# SIMPLE FOUR-MIRROR ANASTIGMATIC SYSTEMS WITH AT LEAST ONE INFINITE CONJUGATE

---

A thesis submitted in partial fulfilment of the

requirements for the Degree

of Doctor of Philosophy

in the University of Canterbury

by Andrew Rakich

University of Canterbury

April, 2007

---

## Table of Contents

**I. Acknowledgments** ..... **4**
**II. Abstract** ..... **6**
**1. Introduction** ..... **9**
**2. Method** ..... **30**
**2.1 Aberration coefficients in wavefront measure in forms useful for Plate Diagram analysis.** ..... 30
**2.2 The Plate Diagram method applied to a survey of four-spherical-mirror telescopes** ..... 42
**2.3 Extension to four-mirror systems containing one, two or three conicoid mirrors** ..... 53
**2.3.1. Three conicoid mirrors** ..... 54
**2.3.2. Two conicoid mirrors** ..... 56
**2.3.3. One conicoid mirror** ..... 59
**2.4 Techniques for filtering solution sets** ..... 62
**3. Results: Four spherical mirrors with no element larger than the entrance pupil** ..... **67**
**4. Results: Four-mirror anastigmats with useful first-order layouts and containing one, two or three conicoid elements** ..... **84**
**4.1 Three-conicoid solution** ..... 84
**4.2 Two-conicoid solutions** ..... 86
**4.3 One-conicoid solutions** ..... 90
**5. Results: Four-spherical-mirror anastigmats with elements larger than the entrance pupil** ..... **97**
**5.1 AA Solutions** ..... 99
**5.2 AB Solutions** ..... 100
**5.3 AC Solutions** ..... 106
**5.4 BA Solutions** ..... 107
**5.5 BB Solutions** ..... 109
**5.6 BC Solutions** ..... 112
**5.7 CA Solutions** ..... 115
**5.8 CB Solutions** ..... 119
**5.9 CC Solutions** ..... 123
**6. Concluding comments** ..... **126**
**Appendix A: Four-mirror anastigmats I: A complete solution set for all-spherical telescopic systems** ..... **130**
**Appendix B: Four-mirror anastigmats II: A complete solution set for all-spherical telescopic systems** ..... **159**

**Appendix C: Four-mirror anastigmats III: all-spherical systems with elements larger than the entrance pupil ..... 179**
**Appendix D: Sample Mathematica File ..... 206**
**Appendix E: Schwarzschild Paper ..... 213**
**Appendix F: SPIE Four-spherical-mirror paper ..... 233**
**Appendix G: SPIE 1, 2 or 3 conicoid mirror paper ..... 246**
**References ..... 269**

## List of Figures

Figure 1.1. Two examples of two-mirror anastigmats ..... 15
Figure 1.2. Two-concentric-spherical-mirror anastigmats ..... 26
Figure 2.1.1. Refraction at a surface. ..... 31
Figure 2.1.2. The annulling plate. ..... 38
Figure 2.1.3. Quantities in the plane of the plate ..... 39
Figure 2.2.1. Stop Shift ..... 43
Figure 2.2.2. Plate Diagram for a Paul three-mirror anastigmat. ..... 45
Figure 2.4.1. Classification based on the order of optical components. ..... 66
Figure 3.1. Schwarzschild anastigmats ..... 68
Figure 3.2. Three-mirror anastigmats with two strictly spherical mirrors ..... 70
Figure 3.3. One of the five solution families ..... 71
Figure 3.4. Two afocal four-spherical-mirror anastigmats. ..... 73
Figure 3.5. Two examples of focal versions ..... 74
Figure 3.6. An afocal four-spherical-mirror anastigmat ..... 75
Figure 3.7. Focal versions of the second type of solution ..... 76
Figure 3.8. An example of high-order aberration correction. ..... 80
Figure 3.9. On-axis WFE residuals ..... 81
Figure 3.10. Schiefspiegler example. ..... 82
Figure 4.1. Baseline system. ..... 85
Figure 4.2. SA, SB and SC solution curves. ..... 87
Figure 4.3. An example of a solution for two-conicoid anastigmats ..... 88
Figure 4.4. Examples from the SB family of solutions. ..... 89
Figure 4.5. Two examples of solutions from the SC curves. ..... 90
Figure 4.6. Three independent sets of solutions ..... 91
Figure 4.7. An example of a completely impractical solution. ..... 93
Figure 4.8. Representative examples from the SB solution set. ..... 94
Figure 4.9. Solution from the SC solution set ..... 95
Figure 5.1.1. An AA-type 42135 system with convex primary mirror. ..... 100
Figure 5.2.1. Three AB-type concave primary mirror solutions. ..... 102

Figure 5.2.2. Two AB-type concave primary mirror solutions. .....103
Figure 5.2.3. Three examples for AB-type convex primary systems. .....105
Figure 5.3.3. AC-type convex primary mirror solutions.....107
Figure 5.4.1. BA-type convex primary mirror solutions.....108
Figure 5.5. BB-type concave primary solutions.....110
Figure 5.5.2. BB-type convex primary mirror solutions. .....111
Figure 5.6.1. BC-type convex primary mirror systems.....114
Figure 5.7.1. CA-type concave primary mirror solutions .....116
Figure 5.7.2. CA-type convex primary mirror solutions.....118
Figure 5.8.1. Three families of CB-type concave primary solutions.....120
Figure 5.8.2. Three families of CB-type convex primary systems .....122
Figure 5.9.1. CC-type concave primary mirror systems. .....123
Figure 16. CC-type convex primary mirror systems.....124

## List of Tables

Table 1. System parameters for the systems depicted in figures 3.4-3.7. .....77
Table 2. Optical design data for the systems shown in figure 3.8. .....80
Table 3. Optical design data for chapter 4 systems. .....96
Table 4. Optical design data for figure 5.1.1. .....100
Table 5. Optical design data for AB-type systems .....104
Table 6. Optical design data for the figure 5.3.1.A system. .....106
Table 7. Optical design data for BA-type systems .....109
Table 8. Optical design data for BB systems from figures 5.5.1 -2.....112
Table 9. Optical design data for BC-type solutions .....113
Table 10. Optical design data for CA-type solutions. .....117
Table 11. Optical design data for CB-type systems .....121
Table 12. Optical design data for CC-type systems .....125

# I. Acknowledgments

A number of individuals have contributed to my being able to complete this work and I would like to take this opportunity to thank them here. First and foremost amongst them is Norman Rumsey, my great friend and teacher. Norman was one of my co-supervisors during my work on this subject, and he passed away three months prior to its completion, in January 2007. Without Norman's support and encouragement, and his dedicated effort to give me a comprehensive education in the area of optical design over a period of 17 years, I certainly would not have the interesting career that I do, or be presenting the interesting results that are presented in this thesis.

Prof. John Hearnshaw and Dr William Tobin at the University of Canterbury, Department of Physics and Astronomy, have been co-supervisors for both my M.Sc. and Ph.D. work and have been of great assistance throughout. Dr Craig Smith is not only the final co-supervisor for my Ph.D. but also my immediate superior at work, and I am grateful for the support that he and my employer, EOS Space Systems, have provided during the course of this work. Dr Raymond Wilson has been the source of much encouragement and interesting conversations on the history of optics and aberration theory. David Shafer has also been helpful. With his extensive background in this field he has been

helpful in confirming some of my claims of originality, as well as informing me of the only existing cases of “prior art” for all-spherical four-mirror anastigmatic telescopes. Of course my wife, Thawee, has been tremendously patient and supportive, as have my children Ivan, Joseph and Marissa, who now have many missed trips to the park and such like owing to them.

# II. Abstract

This thesis describes an analytical approach to the optical design of four-mirror anastigmatic optical systems. In all cases investigated here the object is at infinity. In the introduction the field of reflecting, or "catoptric", optical system design is discussed and given some historical context. The concept of the "simplest possible reflecting anastigmat" is raised in connection with Plate Diagram analysis. It is shown that four-plate systems are in general the simplest possible anastigmats, and that four-plate systems comprised of four spherical mirrors are the last family of "simplest possible reflecting anastigmats" for which the complete solution set remains unknown. In chapter 2 third-order aberration coefficients in wavefront measure are derived in a form that is particularly suitable for Plate Diagram analysis. These coefficients are subsequently used to describe the Plate Diagram, and to detail the application of the Plate Diagram to the survey of all possible solutions for four-spherical-mirror anastigmats. The Plate Diagram technique is also generalized to investigate its use as an optical design tool. In the example given a generalized Plate Diagram approach is used to determine solutions for four-mirror anastigmats with a prescribed first-order layout and a minimum number of conicoids.

In chapter 3 results are presented for the survey of four-spherical-mirror anastigmats in which all elements are required to be smaller than the primary mirror. Two novel families of four-spherical-mirror anastigmats are presented and these are shown to be the only examples of four-spherical-mirror systems that exist under the given constraints.

Chapter 4 gives an example of the application of Plate Diagram analysis to the design of an anastigmatic system with a useful first-order layout and a minimum number of conicoid mirrors. It is shown that systems with useful first-order layouts and only one conicoid mirror can be obtained using this method.

In chapter 5 results are presented of the survey of all remaining four-spherical-mirror anastigmatic systems: that is systems in which elements are allowed to exceed the diameter of the entrance pupil, which includes systems with concave and convex primary mirrors. A wide variety of solutions are presented and classified according to both the underlying geometry of the solutions and the first-order layouts. Of these systems only one has been reported in previously published literature.

The results presented in this thesis complete the set of "four-plate" reflecting anastigmats, and it can now be said that all possible solutions for four-spherical-mirror anastigmatic systems have been determined.

# 1. Introduction

Anastigmatic optical systems are systems in which (at least) the third-order aberrations that produce blurring in the images of point sources are simultaneously brought to zero. These aberrations are spherical aberration, coma and astigmatism. The two remaining third-order aberrations are distortion and Petzval curvature. While these two aberrations respectively stretch (or squash) and curve the image of a plane object, they do not affect the sharpness of the image, and therefore do not increase the size of the minimum resolvable detail in an image.

With one notable exception[1], prior to the nineteenth century optical imaging systems were limited to the correction of spherical aberration only. Indeed it would have been difficult to correct for the off-axis aberrations as there existed no theoretical basis for classifying or quantifying the off-axis aberrations of an

[1] The exception referred to is the afocal two-mirror system proposed by Marin Mersenne in 1636, which was a system consisting of confocal paraboloid mirrors in either the "Cassegrain" or "Gregory" forms. While these names now have a particular meaning for two-mirror geometries, Mersenne's work predated either of these two. Mersenne's system was, entirely accidentally, the world's first anastigmatic optical design. It is not clear who it was that first recognized the anastigmatic properties of the confocal paraboloid pair. Evidence suggests that it was McCarthy (1940). As to the first person to realize that Mersenne was the accidental inventor of the world's first anastigmat, that was much later, possibly Willstrop in the 1980s.

optical system until pioneering work by Hamilton (1833) (though it does appear that Fraunhofer had achieved coma correction in his well known "aplanatic" refracting objective lenses, though how he achieved this correction is not clear, and the coma correction was not nearly so perfect as would be implied by the modern use of the term "aplanat" (King 1955)). While Hamilton's work laid the basis for completely defining the properties of off-axis point images, it wasn't of much practical use to optical designers, as Hamilton's Characteristic Function did not directly involve system constructional parameters. The first recorded instance of the formulation of aberration coefficients in terms of system constructional parameters was the work of Seidel (1856). The five third-order aberrations, now commonly referred to as "Seidel aberrations" are: spherical aberration, coma, astigmatism, distortion and Petzval curvature.

It is interesting to note that there exists a strong set of circumstantial evidence suggesting that Petzval had independently developed an aberration theory useful for practical optical design, and encompassing higher orders of aberration that were not otherwise known until the work of Buchdahl (1954). A brief summary of this evidence follows:

1) Von Rohr (1899) states categorically that Petzval did not utilize iterative trigonometric ray-tracing in his lens design. However, the first

Petzval portrait objectives had high-order spherical aberration balanced against third-order spherical aberration; if trigonometric ray tracing was not used for this then this balance could only practically have been achieved by balancing aberration coefficients.

2) Aldis (1900) directly attributes the third-order aberrations to Petzval (with no reference).

3) Schwarzschild (1905a) says "Petzval, the calculator of the first "portrait lens" gave this number (of fifth order aberration coefficients) as 12, from which seems to follow that despite his calculations extending to aberration coefficients of the $9^{th}$ order, he did not see through the relationship all too deeply". In fact relatively recent work (De Meijère and Velzel 1989) shows that one can formulate either 9 or 12 fifth order aberration coefficients, depending on an arbitrary choice of definition of the pupil coordinates.

This and other supporting evidence is to be the subject of a paper at the 2007 SPIE annual general meeting (Rakich 2007).

In 1874 Piazzi-Smyth invented the field-flattening lens, which allowed the transformation of, for example, a Petzval lens (which, ironically, suffered from Petzval curvature) to a flat-field anastigmat (Piazzi-Smyth 1874). Prior to this

development optical designers had resorted to using astigmatism to balance optimally against Petzval curvature. In this they sought to achieve a flat tangential focal surface, minimizing the residual aberration blur on a flat surface. Piazzi-Smyth commented that when optical designers deliberately introduced astigmatism to flatten the image they "relieved us of a blunder by substituting a sin".

By the early 1900s there existed a number of anastigmatic lens designs, notably the Rudolph's "Tessar" and Taylor's "Cooke Triplet" (Kingslake 1980).

While progress in the optical design of refracting systems had proceeded at pace, largely driven by the development of photography as well as increasing demands from the field of microscopy, prior to 1905 no-one had thought to apply aberration theory to correcting the field aberrations of reflecting telescopes. The optical design of two-mirror telescopes had not progressed since the pioneering work of Mersenne in 1636, followed by Gregory in 1663 and Cassegrain in 1672 (Wilson 2004a). The same could be said of the reflecting microscope objective, first proposed by Newton, with Cassegrain forms given by Smith in 1738 (Burch 1947). In neither case had any attempt been made to address and control field aberrations; this is not surprising as the theoretical development simply didn't exist at that point.

In the early 1900s the astronomer Karl Schwarzschild, conscious when comparing mirrors to lenses of both the price advantage and the lack of chromatic aberration available with mirror systems, became interested in all-reflecting equivalents of the refracting astrograph objectives that were then in common use for astronomical sky surveys.

In the first two of a series of three papers Schwarzschild revolutionized the field of optical design by developing a complete theory for the design of two-mirror telescope systems compensated for field aberrations (Schwarzschild 1905-1, 2). In the first of these papers Schwarzschild formulated third and fifth order aberration coefficients in wavefront measure in terms of optical system parameters. In the course of doing this he invented a convenient mathematical parameter used to define the asphericity of conic surfaces of revolution which has become the modern standard in optics, the conic constant. In the second paper Schwarzschild applied the third-order coefficients to an investigation of the on- and off-axis imaging properties of reflecting systems with one and two mirrors. In the course of this work he gave explicit formulae for aplanatic two-mirror systems (systems simultaneously free of spherical aberration and coma, at least to the third order), but did not pursue such systems as the residual astigmatism would have intolerably limited the field of view that he was trying to achieve.

Later aplanatic two-mirror telescopes were independently re-discovered by Chrétien (1922) and the telescope that came to be known as the Ritchey-Chrétien has dominated the field of large professional astronomical telescopes throughout the latter half of the twentieth century and up to the present day.

Schwarzschild was primarily interested in anastigmats and gave explicit formulae for two-mirror anastigmats and two solved examples. One of these was for the special case of a two-mirror anastigmat with zero Petzval curvature, and the second was for an anastigmat with a concave primary mirror and non-zero Petzval curvature (figure 1.1). He showed that all focal two-mirror anastigmats would have a mirror separation equal to twice the system focal length, and that the only flat-field two-mirror anastigmat possible would have a convex primary mirror and a much larger concave secondary mirror. Disappointed, Schwarzschild abandoned his search for a two-mirror flat-field anastigmat and concentrated instead on the design of a two-mirror aplanat with an astigmatism flattened field. This system was later improved by Couder, who reverted to a two-concave-mirror anastigmatic system with residual Petzval curvature, and flattened the field by way of a singlet field-flattening lens (Danjon and Couder 1935).

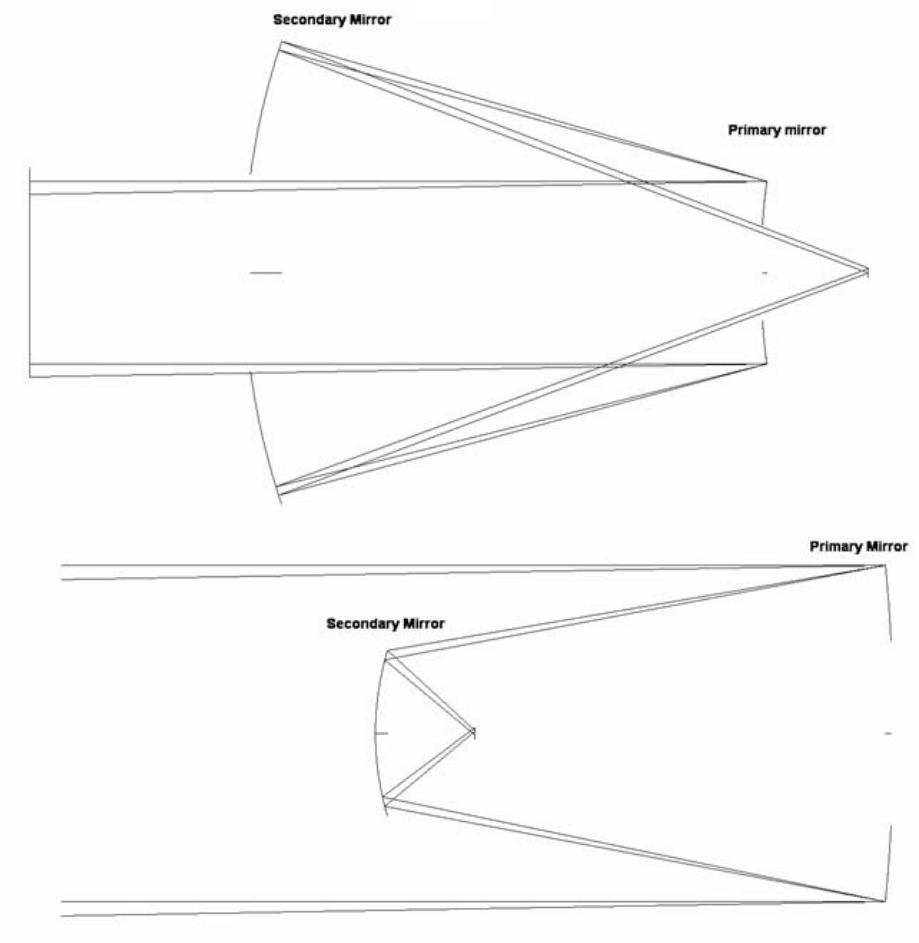


**Figure 1.1. Two examples of two-mirror anastigmats, similar to examples given by Schwarzschild. The upper system has a convex primary mirror, both mirrors are oblate spheroids and the Petzval curvature is zero. The lower system is a concave primary system, later adapted by Couder to include a field-flattening lens near the focal plane. In his 1905 paper Schwarzschild reintroduced astigmatism to this system to flatten the field. As with all focal two-mirror anastigmats, the separation of the two mirrors is equal to twice the system focal length.**

A summary of Schwarzschild's two papers is provided by the author (Rakich 2005), and that paper is attached to this document as appendix E.

While Schwarzschild's investigations did not lead to any particularly attractive systems for the application he had in mind (only two of his aplanats are known to have been made (Wilson 2004b)) Schwarzschild's development of a practically useful aberration theory for reflecting systems opened up a whole new field for modern optical design. Within a relatively short space of time designs were also being proposed for anastigmatic catoptric microscope objectives (e.g. Maksutov 1932, Burch 1943-1, 1947, Brumberg 1943, Linfoot 1938, 1943, Clay 1939), anastigmatic spectrograph cameras (McCarthy 1940), the Schmidt telescope (Schmidt 1936) and new three-mirror-anastigmat telescopes (Paul 1935, Dimitrov and Baker 1945).

The field of reflecting optics, and in particular the area of three-or-more-mirror systems expanded rapidly in the second half of the 20$^{th}$ century. A thorough treatment of this development, at least with respect to reflecting telescope systems is given by Wilson (2004c).

A little before the time that Schwarzschild began working in optics, Aldis (1900) published an interesting but little known paper. Using third-order aberration coefficients (that he ascribed to Petzval), he showed that anastigmatic optical correction could be achieved by means of four spherical surfaces. This work was subsequently picked up by Burch, who in a series of papers generalized Aldis' approach and applied it to mirror systems in which

the elements could either be spheres or conicoids (for example Burch 1943-2). As will be described in the next chapter, Burch showed how a spherical mirror, which has optical power, could be replaced with a zero-power Schmidt-like plate that produced the same aberrations as the spherical mirror without introducing power, and how a conicoid mirror could be replaced by two such plates, one representing the spherical aberration contribution of the vertex sphere, and the other representing the spherical aberration contributed by the conic departure from the vertex sphere. In this elegant analysis, Burch showed how system sums of third-order aberrations could be represented as a mechanical system, which he called alternatively the "Optical See-Saw Diagram" or "Plate Diagram".

The main strength of the Plate Diagram was that it provided a way to cut through the complex algebra used to describe multi-mirror systems, giving an alternative representation of such systems that was much more amenable to intuitive grasp and manipulation. Fundamental optical concepts such as the stop-shift theorem and the optical properties of concentric systems become perfectly obvious when optical systems are transformed into a Plate Diagram. On this subject, Burch himself said "When one conducts an extended-paraxial analysis in term of these *natural co-ordinates* − as I regard them − the equations automatically assume a particularly suggestive form, the relations

appear which, though they must also be contained in the equally exact analysis, e.g. of Conrady, have remained to me, at least, hitherto invisible − shrouded in a dark miasma of algebraic artificial fog".

Using the Plate Diagram, Burch was able to generalize Aldis' result for four spherical surfaces as mentioned above, and showed that an anastigmatic telescope (or microscope with an infinite long conjugate) could be arrived at with either two conicoid mirrors, three mirrors one of which was a conicoid or four spherical mirrors. Each of these classes of system could be represented by a Plate Diagram of four plates.

In this sense the three possible types of four-plate systems can be regarded as the simplest possible reflecting anastigmats[2]. While two-mirror systems can be

[2] There do exist certain degenerate special cases, such as the concentric spherical mirror pair, which happens to be anastigmatic and forms a real image of an infinitely distant object when the primary mirror is convex, the secondary concave, and the separation of the mirrors is in the ratio 1: 1.618 (the golden ratio) to the radius of the secondary mirror. When these conditions are met, the central obstruction ratio for the axial pencil is also in the golden ratio. It is interesting to note that this system is almost universally attributed to Schwarzschild, but it is clear from reading his papers that he did not realize that an all-spherical anastigmatic two-mirror system was possible. Shafer (1978), in pointing this out, credits Burch with the discovery (Burch 1943). However, in the reference given, Burch makes no claim of originality and, in his discussions of two-concentric spherical-mirror anastigmats in his other published works, he treats them as if they are already well known.

represented by at most four plates, three-mirror systems can give rise to a maximum of six plates and four-mirror systems to eight (if all of the mirrors are aspheric). Therefore, for three- and four-mirror systems the four-plate systems represent interesting special cases of good correction with minimum optical complexity.

The two-aspheric-mirror case, first investigated by Schwarzschild (1905-2), has received considerable attention throughout the twentieth century. Aside from the references already given for Burch and Linfoot, examples of explorations and developments for two-mirror systems can be found in Steele (1950), Grey (1951), Erdös (1959), Stavroudis (1967), Rosin (1968), Wynne (1969), Gelles (1975), Sasian (1990) and Hannan (1992).

The first three-mirror anastigmat design was presented by Paul (1935). This system, later described by Willstrop (1984, 1985) as the "Mersenne-Schmidt", was indeed a combination of the afocal Mersenne confocal paraboloid pair with a Schmidt telescope. As pointed out in footnote 1, the Mersenne system is in fact anastigmatic. If a spherical mirror is used to form an image from the afocal output of a Mersenne system it will, in general, introduce aberration to the final image. However, if the concave spherical tertiary mirror is chosen such that its centre of curvature lies on the pole of the convex secondary

mirror of the Mersenne system, then it can be seen, by imagining the stop is placed at the secondary mirror, that the spherical tertiary mirror will not introduce any coma or astigmatism for exactly the same reason that these aberrations are absent from a Schmidt telescope. As with the mirror of a Schmidt telescope, this tertiary mirror will still introduce spherical aberration. However, if the radius of curvature of the tertiary mirror is chosen to be equal to that of the secondary mirror, then the amount of spherical aberration introduced by the tertiary mirror is exactly the same as the amount of spherical aberration introduced to the system by the paraboloidal figuring of the secondary mirror. Therefore, if the secondary mirror is made spherical instead of paraboloidal, the three-mirror system sum for spherical aberration is reduced to zero, and as this change happened at the system stop, there is no effect on the correction of coma and astigmatism. Of course, once it is realized that such a system is anastigmatic, there is no restriction on the stop position, as by the stop-shift theorem the stop can be moved to any location within the system without re-introducing any of the first three third-order aberrations (and without having any effect on the residual third-order distortion).

Paul's system was the first, and arguably the most geometrically elegant, of the many possible "four-plate systems" obtainable with three mirrors, only one of which is aspheric. This system was independently re-discovered by

Dimitroff and Baker (1945) who improved it by making the secondary mirror ellipsoidal, which allowed the tertiary mirror to change its radius by the amount required to bring the Petzval sum to zero, without disturbing the anastigmatic correction of the system. Baker was unaware of Paul's work, and it was brought to his attention in a private communication from Rumsey, which he acknowledged in a subsequent publication (Baker, 1969).

A final variant of the Paul system was proposed by an amateur astronomer (Stevick 1993) who also independently re-discovered the Paul system while investigating Schiefspiegler designs[3]. Stevick was the first person to consider using the Paul system off-axis. The Paul system is particularly well suited to this approach as the Stevick-Paul variant uses the complete rotationally symmetrical paraboloid primary mirror, and the off-axis components are

[3] While "Schiefspiegler" literally means "tilted mirrors", it has come to mean reflecting telescope systems which are free from central obstruction. These can indeed be obtained by using mirrors that have been tilted with respect to the optical axis. However the common usage of the term Schiefspiegler also includes unobstructed systems that are based on portions of parent systems that are symmetrical about some common axis. An axially-symmetrical parent system can be rendered as a Schiefspiegler by using an off-axis portion of the pupil, or by using only a small range of field points surrounding some off-axis field point, or by a combination of both of these approaches. The Stevick-Paul system is based on the axially-symmetrical Paul parent system, and is off-axis in field but retains an axially-symmetrical pupil.

strictly spherical, and so do not pose the difficulties of manufacture or alignment that would be associated with off-axis aspheric components.

Following Paul, the next "simplest possible" three-mirror anastigmats were produced in two papers by Rumsey (1971, 1972). In the first of these, Rumsey investigated pairs of spherical-mirror correctors capable of giving anastigmatic performance to a paraboloidal primary mirror. Rumsey showed that, apart from the Paul form, there were two other possible types of two-spherical-mirror corrector for a concave paraboloid mirror. In his second paper, Rumsey showed that there existed four types of correctors for the case in which the primary mirror was a mild hyperboloid. In fact that primary mirror to which Rumsey applied his results was the hyperboloid primary mirror of the Anglo-Australian Telescope, a Ritchey-Chrétien system.

Cook (1987) produced another three-mirror, one-mirror-aspherized, Schiefspiegler design. This system was unique among the simplest possible three-mirror designs produced up until that point, in that it achieved zero Petzval curvature while maintaining two strictly spherical mirrors.

Despite a large amount of work in the area of the analytical design of three-mirror anastigmats in the last three decades of the twentieth century, for example Rumsey (1970), Korsch (1973), Robb (1978), Yamashita and Nariai

(1983), Epps and Tadeka (1983) and Stone and Forbes (1991), it wasn't until 2001 that new solutions in the simplest possible three-mirror anastigmat family were produced.

Here, the author, together with Rumsey, produced a complete solution set containing all possible solutions for three-mirror telescopes in which the primary mirror was concave and two mirrors were kept strictly spherical (Rakich 2001, Rumsey and Rakich 2002). This work utilized the simplicity of the Burch analysis to formulate an analytical solution for three-mirror anastigmats in three separate cases, depending on which of the primary, secondary or tertiary mirrors were aspherized. In each case, for a given set of starting parameters, a cubic equation could be defined which would lead to three unique anastigmat solutions. By applying this solution to all points in a plane defined by two of the optical system constructional parameters, Rumsey and Rakich generated geometrically nine distinct families of solution. On investigation these solution sets were shown to contain, as expected, all of the "simplest possible" three-mirror systems described above, as well as a number of examples of new design variants.

Perhaps the most notable among these was a system the author referred to as the "Paul-Rumsey" system. In this case the Paul system was modified to produce a system with a flat field while retaining two strictly spherical mirrors.

This was achieved by changing the primary mirror from the paraboloid of the Paul system to an ellipsoid with a conic constant quite close to -1.

Following the success of this survey it was decided to explore the final set of simplest possible reflecting anastigmats, the four-spherical-mirror set, using a similar approach.

While four-mirror systems in general have received some attention since the first investigation by Steele (1953), the field has not developed at the same pace as that of the two or three-mirror anastigmats. While it is true that until relatively recent improvements in coating technology, making possible high efficiency broadband multilayer dielectric optical coatings, such systems would have been considered by many as too "lossy", it is also undoubtedly the case that many have considered the algebraic complexity of an analytical approach to four-mirror system design as impractical. For example, Lerner et al. (2000) refer to the idea of an analytical solution for four-mirror lithography systems as "unfeasible".

While analytical approaches to four-mirror systems do exist in the literature, for example those of Korsch (1973, 1991), and also Howard and Stone (2000), most publications concerning four-mirror anastigmatic or aplanatic telescopes focus on a particular design, or few designs, rather than on a general

analytical solution and its application to a survey of the field of possible solutions. As well as in the reference listed immediately above, examples of work on four-mirror telescope systems can be found in Meinel et al. 1984, Sasian 1987, Wilson and Delabre 1994, Gilmozzi et al. 1998 and Goncharov 2004 .

In all of the work done in the field of four-mirror telescope systems, the only author who has produced designs for anastigmats comprised of four spherical mirrors is Shafer (1978, 1988). In the first of these papers, Shafer started by coupling anastigmatic subsystems to produce systems with four or five reflections that were themselves anastigmatic. Shafer showed how the two-concentric-spherical mirror telescope described above was also anastigmatic when used in reverse, i.e. with collimated light from an infinitely distant object incident on the larger primary mirror instead of on the smaller convex mirror (figure 1.2). However, in this case a virtual image is formed behind the secondary mirror, though this image is still anastigmatic. Shafer showed how, by combining this system with a two-concentric-spherical mirror anastigmatic relay system, the virtual image could be re-produced as a real image by the resultant four-spherical mirror anastigmatic system. In Shafer's example the base system produced 100% central obstruction, but Shafer was able to produce a Schiefspiegler free from obstruction, by using off-axis portions of

the pupil and an off-axis field. This system remains the only existing example in the published literature, prior to the author's work, of a four-spherical-mirror anastigmatic telescope in which the primary mirror is the element with the largest diameter.

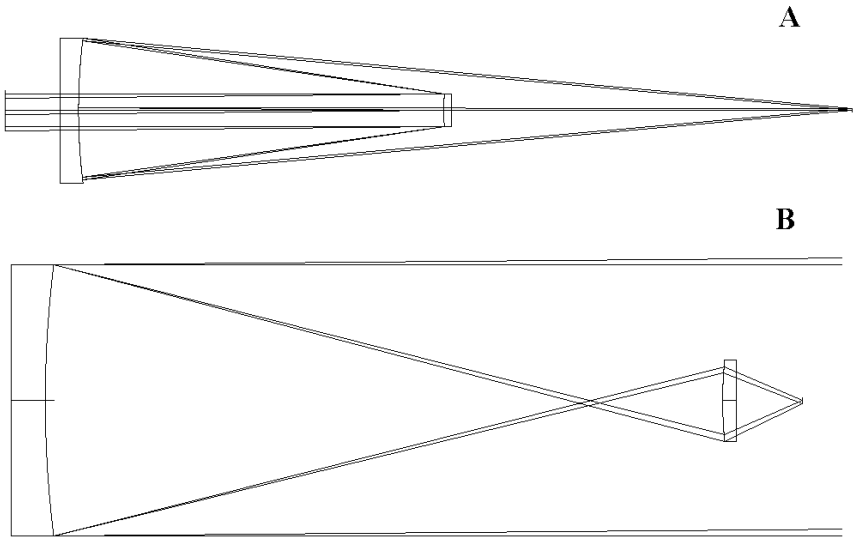


**Figure 1.2. Two-concentric-spherical-mirror anastigmats**

- **A) The two-concentric-spherical-mirror anastigmat produces a real curved image of an object at infinity. In this diagram collimated light from the object is incident on the smaller, convex primary mirror from the left of the page.**
- **B) When the same system is used in reverse, with light from an infinitely distant object now incident first on the larger concave mirror, the system is still anastigmatic, but the image is now virtual, behind the smaller convex mirror.**

The only other example in the literature of a four-spherical mirror anastigmatic telescope is in Shafer's 1983 paper. Here he describes a system with a convex primary mirror which is used on axis.

This thesis presents the results of a complete survey of all possible four-spherical mirror telescope systems. The survey utilizes an analytical solution for four-spherical-mirror anastigmats derived by using an approach based on Burch's Plate Diagram analysis. This survey and its results are primarily described in two papers. At the time of writing both of these papers have been submitted and accepted by *Optical Engineering*. These papers are included in this document as appendices A and C.

The paper attached as appendix A details the method employed in the four-spherical-mirror survey in the case where the primary mirror is concave and is also the optical element with the greatest diameter in the system. The paper attached as appendix C details the results of an equivalent survey conducted in the case where the primary mirror is allowed to be either convex or concave, and optical elements subsequent to the primary mirror are allowed to be larger in diameter than the primary mirror itself. The paper attached as appendix B presents the results of a separate but related investigation. In this case, an investigation is made into the feasibility of using surveys of solution space analogous to those used for the four-spherical-mirror surveys as a more

general optical design tool. The aim of the investigation is to locate anastigmatic systems with a minimum number of conic surfaces when one starts from a four-mirror system that has a useful first-order layout (but is not corrected for spherical aberration, coma or astigmatism). It is demonstrated in the example given in the paper that, using such a baseline system, the survey method is capable of throwing up both unthought-of geometries and also solutions similar in first-order layout to the baseline system that are also anastigmatic with only one mirror required to be a conicoid.

This document is intended to provide some background and context for these papers. Hence, following this introduction, the next chapter of this document will elaborate on the method employed for the survey, including details of the analytical solutions derived. Chapter 3 will then give a description and summary of the papers attached in appendices A, B and C. Appendix D contains an example of the Mathematica™ code used to conduct the surveys described in appendices A and C. Appendix E is a copy of an SPIE conference paper given on the subject of Schwarzschild's first two 1905 papers on optics, which the author, with the assistance of Dr Werner Friedrich of Industrial Research Limited, New Zealand, had translated in 2002. It is included in this document, as it provides useful and relevant background information to the work presented in this thesis, helping to set it in its

historical context. Appendices F and G are copies of SPIE conference papers on which the Optical Engineering papers in appendices A and B respectively are based. The conference papers are in fact superseded by the journal papers, but are included in this document for completeness.

# 2. Method

This chapter summarizes the methods used in the surveys conducted in the papers presented as appendices A, B, C, F and G of this thesis. In section 2.1 primary aberration coefficients in wavefront measure will be derived in forms useful to the Plate Diagram analysis. Section 2.2 will be a general discussion of the Plate Diagram method applied to the survey of four-spherical-mirror telescopes as developed and used in the papers provided in appendices A and C. Section 2.3 will look at how this method was generalized in the paper of appendix B to investigate four-mirror systems with one, two or three conicoid mirrors.

## *2.1 Aberration coefficients in wavefront measure in forms useful for Plate Diagram analysis.*

For the analysis of multi-mirror systems the wavefront measure of aberration (as opposed to the transverse or longitudinal measures) is particularly useful. This is because the system sum of third-order aberrations in wavefront measure can be obtained by simple addition of contributions from each individual element in the system, whereas with transverse or longitudinal measures more algebra is required to take into account scaling changes from

surface to surface. The following derivations give third-order coefficients for spherical aberration, coma and astigmatism in forms useful and directly applicable to Plate Diagram analysis. The derivation of the first spherical aberration coefficient in eq. 2.16 below follows Hopkins (1950), while the derivations for coma and astigmatism coefficients were presented by Rakich (2001) based on analysis by Aldis (1900) and Burch (1943-2).

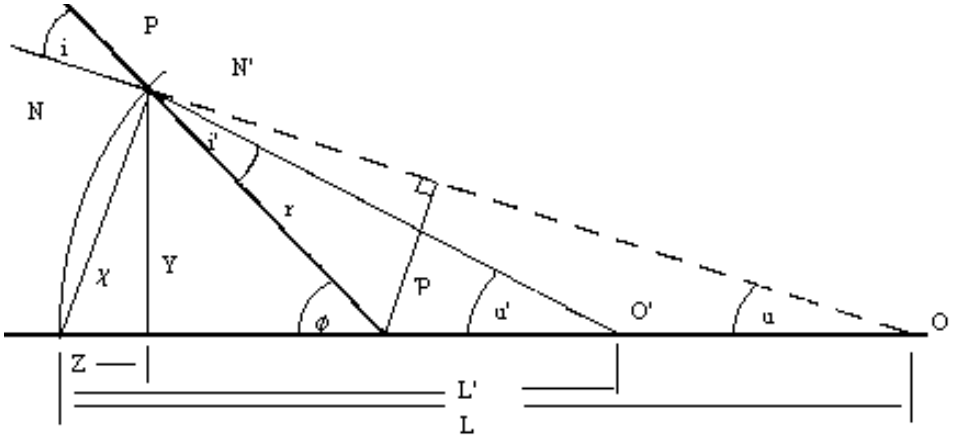


**Figure 2.1.1. Refraction at a surface. All quantities shown here are positive. $N$ and $N'$ are refractive indices before and after refraction and P is the point at which the marginal ray is incident on the surface. All other quantities are either self-evident from the diagram or will be explained as they are used in the text.**

The spherical aberration in wavefront measure arising at an optical surface is usually quantified in terms of the maximum optical path difference (OPD) introduced between the incident and transmitted wavefronts, where the incident wavefront emanates from an axial object point (i.e. the wavefront has

axial symmetry about the optical axis of the surface). In this case the marginal ray of the axial pencil is the only ray required to quantify the primary spherical aberration contribution from a given surface.

Figure 2.1.1 above shows a ray refracting at a spherical surface. All quantities shown in figure 2.1.1 are positive, defining the sign convention used here. Using these symbols, the OPD introduced to the ray by the surface can be written as

$$W = N'(L' - \mathrm{PO}') - N(L - \mathrm{PO}). \tag{2.1}$$

Observing that

$$\begin{aligned} \mathrm{PO}^2 &= Y^2 + (L - Z)^2 \\ &= L^2 + Y^2 - 2LZ + Z^2 \end{aligned} \tag{2.2}$$

and that for a spherical surface the profile equation is

$Y^2 = 2rZ - Z^2$, we obtain (2.3)

$$2rZ = Y^2 + Z^2 = X^2, \text{ or} \tag{2.4}$$

$$2Z = \frac{X^2}{r}. \tag{2.5}$$

Therefore,

$$\begin{aligned}\mathrm{PO}^2 &= L^2 - \frac{LX^2}{r} + X^2 \\ &= L^2\left(1 - \frac{X^2}{Lr} + \frac{X^2}{L^2}\right) \\ &= L^2\left(1 - \frac{X^2}{L^2}\left(\frac{1}{r} - \frac{1}{L}\right)\right).\end{aligned} \tag{2.6}$$

Using the binomial theorem,

$$\mathrm{PO} = L\left(1 - \frac{X^2}{2L}\left(\frac{1}{r} - \frac{1}{L}\right) - \frac{X^4}{8L^2}\left(\frac{1}{r} - \frac{1}{L}\right)^2 - \mathrm{O}(6)\right). \tag{2.7}$$

Excluding high-order terms and rearranging gives

$$\begin{aligned}N(L - \mathrm{PO}) &= \frac{1}{2}X^2 N\left(\frac{1}{r} - \frac{1}{L}\right) + \frac{1}{8}X^4\left(N\left(\frac{1}{r} - \frac{1}{L}\right)\right)^2 \frac{1}{NL}, \\ N'(L' - \mathrm{PO}') &= \frac{1}{2}X^2 N'\left(\frac{1}{r} - \frac{1}{L'}\right) + \frac{1}{8}X^4\left(N'\left(\frac{1}{r} - \frac{1}{L'}\right)\right)^2 \frac{1}{N'L'}.\end{aligned} \tag{2.8}$$

Now $W$ from 2.1 can be defined in terms of 2.8.

In the paraxial limit Snell's law becomes

$$Ni = N'i' \tag{2.9}$$

Adopting the convention of replacing upper-case symbols with the corresponding lower-case symbols, when the quantity that they represent is a paraxial quantity, gives:

$$
\begin{aligned}
&i = \phi - u = \frac{y}{r} - \frac{y}{l};\\
&i' = \phi - u' = \frac{y}{r} - \frac{y}{l'};\\
&\rightarrow N(\frac{1}{r} - \frac{1}{l}) = N'(\frac{1}{r} - \frac{1}{l'}).
\end{aligned}
\tag{2.10}
$$

Also,

$$X \rightarrow y. \tag{2.11}$$

Applying the paraxial approximations to $W$ and disregarding high-order terms gives:

$$
\begin{aligned}
W &= \frac{1}{8} y^4 (N(\frac{1}{r} - \frac{1}{l}))^2 (\frac{1}{N'l'} - \frac{1}{Nl})\\
&= \frac{1}{8} y (N(\frac{y}{r} - \frac{y}{l}))^2 (\frac{y}{N'l'} - \frac{y}{Nl})\\
&= \frac{1}{8} y (Ni)^2 (\frac{u'}{N'} - \frac{u}{N}).
\end{aligned}
\tag{2.12}
$$

This is the third-order spherical aberration coefficient for a single spherical optical surface in wavefront measure. In this thesis two alternative forms of this coefficient are used, both of which are simplified versions of the general result above. The simplified versions only apply to the spherical aberration arising at a spherical reflecting surface in air, where:

$$N = \pm 1, N^2 = 1, N' = \mp 1, N'^2 = 1. \tag{2.13}$$

A variable introduced here is the surface reciprocal radius, or curvature, $c = \frac{1}{r}$. Using this and quantities defined in figure 2.1.1 the following relationships can be obtained:

$$\begin{aligned} u &= \phi - i = \frac{(y - \mathrm{P})}{r} = c(y - \mathrm{P}) \\ \rightarrow y &= \frac{(u + c\mathrm{P})}{c}; \\ u + i &= u' + i' = \frac{y}{r} = cy, \end{aligned} \tag{2.14}$$

and,

$$\begin{aligned} \frac{u'}{N'} - \frac{u}{N} &= N'^2 \frac{u'}{N'} - N^2 \frac{u}{N} = N'u' - Nu = N'(u' + i') - N(u + i), \\ &= y\frac{(N' - N)}{r} = yc(N' - N), \\ &= -2Ncy. \end{aligned} \tag{2.15}$$

Substituting this result into 2.12 gives:

$$\begin{aligned} W &= \frac{1}{8}(Ni)^2 y(-2Ncy) \\ &= -\frac{1}{4}N^3 i^2 cy^2 \\ &= -\frac{1}{4}Nci^2 y^2. \end{aligned} \tag{2.16}$$

In collimated light, where $u = 0$ for the axial pencil, $i = \frac{y}{r} = yc$, and 2.16 becomes:

$$W = -\frac{1}{4} N c^3 y^4. \tag{2.17}$$

Finally, by noting that $i = c\mathrm{P}$, and using relationships from 2.14 and 2.16 another form of the spherical aberration coefficient is obtained as follows:

$$\begin{aligned} W &= -\frac{1}{4} N c i^2 y^2 \\ &= -\frac{1}{4} N c (cP)^2 (\frac{(u + cP)}{c})^2 \\ &= -\frac{1}{4} N c \mathrm{P}^2 (u + cP)^2. \end{aligned} \tag{2.18}$$

Note that the "*P*" used in 2.14 and 2.18 is the length of the perpendicular from the centre of curvature of the surface to the incident ray, and is not to be confused with the point of incidence of the ray on the surface, P. Also note that 2.18 $\rightarrow$ 2.17 as $u \rightarrow 0$.

The design of anastigmatic systems also requires coefficients for third-order coma and astigmatism in wavefront measure. To derive these in a form that is

particularly convenient for Plate Diagram analysis we start by considering Burch's concept of the "annulling plate" (Burch, 1943-2).

The annulling plate is a zero-powered Schmidt plate that replaces a spherical mirror. By the correct choice of strength and location for the plate it can introduce exactly the same aberrations into the optical system as the spherical mirror it replaces.

Figure 2.1.2 below shows how a spherical mirror can be replaced by an "anti-Schmidt plate" which contributes exactly the same aberrations as the mirror it replaces, without contributing any power.

To proceed we consider a single spherical mirror which can be thought of as being illuminated by collimated, divergent or convergent pencils of rays from on- and off-axis objects. The spherical aberration, as defined by 2.1, is first determined for the mirror surface using 2.16, 2.17 or 2.18 as appropriate. Having established the magnitude of the spherical aberration contributed by the mirror we now determine the profile equation of an annulling plate, placed at the centre of curvature of the spherical mirror, which will produce exactly this quantity of spherical aberration.

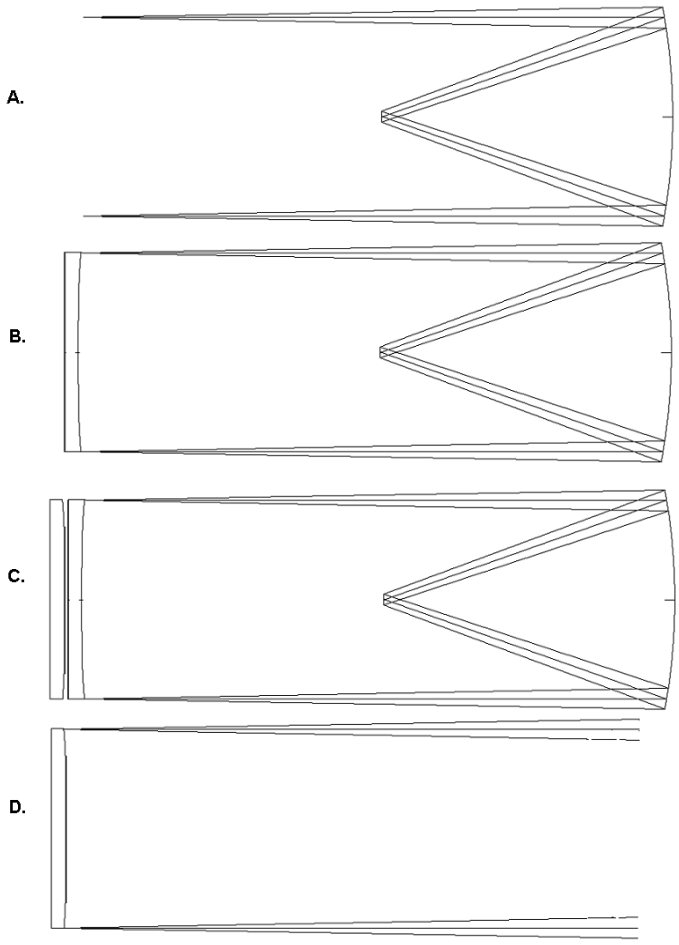


**Figure 2.1.2. The annulling plate.**
**A) Spherical mirror with the aperture stop at the centre of curvature. Coma and astigmatism free, but image suffers from spherical aberration over a curved field.**
**B) Introducing a Schmidt plate with a spherical contribution equal in magnitude and opposite in sign to that of the mirror, at the centre of curvature, corrects spherical aberration. By the Stop-Shift Theorem, the stop can now be moved anywhere without re-introducing coma or astigmatism.**
**C) Introducing an "anti-Schmidt plate" cancels the correction described in B, returning the aberration condition to that of the original spherical mirror.**
**D) Removing the original spherical mirror and Schmidt correcting plate leaves the anti-Schmidt plate, giving the same aberrations as the original spherical mirror, including astigmatism and coma as the stop moves away from the plate.**

This plate will advance or retard a wavefront in proportion to $y^4$, where $y$ is the distance from the axis at which the ray is incident on the plate. The constant of proportionality, $\kappa$, is chosen so that the wavefront reached the value $W$ at $y_c$, where $y_c$ is the value at the plate for the marginal ray of the axial pencil. In general $y_c$ at the plate is not equal to $y$ at the mirror surface, $y_c = y - ru$ and:

$$\kappa y_c^4 = W \rightarrow \kappa = \frac{W}{y_c^4}. \tag{2.19}$$

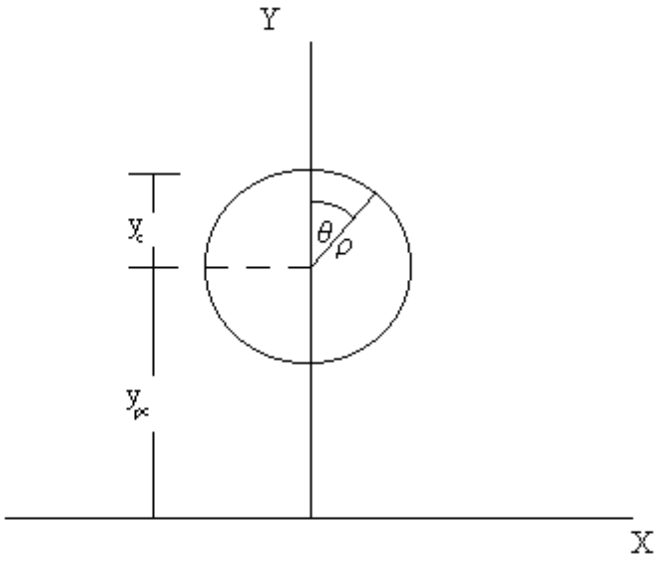


**Figure 2.1.3. Quantities in the plane of the plate.**

Now consider an oblique pencil for which the principal ray crosses the plate at the height $y_{pc}$, as depicted in figure 2.1.3. Here the pencil has a semi-diameter of $y_c$. In the cross section of the pencil we set up polar co-ordinates $(\rho,\theta)$, with the origin on the principal ray, with $\theta = 0$ for the vertically upwards direction and with $\rho$ ranging from zero to $y_c$.

Then, if $(X,Y)$ denote co-ordinates in the plane of $(\rho,\theta)$, but with an origin at the optical axis:

$$\begin{aligned} X &= \rho \sin\theta \\ Y &= y_{pc} + \rho\cos\theta. \end{aligned} \tag{2.20}$$

Using 2.19, the advance or retardation, $\delta W$, for any point on the plate is:

$$\begin{aligned} \kappa(X^2+Y^2)^2 &= \kappa((\rho\sin\theta)^2 + (y_{pc}+\rho\cos\theta)^2)^2 \\ &= \kappa(\rho^2\sin^2\theta + y_{pc}^2 + 2y_{pc}\rho\cos\theta + \rho^2\cos^2\theta)^2 \\ &= \kappa(y_{pc}^2 + 2y_{pc}\rho\cos\theta + \rho^2)^2 \\ = \kappa(y_{pc}^4 + 4y_{pc}^3\rho\cos\theta + 4y_{pc}^2\rho^2\cos^2\theta + 4y_{pc}\rho^3\cos\theta + \rho^4 + 2y_{pc}^2\rho^2). \end{aligned} \tag{2.21}$$

The six terms in the final line of equation 2.21 represent, in order of appearance, a constant displacement (piston) term, distortion, astigmatism$_1$, coma, spherical aberration and astigmatism$_2$. The two astigmatism terms can

be written $2y_{pc}^2\rho^2(1+2\cos^2\theta)$. Equation 2.21 shows the dependence of various aberrations on $\rho$, $\theta$ and $y_{pc}$. We most often wish to have a single number for each aberration. This is usually the maximum value for the permitted range of $\rho$, $\theta$ and $y_{pc}$, though an exception is usually made in the case of astigmatism, where we still use the maximum values of $\rho$ and $y_{pc}$, but most commonly set $\cos\theta = 0$.

For the investigation of anastigmatic systems we can discard the piston and distortion terms. Setting $\rho$ to its maximum value, $y_c$, assuming $y_{pc}$ has its maximum value, substituting $\cos\theta = 1$ for the coma term and $\cos\theta = 0$ for the astigmatism term, and substituting $\frac{W}{y_c^4}$ for $\kappa$, we obtain the following expression for the total third-order aberration:

$$\begin{aligned} \textit{Total third order aberration} &= (y_c^4 + 4y_{pc}y_c^3 + 2y_{pc}^2y_c^2)\frac{W}{y_c^4} \\ &= (1 + 4\frac{y_{pc}}{y_c} + 2\frac{y_{pc}^2}{y_c^2})W. \end{aligned} \tag{2.22}$$

### *2.2 The Plate Diagram method applied to a survey of four-spherical-mirror telescopes*

The Plate Diagram method of Burch forms the basis of the analytical approach to all of the work produced in this thesis. It is described in detail in the "method" section of "Four-mirror anastigmats I: A complete solution set for all-spherical telescopic systems", which is attached as appendix A. That section is repeated with some additional clarification below.

The Plate Diagram analysis of an optical system gives a system of Schmidt plates in collimated light which reproduce exactly the wavefront primary aberration condition of a system consisting of any number of concave or convex, conicoid or spherical, refracting or reflecting optical surfaces and spaces. In this work we are limited to considering systems of mirrors.

It was shown in section 2.1 that a spherical mirror can be replaced by an "anti-Schmidt plate" which contributes exactly the same aberrations as the mirror it replaces, without contributing any power.

The "strength" of the anti-Schmidt plate representing the spherical mirror can be thought of as $W$, with $W$ as defined in equations 2.16, 2.17 or 2.18 as appropriate.

Remembering that $y_{pc}$ is the height of the principal (chief) ray of the most oblique pencil in the plane of the centre of curvature of the mirror, it can be seen that this quantity will be zero if the stop position coincides with that of the plate representing the spherical mirror, and non-zero as the stop moves away from the plate. As can be seen from figure 2.2.1, $y_{pc}$ is directly proportional to $x$, the axial distance from the stop to the plate representing the mirror, so following from equation 2.22 we have the following proportionalities:

$$\begin{aligned} \text{Coma} &\propto xW \\ \text{Astigmatism} &\propto x^2W \end{aligned} \tag{2.23}$$

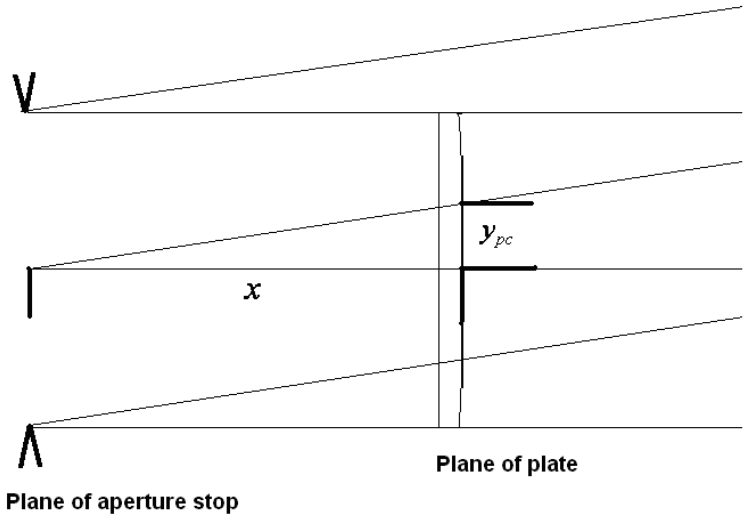


**Figure 2.2.1. As the plate is moved axially away from the stop, the height of the intercept of the principal ray of the most oblique pencil with the plate, $y_{pc}$, grows in direct proportion to the axial separation of the plate and the stop, $x$.**

A conicoidal mirror can be thought of as consisting of two plates. One plate represents the vertex sphere as described above, and the other plate represents the primary wavefront spherical aberration induced by the aspheric departure, given by:

$$W_{Conicoid} = \frac{kc^3 y_c^4}{4}. \tag{2.24}$$

Here $k$ represents the conic constant of the conicoid. The conic constant, first introduced by Schwarzschild (1905-1), is given by $k = -e^2$, where $e$ is the eccentricity of the conic section that is rotated about its axis to produce the conicoid. This plate lies on the pole of the conicoid mirror. Coma and astigmatism introduced by this plate arise exactly as for the spherical mirror as described in equation 2.22.

For multiple-mirror telescope systems the positions of the plates are determined by imaging the centre of curvature of spherical mirrors (or vertex spheres) and mirror poles in the case of conic contributions, into infinite conjugate space through all preceding elements in the system. Figure 2.2.2 gives an example of the Plate Diagram for a Paul three-mirror anastigmat.

With plate strengths and distances from the entrance-pupil evaluated for multiple mirrors it is a simple matter to determine the aberration condition of a

multi-mirror system. The primary wavefront aberration contributions from each mirror are simply additive, so for a system of $N$ plates, the system sum for spherical aberration can be given as:

$$\text{Spherical aberration}_{\text{SYS}} = \sum_{i=1}^{n} W_i. \tag{2.25}$$

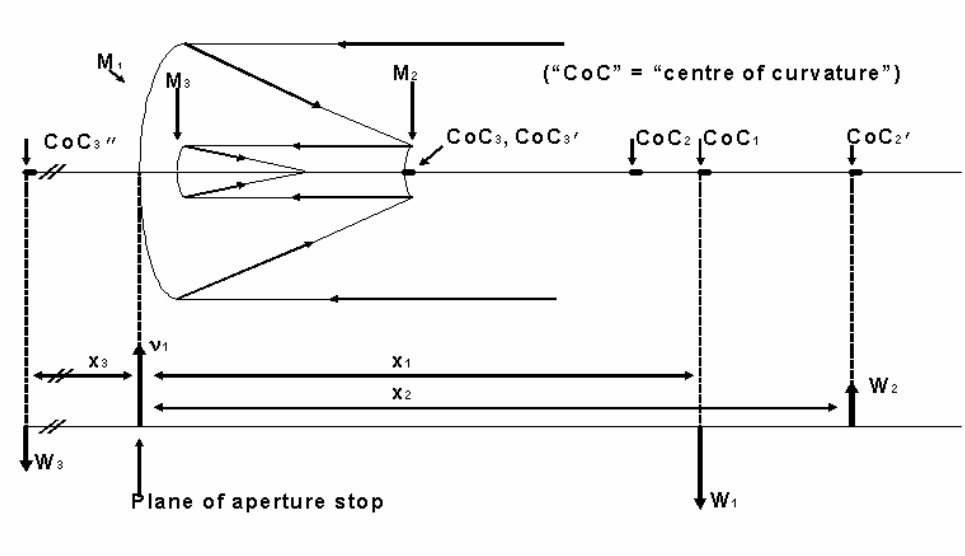


**Figure 2.2.2. Plate Diagram for a Paul three-mirror anastigmat. The primary mirror is a paraboloid giving rise to two plates, $W_1$ from the vertex sphere and $\nu_1$ from the conic departure. Note that the plates are of equal magnitude and opposite sign, consistent with the fact that the paraboloid has no spherical aberration. The plate representing the spherical secondary mirror, $W_2$, is in object space at $CoC_2$, the image of the centre of curvature of the secondary mirror through the primary. Similarly the plate representing the spherical tertiary mirror, $W_3$ is at $CoC_3$'', the image of the centre of curvature of the tertiary mirror through the secondary, then the primary. Note that $W_2$ and $W_3$ are also equal in magnitude and opposite in sign, so the system spherical aberration is zero. Using the Plate Diagram it is a simple matter to prove that system sums for coma and astigmatism are also zero. See also the description of this "Mersenne-Schmidt" system given in the introduction.**

Following from equation 2.23, sums linearly proportional to the system totals of coma and astigmatism are given by:

$$\begin{aligned} \text{Coma}_{\text{SYS}} &\propto \sum_{i=1}^{n} x_i W_i, \\ \text{Astigmatism}_{\text{SYS}} &\propto \sum_{i=1}^{n} x_i^2 W_i. \end{aligned} \tag{2.26}$$

In seeking anastigmatic systems, the goal is to drive these aberrations to zero, so only relative quantities are required. The extra step of calculation required in finding actual system sums for coma and astigmatism is not necessary.

In the case of four spherical mirrors there are four plates, one for each of the mirrors. If the height of the marginal paraxial ray on the primary mirror is $y_1$ and the reciprocal of the radius of the primary is $c_1$, then the plate strength, $W_1$, of the plate replacing the primary mirror is given by equation 2.17. Subsequent mirrors in the system will not in general be in collimated light so the plate strengths of these mirrors can be found using equation 2.16.

Without loss of generality we can fix the radius of the primary mirror as 2 m (unit focal length) and the diameter as 0.4 m. Then, by equation 2.17, we have:

$$W_1 = 0.00005\,\mathrm{m}. \tag{2.27}$$

The plate equations 2.25 and 2.26 can now be formulated as a system of simultaneous equations:

$$\begin{aligned} 0.00005\,\mathrm{m} + W_2 + W_3 + W_4 &= 0 \quad (\text{spherical aberration}) \\ 0.00005\,\mathrm{m} \times x_1 + W_2 x_2 + W_3 x_3 + W_4 x_4 &= 0 \quad (\text{coma}) \\ 0.00005\,\mathrm{m} \times x_1^2 + W_2 x_2^2 + W_3 x_3^2 + W_4 x_4^2 &= 0 \quad (\text{astigmatism}). \end{aligned} \tag{2.28}$$

An interesting step at this point is the key to solving these equations. The position of the entrance-pupil is of fundamental importance to the plate equations, as all $x_i$ are measured from this. If we now state that the aperture stop for the system lies at the centre of curvature of the quaternary mirror we can immediately simplify the coma and astigmatism equations in 2.28, as $x_4$ will be zero.

Here it is important to take note of the Stop Shift Theorem (Schwarzschild 1905-1). The Stop Shift Theorem orders the four Seidel aberrations spherical aberration, coma, astigmatism and distortion by the power to which the changes in the quantities of different types of aberrations that are contributed to a system by a spherical optical element are dependent on the position of the aperture stop. It can be shown that the change in spherical aberration is independent of this position, the change in coma is linearly proportional, the change in astigmatism is quadratically proportional and the change in

distortion is cubically proportional to the change in aperture stop position. Disregarding distortion, equations 2.25 and 2.26 imply this. The Stop Shift Theorem also shows that if the system sums for "lower ranked aberrations", using the ranking by dependence on aperture stop position described above, are zero, then the zero system sums of all of these lower ranked aberrations, and also the quantity of the lowest ranking of system aberration that is non-zero, will be independent of stop position. Therefore, the corrected spherical aberration, and uncorrected coma in a Newtonian telescope are independent of stop position, as are the corrected spherical aberration and coma and uncorrected astigmatism in a Ritchey-Chrétien system. Also, the system sum for distortion in an anastigmatic system will be independent of stop position, but more importantly for the work presented in this thesis, so will the system sums for spherical aberration, coma and astigmatism.

It is important to note that while setting the position of the aperture stop is a necessary step in the formulation presented here, the resultant anastigmat is not limited by this; the position of the aperture stop can be set anywhere in the system without disturbing the correction of an anastigmatic system.

Setting $x_4$ to zero, the coma and astigmatism equations in 2.28 can be rearranged to give:

$$W_3 x_3 = -W_2 x_2 - 0.00005\,\mathrm{m} \times x_1, \text{ and} \tag{2.29}$$

$$W_3 x_3^2 = -W_2 x_2^2 - 0.00005\,\mathrm{m} \times x_1^2. \tag{2.30}$$

At this point two further simplifications are made. Firstly the entrance-pupil position is set, and it can be set to any point in object space. By definition, the entrance-pupil position is the image in object space of the system aperture stop, which has been set at the yet-to-be-located centre of curvature of the quaternary mirror. We are free to place the entrance-pupil anywhere in object space because at this point the secondary and tertiary mirrors are undefined.

If we define the entrance-pupil position as the axial distance from the pole of the primary mirror, and give it the symbol $\varepsilon$, we can immediately evaluate $x_1$ (which is simply $\varepsilon - R_1$, where $R_1$ is the radius of curvature of the primary mirror). At this point we also assign arbitrary values to $t_1$, the separation of primary and secondary mirrors, and $c_2$, the curvature of the secondary mirror. With these, $W_2$ and $x_2$ can be calculated using 2.16 and standard relationships in paraxial optics to calculate the required values for $i_2, y_2$ and $x_2$. Now the right-hand sides of equations 2.29 and 2.30 can be completely evaluated.

This allows us to calculate $W_3$ and $x_3$ by first dividing equation 2.30 by equation 2.29 to give $x_3$, and then dividing equation 2.29 by the newly-acquired value of $x_3$ to give $W_3$.

We now need to translate the plate quantities $x_3$ and $W_3$ back into optical-system constructional parameters. These are needed to determine the actual position of the centre of curvature of the quaternary mirror, and finally the curvature of the quaternary mirror. To proceed we rearrange equation 2.18 as follows:

$$W_3 = -\tfrac{1}{4} N_3 c_3 P_3^2 (u_3 - c_3 P_3)^2 \rightarrow -\tfrac{1}{4} N_3 c_3 P_3^2 (u_3 - c_3 P_3)^2 - W_3 = 0. \qquad (2.31)$$

Here $u_3$ is the angle that the marginal paraxial ray from the secondary to the tertiary mirror makes with the optical axis and $P_3$ is the length of the perpendicular to this ray from the centre of curvature of the tertiary mirror. Equation 2.31 is cubic in $c_3$ and as all other quantities in equation 2.31 can be obtained from standard paraxial relationships, $c_3$ can immediately be evaluated. Analytical expressions for the solutions for the general cubic equation:

$$a_0 + a_1 x + a_2 x^2 + x^3 = 0, \qquad (2.32)$$

can be given as:

$$SA = \frac{-a_2}{3} - \frac{\sqrt[3]{2}Y}{3\sqrt[3]{Z+Q}} + \frac{\sqrt[3]{Z+Q}}{3\sqrt[3]{2}}, \tag{2.33}$$

$$SB = \frac{-a_2}{3} + \frac{(1-i\sqrt{3})Y}{3\sqrt[3]{4(Z+Q)}} - \frac{(1+i\sqrt{3})\sqrt[3]{Z+Q}}{6\sqrt[3]{2}}, \tag{2.34}$$

$$SC = \frac{-a_2}{3} + \frac{(1+i\sqrt{3})Y}{3\sqrt[3]{4(Z+Q)}} - \frac{(1-i\sqrt{3})\sqrt[3]{Z+Q}}{6\sqrt[3]{2}}, \tag{2.35}$$

where,

$$Y = 3a_1 - a_2^2;\ Z = -27a_0 + 9a_1a_2 - a_2^3;\ Q = +\sqrt{4Y^3 + Z^2}. \tag{2.36}$$

Here $i = \sqrt{-1}$. With each of the three values of $c_3$ thus obtained, and the locations of the tertiary mirror set by imaging the plate position $x_3$ through the primary and secondary mirrors respectively, a different position of the centre of curvature of the quaternary mirror can now be calculated by imaging the position of the entrance pupil that was defined at an earlier stage back through the primary, secondary and tertiary mirrors. This determines the position of the centre of curvature of the quaternary mirror. With the system up to the tertiary mirror defined (three times, once for each solution to equation 2.31) the quantities $u_4$ and $P_4$ can be determined, and $W_4$ can be obtained from rearranging the spherical aberration equation in 2.28 and substituting in values for $W_3$ and $W_2$ obtained above to give :

$$W_4 = -(W_2 + W_3 + 0.00005\,\mathrm{m}). \tag{2.37}$$

Now it only remains to formulate a similar cubic to equation 2.31 and solve for $c_4$:

$$W_4 = -\tfrac{1}{4} N_4 c_4 P_4^2 (u_4 - c_4 P_4)^2 \rightarrow -\tfrac{1}{4} N_4 c_4 P_4^2 (u_4 - c_4 P_4)^2 - W_4 = 0. \tag{2.38}$$

Again, there will be three solutions to this cubic in $c_4$.

To summarize, for each point in the three-dimensional parameter space defined by $t_1, c_2$, and $\varepsilon$, there will be a total of nine geometrically distinct anastigmatic systems, arising from the nine possible combinations of the solutions to equations 2.31 and 2.38.

This completes the derivation of the constructional parameters of nine distinct four-spherical-mirror anastigmats for any given input values of $t_1, c_2$, and $\varepsilon$.

Using the method described above nine distinct anastigmatic solutions are obtained, because as we have seen, for each of the three values of $c_3$ there are three distinct values of $c_4$. These nine anastigmats can justifiably be thought of as belonging to geometrically distinct families; the remaining members of each family can be found by repeating the method described above for a large

number of different points, sampling the 3-space defined by $t_1, c_2$, and $\varepsilon$ with sufficient density so as to accurately map out the solution spaces. By solving for enough points in this parameter space the entire set of solutions for four-spherical-mirror anastigmats can be mapped with a large but not unmanageable amount of computing.

### *2.3 Extension to four-mirror systems containing one, two or three conicoid mirrors*

An exploration was made into the application of the Plate Diagram based method described above to systems which could be described as five, six or seven plate systems (four-mirror systems with one, two or three conicoid mirrors). The aim in this case was to start from a system with a first-order layout chosen for its desirable characteristics, for example, relatively low central obstruction, convenient focal plane location, reasonably sized optics and so on, and then to investigate what sort of systems could be obtained with decreasing numbers of mirrors from the original four-sphere system allowed to become conicoids.

In general, for a system of fixed spherical mirrors, allowing $N$ mirrors to have conicoid departures superposed on the original base spheres will allow for the correction of $N$ third-order aberrations, excluding Petzval curvature. This idea

is referred to by Wilson (2004e) as the "generalized Schwarzschild theorem", recognizing that Schwarzschild first pointed this fact out in 1905 (Schwarzschild 1905-2).

Starting from a chosen base system of four spherical mirrors, this investigation has looked at rendering the system anastigmatic with, at first, three conicoids and all base mirrors fixed in their original radii and positions, then with two conicoids and the curvature and position of the quaternary mirror free to vary, then finally with one conicoid and the radius and position of both tertiary and quaternary mirrors free to vary. By choosing spacing and radii variables to be as close to the focal plane (close in terms of their sequential order) as possible, the disturbance to the baseline first-order layout is minimized.

### *2.3.1. Three conicoid mirrors*

In the first case considered here, three mirrors are allowed to become conicoids and conic constants are found that simultaneously zero spherical aberration, coma and astigmatism. This is a trivial exercise in a modern ray-tracing program but the Plate Diagram approach is included here as an example.

With the radii and positions of the four mirrors set we can immediately calculate plate strengths and positions for the plates representing the four

baseline spheres in object space using equations 2.16 or 2.17 and simple paraxial optics. Setting the position of the entrance pupil to any convenient location allows us to calculate $x_i$ and hence system sums for spherical aberration, coma and astigmatism arising from the baseline system, following equations 2.25 and 2.26:

$$\begin{aligned} \text{spherical}_{\text{SYS}} &= \sum_{i=1}^{n} W_i \\ \text{coma}_{\text{SYS}} &\propto \sum_{i=1}^{n} x_i W_i \\ \text{astigmatism}_{\text{SYS}} &\propto \sum_{i=1}^{n} x_i^2 W_i . \end{aligned} \tag{2.39}$$

As mentioned earlier, the coma and astigmatism "sums" are only proportional to the actual values for coma and astigmatism, but as these quantities are being used to drive the final system sum to zero that does not matter. To obtain the necessary combination of conicoids required for anastigmatic correction it is simply a matter of formulating and solving the following linear system of plate equations for $W_{ki}$, using standard paraxial optics relationships to determine the fixed values of $x_{ki}$ and placing the system sums from equation 2.39 on the *RHS*:

$$\begin{aligned} W_{k2} + W_{k3} + W_{k4} &= -\text{spherical}_{\text{SYS}} \\ x_{k2}W_{k2} + x_{k3}W_{k3} + x_{k4}W_{k4} &= -\text{coma}_{\text{SYS}} \\ x_{k2}^2W_{k2} + x_{k3}^2W_{k3} + x_{k4}^2W_{k4} &= -\text{astigmatism}_{\text{SYS}} \end{aligned} \tag{2.40}$$

Once the $W_{ki}$ are thus determined, $k_2, k_3$ and $k_4$ can be obtained by rearranging and evaluating equation 2.24 for each case. The subscripts $k_2, k_3$ and $k_4$ refer to the fact that in the example given here the primary mirror remains spherical and conicoids are sought for the secondary, tertiary and quaternary mirrors. In practice any of the four mirrors could have been chosen to remain spherical without any further complication.

While this case was relatively trivial, the next case, which departs from the generalized Schwarzschild theorem in that two conicoids are being used to correct three aberrations, is somewhat more interesting.

### *2.3.2. Two conicoid mirrors*

Here the position of and curvature of the quaternary mirror are also being allowed to vary. In this way four variables, two conic constants, one position and one surface power, are being used to solve for three aberrations. The result is that the solutions form a set that can be mapped as a 1-dimensional curve in some 2-parameter space.

In this example two mirrors, the primary and quaternary mirrors, will remain strictly spherical. This is only one of six possible arrangements of two conicoids amongst four mirrors, but serves as a representative example. The secondary and tertiary mirrors are allowed to be conicoids. To achieve anastigmatic correction the position and curvature of the quaternary mirror must be varied. In this case we will start with the primary, secondary and tertiary mirrors retaining some arbitrary but promising first-order layout. We then will solve for the position and radius of the quaternary mirror.

To proceed we imagine that the aperture stop is placed at the centre of curvature of the quaternary mirror. Also, we assign some arbitrary position to the entrance pupil, which after imaging through primary, secondary and tertiary mirrors, will locate the centre of curvature of the quaternary mirror. In this way, the coma and astigmatism equations in 2.40 are reduced to:

$$\begin{aligned} x_{k2}W_{k2} + x_{k3}W_{k3} &= -\text{coma}_{\text{SYS}} \\ x_{k2}^2W_{k2} + x_{k3}^2W_{k3} &= -\text{astigmatism}_{\text{SYS}} \end{aligned} \tag{2.41}$$

That is, only contributions from the two conicoids provide variables to balance against system coma and astigmatism; by placing the stop on the centre of curvature of the quaternary mirror the $x_4$ value for the plate associated with this mirror is now zero so its coma and astigmatism contributions are necessarily zero. Note that here $\text{coma}_{\text{SYS}}$ and $\text{astigmatism}_{\text{SYS}}$ are values calculated from the

spherical primary and vertex spheres of the secondary and tertiary mirrors. Values of $x_{ki}$ can be obtained and equations 2.41 can be used to solve for $W_{ki}$ and hence, by re-arranging equation 2.24, for $k_2$ and $k_3$. Using the values of $W_{ki}$ thus obtained we can now solve for the spherical aberration contribution of the quaternary mirror by rearranging the spherical aberration equation in equations 2.4 (and substituting $W_{\text{quat}}$ for $W_{k4}$ in this case):

$$W_{\text{quat}} = -spherical_{\text{SYS}} - W_{k2} - W_{k3}. \tag{2.42}$$

Now we have the position of the centre of curvature of the quaternary mirror (from setting the initial position of the entrance pupil) and the spherical aberration contribution of the quaternary mirror from equation 2.42. Also, by simple paraxial optics we can obtain $u_4$, the angle the marginal ray of the axial paraxial pencil makes with the axis after reflection from the tertiary. We can also calculate the quantity *P*, which from figure 2.1.1 is the length of the perpendicular from the centre of curvature of the quaternary mirror to the marginal ray of the axial paraxial pencil after reflection from the tertiary mirror. Using these, and equation 2.38, we can solve the resultant cubic equation in $c_4$ (the curvature of the quaternary mirror).

Using these three solutions, for each initial position of the entrance pupil (and therefore the position of centre of curvature of the quaternary mirror) we obtain a maximum of three distinct anastigmatic telescopes. These telescopes differ only in the position and curvature of the quaternary mirror (and hence in other related parameters such as focal ratio, Petzval curvature and central obstruction). It remains to scan through the available solution space, there will be three solutions for each initial choice of entrance pupil position. By plotting some system parameter, such as $c_4$, against the position of the image of the centre of curvature of the quaternary mirror in object space (which was the original position of the entrance pupil for the system) we can build up three curves representing available solutions.

Note also that while the position of the aperture stop and hence entrance pupil was set initially to reduce the number of unknowns in equations 2.40, once an anastigmatic system is achieved the aperture stop can be moved to any convenient location without affecting the anastigmatic correction, as given by the stop shift theorem.

### *2.3.3. One conicoid mirror*

In this final example we look at the case in which there is one conicoid mirror and three spheres. While in this case the secondary mirror has been chosen to

be the conicoid, the method described below is readily adapted to accommodate any choice of mirror as the conicoid. The primary and secondary mirrors can be imagined to have the same characteristics and positions as in the system considered in 2.3.1 and 2.3.2. Now the curvatures and positions of the tertiary and quaternary mirrors are varied to solve for anastigmats. The first step is similar to that described in the previous section 2.3.2. As in the previous example, the initial position of the aperture stop is chosen to eliminate one set of variables from the plate equations. In this case placing the aperture stop at the pole of the secondary mirror prevents the plate associated with the conic constant of the secondary mirror from having any effect on the coma or astigmatism of the system. Now we can form the following equations:

$$\begin{aligned} x_{\text{tert}}W_{\text{tert}} + x_{\text{quat}}W_{\text{quat}} &= -(x_{\text{prim}}W_{\text{prim}} + x_{\text{sec}}W_{\text{sec}}) \\ x_{\text{tert}}^2W_{\text{tert}} + x_{\text{quat}}^2W_{\text{quat}} &= -(x_{\text{prim}}^2W_{\text{prim}} + x_{\text{sec}}^2W_{\text{sec}}). \end{aligned} \tag{2.43}$$

Here “prim, “sec”, “tert” and “quat” refer to quantities derived from the spherical primary through quaternary mirrors respectively (or vertex sphere in the case of the conicoid secondary mirror). The upper equation is the condition for zero coma and the lower equation is the condition for zero astigmatism. Quantities on the RHS are known. To proceed further we assign values to $t_2$,

the separation of the secondary and tertiary mirrors and $r_3$, the radius of the tertiary mirror, from which we can calculate $x_{\text{tert}}$ and $W_{\text{tert}}$.

Moving all known quantities in the above equations to the RHS, and dividing the astigmatism equation by the coma equation from equations 2.43 gives:

$$x_{\text{quat}} = \frac{x_{\text{prim}}^2 W_{\text{prim}} + x_{\text{sec}}^2 W_{\text{sec}} + x_{\text{tert}}^2 W_{\text{tert}}}{x_{\text{prim}} W_{\text{prim}} + x_{\text{sec}} W_{\text{sec}} + x_{\text{tert}} W_{\text{tert}}}, \tag{2.44}$$

from which we obtain:

$$W_{\text{quat}} = -\frac{(x_{\text{prim}} W_{\text{prim}} + x_{\text{sec}} W_{\text{sec}} + x_{\text{tert}} W_{\text{tert}})}{x_{\text{quat}}}. \tag{2.45}$$

Now that all $W_i$ are known apart from the one associated with the conicoid, we can solve for the conicoid using the spherical aberration plate sum equation 2.39 and a rearranged 2.24:

$$k_2 = \frac{-4}{c_2^3 y_2^4}(W_{\text{prim}} + W_{\text{sec}} + W_{\text{tert}} + W_{\text{quat}}). \tag{2.46}$$

It is interesting to note that in the above derivation the necessary spherical aberration contribution from the quaternary mirror is defined before the radius or position of the quaternary mirror is determined. The final remaining step is

to solve for the radius and position of the quaternary mirror, which is done exactly by deriving necessary paraxial quantities and formulating and solving equation 2.38. As in the previous case, this leads to three distinct systems, this time for each choice of the starting values $t_2$ and $c_3$. Again, as in the previous case, each of the three exact algebraic solutions to equation 2.38 can be evaluated independently for a large number of initial values of the parameters $t_2$ and $c_3$. In this way a map of the solutions can be built up over this 2-parameter space for solutions SA, SB and SC.

In these maps anastigmats that are physically impossible can be filtered out, and there is also the opportunity to write custom filters targeting systems with particular characteristics, for example sizes of mirrors, space envelope, central obstruction etc. Approaches to filtering the large solution sets obtainable by applying the methods described in sections 2.2 and 2.3 will now be discussed.

### *2.4 Techniques for filtering solution sets*

The methods described in sections 2.2 and 2.3, with one exception, produce one, two or three dimensional solution sets of anastigmatic systems. The basis vectors for these solution sets are certain system constructional parameters, such as mirror separations, curvatures or conic constants. While it is true that in the methods discussed in the sections above there are always anastigmatic

solutions for each point in the specified parameter space, there is no guarantee that these solutions are physically valid.

For example solutions SA, SB or SC from equations 2.33, 2.34 and 2.35 respectively may have imaginary components. In this case the solutions do not give physically-realizable anastigmatic systems. It is also possible for real solutions to be physically invalid if they require mirrors or the focal plane to occupy virtual spaces (the word "virtual" is used here in the sense of optical imaging). Solutions with all-real components may still be uninteresting because of excessively large optical elements or mirror separations. These systems can also suffer from total, or at least, unacceptably high, self-obstruction.

In the general approach described in preceding sections, points in the relevant parameter space are iteratively sampled with a relatively high density. At each sampled point the relevant analytical solution for an anastigmatic reflecting system is applied, and for systems not containing imaginary components in some part of their solutions, all system constructional parameters are evaluated. Once the system constructional parameters are obtained the system can be screened with logical operators in the program. For example, airspaces can be checked for sign, and systems containing airspaces requiring virtual

mirrors for example can be rejected. Similarly, upper and/or lower limits can be set on acceptable mirror separations, mirror sizes etc.

The filters described so far are trivial to implement in practice. A more complicated example of filtering arises when we try to control the central obstruction. To calculate the central obstruction of a four mirror system an approach has been adopted here that first sorts systems by the relative arrangement of all of the mirrors and of the focal plane, and then to assign two rays, one a marginal ray of the axial pencil, and one an axial pencil ray that is selected to lie at some height between the axis and the marginal ray. These rays are traced through the system and for each portion of their path through the system, for example, from the object to M1, then from M1 to M2, from M2 to M3, from M3 to M4 and from M4 to the focal plane, checks are made to see whether or not the beam encompassed by the two selected rays will be obstructed by any of the mirrors, or the focal plane if applicable, that lie in that portion of the path.

If we label the primary through quarternary mirrors as 1 through 4 and the image space as 5, then a 5-digit number comprised of these five numerals can be used to categorize the system according to the order that the optical components are arranged. For example, with incident collimated light traveling from left to right, a system designated “21435” would be a system in

which the order of placement of elements from left to right would be secondary mirror, primary mirror, quaternary mirror, tertiary mirror and focal plane. An example of a 45231 system is given in figure 2.4.1.

It turns out that there are 16 possible permutations of the "order of occurrence" of four mirrors and focal plane in valid four-mirror imaging systems. Using the system described above, these can be represented by the following sets of digits:

21435, 21453, 24513, 24153, 24135, 24531, 24351, 24315, 45213, 42513, 42153, 42135, 45231, 42531, 42351 and 42315.

This classification system can be useful. For example, when designing microscope objectives it would make sense to limit the investigation to systems with "5" as the last digit, representing systems for which the "image" was beyond all of the optics (though for a microscope objective the "image" here would typically be the object and the image space would have the infinite long conjugate).

To apply a filter to remove systems with unacceptable central obstruction, a system having passed successfully through the other filter processes described above, is then sorted into one of the sixteen possible categories of element arrangement. For each different arrangement, there are now known potential

obstructions for each portion of the optical path through the system, and appropriate calculations can now be made to check whether or not appropriate components impinge on the beam over each of these portions.

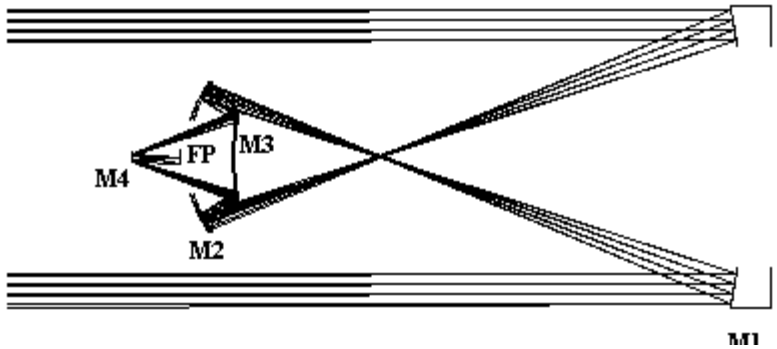


**Figure 2.4.1. Classification based on the order of optical components. In the classification system described in the text this system would be described as a "45231" system.**

# 3. Results: Four spherical mirrors with no element larger than the entrance pupil

It is interesting to note at this point that of the three four-plate systems referred to in the introduction, the two-conicoid mirror solutions lie along a curve in 2-parameter space (figure 3.1) and the three-mirror, one conicoid solutions lie in 2-dimensional regions (figure 3.2). Now we have four-spherical-mirror solutions occupying 3-dimensional solution spaces (figure 3.3). While in each case there are four plates involved, in the case of systems with conicoid mirrors the two plates representing the conicoid have an extra element of coupling which effectively reduces the dimensionality of the solution space.

As described in section 2.4, solutions from the initial "unfiltered" solution set, as depicted in figure 3.3, are not necessarily physically-realizable anastigmats. Physically-unrealizable solutions fall into two categories. In one, the solution involves at least one mirror located in a virtual space. Also, any solutions with imaginary components will not be physically-realizable anastigmats.

The plot in figure 3.2 shows an example of an unfiltered solution-set map, in this case for three-mirror anastigmats with two spherical mirrors. In this map gray areas represent physically-unrealizable solutions, while white and black regions are possible anastigmats with positive and negative Petzval curvature respectively. While a large range of different system metrics could be plotted for the valid solutions, the Petzval curvature has been chosen in this case to allow for the ready identification of flat-field solutions.

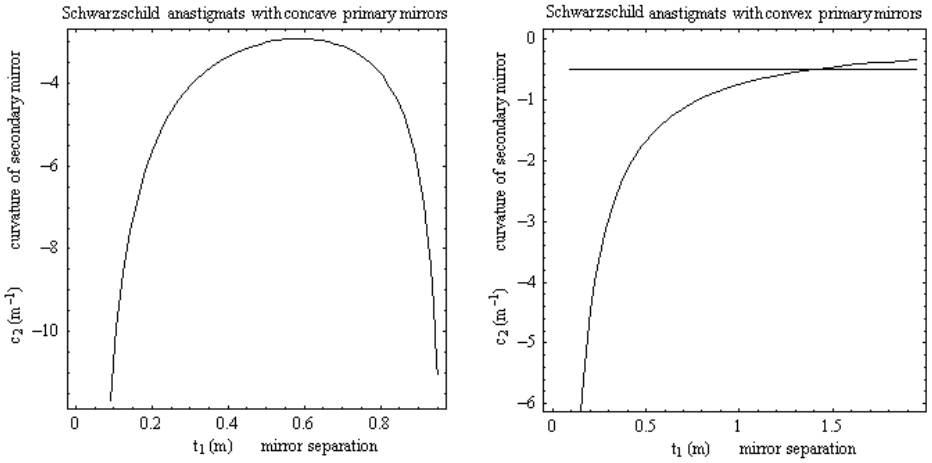


**Figure 3.1. These two plots represent the complete solution set for two-mirror or Schwarzschild anastigmats. In both cases the primary mirror has been set with a focal length of +/- 1 m (so $c_1$ = +/- 0.5 $m^{-1}$). In both cases the secondary mirrors are concave. The horizontal line in the right-hand plot intersects the solution curve at the point representing a flat-field anastigmat. In both cases the mirrors are, in general, conicoids.**

The mapping of four-spherical-mirror anastigmat sets has now been carried out. Of the nine distinct families of solution, four were empty sets when physically-unrealizable solutions were filtered out. The remaining five solution

sets contain a large amount of data. Figure 3.3 is an example of several cross sections of one of these as defined for figures 3.1 and 3.2. As in figure 3.2, gray areas represent physically-unrealizable solutions, and white and black regions represent solutions with positive and negative Petzval curvature respectively.

Once a set of physically-realizable solutions has been achieved, the physically-realizable set represents the complete range of possible solutions, and is thus a truly global solution set. Nevertheless, various conditions for practicality can be used to further refine the set.

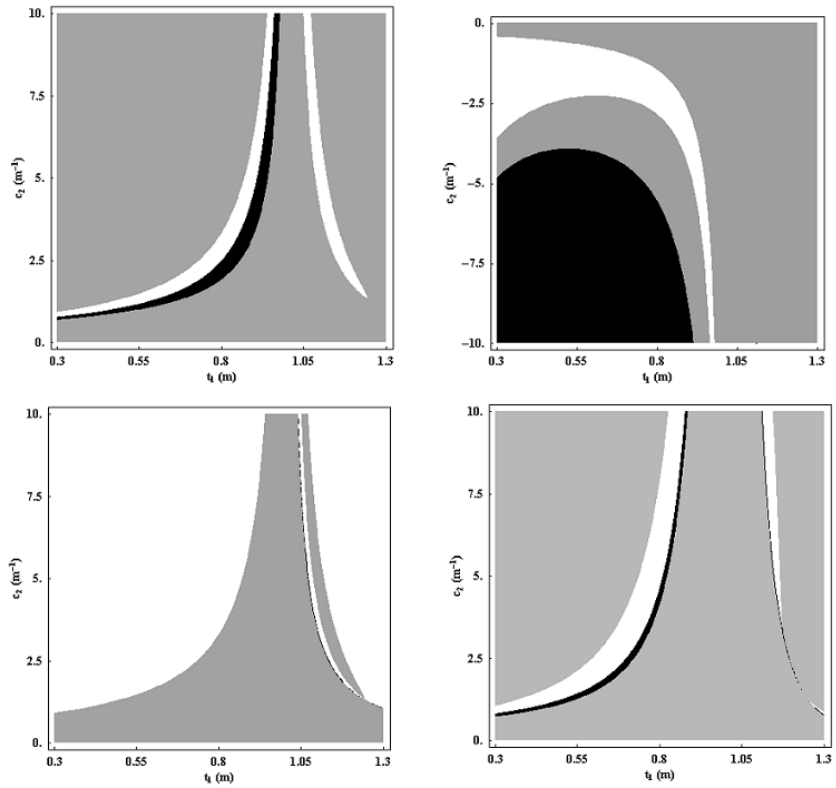


**Figure 3.2. These plots are four out of the seven plots representing the complete solution set for three-mirror anastigmats with two strictly spherical mirrors. In these plots solutions with positive Petzval curvature are plotted white and solutions with negative Petzval curvature are plotted black (grey points correspond to non-physical solutions). Hence flat-field solutions lie along loci where black and white regions abut. Clearly there are 4 families of flat-field three-mirror anastigmat with two spherical mirrors: only one of these appeared in the literature prior to Rakich (2001).**

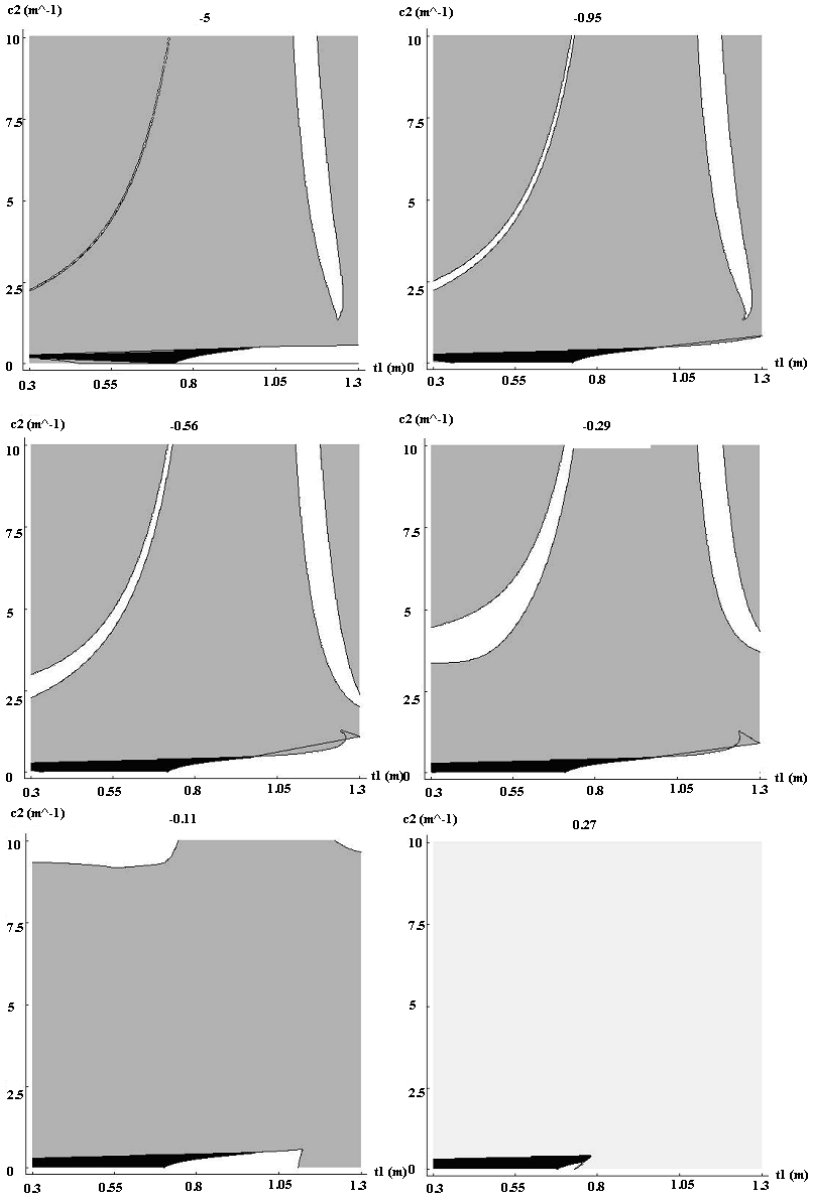


**Figure 3.3. A number of cross sections taken from one of the five solution families for four-spherical-mirror anastigmats with concave primary mirrors. The horizontal and vertical axes represent $t_1$ and $c_2$ respectively. The number in the centre top of each plot is related to $\varepsilon$, the initial position of the entrance-pupil, for each cross section. White points represent solutions with positive Petzval curvature, black points systems with negative Petzval curvature. Flat field solutions lie along curves where white regions abut black regions.**

Possible impracticalities include mirrors with huge diameters, large inter-mirror distances, and large or complete self-obstruction by system elements. Removing such systems from consideration is achieved by writing "filters" into the program used to map the solution space, as described in section 2.4.

When further filtering is introduced to remove systems with unfeasibly large element spacing and diameters larger than the primary mirror, the number of populated solution sets for four-spherical-mirror anastigmats with no elements larger than the entrance pupil reduces from 5 to 2. It was initially reported that there were no such viable solutions with usefully-low central obstructions (Rakich, 2004), but recent automation of the search process for low-obstruction systems has produced useful systems (Rakich, 2007-2). These systems represent the viable systems when axially-symmetrical systems are considered. Figures 3.4-3.7 contain examples of both afocal and focal systems of each solution type. Table 3.1 gives corresponding design parameters. As a result of the analytical approach taken in this work it can now be stated with certainty that the sets of solutions represented by figures 3.4-3.7, and in table 3.1, are the only feasible all-spherical reflecting anastigmats with concave primary mirrors, in the case where no element is allowed to exceed the entrance pupil in diameter.

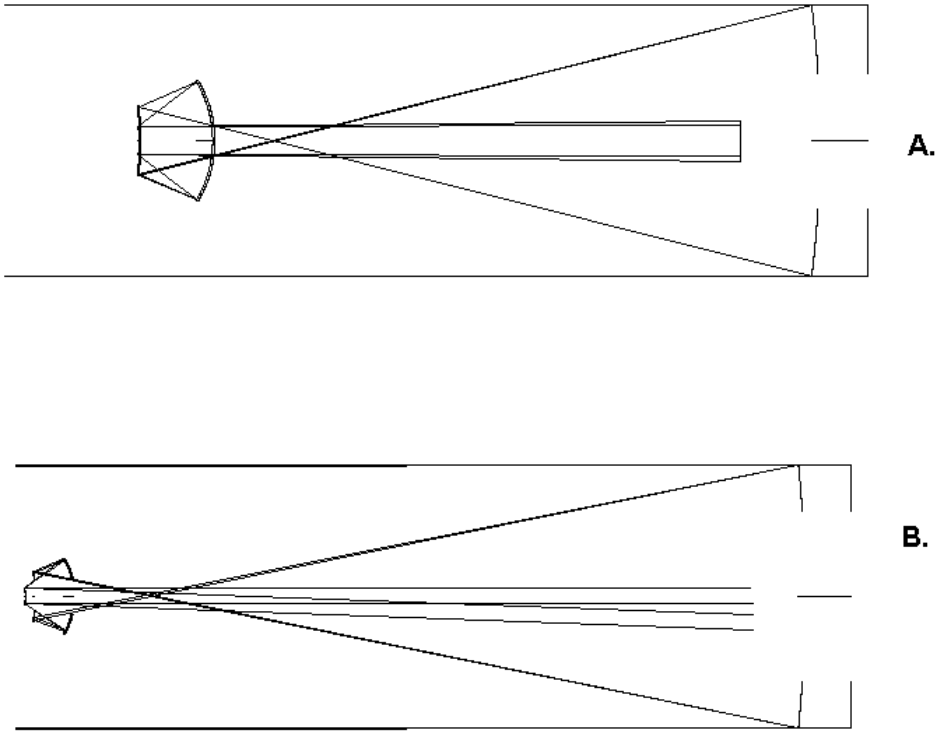


**Figure 3.4. Two afocal four-spherical-mirror anastigmats. System A is comprised of coupled pairs of two-concentric-spherical-mirror anastigmatic systems. The linear central obstruction of this system is 50%. System B is a more general version that can not be broken down into individually-anastigmatic sub-systems.**

The linear central obstructions of the systems presented here range from 50% to 75%. With 50% central obstruction, the afocal system in figure 3.4A represents the minimum possible central obstruction for the class of system under discussion. This fact has been determined by successively eliminating systems while reducing the central obstruction allowed until finally only one solution point remains out of the 3-dimensional solution space. For focal

systems of focal ratio less than f/15, the minimum-achievable linear central obstruction appears to be approximately 60% as represented by figure 3.5C.

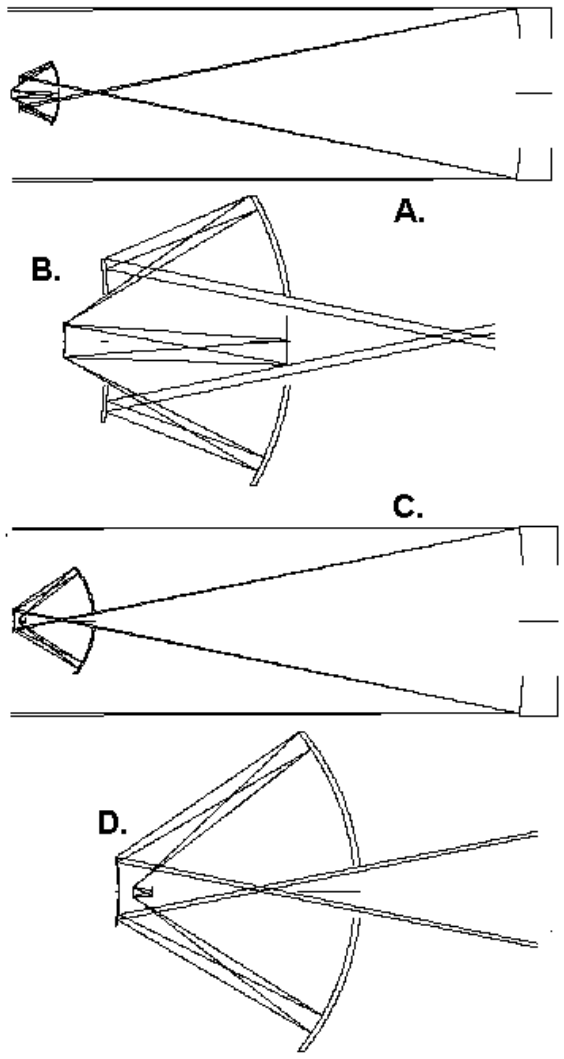


**Figure 3.5. Two examples of focal versions of the solution type shown in figure 3.4. Drawings B and D give an expanded view of the last three elements of systems A and C respectively. This solution type contains as special cases systems that are comprised of two pairs of concentric two-spherical-mirror anastigmats.**

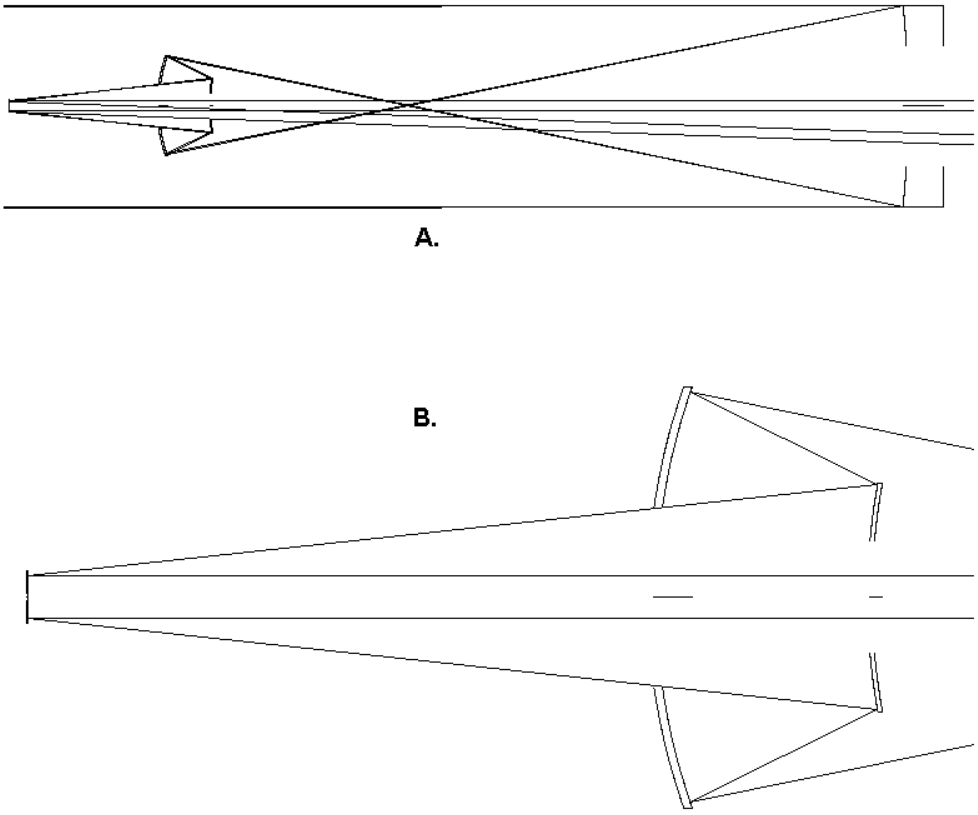


**Figure 3.6. An afocal four-spherical-mirror anastigmat of the second kind. Unlike the solutions of figures 3.4 and 3.5, this solution type has no special case that is comprised of coupled pairs of concentric mirrors. B above gives a close up view of the last three mirrors of the system in A.**

As can be seen in figures 3.4 and 3.5, this first solution family has convex secondary mirrors, concave tertiary mirrors, and convex quaternary mirrors. The second solution family represented by figures 3.6 and 3.7 has concave secondary mirrors and convex tertiary and quaternary mirrors. These systems have slightly higher central obstructions: around 70% linear central obstructions at best.

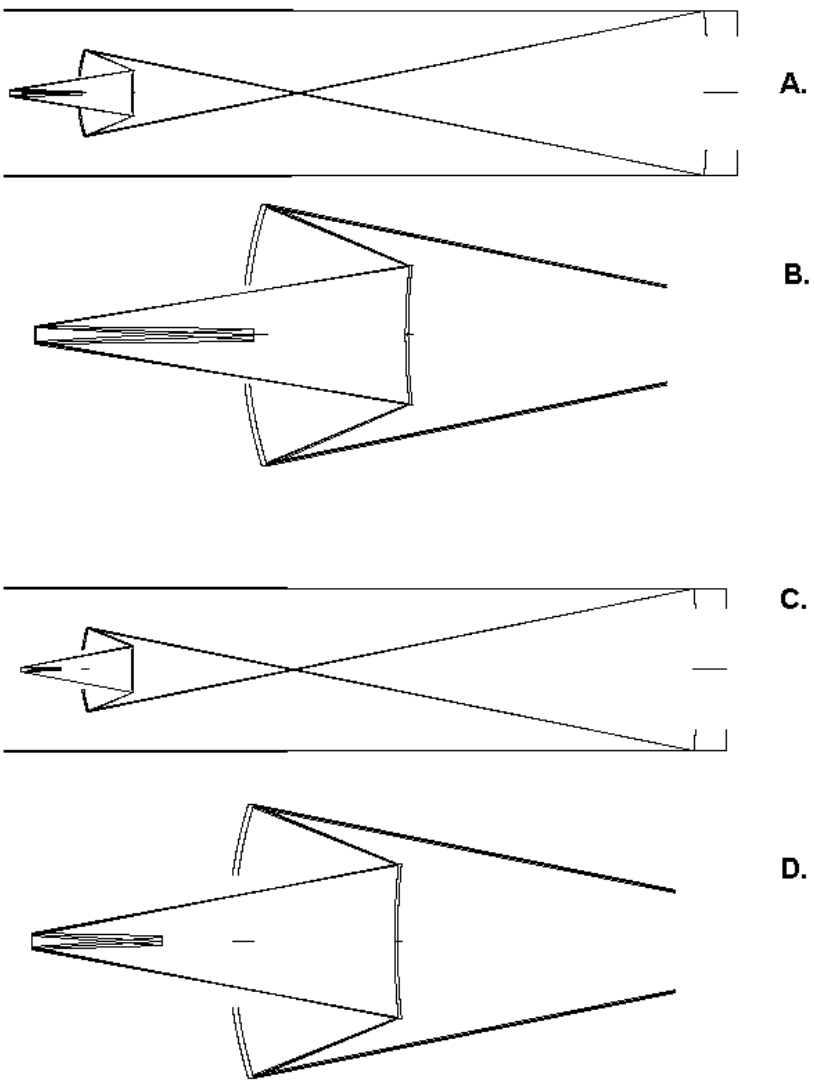


**Figure 3.7. Focal versions of the second type of solution as shown in figure 3.6. Drawings B and D give an expanded view of the last three elements of systems A and C respectively. There is a continuum of solutions with focal ratios ranging from the afocal case down to about f/8 (for the scale given for these systems). In practice the image could be picked off to a more convenient location with a fold mirror. This type of system in general suffers from less high-order aberration than the systems shown in figures 3.4 and 3.5. The minimum linear central obstruction achievable with this type of system is approximately 67%.**

| | 3.4.A | 3.4.B | 3.5.A | 3.5.C | 3.6 | 3.7.A | 3.7.C |
|---|---|---|---|---|---|---|---|
| **R1** | −1.61838 | −2 | −2 | −2 | −2 | −2 | −2 |
| **t1** | −1.0 | −1.17050 | −1.17050 | −1.09550 | −1.49005 | −1.52005 | −1.51005 |
| **R2** | −0.61838 | −0.40401 | −0.40818 | −0.12618 | 0.29939 | 0.35087 | 0.35087 |
| **t2** | 0.10615 | 0.05809 | 0.09052 | 0.16859 | 0.10022 | 0.12631 | 0.12058 |
| **R3** | −0.17129 | −0.11475 | −0.15052 | −0.18226 | 0.30119 | 0.47371 | 0.57943 |
| **t3** | −0.10595 | −0.07272 | −0.11237 | −0.15859 | −0.39783 | −0.29493 | −0.27074 |
| **R4** | −0.06545 | −0.04015 | −0.03536 | −0.01375 | −0.18985 | −0.09802 | −0.07472 |
| **t4** | ∞ | ∞ | 0.11148 | 0.01289 | ∞ | 0.17378 | 0.09704 |

**Table 1. System parameters for the systems depicted in figures 3.4-3.7. Units are metres. R1-R4 are the radii of the primary – quaternary mirrors. t1–t4 are inter-mirror or in the case of t4, the mirror-focal plane separation. In each case the aperture stop has been set at the primary mirror, though as these systems are anastigmats the stop position can be set anywhere without affecting the correction of the third-order aberrations. The stop diameter (and hence that of the primary mirror) has been set at 0.4 m in all cases.**

It is interesting to note that the system shown in figure 3.4.A is actually a system formed by coupling two pairs of concentric spherical anastigmats: the well known two-concentric-mirror anastigmat with convex primary mirror and the less well known two- concentric-mirror anastigmat with concave primary mirror that produces a virtual image. These pairs were discussed individually by Burch (1943-2) and Rosin (1968), and later, in combination to produce four-mirror systems, by Shafer (1978). It is surprising that Shafer did not propose the more fundamental on-axis systems presented here, despite

identifying both pairs of two-concentric-mirror anastigmats, and also proposing the concept of relaying the virtual image of the concave-primary-mirror version of the two-concentric-mirror anastigmat using either finite conjugate or afocal anastigmatic relay systems. Shafer, who was the first to present four-spherical-mirror anastigmatic systems, reported only off-axis systems, that is, systems in which both the central field angle and the entrance pupil were offset from the system axis.

Figure 3.4.B represents a version of the four-spherical-mirror afocal system that does not consist of individually-anastigmatic two-mirror pairs. Similarly, the focal family of solutions as illustrated in figure 3.5 contains, but is not limited to, solutions formed by pairs of individually-anastigmatic and concentric two-spherical-mirror systems.

Unlike the solutions in figures 3.4 and 3.5, the solutions in figures 3.6 and 3.7 do not have any versions that can be reduced to pairs of individually-anastigmatic two-mirror systems. There are no systems corresponding to these in the published literature.

It should be noted that all of these systems can be scaled in aperture without affecting their anastigmatic correction in the third-order aberration sense, though the magnitude of high-order aberration residuals will of course change with this scaling.

It should also be noted that, while these systems have valid correction in the "extended paraxial region", they do suffer from residual high-order aberration. The third-order solutions discussed here, and in many of the references provided in this work, are generally understood to be good starting points for design. Typically, high-order aberrations can be removed by optimization and either introducing high-order aspheric terms, or "tweaking" the various constructional parameters to reintroduce small balancing quantities of third-order aberration. An example of the latter approach is given in figures 3.8, 3.9 and table 2.

Other practical systems can still be extracted from the large number of solutions produced by this survey. There exist a number of systems within the solution set that are excluded because of self-obstruction when considered as axially-symmetrical systems, but that yield systems with small or even zero self-obstruction when off-axis or multi-axis systems are considered.

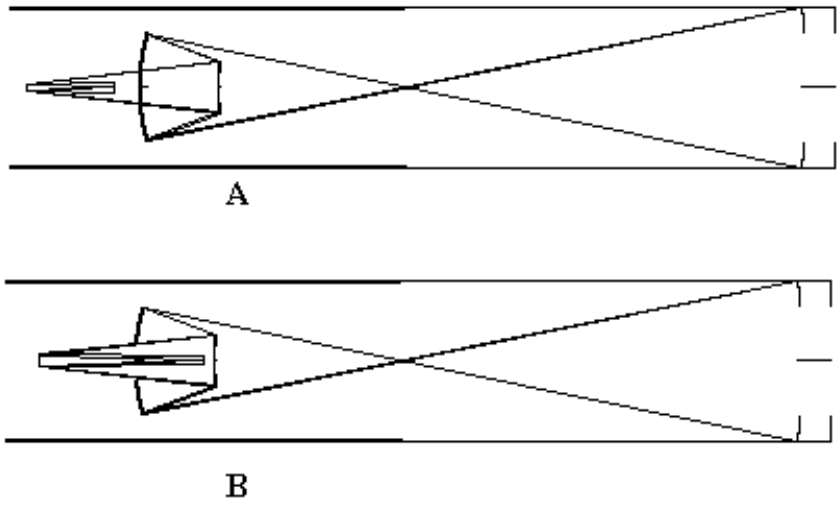


**Figure 3.8. An example of high-order aberration correction. System A is the layout of a third-order solution. If one starts from system A, creates a merit function in an optimization routine in optical design software that attempts to minimize the total residual RMS wavefront error and re-optimizes allowing the radii of all mirrors subsequent to the primary mirror to vary, along with some of the air-spaces, the result is shown in system B. In system B, 1076 nm of third-order spherical aberration, 95 nm of third-order coma and 82 nm of third-order astigmatism are balanced against the high-order residual aberrations in an optimal manner.**

| System | R1 | T1 | R2 | T2 | R3 | T3 | R4 | T4 |
|---|---|---|---|---|---|---|---|---|
| **3.8 A** | -2.0 | -1.67 | 0.4757 | 0.1945 | 0.5179 | -.4725 | -.1687 | 0.2117 |
| **3.8 B** | -2.0 | -1.67 | 0.4719 | 0.1941 | 0.4852 | -.4269 | -.4331 | 0.4154 |

**Table 2. Optical design data for the systems shown in figure 3.8. In both cases the system stop was set on the primary and the entrance pupil diameter was set at 0.4 m. All units are metres. System A has a focal ratio of f/15.0; system B has a focal ratio of f/13.3.**

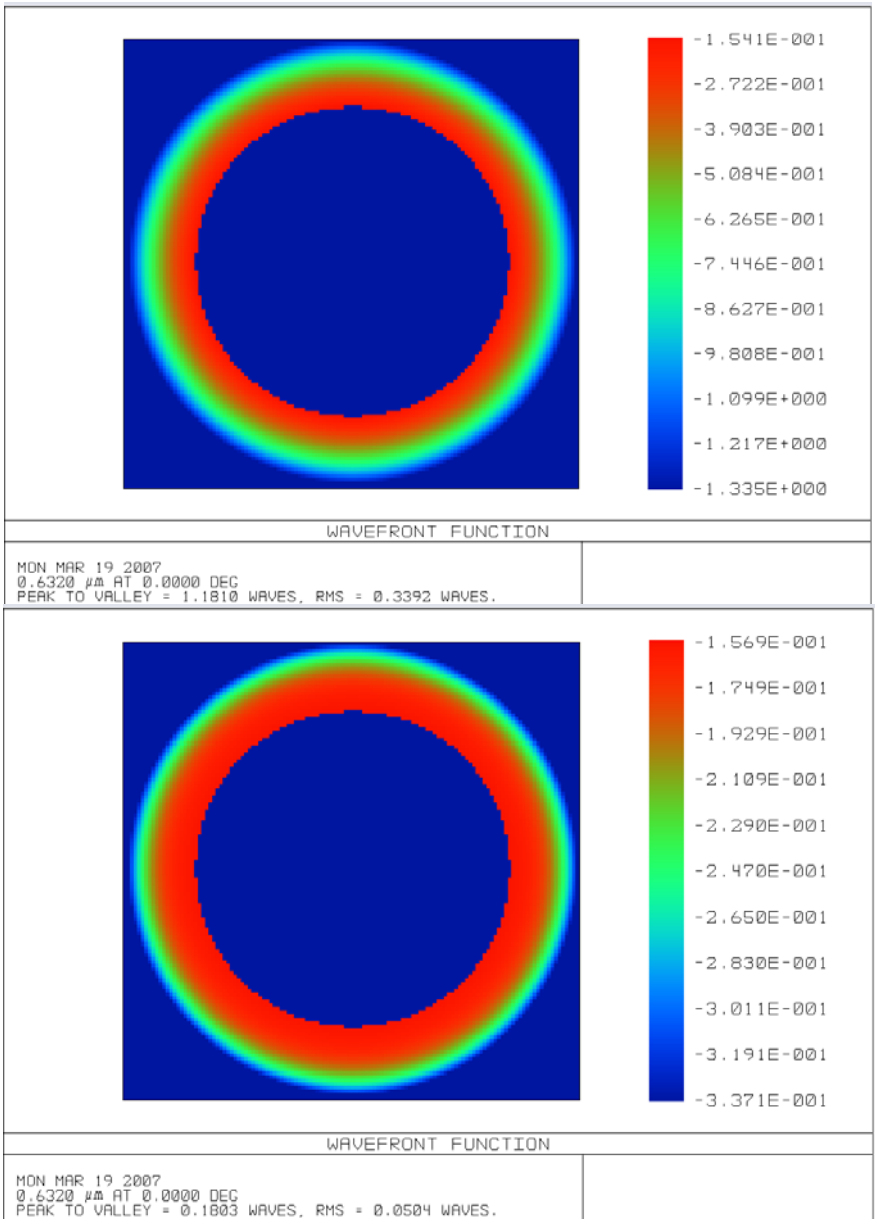


**Figure 3.9. On-axis WFE residuals, for the third-order solution from figure 3.8A (top), and the solution in which third-order aberration is reintroduced so as optimally to balance against high-order aberration from figure 3.8B (bottom). The total wavefront error in the system with high-order aberration taken into account is reduced by a factor of 6.7 from that of the third-order solution in this example.**

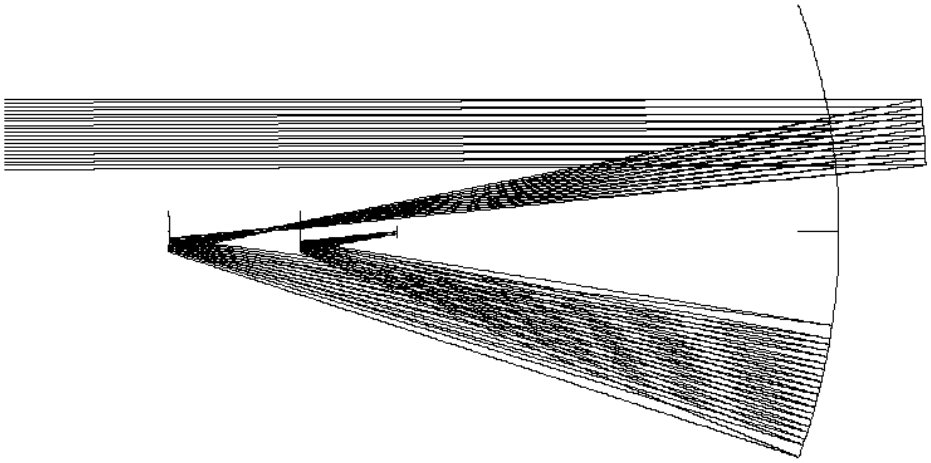

**Figure 3.10. An example of a four-spherical-mirror anastigmatic Schiefspiegler. Numerous examples of anastigmatic Schiefspiegler are presented in chapter 5.**

Figure 3.10 gives an example of one such Schiefspiegler system. In comparison to off-axis systems comprised of aspheric mirrors, there is a greatly reduced manufacturing and alignment difficulty associated with systems consisting of "off-axis" spherical mirrors, which of course remain spherical.

While "shiefspiegler" literally means "oblique mirror", and was originally used to describe systems comprised of tilted mirrors that could not be derived from axially-symmetrical parent systems (Kutter, 1953), it has come to mean reflecting telescope systems which are free from central obstruction. These can indeed be obtained by using mirrors that have been tilted with respect to the

optical axis. However the common usage of the term Schiefspiegler also includes unobstructed systems that are based on portions of parent systems that are symmetrical about some common axis.

An axially-symmetrical parent system can be rendered as a Schiefspiegler by using an off-axis portion of the pupil, or by using only a small range of field points surrounding some off-axis field point, or by a combination of both of these approaches. An interesting point to note about these Schiefspiegler systems is that because they are derived from axially-symmetric parent systems, the centres of curvature of the mirrors are collinear. This fact presents the opportunity for Schiefspiegler systems that can be brought into alignment with remarkable ease when compared to the general case. Numerous examples of Schiefspiegler systems will be given in chapter 5.

Also, systems with convex primary mirrors, while not deemed appropriate here for telescope systems, are still of interest for a variety of applications. A full discussion will be given of solutions in which elements are allowed to exceed the diameter of the primary mirror (which allows convex-primary-mirror solutions that were disqualified from the search presented above, as well as concave-primary-mirror systems with large secondary-quaternary optics) in chapter 5 below.

# 4. Results: Four-mirror anastigmats with useful first-order layouts and containing one, two or three conicoid elements

The results from chapter 3 are interesting, but it is unfortunate that the valid solution sets contain only a limited range of viable geometries. One way to obtain a wider range of potentially useful geometries is to introduce more degrees of freedom to the four-mirror system. As was discussed in section 2.3, with three more degrees of freedom introduced to the four-spherical-mirror systems, obtained by allowing three of the mirrors to become conicoids, any arbitrary geometrical arrangement of four mirrors can be rendered anastigmatic. Such a system would be a seven-plate system. While anastigmatic correction is easily obtained in this way, the advantage is lost of having a relatively simple optical system, with all-spherical surfaces that are much less difficult to fabricate and align than conicoids.

## *4.1 Three-conicoid solution*

Section 2.3 described how the Plate Diagram algebra developed for four spherical mirrors could be generalized to include one, two or three conicoid mirrors. Following below is an example of the methods described in section 2.3 applied to the system shown in figure 4.1.A.

In figure 4.1, system A is presented as a baseline system of four mirrors which has a potentially useful first-order layout and for which no attempt at third-order correction has yet been made. The large transverse aberration of the marginal rays is clearly visible at the focal plane. System B is identical to system A in its first-order properties, but now has in addition on three of its mirrors a conicoid term giving a departure from sphericity, with the conic constants chosen to render the system anastigmatic.

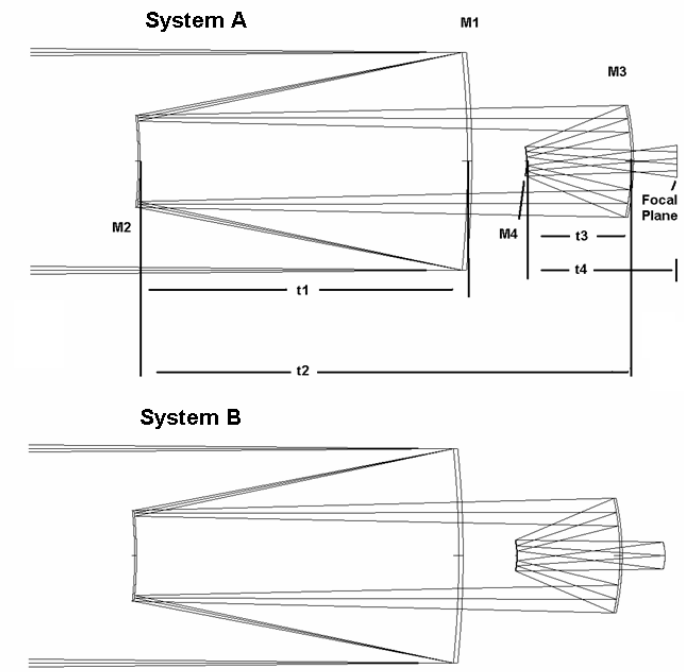


**Figure 4.1. System A represents an example of a potentially useful first-order layout of a four-spherical-mirror system. The system is not corrected for aberration and the aberration is clearly visible at the focal plane. System B represents the same system, but in this case the aberration has been removed by a suitable choice of conicoids for mirrors M2, M3 and M4.**

The method for deriving the required conic constants for these three mirrors is described in section 2.3.1. Table 3 gives optical parameters for the systems shown in figure 4.1.

### *4.2 Two-conicoid solutions*

The first "non-trivial" example of the application of plate theory to producing four-mirror systems with some mirrors allowed to be conicoids is described in section 2.3.2. In applying that method in the investigation presented here, the baseline system from figure 4.1.A is used. While maintaining the vertex radii for the first three mirrors of this system, two mirrors are allowed variable conic constants, the secondary and tertiary mirrors in this case, and also the position of the centre of curvature and the radius of the quaternary mirror is allowed to vary. For each position of the centre of curvature of the quaternary mirror there will be three geometrically-distinct anastigmatic solutions, which are the three solutions to equation 2.38 as given in equations 2.32-2.35. Plotting the curvature of the quaternary versus $L$, the position of the image of the centre of curvature of the quaternary mirror in object space, with $c_4$ determined by equation 2.32, 2.33 or 2.34, gives rise to the three solution sets shown in figure 4.2.

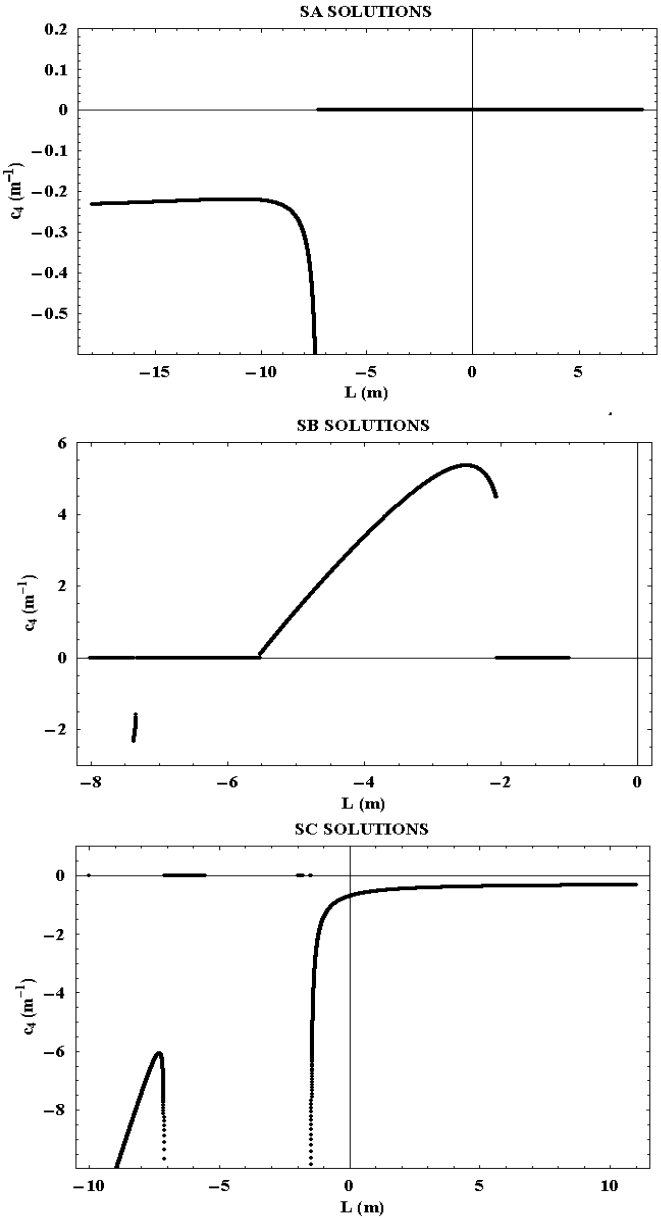


**Figure 4.2. SA, SB and SC solution curves for the case in which the baseline system is as given in table 3, and mirrors 2 and 3 are allowed to become conicoids. SA solutions are given by equation 2.33, SB solutions by equation 2.34 and SC solutions by equation 2.35. The horizontal axis here represents the initial position of the entrance pupil as measured from the primary mirror in object space, L, and the vertical axis represents the curvature of the quaternary mirror, $c_4$. Representative examples of optical systems from these solution sets are given in figures 4.3-4.5 and in table 3.**

Examples of optical systems from these three solution sets are given in figures 4.3- 4.5. A system closely resembling the baseline system exists, and is shown in figure 4.4. Interestingly, other valid solution types that are not so clearly related to the baseline system are also apparent. The Schiefspiegler system shown in figure 4.3 is an interesting and novel four-mirror anastigmatic design, and is similar in some respects to a design recently presented by Cook (2004).

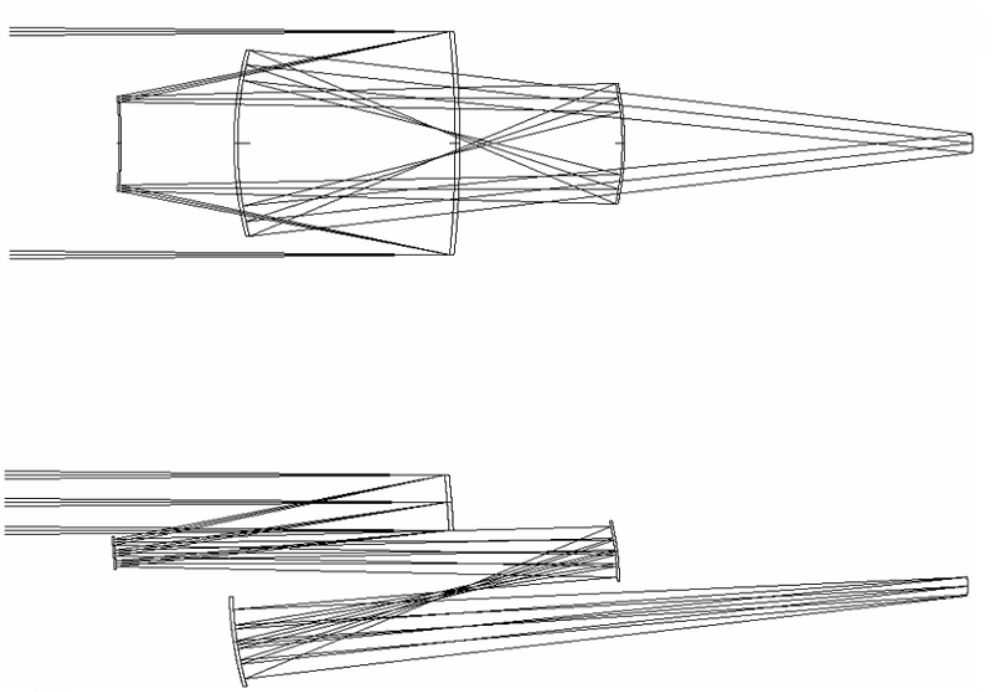

**Figure 4.3. An example of a solution for two-conicoid anastigmats using the SA solution. While the axially-symmetric system at top is clearly impractical because of 100% obstruction by the quaternary mirror of the light from the primary to the secondary mirror, a system obtained by using an off-axis portion of this parent system gives a useful unobstructed design. The optical design presented above is similar to but distinct from a system proposed by Cook (2004).**

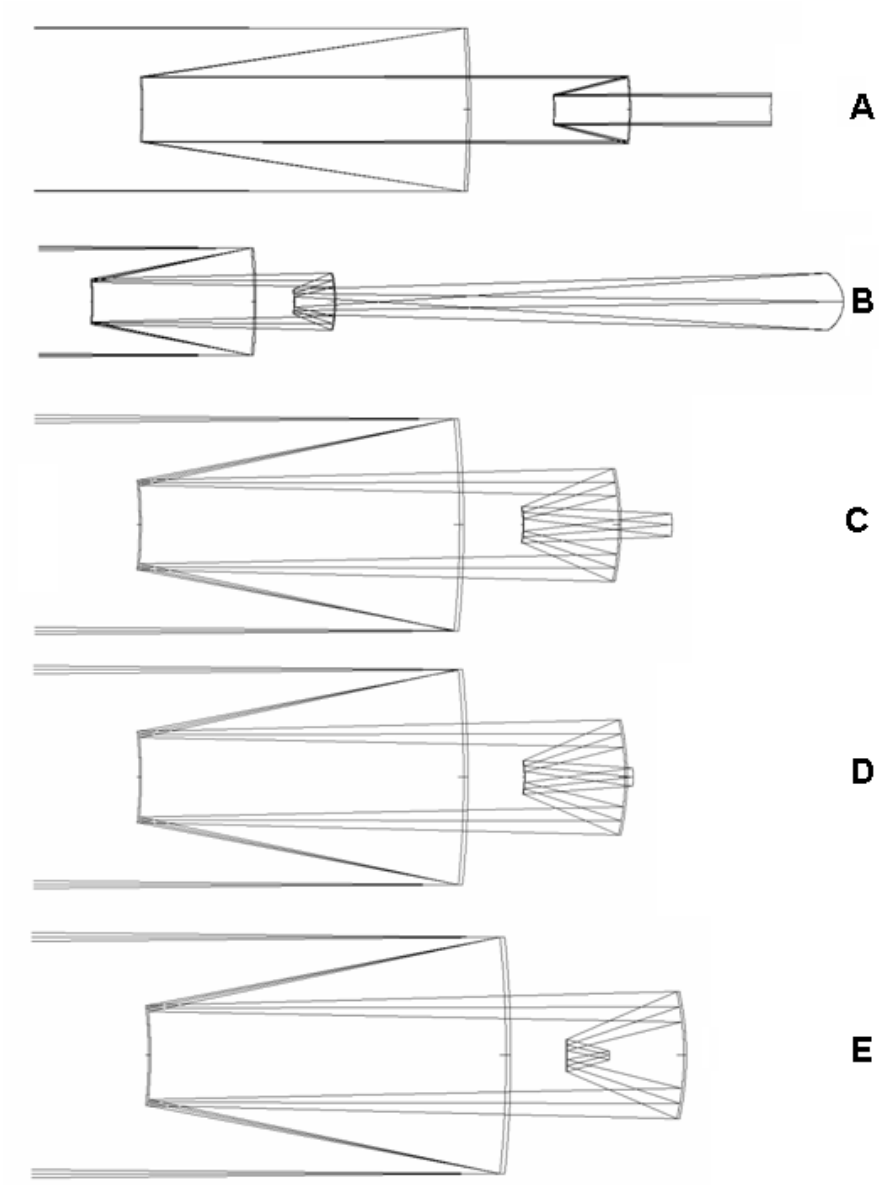


**Figure 4.4. Examples of the SB family of two-conicoid, two-sphere anastigmatic solutions. Systems ordered from A to E in this figure are solutions taken from points on the SB solution curve of figure 4.2 from right to left. Note that the system A is afocal, with systems of reducing (faster) focal ratio going down the page from A to E. System C is closely related to the baseline system in its first-order properties, and achieves anastigmatic correction with only two conicoids. Optical design data for system C are given in table 3.**

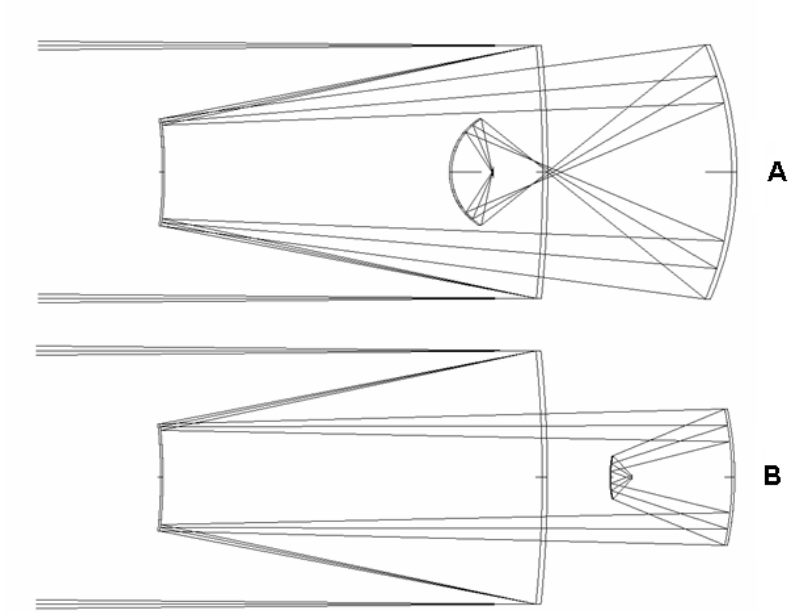


**Figure 4.5. Two examples of solutions from the SC curves shown in figure 4.2. While these systems do not exhibit a particularly favourable geometry, they serve as examples of the varied geometrical forms of valid anastigmatic systems that can be produced by this method.**

### *4.3 One-conicoid solutions*

The final example considered in this investigation is one in which only one mirror is allowed to become a conicoid. As will be shown below, it is possible to determine solutions with first-order properties close to those of the baseline system shown in figure 4.1, and with anastigmatic correction achieved with only one mirror allowed to become a conicoid. This addition of one conicoid surface represents the minimum compromise towards system complexity that one must make in order to obtain anastigmatic correction in a system that still

resembles the baseline system in its first-order properties. It should be noted that this investigation has focussed on a specific example, not the general case.

The algebraic method used to determine anastigmatic systems with one conicoid mirror is described in section 2.3.3. In the example given here the secondary mirror is allowed to become a conicoid. While it has not been shown here, it can be demonstrated that any mirror can be chosen to be the conicoid without adding complexity to the algebraic method given in section 2.3.3.

Figure 4.6 plots the solution sets over the basis vectors $c_3$, the curvature of the tertiary mirror, and $t_2$, the separation of the secondary and tertiary mirrors.

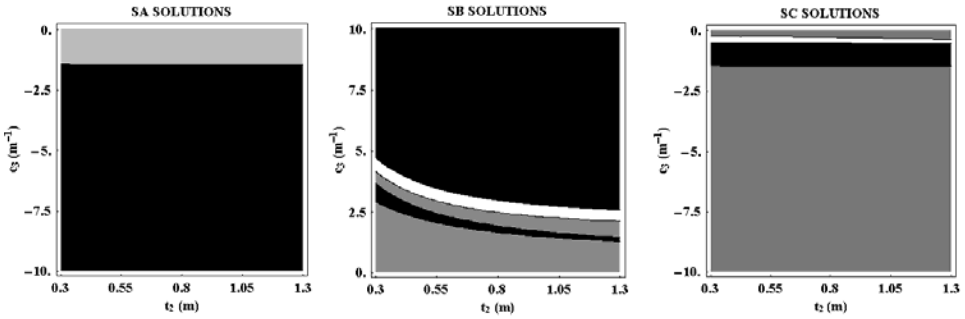


**Figure 4.6. Three independent sets of solutions for the case where only $M_2$ is allowed to be a conicoid. SA solutions are given by equation 2.16, SB by equation 2.17 and SC by equation 2.18. In these plots the vertical axis represents the curvature of the tertiary mirror while the horizontal axis represents the separation of the secondary and tertiary mirrors. Solutions are represented by either black or white regions, representing solutions with either negative or positive Petzval sums. Grey regions represent regions for which no valid anastigmatic solution exists. Note that there exist solution regions which have the corresponding coordinates in different sets. These represent systems that differ only in the radius and position of the quaternary mirror.**

To explain the increase in dimensionality of the solution sets in figure 4.6 compared to those in figure 4.2, one must consider that in going from the two-conicoid-mirror solution sets to the one-conicoid-mirror solution sets, we have removed one conicoid as a variable, in this case the conicoid variable assigned to the tertiary mirror, but then allowed both the position of the centre of curvature, and the actual curvature, of the tertiary mirror to become variable.

This increase in variables by one explains the change from 1-dimensional to 2-dimensional solution sets.

Figure 4.7 gives an example of a solution type obtained from the SA solution set of figure 4.6. While it would obviously be unsuitable as a telescope design, it does have potential as a microscope objective. Numerous systems of this type, that is, systems with elements much larger than the entrance pupil, are discussed in the following chapter.

Figure 4.8 shows a range of solutions from the SB solution set of figure 4.6. Clearly the SB solution set contains examples somewhat similar to the baseline system in the one-conicoid case, as was also the case in the two-conicoid example discussed above. In particular the system in figure 4.8.A gives the focal plane in approximately the same position as the baseline system, but with a slower relative aperture of f/13.6. The system in figure

4.8.C has the same focal ratio as the baseline system, but with the focal plane now between the tertiary and quaternary mirrors. The optical design data for this system are also given in table 3.

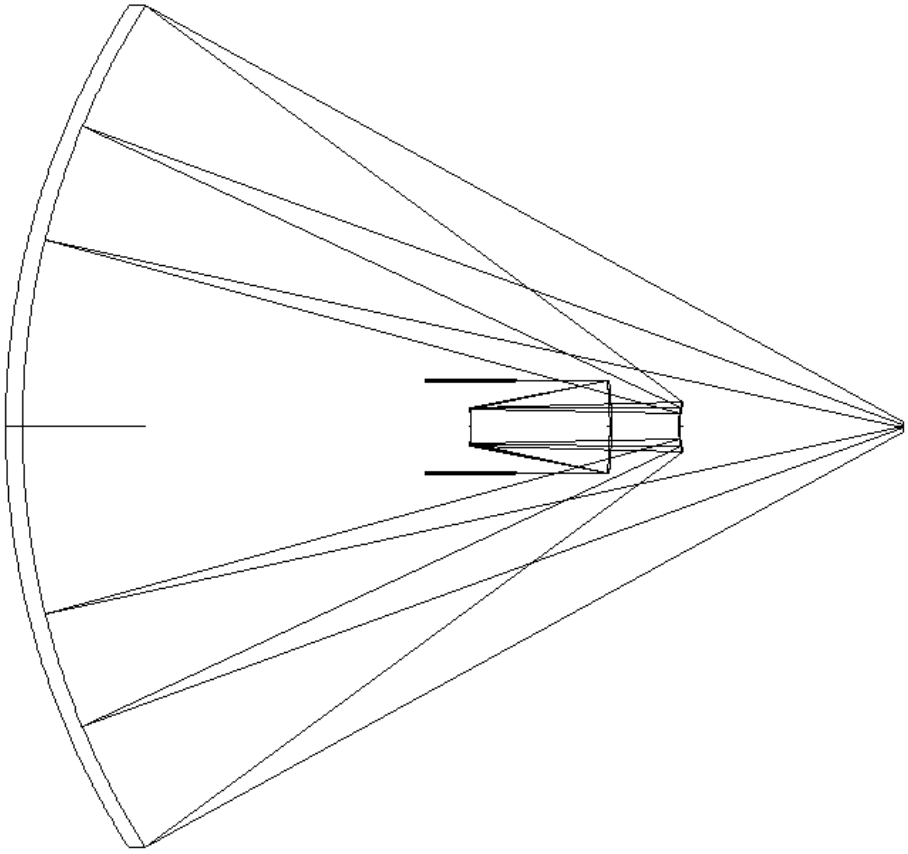

**Figure 4.7. An example of a completely impractical solution for the SA solution set of figure 4.6. When filters which exclude solutions with impractically large mirrors are applied, this solution set vanishes.**

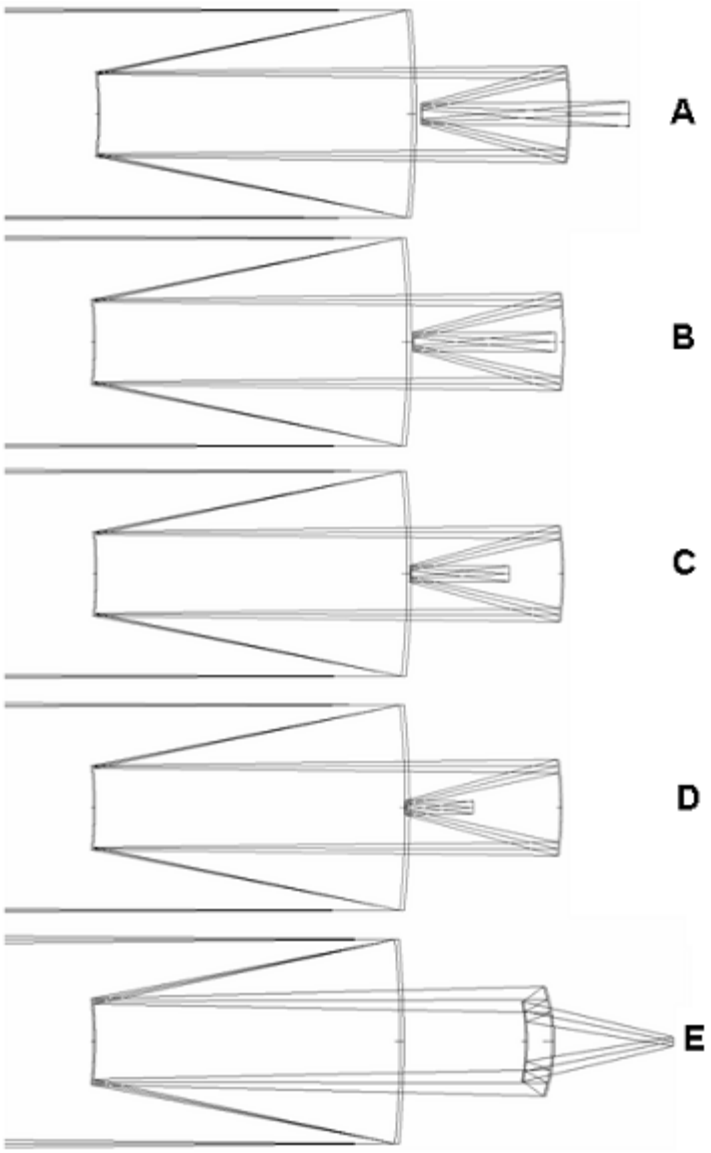


**Figure 4.8. Representative examples from the SB solution set shown in figure 4.6. In particular, systems A through D inclusive come from the thin black curving region in the SB solution plot, while system E is from the white region. System A most closely resembles the layout of the baseline system. This system has a focal ratio of f/13.6. System C most closely resembles the focal ratio of the baseline solution. Optical design data for system C are given in table 3.**

The final system here considered is shown in figure 4.9. This system comes from the SC solution set of figure 4.6. It bears a superficial resemblance to a system proposed by Steele (1953) and also to one of the proposed "INCA" systems of Rosin (1968), but unlike these systems, which both incorporate four conicoidal mirrors and suffer from Petzval curvature, the system presented in figure 4.9 is a flat-field anastigmat, and achieves this performance with only one mirror aspherized.

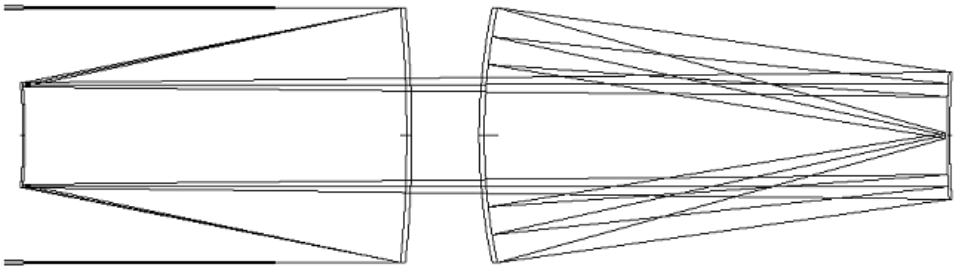

**Figure 4.9. This solution from the SC solution set of figure 4.6 bears some resemblance to a system proposed by Steele (1953). In this case however anastigmatic performance, and zero-Petzval curvature, are achieved, and these with only one conicoid mirror. Optical design data for this system are given in table 3.**

The results in this chapter show that an application of an algebraic-based search method to optical designs of four-mirror systems with pre-determined first-order characteristics is capable of yielding not only anastigmats with two less conicoids than are required for anastigmatic correction according to the generalized Schwarzschild theorem, but also that this approach delivers a variety of alternative solutions that may not have been previously considered.

| System | 4.1.A | 4.1.B | 4.3 | 4.4.C | 4.8.C | 4.9 |
|---|---|---|---|---|---|---|
| **R1** | -2.0 | -2.0 | -2.0 | -2.0 | -2.0 | -2.0 |
| **t1** | -0.6 | -0.6 | -0.6 | -0.6 | -0.6 | -0.6 |
| **R2** | -0.8 | -0.8 | -0.8 | -0.8 | -0.8 | -0.8 |
| **k2** | 0 | 3.1662 | 4.2813 | 3.2308 | 2.8618 | 2.3005 |
| **t2** | 0.9 | 0.9 | 0.9 | 0.9 | 0.9 | 1.45 |
| **R3** | -0.5 | -0.5 | -0.5 | -0.5 | -0.68027 | 1.55134 |
| **k3** | 0 | -0.3506 | -1.3680 | -0.2344 | 0 | 0 |
| **t3** | -0.19107 | -0.19107 | -0.69092 | -0.17652 | -0.29289 | -0.72812 |
| **R4** | -0.15 | -0.15 | 0.66118 | -0.19230 | -0.12558 | 0.97917 |
| **k4** | 0 | -0.2667 | 0 | 0 | 0 | 0 |
| **t4** | 0.27500 | 0.27500 | 1.32113 | 0.31166 | 0.19090 | 0.72592 |

**Table 3. Optical design data for the systems as indicated by the column headings. The quantities $k_i$ are the conic constants for the mirror indicated by the index number.**

# 5. Results: Four-spherical-mirror anastigmats with elements larger than the entrance pupil

This final results chapter presents the results of a survey of four-spherical-mirror systems in which optical elements are allowed significantly to exceed the size of the entrance pupil. This relaxation of the conditions that were used in chapter 3 leads to systems that in general would not be considered useful as telescopes. However, there are a wide range of applications, including but not limited to EUV lithography, high-energy laser systems, microscopy, projection and hyper-spectral imaging, which all benefit from the advantages catoptric systems offer, such as zero chromatic dispersion, high transmission efficiency, high damage thresholds and good correction of optical aberrations achievable with relatively simple systems. In many of these applications, systems that have elements many times larger than the entrance pupil would not be considered impractical.

One immediate result of relaxing the constraint on the size of optical elements is that now systems with convex primary mirrors can be considered. These

were previously ruled out as the secondary mirror is always larger than the entrance pupil for a convex primary system.

To complete this survey, only minor modifications were required to be made to the Mathematica™ program that was used to generate solutions in chapter 3. Firstly, constraint equations governing the maximum diameters of optics needed to be set new targets; in this case a cutoff was chosen that allowed mirrors up to fifteen times the diameter of the primary mirror.

Then the program could be run to generate nine families of solutions for concave-primary-mirror systems as discussed in chapter 3, but this time with much larger elements allowed. Also, by simply changing the sign of the input value for the primary mirror radius, the program could be run again to generate nine families of solution for the case where the primary mirror is convex.

The results of this new survey are presented below. There are a very large number of distinct anastigmatic solutions generated by this survey, a much larger and more varied set than in the more constrained case examined in chapter 3. To differentiate the various solutions, two classification systems have been employed. Firstly, solutions are identified as either having convex or concave primary mirrors. Then, for each family of solutions, two letters are assigned to show which of the three algebraic solutions to the cubic equation

used to determine the curvature of the tertiary and quaternary mirrors was employed in generating that solution set. For example, referring to SA, SB and SC as defined in equations 2.33-2.35, a solution set in which SB was used to determine the curvature of the tertiary mirror and SA was used to determine the curvature of the quaternary mirror would simply be referred to as the BA solution set. Thus the nine possible solution sets are named according to the nine possible permutations of the analytical solutions to the two cubic equations that are formulated in the method described in section 2.2.

Finally, within each solution set there are often a wide variety of available system geometries, and the digit-based classification system described in section 2.4 and detailed in figure 2.4.1 is employed further to refine the description of available solutions.

### *5.1 AA Solutions*

There are no AA-type solutions for concave-primary-mirror systems. Only one type of solution exists for convex-primary AA-type solutions, as shown in figure 5.1.1. Optical design data for this figure are given in table 4. All members from the relatively limited range of solutions in this family are of the 42135 type.

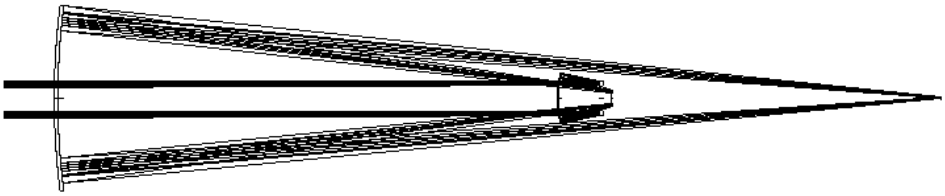

**Figure 5.1.1. An AA-type 42135 system with a convex primary mirror. In this figure, and in all subsequent figures in this chapter, collimated light incident on the primary mirror from the object at infinity is travelling from left to right.**

| System | R1 | t1 | R2 | t2 | R3 | t3 | R4 | t4 |
|---|---|---|---|---|---|---|---|---|
| **5.1.1.** | 2.0 | -0.47672 | 1.11099 | 0.62439 | 0.37561 | -6.51739 | 8.47899 | 10.403 |

**Table 4. Optical design data for the AA-type system shown in figure 5.1.1. The primary mirror in this and all other non-Schiefspiegler systems presented in this paper is 0.4 m diameter, though this is an arbitrary value as all these systems can be scaled. Units are metres. The sign convention employed should be obvious from the figure and table.**

### *5.2 AB Solutions*

AB-type solutions exist for both concave- and convex-primary-mirror types. Concave-primary-mirror solutions are shown in figures 5.2.1 and 5.2.2, with design data for these systems given in table 5. There exist two distinct sub-regions of solution in the AB concave primary mirror case. Examples from the first sub-region are given in figure 5.2.1. The three systems shown here can be classified as 24135, 24153 and 24513 systems, and they are indicative of the continuum of solutions within their solution family. Afocal versions also exist.

24531, 24351 and 24315 versions of this family also exist and some of these were reported in chapter 3. In these cases the tertiary mirror lies between the primary and secondary mirrors (the digit “3” is always between the digits “2” and “1” in the five-digit naming system in these cases) and is in general smaller in diameter than the primary mirror. There are no members of this family for which Petzval curvature is zero.

Two solutions from the second solution sub-region are shown in figure 5.2.2. Within this particular family there also exist afocal solutions. Solution 5.2.2.A is an example of one of the members of this solution family that has zero Petzval curvature. This solution family, which can be seen to be geometrically distinct from the solution family shown in figure 5.2.1, contains 21435 and 21453 type solutions.

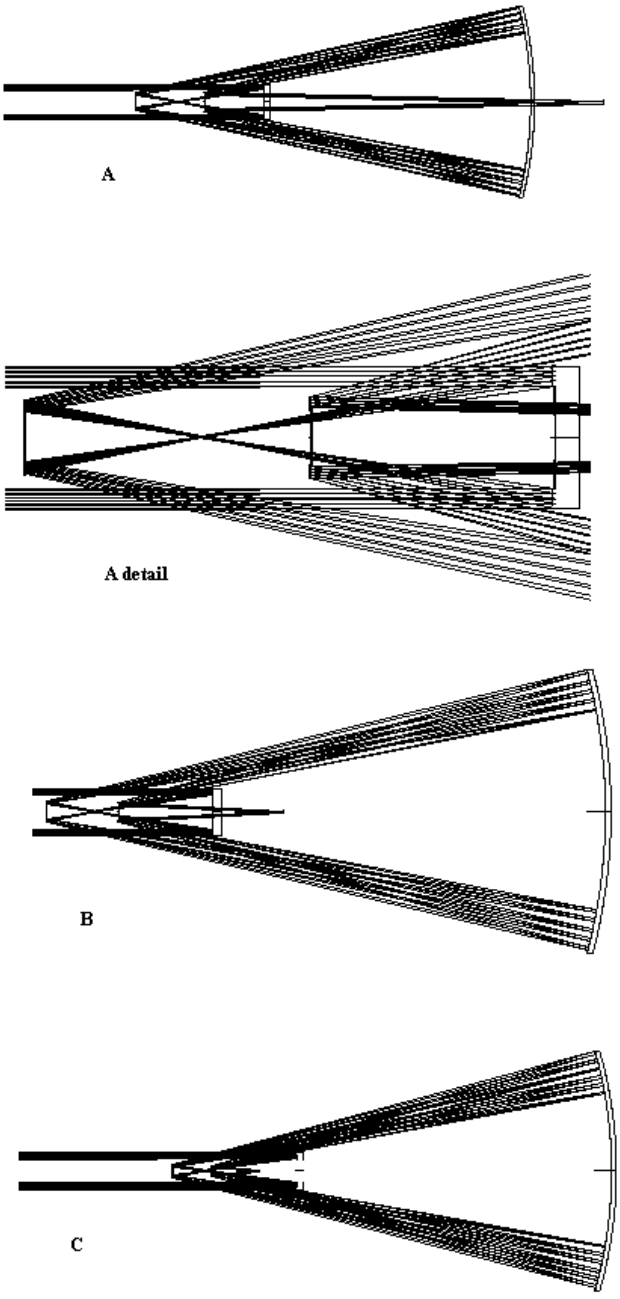


**Figure 5.2.1. Three examples, each from the first sub-region of AB-type concave-primary-mirror solutions.**

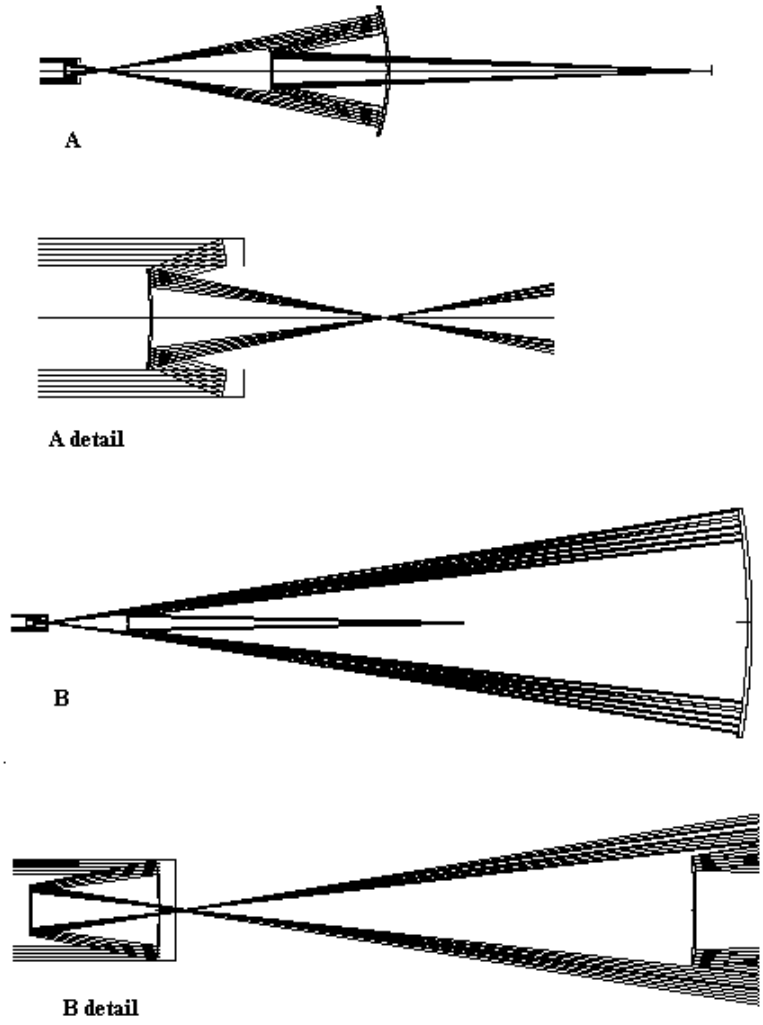


**Figure 5.2.2. Two examples, each from the second sub-region of AB-type concave-primary-mirror solutions.**

Convex-primary-mirror solutions are shown in figure 5.2.3. All of these solutions occupy a single connected "volume" in solution space. Within this

solution family there exist examples of 21435 and 21453 systems. The system depicted in figure 5.2.3.C is a system previously described by Shafer (1988). Of the systems presented in this thesis, this is the only one that has previously appeared in published literature. Shafer's system is an example of this solution type that has zero Petzval curvature. Optical design data for the convex primary systems can be found in table 5.

| System | R1 | t1 | R2 | t2 | R3 | t3 | R4 | t4 |
|---|---|---|---|---|---|---|---|---|
| **5.2.1.A** | -2.0 | -1.49005 | -10.0100 | 4.57732 | -4.57732 | -3.76881 | -0.96077 | 4.605 |
| **5.2.1.C** | -2.0 | -1.41005 | -5.00250 | 4.73340 | -4.73340 | -4.12223 | -0.77917 | 1.395 |
| **5.2.2.A** | -1.0 | -0.19774 | -1.22416 | 5.08832 | -3.38817 | -1.81143 | -2.09091 | 6.947 |
| **5.2.2.C** | -2.0 | -0.51005 | -5.0025 | 18.86250 | -17.8625 | -16.1996 | -3.02074 | 8.775 |
| **5.2.3.A** | 2.0 | -3.30005 | 6.28465 | 5.26039 | -3.78465 | -0.22825 | -1.62752 | 0.199 |
| **5.2.3.B** | 2.0 | -2.13005 | 2.77701 | 2.31242 | -0.61242 | -0.04667 | -0.18168 | 0.269 |
| **5.2.3.C** | 2.0 | -3.60794 | 5.60795 | 6.95518 | -1.34723 | -0.07000 | -1.27723 | 0.103 |

**Table 5. Optical design data for the AB-type systems shown in figures 5.2.1, -2 and -3.**

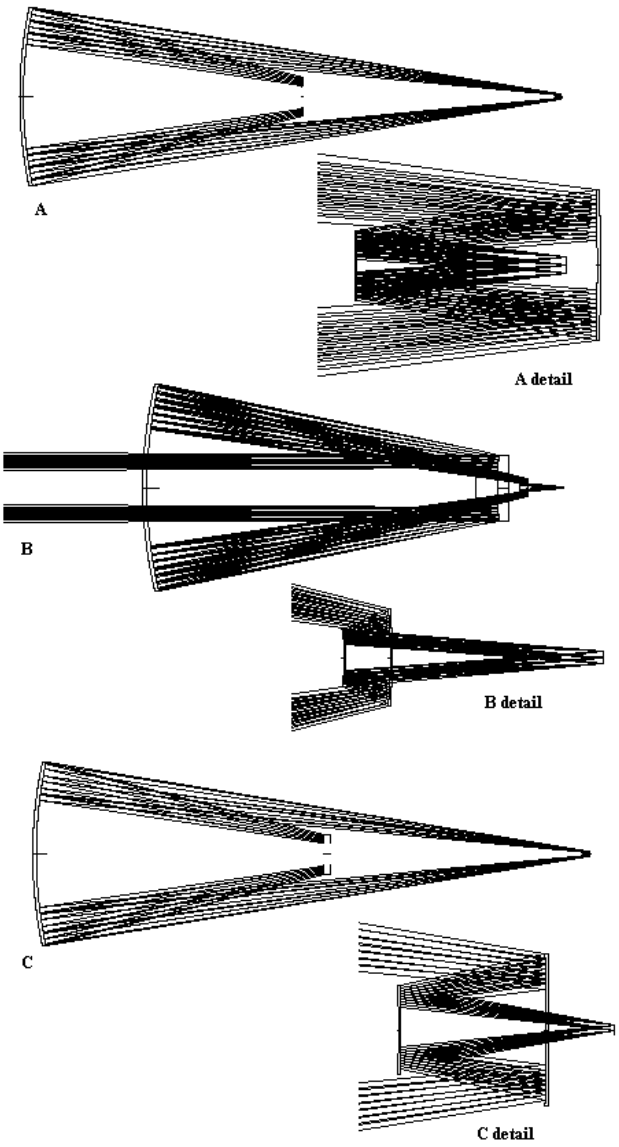


**Figure 5.2.3. Three examples from the single solution set for AB-type convex-primary-mirror systems. A is a flat-field system originally given by Shafer (1988) and is the only example of an axially-symmetrical four-spherical-mirror anastigmat with infinite object conjugate to have appeared in previously published literature.**

### *5.3 AC Solutions*

No concave-primary-mirror AC-type solutions exist. A limited range of convex-primary-mirror AC-type solutions exist, and a typical example is given in figure 5.3.1. All of these systems are of the 45213 type. Optical design data for these systems are given in table 6. As can be seen in figure 5.3.1.A, these systems suffer from a high central obstruction ratio. One way around this problem is illustrated in figure 5.3.1.B, which shows a completely unobstructed system taken from an axially-symmetrical parent system. This family of solutions contains no afocal systems, and no systems for which the Petzval curvature is zero.

| System | R1 | t1 | R2 | t2 | R3 | t3 | R4 | t4 |
|---|---|---|---|---|---|---|---|---|
| **5.3.1** | 2.0 | -1.10000 | -5.00250 | 6.96588 | -7.96588 | -7.57213 | 0.80757 | 0.157 |

**Table 6. Optical design data for the AC-type system shown in figure 5.3.1.A. The Schiefspiegler shown in figure 5.3.1.B is simply a system produced by using an off-axis portion of the pupil of this system.**

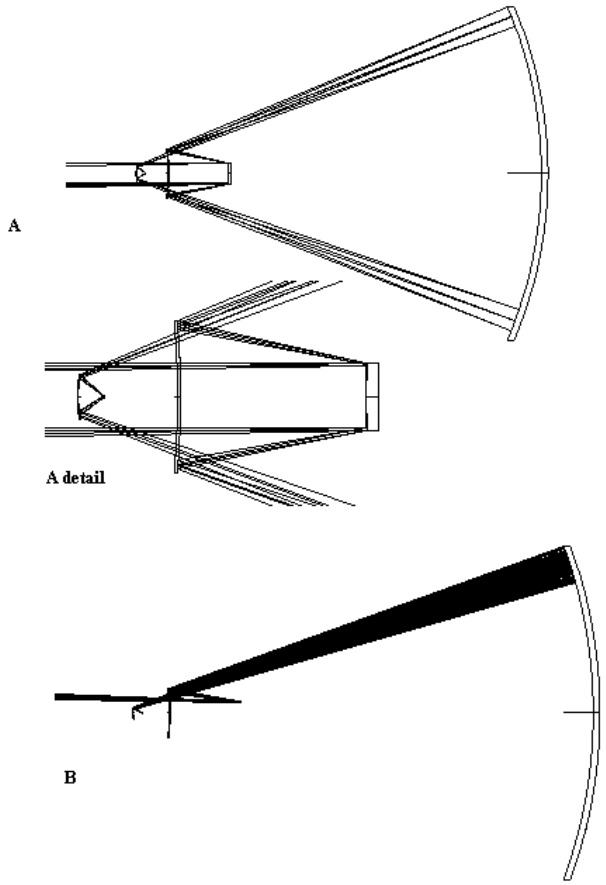


**Figure 5.3.1. AC-type convex-primary-mirror solutions all resemble this solution. B shows a Schiefspiegler formed by using an off-axis portion of the A system.**

### *5.4 BA Solutions*

There are no BA-type concave-primary-mirror solutions. There is a relatively limited range of BA convex-primary solutions. Examples of 42315, 42135, 24135 and 21435 variants are given in figure 5.4.1, with system design parameters given in table 7. There are no variants free of Petzval curvature.

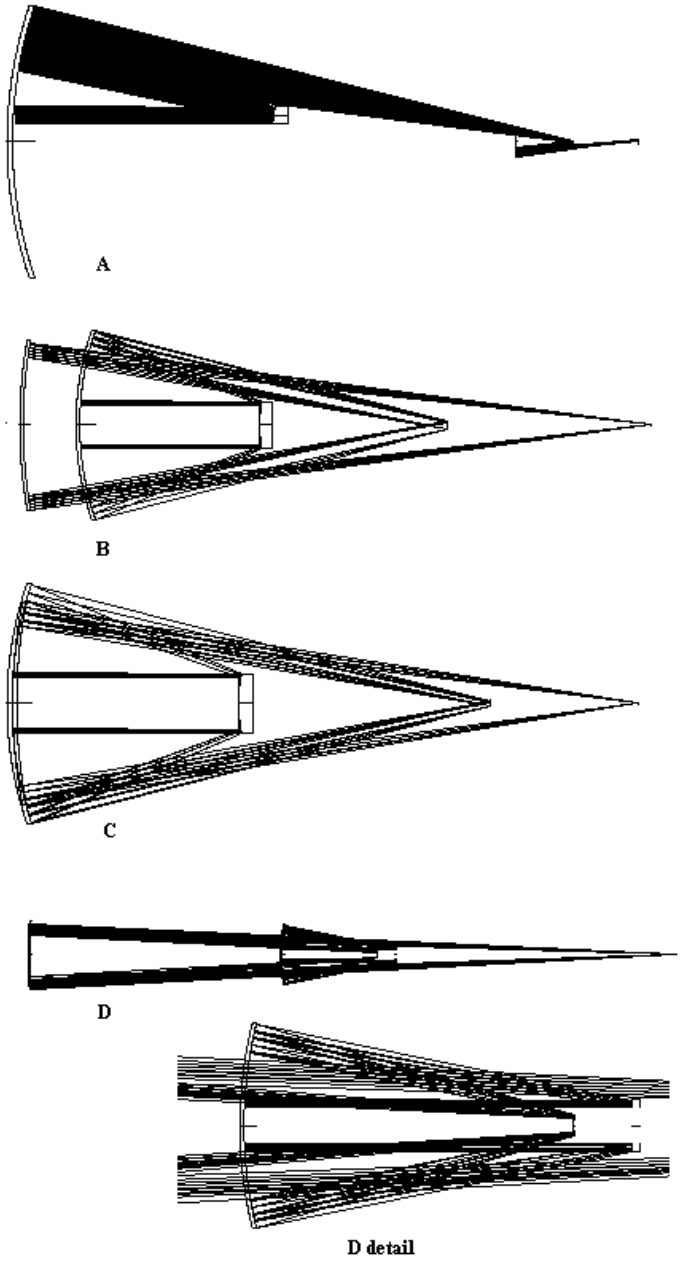


**Figure 5.4.1. BA-type convex-primary-mirror solutions. A is an example of a 21435 system that only works as a Schiefspiegler; the axially-symmetrical parent system is 100% self-obstructing. B, C and D are all solution types from one connected volume of solutions within the solution space.**

| System | R1 | t1 | R2 | t2 | R3 | t3 | R4 | t4 |
|---|---|---|---|---|---|---|---|---|
| **5.4.1.A** | 1.0 | -1.51502 | 2.49875 | 3.27763 | 0.22237 | -0.33542 | 0.44547 | 0.713 |
| **5.4.1.B** | 2.0 | -3.06005 | 4.99750 | 6.24161 | 2.75839 | -7.20474 | 8.37344 | 10.671 |
| **5.4.1.C** | 2.0 | -3.04005 | 4.99750 | 6.42442 | 1.57558 | -6.36053 | 7.11601 | 8.379 |
| **5.4.1.D** | 2.0 | -3.02005 | 3.33222 | 2.56571 | 0.43429 | -9.31763 | 12.9222 | 17.367 |

**Table 7. Optical design data for BA-type systems as shown in figure 5.4.1. The figure 5.4.1.A system is an example of a system that only works as a Schiefspiegler; the axially-symmetrical system is totally self-obstructing.**

### *5.5 BB Solutions*

One connected volume of BB-type concave-primary-mirror solutions exists. 24351, 24315, 42315, 42351, 42531, and 45231 variants are shown in figure 5.5.1, with optical design data given in table 8.

There is a relatively limited range of BB convex primary solutions. Examples of 45213, 42135 and 21435 variants are given in figure 5.5.2, with system design parameters given in table 8. There are no variants free of Petzval curvature. The system in figure 5.5.2.A only works as a Schiefspiegler as a result of self-obstruction in the axially-symmetrical system. It is interesting to note the clear first-order differences between the 45213 system in figure 5.5.2.D and the 45213 systems in figure 5.3.1.

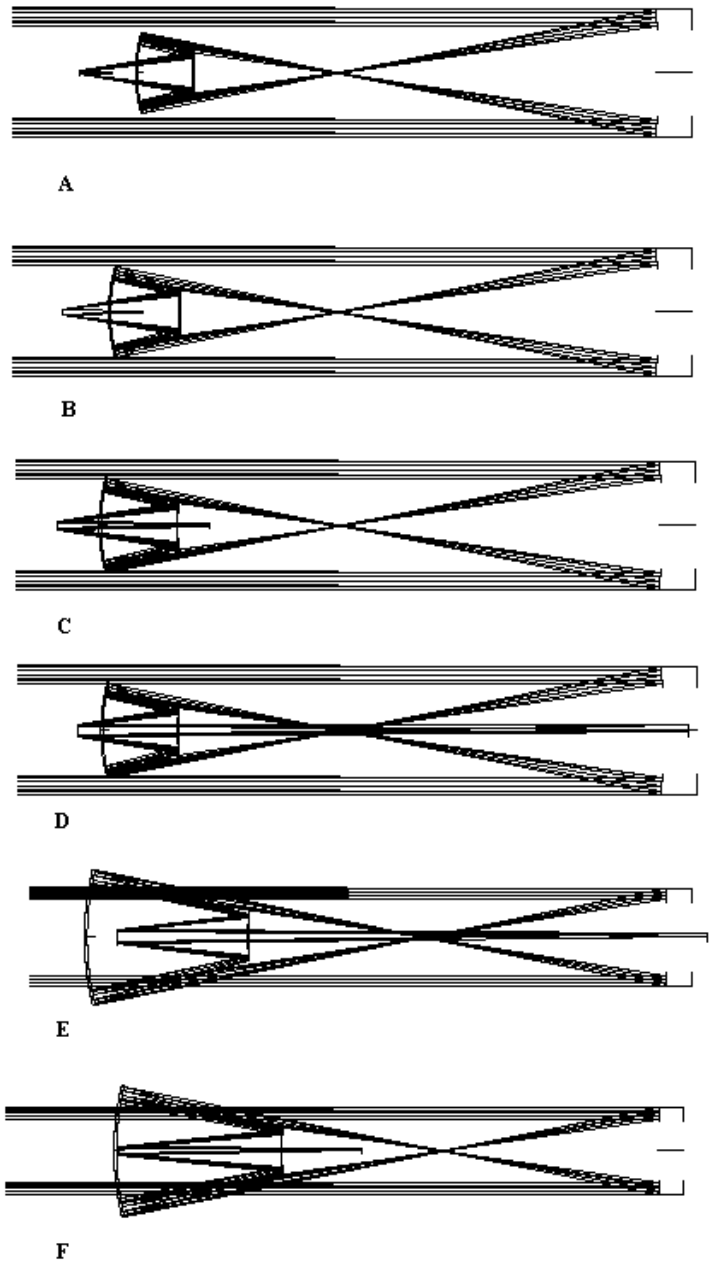


**Figure 5.5.1. BB-type concave-primary solutions. The first four systems here, A-D, were previously reported in chapter 3, and are included here for comparison to other members of this solution family. The systems shown in E and F are clearly members of this family.**

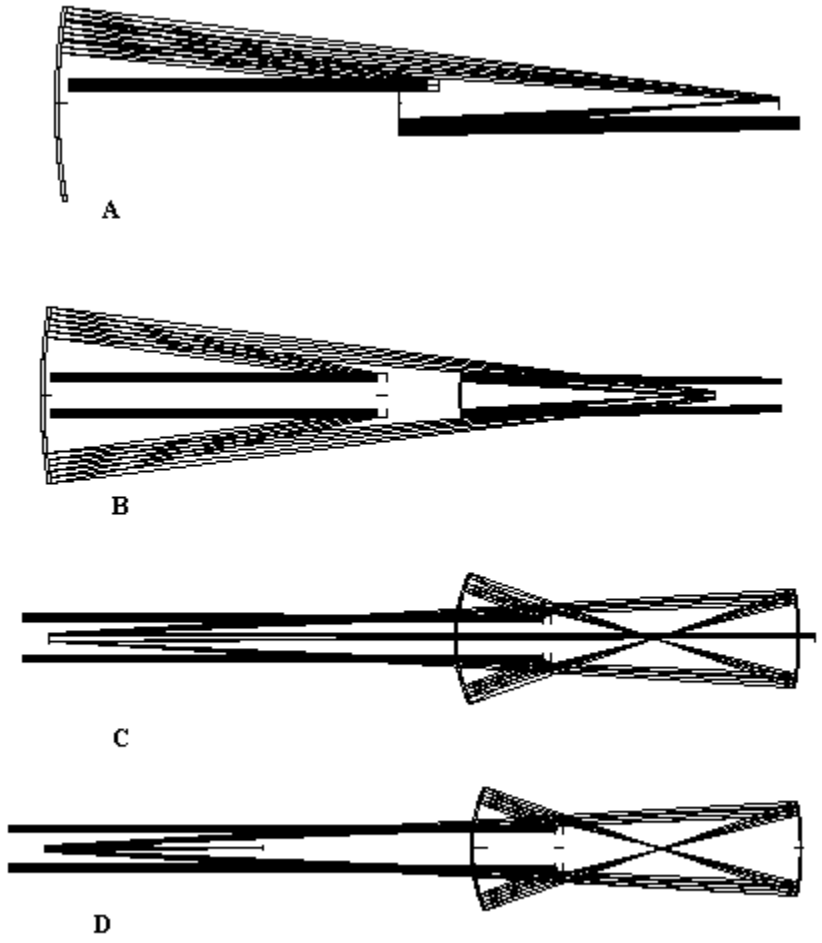


**Figure 5.5.2. BB-type convex-primary-mirror solutions. The 24135 system shown in A is another example of a system that only works as a Schiefspiegler because of self-obstruction. B, C and D are 21435, 42135 and 45213 type arrangements respectively.**

| System | R1 | t1 | R2 | t2 | R3 | t3 | R4 | t4 |
|---|---|---|---|---|---|---|---|---|
| **5.5.1.A** | -2.0 | -1.61747 | 0.44803 | 0.17183 | 0.68119 | -0.34970 | -0.08908 | 0.100 |
| **5.5.1.B** | -2.0 | -1.70005 | 0.52081 | 0.21256 | 0.78744 | -0.36063 | -0.13957 | 0.250 |
| **5.5.1.C** | -2.0 | -1.74005 | 0.55246 | 0.23475 | 0.76525 | -0.36985 | -0.18222 | 0.470 |
| **5.5.1.D** | -2.0 | -1.72000 | 0.52869 | 0.22013 | 0.78703 | -0.28804 | -0.23104 | 1.860 |
| **5.5.1.E** | -2.0 | -2.37005 | 1.16266 | 0.65589 | 1.34411 | -0.53018 | -0.47801 | 2.40928 |
| **5.5.1.F** | -2.0 | -2.49005 | 1.28189 | 0.75225 | 1.24775 | -0.73961 | -0.44377 | 1.112 |
| **5.5.2.A** | 2.0 | -3.08005 | 4.9975 | 6.04405 | 3.95595 | -3.18582 | 4.67821 | 18.418 |
| **5.5.2.B** | 2.0 | -3.07005 | 4.99750 | 6.20993 | 2.79007 | -2.35117 | 3.48385 | 12.352 |
| **5.5.2.C** | 2.0 | -1.78765 | 3.33322 | 7.21546 | -5.21546 | -15.8551 | -3.12821 | 16.196 |
| **5.5.2.D** | 2.0 | -1.78385 | 3.33322 | 7.21216 | -5.21216 | -16.6497 | -2.33138 | 4.784 |

**Table 8. Optical design data for BB-type systems as shown in figures 5.5.1 and 5.5.2. The systems shown in figures 5.5.2.C and 5.5.2.D have for the sake of clarity been scaled in aperture to 1 m (the primary mirror has a 1 m diameter with the stop on the primary).**

### *5.6 BC Solutions*

No concave-primary-mirror BC-type solutions exist. There is one connected volume of BC solutions with convex primary mirrors. Within this family there exist 24153, 24513, 24531 and 21453 variants as shown in figures 5.6.1.A, B, C and D respectively. The example given in figure 5.6.1.C has zero Petzval curvature.

The first–order layout of the first two mirrors of the system in figure 5.6.1.D is very similar to the two-mirror Schwarzschild flat-field anastigmat, though in that case both mirrors are conicoids. Here, instead of requiring two conicoid mirrors, correction of coma and astigmatism is achieved with the small set of tertiary and quaternary spherical mirrors. However the system has a curved focal plane. Optical design data for the BC solutions are given in table 9.

| System | R1 | t1 | R2 | t2 | R3 | t3 | R4 | t4 |
|---|---|---|---|---|---|---|---|---|
| **5.6.1.A** | 2.0 | -1.37005 | 1.99960 | 1.53636 | 0.46364 | -0.22866 | 0.30563 | 0.131 |
| **5.6.1.B** | 2.0 | -1.40005 | 1.99960 | 1.49873 | 0.50127 | -0.29596 | 0.35824 | 0.156 |
| **5.6.1.C** | 2.0 | -1.51005 | 1.99960 | 1.36335 | 0.63665 | -0.66006 | 0.62166 | 0.28887 |
| **5.6.1.D** | 2.0 | -2.85005 | 3.33222 | 2.90352 | 0.09648 | -0.02224 | 0.04863 | 0.019 |

**Table 9. Optical design data for BC-type solutions as shown in figure 5.6.1.**

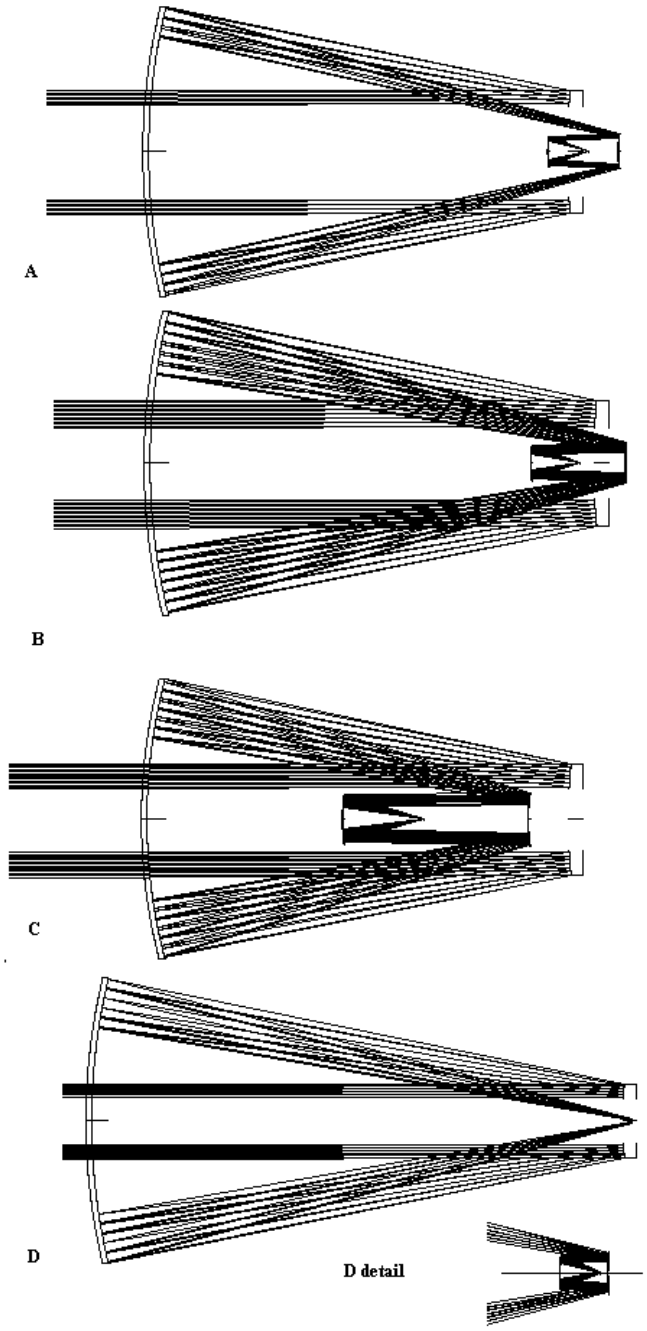


**Figure 5.6.1. BC-type convex-primary-mirror systems from one connected volume of solutions. The 24531 system in C is an example of a flat-field anastigmat.**

### *5.7 CA Solutions*

There are two separate solution volumes for CA-type systems with concave primary mirrors, and these are shown in figure 5.7.1, with optical design data in table 10. Both 42315 and 42351 arrangements exist. These two systems have relatively high numerical apertures. Also, both these systems are characterized by the high angles of incidence that rays make on the tertiary mirror. These two facts mean that these systems are less well approximated by third-order theory than is the norm, as the proportion of high-order to low order aberration in these types of system is much greater than in other systems so far presented.

The convex-primary CA-type systems are shown in figure 5.7.2. The solution set contains systems with 21435, 24135 and 42135 arrangements. All solutions come from one connected volume of solutions, and there are some interesting variants, including versions with zero Petzval curvature (shown in figures 5.7.2.A, B, C and D). The flat-field system shown in figure 5.7.2.D is similar to the system shown in figure 5.6.1.D, though the arrangement of the "small corrector pair" of the tertiary and quaternary mirrors is somewhat different. Optical design data for these systems is given in table 10.

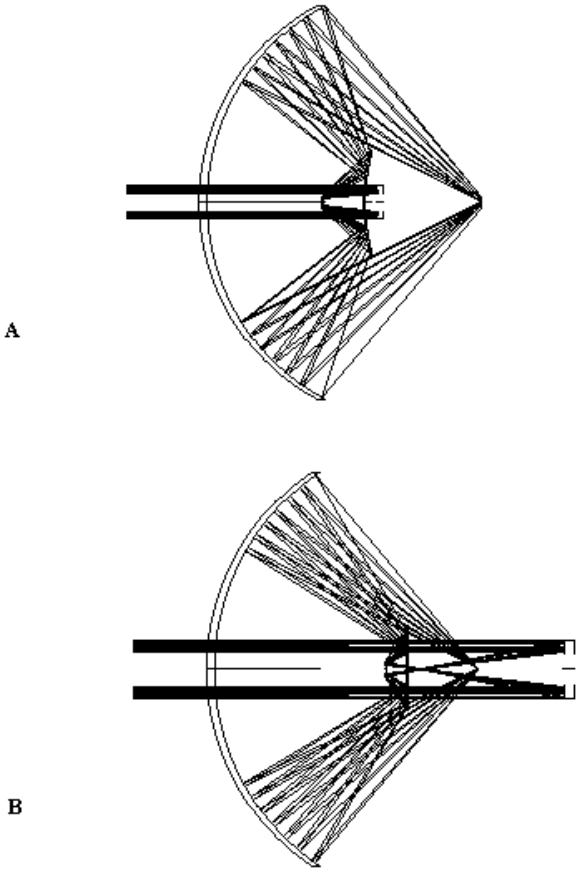


**Figure 5.7.1. CA-type concave-primary-mirror solutions, from two unconnected volumes of solution space. Both systems are characterized by high numerical aperture and large angles of incidence on the tertiary mirror.**

| System | R1 | t1 | R2 | t2 | R3 | t3 | R4 | t4 |
|---|---|---|---|---|---|---|---|---|
| **5.7.1.A** | -2.0 | -0.66005 | -0.14085 | 0.48884 | 2.51116 | -1.87143 | 2.69156 | 3.282 |
| **5.7.1.B** | -2.0 | -1.24005 | -0.13889 | 0.13430 | 6.8657 | -1.32947 | 1.65190 | 1.826 |
| **5.7.2.A** | 2.0 | -0.61005 | 1.24984 | 1.24944 | 0.75056 | -0.67398 | 0.96508 | 1.181 |
| **5.7.2.C** | 2.0 | -1.21005 | 1.99960 | 3.23066 | 4.76934 | -3.24174 | 5.06698 | 6.564 |
| **5.7.2.D** | 2.0 | -2.87005 | 3.33186 | 2.94074 | 0.05962 | -0.03519 | 0.05794 | 0.080 |
| **5.7.2.E** | 1.618 | -2.61798 | 4.23598 | 7.00000 | 1.28818 | -7.47487 | 8.76305 | 9.805 |

**Table 10. Optical design data for CA-type solutions as shown in figures 5.7.1 and 5.7.2. Figure 5.7.2.B is an example of a flat-field Schiefspiegler obtainable by using an off-axis portion of the pupil of the system in figure 5.7.2.A.**

The system shown in figure 5.7.2.E is an example of a four-spherical-mirror anastigmat that consists of two individually-anastigmatic pairs of concentric spherical mirrors. In this case the primary and secondary mirrors form a two-concentric-spherical-mirror anastigmat with the object at infinity, and the tertiary and quaternary mirrors are a two-concentric-spherical-mirror anastigmatic relay.

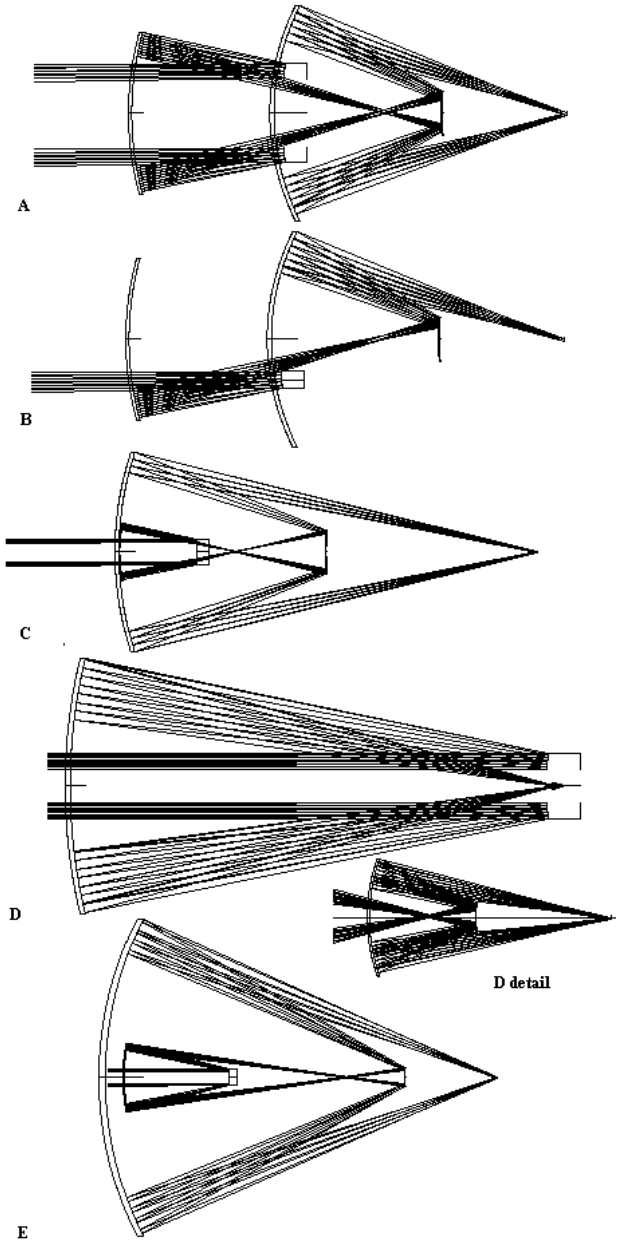


**Figure 5.7.2. Each of the first four CA-type convex-primary-mirror solutions shown here has zero Petzval curvature. B is a Schiefspiegler with a relatively fast numerical aperture taken from the axially-symmetrical parent in A. System E is comprised of two individually-anastigmatic concentric-spherical-mirror pairs. Solutions such as this are a special case, lying in a 2-dimensional sub-space of the 3-dimensional solution space.**

### *5.8 CB Solutions*

Concave-primary CB-type solutions exist in three unconnected volumes within the solution space. The 45213 solutions as shown in figure 5.8.1.A come from one of the solution volumes. These systems only work as Schiefspieglers, and have relatively uninteresting geometries. The 21453 solutions as in figure 5.8.1.B come from another distinct family of solutions and the 21453- and 24135-type solutions as shown in figure 5.8.1.C come from the third family of solutions. There are no afocal systems or systems with zero Petzval curvature among these solutions. Optical design data for these systems are given in table 11.

There is a relatively wide variety of convex-primary-mirror CB-type solutions, including flat-field systems and afocal systems. 21435, 24135, 42153, 42135 and 45213 geometries exist and examples are given in figure 5.8.2 and table 11. These solutions come from three unconnected volumes of solution. The 45213 example in figure 5.8.2.E shows in effect a three-spherical-mirror anastigmat with the secondary mirror as a flat fold mirror. While technically the example given has four powered mirrors, there does exist a very similar system to the one shown in which the secondary mirror has no power.

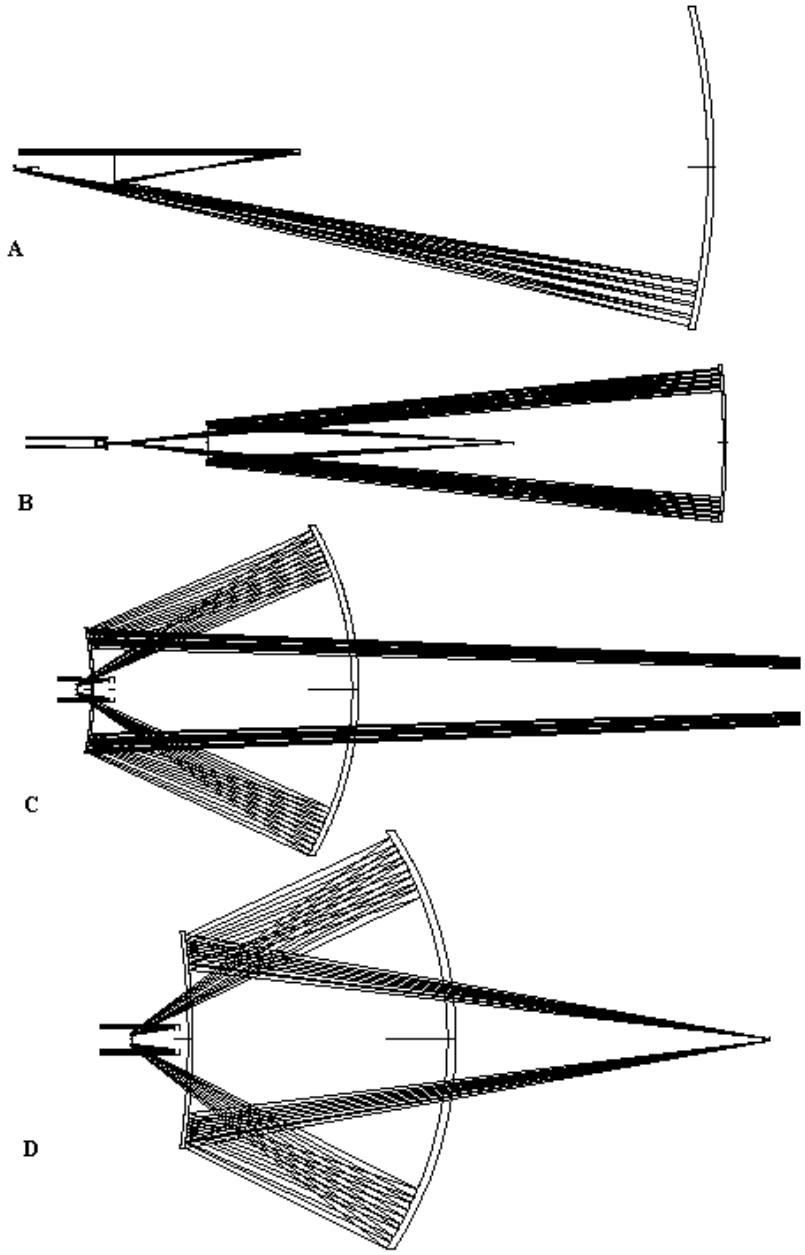


**Figure 5.8.1. Three distinct families of CB-type concave-primary-mirror solutions are shown here. The 45213 system in A comes from one family, the 21453 solution in B from a second and the 24135 and 21435 systems in C and D from the third.**

| System | R1 | t1 | R2 | t2 | R3 | t3 | R4 | t4 |
|---|---|---|---|---|---|---|---|---|
| **5.8.1.A** | -2.0 | -1.95005 | -10.0100 | 6.46323 | -7.46323 | -7.55919 | -0.42120 | 0.264 |
| **5.8.1.B** | -2.0 | -0.38005 | -3.33440 | 23.8200 | -24.8200 | -19.5608 | -44.4246 | 11.610 |
| **5.8.1.C** | -2.0 | -0.54005 | -0.23256 | 4.65637 | -5.65637 | -4.38337 | -5.48759 | 25.449 |
| **5.8.1.D** | -2.0 | -0.58005 | -0.19608 | 4.26324 | -5.26324 | -3.45058 | -10.3864 | 7.797 |
| **5.8.2.A** | 2.0 | -2.01054 | 3.31934 | 4.54919 | 3.45264 | -0.71567 | 2.04974 | 5.056 |
| **5.8.2.B** | 2.0 | -2.25005 | 1.99960 | 7.24702 | -6.24702 | -5.37939 | -3.11477 | 12.531 |
| **5.8.2.C** | 2.0 | -1.82005 | 3.33220 | 20.8835 | -19.8835 | -23.1106 | -3.44192 | 4.166 |
| **5.8.2.D** | 2.0 | -1.29005 | -10.0100 | 3.18882 | -5.18882 | -9.15276 | 5.98398 | 22.530 |
| **5.8.2.E** | 2.0 | -1.00005 | 10000 | 2.23341 | -5.23341 | -6.80769 | -3.52854 | 0.043 |

**Table 11. Optical design data for CB-type systems as shown in figures 5.8.1 and 5.8.2.**

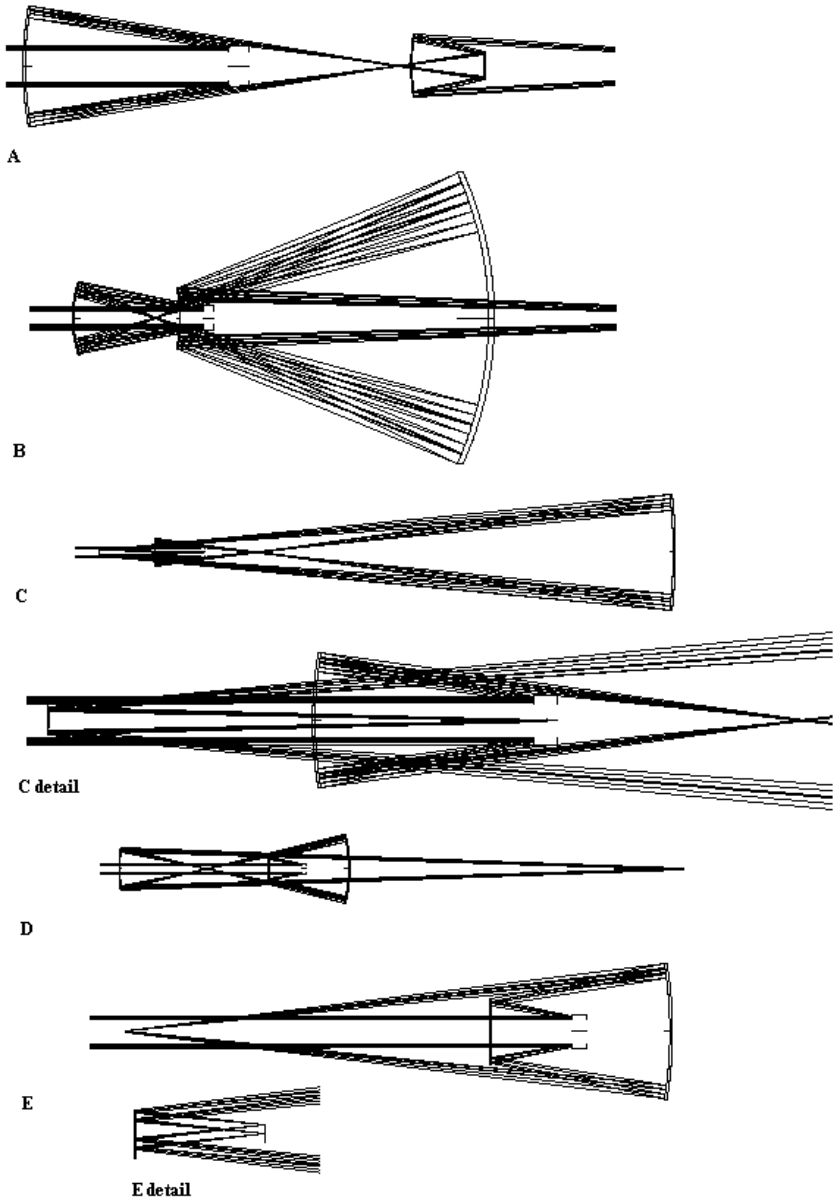


**Figure 5.8.2. Three distinct families of CB-type convex-primary systems exist. A is an example of a flat-field system from one of these families. E is very close to a special-case system in which the secondary mirror has zero power; essentially a three-spherical-mirror anastigmat.**

### *5.9 CC Solutions*

A very limited range of concave primary CC-type solutions exists as shown in figure 5.9.1. All solutions of this type are in the 42135 configuration.

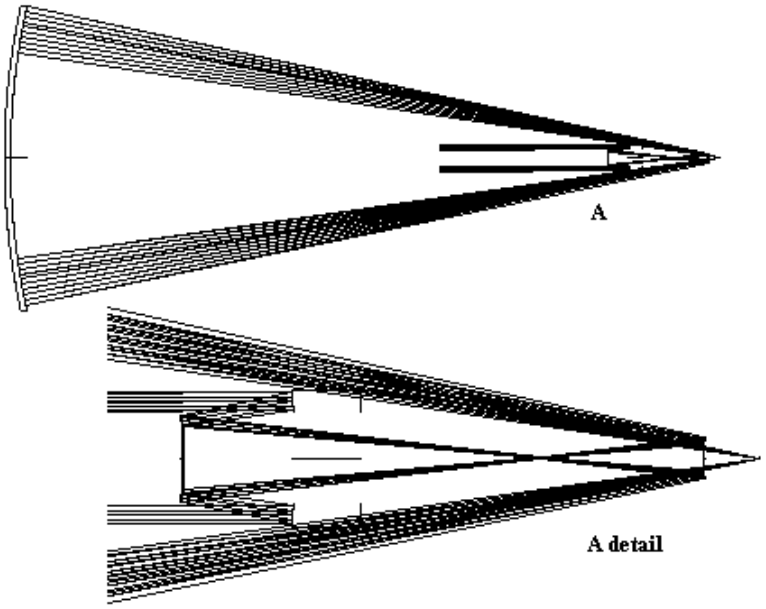


**Figure 5.9.1. The system depicted here is typical of the very limited range of available CC-type concave-primary-mirror systems.**

While there is somewhat more variety with the convex-primary CC-type solutions, with 45231, 42531, 42351 and 42135 geometries available, all members of this family of solution are characterized by an extremely fast focal ratio. This means that the third-order aberration approximation is not so close to an optimum solution for this family of systems, as was the case with the CA

concave-primary-mirror systems. Convex-primary CC-type solutions are shown in figure 5.9.2, with optical design data given in table 12.

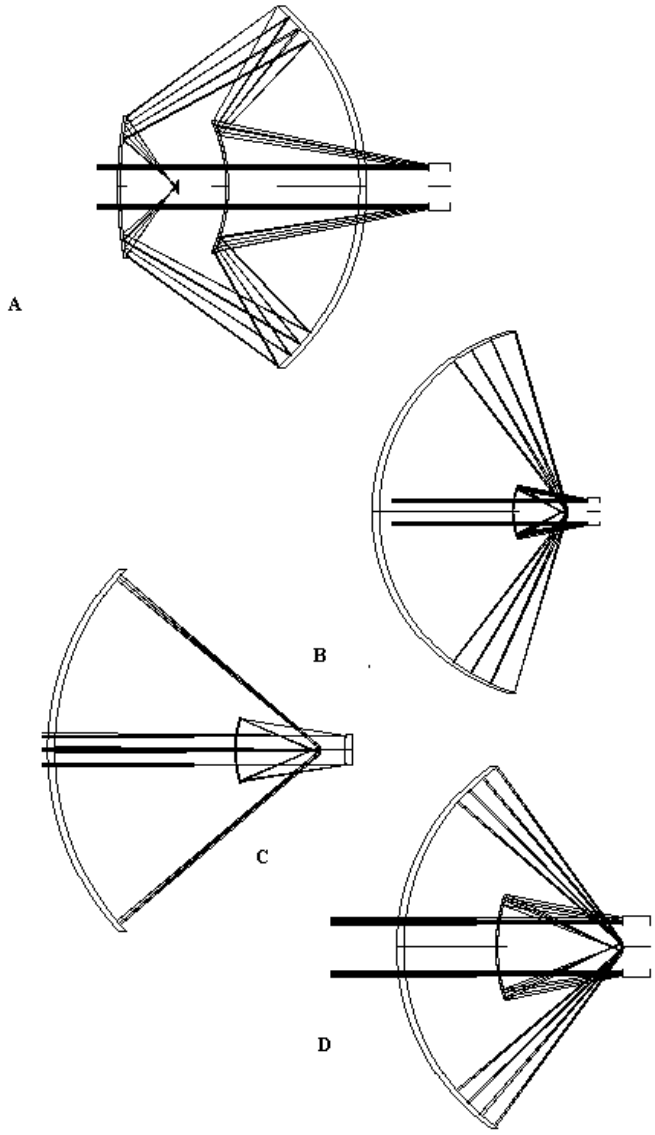


**Figure 5.9.2. CC-type convex-primary-mirror systems from the single available solution family are depicted here. All members of this family have relatively high numerical apertures.**

| System | R1 | t1 | R2 | t2 | R3 | t3 | R4 | t4 |
|---|---|---|---|---|---|---|---|---|
| **5.9.1** | -2.0 | -0.34005 | -3.33444 | 1.58416 | 1.41584 | -11.0188 | 11.2492 | 11.190 |
| **5.9.2.A** | 2.0 | -1.81005 | -1.42878 | 1.18685 | -2.18685 | -2.16756 | 3.71605 | 0.524 |
| **5.9.2.B** | 2.0 | -1.13005 | 1.11099 | 0.82160 | 0.17840 | -2.88205 | 2.89642 | 2.872 |
| **5.9.2.C** | 2.0 | -1.08005 | 1.11099 | 0.82612 | 0.17388 | -2.62531 | 2.64161 | 2.620 |
| **5.9.2.D** | 2.0 | -0.85005 | 1.11099 | 0.85118 | 0.14882 | -1.49641 | 1.52108 | 1.513 |

**Table 12. Optical design data for CC-type systems as shown in figures 5.9.1 and 5.9.2.**

# 6. Concluding comments

A closed-form analytical solution for four-spherical-mirror anastigmats has been derived and used to map out all possible solutions for four-spherical-mirror anastigmatic telescopes with concave or convex primary mirrors. This completes discovery of the full set of "simplest possible anastigmatic reflecting telescopes", a set that also includes two-conicoid-mirror systems and three-mirror systems with one conicoid.

For the case in which all optical elements are constrained to have no greater diameter than that of the entrance pupil, the four-spherical-mirror set as derived in section 2.2 and presented in chapter 3 can be considered to consist of five geometrically distinct families of solutions mapped over 3-space, the basis vectors of which are three constructional parameters of the system.

After exclusion of solutions that are deemed impractical because of large inter-element spacing or extremely large element diameters, there remain two sets of viable four-spherical-mirror anastigmats. These are both novel and unique systems; the analytical approach employed here has shown that no other possibilities exist for rotationally-symmetrical, four-spherical-mirror anastigmats with concave primary mirrors for the case in which no element is allowed to have a diameter that exceeds that of the entrance pupil.

In section 2.3 the four-spherical-mirror algorithm derived in section 2.2 was generalized to include four-mirror systems in which one, two or three mirrors are conicoids. The last case, deemed here the most trivial, is equivalent to Korsch's solution, where three conicoids are used to correct three Seidel aberrations.

An example of the application of the technique has been given in chapter 4, where an initial system with a useful first-order layout is corrected using one, two or three conicoids. Starting from a baseline solution with useful first-order properties, it has been shown that corresponding anastigmatic systems with useful first-order geometries can be found even in the case where the number of conicoid surfaces used to correct the three targeted Seidel aberrations has been reduced to one. Moreover, the technique utilized here has demonstrated the potential to produce useful and unexpected geometries that are not so closely related to the baseline geometry.

This technique is readily generalizable to systems of more than four mirrors, and to systems in which both the object and image conjugates are finite, and therefore is potentially useful to the design of reflecting systems for a wide range of applications.

A large number of solutions for four-spherical-mirror anastigmatic systems have been presented in chapter 5. The difference between these results and those of chapter 3 is that here elements were allowed to exceed the diameter of the entrance pupil by as much as 15 times. An immediate consequence of the relaxation of the constraint on diameter used in chapter 3 is that solutions with convex primary mirrors are considered. Eleven geometrically-distinct families of solution have been found to exist for convex-primary systems. Nine geometrically-distinct families of concave-primary-mirror type solutions have been found. The solution families include focal and afocal systems. Numerous solutions have been found that have zero Petzval curvature. Of the sixteen possible arrangements of four mirrors and focal plane mentioned in section 2.4, only the 42513 arrangement has not been found in this survey.

Together with the systems discussed in chapter 3, the systems described in chapter 5 represent the full range of available possibilities for four-spherical-mirror anastigmats with the object at infinity. Of the systems discussed in this thesis, only one has appeared in previously published work. This was an interesting system described by David Shafer (1988), which can now be seen to be a member of the AB-type convex-primary family of systems.

While many of these systems may seem somewhat impractical, the practicality or otherwise of a given system is strongly dependent on the application. The

main purpose of this work has been to define the range of possible solutions, a task that would be very difficult if not impossible to achieve if conventional optical design software was employed.

The method documented in this thesis illustrates the good results that can be achieved by combining an analytical approach to optical design problems with modern computing power to perform algebra that would have been impractical manually, as it would have had to have been when the Plate Diagram technique was originally developed. For certain classes of system this approach is clearly capable of providing superior global results to those that would be obtainable with modern optical-design software. The fact that this method has produced a large number of novel on-axis, all-spherical, anastigmatic optical designs, and simultaneously has shown that no others can exist, is a testament to the power of the technique.

It would be highly impractical if not impossible to achieve the results and comprehensive knowledge of solution space achieved here using ray tracing and global optimization algorithms alone.

# Appendix A: Four-mirror anastigmats I: A complete solution set for all-spherical telescopic systems

This paper was originally submitted to Optical Engineering in December 2006 and has been provisionally accepted, with a revised manuscript re-submitted in February 2007.

# Four-mirror anastigmats I: A complete solution set for all-spherical telescopic systems

Andrew Rakich [a,b]

[a]EOS Space Systems, 111 Canberra Ave, Griffith, ACT 2603, Australia
[b]Department of Physics and Astronomy, University of Canterbury, Private Bag 4800, Christchurch 8140, New Zealand

## ABSTRACT

The concept of the simplest possible reflecting anastigmat is discussed and anastigmats consisting of four spherical mirrors are introduced in this context as being the last remaining family for which the solution set has not been thoroughly explored. Burch's "Plate Diagram" method is introduced and used to derive a closed-form analytical solution for four-spherical-mirror anastigmatic telescope systems. This solution is then applied to mapping the solution space for four-spherical-mirror anastigmats. Two novel systems are discovered. These represent the first published instances of axially-symmetrical, all-spherical anastigmatic reflecting telescope designs with concave primary mirrors. Due to the completeness of the analytic description of the solution set presented here it can also be stated that there are no other design variants for this class of system.

## 1. INTRODUCTION

Technological advances have led to more interest in the field of multi-element, all-reflecting (i.e. catoptric), optical designs. While these designs are being driven by new demands for aberration correction, wavelength range, and in some cases the physical size of optical components, they are simultaneously being enabled by increasingly sophisticated manufacturing and alignment technologies. Two-mirror systems are limited both in their geometrical variety and potential for aberration correction. Since Paul's[1] development of the three-mirror anastigmat there has been a steadily growing interest in the field of multi-mirror catoptric systems. Today three-mirror anastigmats are increasingly finding applications in astronomy, the LSST[2] and JWST[3] being among the better- known examples.

Early examples of proposals for four-mirror telescope designs are given in Meinel et al.[4] and Robb[5]. With the new generation of Extremely Large Telescopes (ELTs) currently under development there is an increasing need to consider optical designs incorporating four or more mirrors. Reasons for this include the fact that refracting optical components
have a practical limit in size of approximately 1.5 m diameter, and that the magnitude of aberrations requiring correction, particularly in designs with spherical primaries, can not be accommodated with two-mirror designs. It has also been pointed out that four-mirror designs have the potential to place the image in a more favourable location than three-mirror designs. Several approaches to ELT designs using four mirrors have been published[6,7,8]. A comprehensive survey of published three- and four-mirror telescope designs is given by Wilson[9].

Some of the earliest optical designs for four-mirror imaging systems were those of Steele[10]. Steele's designs were achieved by combining pairs of two-mirror solutions. As one of several examples Steele presented a system comprised of a Cassegrain telescope as a "front-end" and a focal two-mirror system resembling the Schwarzschild flat-field anastigmat as a rear-end. In this work Steele was in fact investigating the design possibilities for catoptric microscope objectives, but the results are equally applicable to telescope systems. Later, Shafer[11] independently developed Steele's approach, generalizing it to include systems without axial symmetry and extending it to give exclusively all-spherical, unobscured anastigmatic solutions. For example, one design combined the Offner two-mirror, three-reflection anastigmatic system with an off-axis portion of an axially-symmetrical, concentric two-spherical-mirror anastigmat to give an unobstructed four-mirror, five-reflection anastigmatic system.

In most cases the designs referred to above have been achieved through one of two approaches. In the first case four-mirror systems are composed of sub-systems each of which is an anastigmat, or in the case of Ref. 10, at least corrected for spherical aberration. In the second case optical design software is used to arrive at solutions through optimization.

Analytical approaches to four-mirror system design have generally been regarded as too algebraically complex to be practical. Several authors have used analytical approaches to setting up systems of desirable first-order characteristics, and then resorted to optimization to correct aberrations[12,13,14]. In Ref. 13 Lerner et. al. stated that a closed-form analytical solution for a four-mirror lithography system was "not feasible".

Korsch[15] is the first case in the literature of a true closed form analytical solution for four-mirror anastigmatic telescope systems. This solution relies on $n$ conicoid surfaces to correct $n$ Seidel aberrations, following the well-known principle described by Wilson[16] as the "generalized Schwarzschild theorem". Puryayev et.al.[17] use an approach based on Fermat's theorem and the satisfaction of the Sine Condition for the case of a four-mirror aplanat, requiring two high-order aspheric surfaces to correct spherical aberration and coma to an arbitrary high-order. The authors in this case claim that they have extended their method to solve for third-order astigmatism at the same time, but they do not present the method.

It is interesting to note that of all the cases discussed above, only that of Shafer achieves anastigmatic performance in an all-spherical four-mirror system. Shafer's designs in Ref. 11. all differed from those described below in that they were all systems that were used off-axis in both field and pupil, giving unobscured systems, whereas the systems to be described below are all axially-symmetrical; the central field angle is co-axial with the system axis. As will be explained, these systems of four-spherical-mirrors are one of three families of "simplest possible" reflecting anastigmats.

## 2. SIMPLEST POSSIBLE REFLECTING ANASTIGMATS

In 1900 Aldis[18] showed that an optical system consisting of four spherical surfaces could produce an anastigmatic image. This work was later generalized by C.R. Burch[19,20,21] who showed that systems of two conicoid surfaces, three surfaces, one of which was a conicoid, or four spherical surfaces could all produce anastigmatic images. Burch's generalization of Aldis' work utilized a means of describing and manipulating the Seidel aberrations of an optical system in wavefront measure, which he termed the "Plate Diagram" analysis. Plate Diagram analysis lends itself naturally to the formulation of algebraic systems for multi-mirror telescopes, and a Plate Diagram based approach to determining four-mirror anastigmats will be described in detail in the following section.

Focal anastigmats consisting of two conicoid mirrors were completely described by Schwarzschild[22] in his classic optics papers of 1905. Two distinct families of solution exist, one with concave primary mirrors and the other with convex ones (figure 1). The Schwarzschild anastigmat set has two particularly interesting points on the solution curves, one representing a solution with a flat field (an anastigmat with zero Petzval curvature) and the other representing a special case where both mirrors are strictly spherical (figure 2).

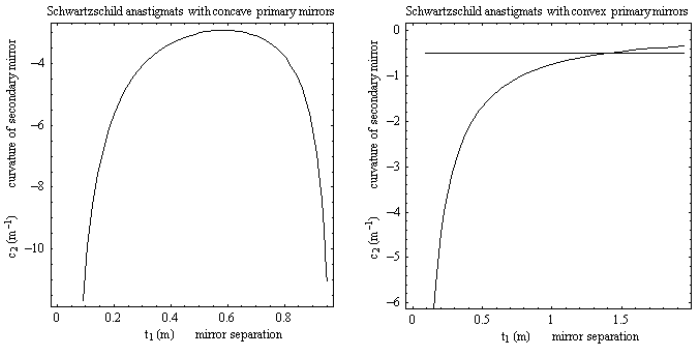


**Figure 1. These two plots represent the complete solution set for two-mirror or Schwarzschild anastigmats. In both cases the primary mirror has been set with a focal length of +/- 1 m (so $c_1$ = +/- 0.5 $m^{-1}$). In both cases the secondary mirrors are concave. The horizontal line in the right-hand plot intersects the solution curve at the point representing a flat-field anastigmat. In both cases the mirrors are, in general, conicoids.**

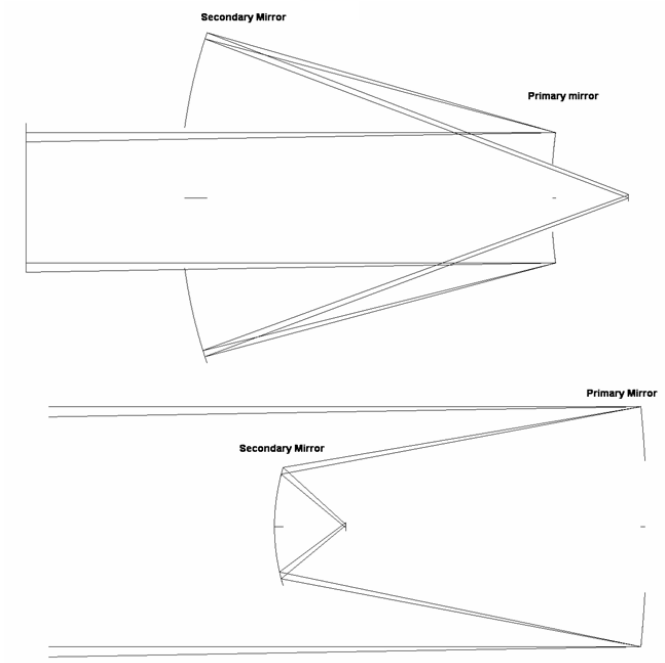


**Figure 2. Two examples of two-mirror anastigmats, similar to examples given by Schwarzschild. The upper system has a convex primary mirror, both mirrors are oblate spheroids and the Petzval curvature is zero. The lower system is a concave primary system. In his 1905 paper Schwarzschild reintroduced astigmatism to this system to flatten the field. As with all focal two-mirror anastigmats, the separation of the two mirrors is equal to twice the system focal length.**

In both of these cases the primary mirror is convex. The concave-primary solutions consist of two concave, aspheric mirrors. In all cases of two-mirror anastigmats the separation of the primary and secondary mirrors is necessarily twice the system focal length. Clearly, the range of advantageous geometries for two-mirror anastigmats is very limited.

Rakich and Rumsey[23] described the complete solution set for three-mirror anastigmats that consist of one conicoid and two spherical mirrors, in the case where the primary mirror was strictly concave. A representative sample of the solution set is given below (figure 3).

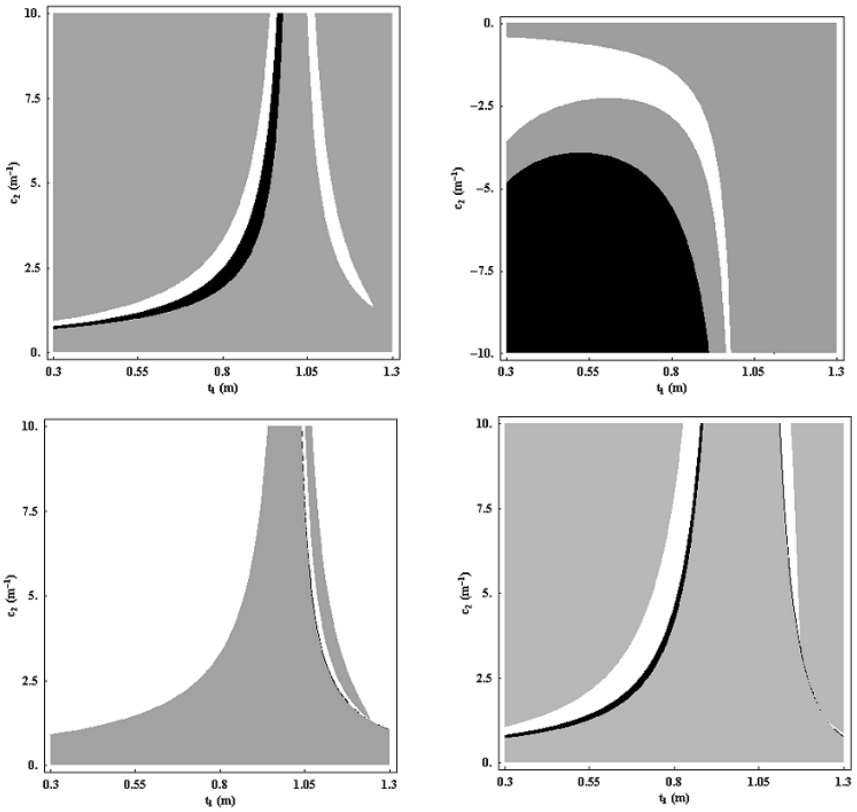


**Figure 3. These plots are four out of the seven plots representing the complete solution set for three-mirror anastigmats with two strictly spherical mirrors. In these plots solutions with positive Petzval curvature are plotted white and solutions with negative Petzval curvature are plotted black (gray points correspond to non-physical solutions). Hence flat-field solutions lie along loci where black and white regions abut directly onto each other. Clearly there are 4 families of flat-field three-mirror anastigmat with two spherical mirrors: only one of these appeared in the literature prior to this work.**

The solution set for simplest possible three-mirror anastigmats contains many more possible system geometries than the two-mirror solution set. In the three-mirror case the solutions occupy 2-dimensional regions of a parameter space defined by system constructional parameters. In this case two parameters were chosen; $t_1$, the separation of the primary and secondary mirrors, and $c_2$ , the curvature of the secondary mirror. The existence of seven geometrically-distinct families of solutions was revealed, with most of the families containing two or more geometrically-distinct "sub-families" of solutions.

These solution sets were obtained by first producing 7 distinct sets of equations, each of which gave, for given input values of $t_1$ and $c_2$, the remaining constructional parameters required to define an anastigmat. Then each of the 7 sets of equations was solved repeatedly for a large number of points in the $t_1$, $c_2$ plane, thus mapping solution sets. A modest amount of computing was able to produce every possible variant within this class of system, leading to the discovery of previously unknown forms of three-mirror anastigmat, including three previously unknown types of flat-field three-mirror anastigmat in which only one mirror is aspherised[24].

A similar method has now been applied to the problem of four-mirror anastigmats consisting entirely of spherical mirrors. The solution for four-spherical-mirror systems completes the Aldis-Burch "triplet" of simplest possible reflecting anastigmats; that is systems with two conicoid mirrors, systems with three mirrors, one of which is a conicoid, and four spherical mirrors. The derivation of the four-spherical-mirror solution and the results of its application to a survey of all possible such systems follow.

## 3. METHOD

### THE PLATE DIAGRAM.

Burch's Plate Diagram method has been used in deriving all the solutions discussed in this paper. The method has been described in detail elsewhere[19, 20, 21, 25], but it seems to be a largely forgotten analysis technique, particularly among the younger generation of optical designers, so a brief summary will be given here.

The Plate Diagram analysis of an optical system gives a system of Schmidt plates in collimated light which reproduce exactly the wavefront third-order aberration condition of a system consisting of any number of concave or convex, conicoid or spherical, refracting or reflecting optical surfaces and spaces. In this work we are limited to considering systems of mirrors.

Figure 4 shows how a spherical mirror can be replaced by an "anti-Schmidt plate" which contributes exactly the same aberrations as the mirror it replaces, without contributing any power. Third-order wavefront spherical aberration for a mirror in air with collimated incident light can be given as:

$$W = \frac{Nc^3 y_c^4}{4}, \tag{3.1}$$

where $c$ is the curvature of the spherical mirror and $y_c$ is the height of the marginal ray of the axial paraxial pencil on the mirror and $N$ is the refractive index of the space immediately preceding the mirror. The "strength" of the anti-Schmidt plate representing the spherical mirror can be thought of as $W$. In the case where the mirror is in convergent or divergent light an alternative expression must be used:

$$W = \frac{Nci^2 {y_c}^2}{4}. \tag{3.2}$$

Here $i$ is the angle of incidence of the marginal ray of the paraxial axial pencil on the mirror. Primary wavefront coma can be given as:

$$Coma = 4\frac{y_{pc}}{y_c}W, \tag{3.3}$$

and astigmatism as:

$$Astigmatism = 2\frac{y_{pc}^2}{y_c^2}W. \tag{3.4}$$

Here $y_{pc}$ is the height of the principal (chief) ray of the most oblique pencil, which will be zero if the stop position coincides with that of the plate representing the spherical mirror, and non-zero as the stop moves away from the plate. As can be seen from figure 5, $y_{pc}$ is directly proportional to $x$, the axial distance from the stop to the plate representing the mirror, so we have the following proportionalities:

$$Coma \propto xW, \tag{3.5}$$

$$Astigmatism \propto x^2 W. \tag{3.6}$$

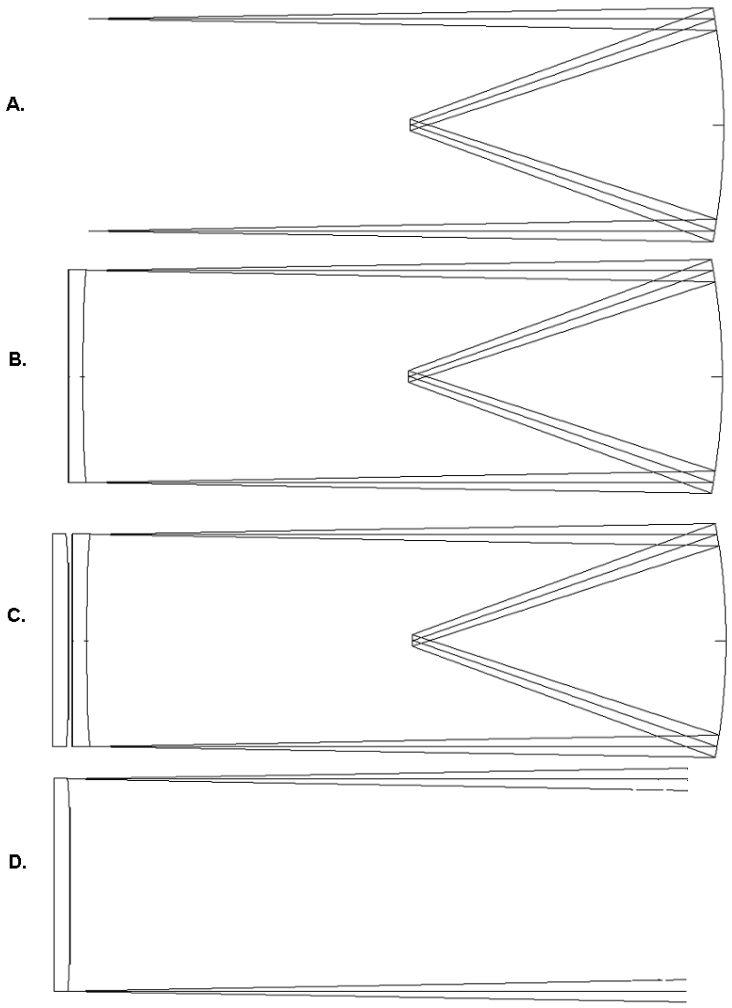


**Figure 4.**
**A. Spherical mirror with the aperture stop at the center of curvature. Coma and astigmatism free, but image suffers from spherical aberration over a curved field.**
**B. Introducing a Schmidt plate with a spherical contribution equal in magnitude and opposite in sign to that of the mirror, at the center of curvature, corrects spherical aberration. By the Stop-Shift Theorem, the stop can now be moved anywhere without re-introducing coma or astigmatism.**
**C. Introducing an "anti-Schmidt plate" cancels the correction described in B, returning the aberration condition to that of the original spherical mirror.**
**D. Removing the original spherical mirror and Schmidt correcting plate leaves the anti-Schmidt plate, giving the same aberrations as the original spherical mirror, including astigmatism and coma as the stop moves away from the plate.**

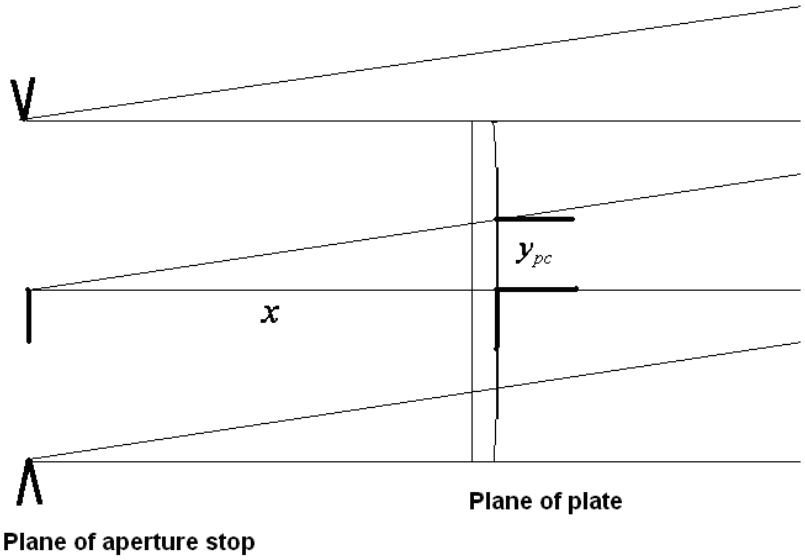


**Figure 5. As the plate is moved axially away from the stop, the height of the intercept of the principal ray of the most oblique pencil with the plate, $y_{pc}$, grows in direct proportion to the axial separation of the plate and the stop, $x$.**

In a similar way a conicoid mirror can be thought of as consisting of two plates. One plate represents the vertex sphere as described above, and the other plate represents the primary wavefront spherical aberration induced by the aspheric departure, given by:

$$W_{Conicoid} = \frac{kc^3 y_c^4}{4}. \tag{3.7}$$

Here $k$ represents the conic constant of the conicoid. This plate lies on the pole of the conicoid mirror. Coma and astigmatism introduced by this plate arise exactly as for the spherical mirror as described in equations 3.3 – 3.6.

For multiple-mirror telescope systems the positions of the plates are determined by imaging the center of curvature of spherical mirrors (or vertex spheres) and mirror poles in the case of conic contributions, into infinite conjugate space through all preceding elements in the system. Figure 6 gives an example of the Plate Diagram for a Paul three-mirror anastigmat.

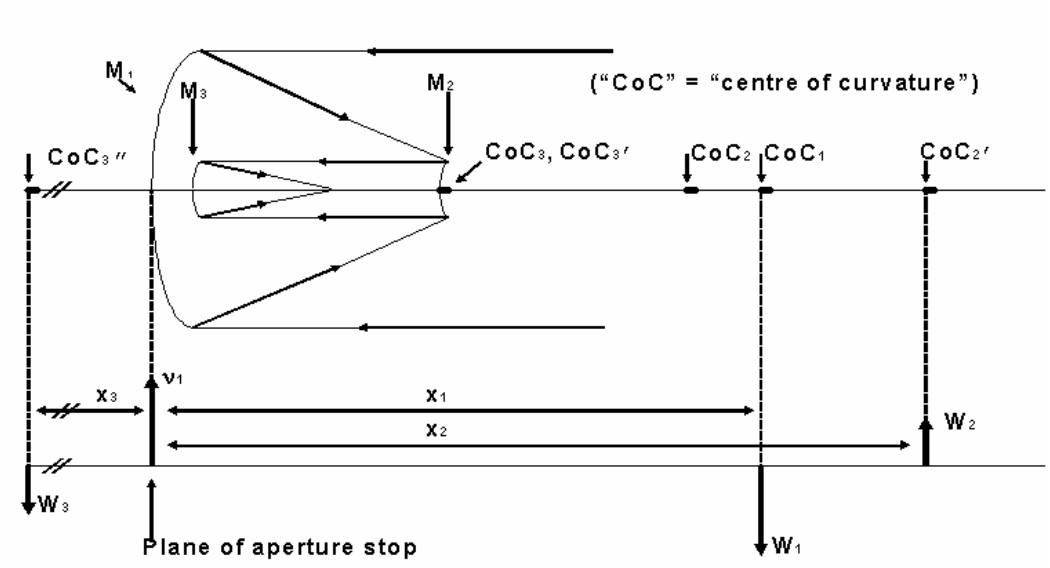


**Figure 6. Plate Diagram for a Paul three-mirror anastigmat. The primary mirror is a paraboloid giving rise to two plates, $W_1$ from the vertex sphere and $\nu_1$ from the conic departure. Note that the plates are of equal magnitude and opposite sign, consistent with the fact that the paraboloid has no spherical aberration. The plate representing the spherical secondary mirror, $W_2$, is in object space at $CoC_2$', the image of the center of curvature of the secondary mirror through the primary. Similarly the plate representing the spherical tertiary mirror, $W_3$ is at $CoC_3$", the image of the center of curvature of the tertiary mirror through the secondary, then the primary. Note that $W_2$ and $W_3$ are also equal in magnitude and opposite in sign, so the system spherical aberration is zero. Using the Plate Diagram it is a simple matter to prove that system sums for coma and astigmatism are also zero.**

With plate strengths and distances from the entrance-pupil evaluated for multiple mirrors it is a simple matter to determine the aberration condition of a multi-mirror system. The primary wavefront aberration contributions from each mirror are simply additive, so the system sum for each aberration can be given as:

$$Spherical_{SYS} = \sum_{i=1}^{n} W_i \tag{3.8}$$

$$Coma_{SYS} \propto \sum_{i=1}^{n} x_i W_i \tag{3.9}$$

$$Astigmatism_{SYS} \propto \sum_{i=1}^{n} x_i^2 W_i \tag{3.10}$$

Note that in using $x$ instead of $y_{pc}$ we are not solving for coma and astigmatism exactly. As our goal is to drive these aberrations to zero only their relative quantities are required. The extra step of calculation is not necessary. For actual values of coma and astigmatism equations 3.3 and 3.4 could be substituted into equations 3.9 and 3.10 respectively. In the methods outlined below, the system sums such as in equations 3.8-3.10 are simultaneously driven to zero to produce anastigmatic systems.

As a final point it should be noted that this approach gives systems that are valid in the "extended paraxial region", or in other words in a third-order approximation to the real aberration condition of an optical system. In general a system corrected for third-order aberrations will have residuals of high-order aberration that can be corrected in a variety of ways. For example, high-order asphericity may be added to element profiles, or positions and radii of spherical elements can be "tweaked" using optimization software, to re-introduce small amounts of third-order aberration that balances against high-order aberration in an optimum manner. While analytical approaches do exist that deal with "total aberration"[26] they are unsuitable for the sort of survey work that is described in this paper.

## FOUR SPHERICAL MIRRORS.

In the case of four spherical mirrors there are four plates, one for each of the mirrors. If the height of the marginal paraxial ray on the primary mirror is $y_1$ and the reciprocal of the radius of the primary is $c_1$, then the plate strength, $W_1$, of the plate replacing the primary mirror is given by equation 3.1:

$$W_1 = -\frac{N_1 c_1^3 y_1^4}{4} \tag{3.11}$$

Subsequent mirrors in the system will not in general be in collimated light so the plate strengths of these mirrors can be found using equation 3.2:

$$W_i = -\frac{N_i c_i i_i^2 y_i^4}{4} \tag{3.12}$$

where $i_i$ is the angle of incidence of the marginal paraxial ray and $N_i$ is the refractive index in the space immediately preceding the $i$ th mirror, following the convention for mirrors in air that the refractive index is of unit magnitude and changes sign on reflection.

Without loss of generality we can fix the radius of the primary mirror as $2\,m$ (unit focal length) and the diameter as 0.4 m. Then , by equation 3.11, we have:

$$W_1 = 0.00005m \tag{3.13}$$

Setting up the system of simultaneous equations described above gives:

$$0.00005m + W_2 + W_3 + W_4 = 0\text{ , (spherical aberration zeroed)} \tag{3.14}$$

$$0.00005m \times x_1 + W_2 x_2 + W_3 x_3 + W_4 x_4 = 0\text{ , (coma zeroed)} \tag{3.15}$$

$$0.00005m \times x_1^2 + W_2 x_2^2 + W_3 x_3^2 + W_4 x_4^2 = 0\text{ , (astigmatism zeroed)} \tag{3.16}$$

An interesting step at this point is the key to solving these equations. The position of the entrance-pupil is of fundamental importance to the plate equations, as all $x_i$ are measured from this. If we now state that the aperture stop for the system lies at the center of curvature of the quaternary mirror we can immediately simplify equations 3.15 and 3.16, as $x_4$ will be zero. It is important to note that while setting the position of the aperture stop is an important step in this formulation, the resultant anastigmat is not limited by this, as, by the Stop Shift Theorem[22], the aperture stop can later be placed anywhere in the system without disturbing the anastigmatic correction. Setting $x_4$ to zero, equations 3.15 and 3.16 can be rearranged to give:

$$W_3 x_3 = -W_2 x_2 - 0.00005m \times x_1 \tag{3.17}$$

$$W_3 x_3^2 = -W_2 x_2^2 - 0.00005m \times x_1^2 \tag{3.18}$$

At this point two further simplifications are made. Firstly the entrance-pupil position is set, and it can be set to any point in object space. By definition, the entrance-pupil position is the image in object space of the system stop, which has been set at the yet-to-be-located centre of curvature of the quaternary mirror. We are free to place the entrance-pupil anywhere in object space because at this point the secondary and tertiary mirrors are undefined.

If we define the entrance-pupil position as the axial distance from the pole of the primary mirror, and give it the symbol $\varepsilon$, we can immediately evaluate $x_1$ (which is simply $\varepsilon - R_1$, where $R_1$ is the radius of curvature of the primary mirror). At this point we also assign arbitrary values to $t_1$, the separation of primary and secondary mirrors, and $c_2$, the curvature of the secondary mirror. With these, $W_2$ and $x_2$ can be calculated using 3.12 and standard relationships in paraxial optics[27]. Now the right-hand sides of equations 3.17 and 3.18 can be completely evaluated.

This allows us to calculate $W_3$ and $x_3$ by first dividing equation 3.18 by 3.17 to give $x_3$ , and then dividing equation 3.17 by the newly-acquired value of $x_3$ to give $W_3$.

We now need to translate the plate quantities $x_3$ and $W_3$ back into optical-system constructional parameters. These are needed to determine the actual position of the center of curvature of the quaternary mirror, and finally the curvature of the quaternary mirror.

To proceed we make use of the following relationship:

$$W_3 = -\tfrac{1}{4} N_3 c_3 P_3^2 (u_3 - c_3 P_3)^2 \rightarrow -\tfrac{1}{4} N_3 c_3 P_3^2 (u_3 - c_3 P_3)^2 - W_3 = 0 \qquad (3.19)$$

Here $u_3$ is the angle that the marginal paraxial ray from the secondary to the tertiary mirror makes with the optical axis and $P_3$ is the length of the perpendicular to this ray from the center of curvature of the tertiary mirror. Equation 3.19 is cubic in $c_3$ and as all other quantities in equation 3.19 can be obtained from standard paraxial relationships, $c_3$ can immediately be evaluated. At this point the three solutions for the cubic are obtained.

With each of the three values of $c_3$ thus obtained, a different position of the center of curvature of the quaternary mirror can now be calculated by imaging the position of the entrance-pupil that was defined at an earlier stage back through mirrors $M_1, M_2$ and $M_3$. This determines the position of the center of curvature of the quaternary mirror. With the system up to the tertiary mirror defined (three times, once for each solution to equation 3.19) the quantities

$u_4$ and $P_4$ can be determined, and $W_4$ can be obtained from rearranging equation 3.14 and substituting in values for $W_3$ and $W_2$ obtained above to give :

$$W_4 = -(W_2 + W_3 + 0.00005m). \tag{3.20}$$

Now it only remains to formulate a similar cubic to equation 3.19 and solve for $c_4$:

$$W_4 = -\tfrac{1}{4} N_4 c_4 P_4^2 (u_4 - c_4 P_4)^2 \rightarrow -\tfrac{1}{4} N_4 c_4 P_4^2 (u_4 - c_4 P_4)^2 - W_4 = 0 \tag{3.21}$$

Again, there will be three solutions to this cubic in $c_4$.

To summarize, for each point in the three dimensional parameter space defined by $t_1, c_2$, and $\varepsilon$, there will be a total of nine geometrically-distinct anastigmatic systems, arising from the nine possible combinations of the solutions to equations 3.19 and 3.21.

This completes the derivation of the constructional parameters of nine distinct four-spherical-mirror anastigmats for given input values of $t_1, c_2$, and $\varepsilon$.

It is a useful precaution to use an independent check that anastigmatic solutions have indeed been reached at this point. In this case the author utilized Zemax© software to check that systems output by the algorithm described above did indeed have zero coefficients for third-order spherical aberration, coma and astigmatism. In practice this is a good way to determine whether any errors have been made in programming.

Using the method described above nine distinct anastigmatic solutions are obtained, because as we have seen, for each of the three values of $c_3$ there are three different values of $c_4$. These nine anastigmats can justifiably be thought of as belonging to geometrically-distinct families; the remaining members of each family can be found by repeating the method described above for a large number of different points, sampling the 3-space defined by $t_1, c_2$, and $\varepsilon$ with sufficient density as to map out the solution spaces. In this work searches were made within the following boundaries for the parameters $t_1, c_2$, and $\varepsilon$:

$$
\begin{aligned}
0.3\,m \le t_1 \le 1.7\,m, \\
-10\,m^{-1} \le c_2 \le 10\,m^{-1}, \\
-10\,m \le \varepsilon \le 10\,m.
\end{aligned}
\tag{3.22}
$$

Solutions occurring outside of those boundaries were considered to have either impractically large central obstructions or impractically high curvatures for the secondary mirror. In each case the sampling was such that at least 200 points were sampled for each basis vector. This was considered to be sufficiently dense sampling that the entire set of solutions for four-spherical-mirror anastigmats could be reliably mapped with a large but not unmanageable amount of computing.

## 4. RESULTS

It is interesting to note at this point that of the three four-plate systems referred to in the introduction, the two-conicoid mirror solutions lie along a curve in 2-parameter space (figure 1) and the three-mirror, one conicoid solutions lie in 2-dimensional regions (figure 3). Now we have four-spherical-mirror solutions occupying 3-dimensional solution spaces. While in each case there are four plates involved, in the case of systems with conicoid mirrors the two plates representing the conicoid have an extra element of coupling which effectively reduces the dimensionality of the solution space.

The solutions obtained in this way described in section 3 are not necessarily physically-realizable anastigmats. Physically-unrealizable solutions fall into two categories. In one, the solution involves at least one mirror located in a virtual space. Obviously in this case the systems are not physically practical. The other case is a result of the derivation given above requiring the solution of two cubic equations. Two of the three algebraic expressions for the solution of a cubic equation allow for a solution with an imaginary component. Any solutions with imaginary components will not be physically-realizable anastigmats.

The plot in figure 3 shows one map made in this way, in this case for three-mirror anastigmats with two spherical mirrors. In this map gray areas represent physically-unrealizable solutions, while white and black regions are possible anastigmats with positive and negative Petzval curvature respectively. While a large range of different system metrics could be plotted for the valid solutions, the Petzval curvature has been chosen in this case to allow for the ready identification of flat field solutions.

The mapping of four-spherical-mirror anastigmat sets has now been carried out. Of the nine distinct families of solution, four were empty sets when physically-unrealizable solutions were filtered out. The remaining five solution sets contain a large amount of data. Figure 7 is an example of several cross sections of one of the five three-dimensional solution sets. The "out of the page" axis represents $\varepsilon$, the entrance-pupil position parameter, and $t_1$ and $c_2$ are system parameters as defined for figures 1 and 3. As in figure 3, gray areas represent physically-unrealizable solutions, and white and black regions represent solutions with positive and negative Petzval curvature respectively.

Once a set of physically-realizable solutions is achieved, various conditions for practicality can be used to further refine the set, but the physically-realizable set represents the complete range of possible solutions, a truly global solution set.

Possible impracticalities include mirrors with huge diameters, large inter-mirror distances, and large or complete self-obstruction by system elements. Removing such systems from consideration is achieved by writing "filters" into the program used to map the solution space. This filtering approach can be implemented in many ways; for example one can specify a certain maximum acceptable central obstruction, mirror size, total system length, minimum back focal length etc. and these specifications can be written into the program producing the solution set as a series of logical operators.

When further filtering is introduced to remove systems with unfeasibly large element spacing and diameters the number of populated solution sets reduces to 2. It was initially reported[28] that there were no such viable solutions with usefully low central obstructions, but recent automation of the search process for low-obstruction systems has produced useful results. These systems represent the viable systems when axially-symmetrical systems are considered. Figures 8-11 contain examples of both afocal and focal systems of each solution type. Table 1 gives corresponding design parameters. As a result of the analytical approach taken in this work it can now be stated with certainty that the set of solutions represented by figure 8-11, and in table 1, are the only feasible all-spherical reflecting anastigmats with concave primary mirrors.

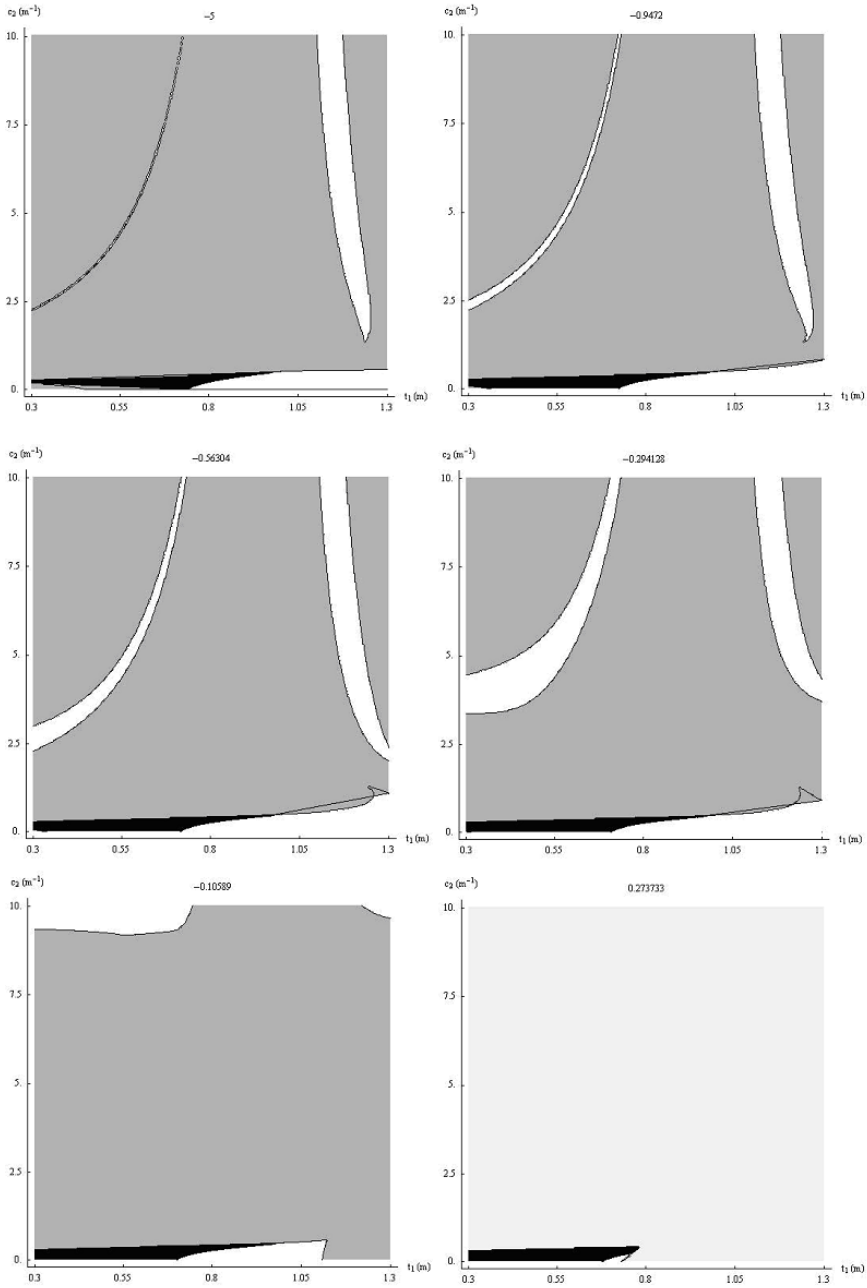


**Figure 7. A number of cross sections taken from one of the five solution families. The horizontal and vertical axes represent $t_1$ and $c_2$ respectively. The number in the center top of each plot is related to $\varepsilon$, the initial position of the entrance-pupil, for each cross section. White points represent solutions with positive Petzval curvature, black points systems with negative Petzval curvature. Flat field solutions lie along curves where white regions abut black regions.**

The linear central obstructions of the systems presented here range from 50% to 75%. With 50% central obstruction, the afocal system in figure 8A represents the minimum possible central obstruction for the class of system under discussion. This fact has been determined by successively eliminating systems while reducing the central obstruction allowed until finally only one solution point remains out of the 3-dimensional solution space. For focal systems of focal ratios less than f/15, the minimum-achievable linear central obstruction appears to be approximately 60% as represented by figure 9C.

As can be seen in figures 8 and 9, this first solution family has convex secondary mirrors, concave tertiary mirrors, and convex quaternary mirrors. The second solution family represented by figures 10 and 11 have concave secondary mirrors and convex tertiary and quaternary mirrors. These systems have slightly higher central obstructions: around 70% linear central obstruction at best.

It is interesting to note that the system shown in figure 8A is actually a system formed by coupling two pairs of concentric spherical anastigmats: the well known two-concentric-mirror-anastigmat with convex primary mirror and the less well know two- concentric-mirror-anastigmat with concave primary mirror that produces a virtual image. These pairs were discussed individually by Burch[20] and Rosin[29] and later by Shafer[11]. It is surprising that Shafer did not propose the more fundamental on-axis systems presented here, despite identifying both pairs of two-concentric-mirror anastigmats, and also proposing the concept of relaying the virtual image of the concave primary mirror version of the two-concentric-mirror anastigmat using either finite conjugate or afocal anastigmatic relay systems. Shafer, who was the first to present four-spherical-mirror anastigmatic systems, reported only off-axis systems, that is, systems in which both the central field angle and the entrance pupil were offset from the system axis (see Ref. 11).

Figure 8B represents a version of the four-spherical-mirror afocal system that does not consist of individually-anastigmatic two-mirror pairs. Similarly, the focal family of solutions as illustrated in figure 9 contains but is not limited to, solutions formed by pairs of individually-anastigmatic and concentric two-spherical-mirror systems.

Unlike the solutions in figures 8 and 9, the solutions in figures 10 and 11 do not have any versions that can be reduced to pairs of individually-anastigmatic two-mirror systems. There are no systems corresponding to these in the published literature.

It should be noted that all of these systems can be scaled in aperture without affecting their anastigmatic correction in the third-order aberration sense, though

the magnitude of high-order aberration residuals will of course change with this scaling.

Other practical systems can still be extracted from the large number of solutions produced by this survey. There exist a number of systems within the solution set that are excluded due to self-obstruction when considered as axially-symmetrical systems, but that yield systems with small or even zero self-obstruction when off-axis or multi-axis systems are considered. Figure 12 gives an example of one such Schiefspiegler system. In comparison to off-axis systems comprised of aspheric mirrors, there is a greatly reduced manufacturing and alignment difficulty associated with systems consisting of "off-axis" spherical mirrors, which of course remain spherical.

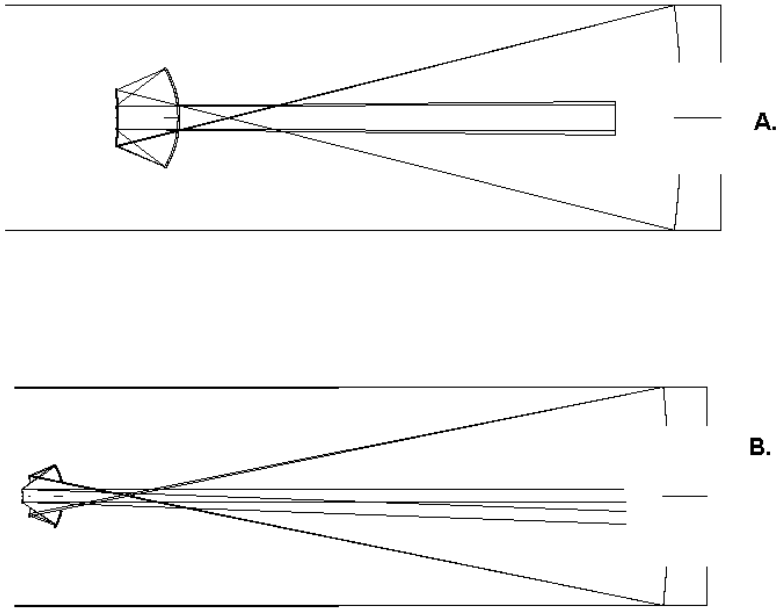


**Figure 8. Two afocal four-spherical-mirror anastigmats. System A is comprised of coupled pairs of two-concentric-spherical-mirror anastigmatic systems. The linear central obstruction of this system is 50%. System B is a more general version that can not be broken down into individually-anastigmatic sub-systems.**

While "shiefspiegler" literally means "oblique mirror", and was originally used to describe systems comprised of tilted mirrors that could not be derived from axially-symmetrical parent systems[30], it has come to mean reflecting telescope systems which are free from central obstruction. These can indeed be obtained by using mirrors that have been tilted with respect to the optical axis. However the common usage of the term Schiefspiegler also includes unobstructed systems that

are based on portions of parent systems that are symmetrical about some common axis. An axially-symmetrical parent system can be rendered as a Schiefspiegler by using an off-axis portion of the pupil, or by using only a small range of field points surrounding some off-axis field point, or by a combination of both of these approaches An interesting point to note about these Schiefspiegler systems is that as they are derived from axial-symmetric parent systems, the centers of curvature of the mirrors are collinear. This fact presents the opportunity for Schiefspiegler systems that can be brought into alignment with remarkable ease when compared to the general case, as will be discussed in detail in a future paper.

Also, systems with convex primary mirrors, while not deemed appropriate here for telescope systems, are still of interest for a variety of applications.

While a thorough investigation of the convex-primary and Schiefspiegler forms latent within the four-spherical-mirror on-axis system solution sets is beyond the scope of this paper, this topic is the subject of ongoing work and will be presented in a future publication.

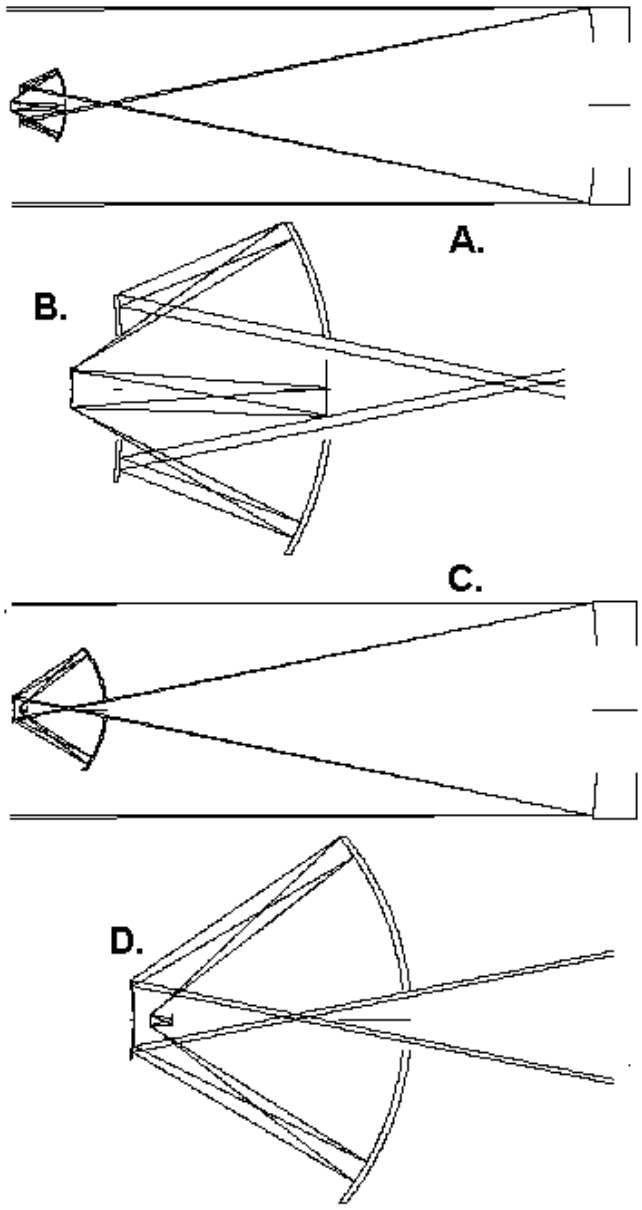


**Figure 9. Two examples of focal versions of the solution type shown in figure 8. Drawings B and D give an expanded view of the last three elements of systems A and C respectively. This solution type contains as special cases systems that are comprised of two pairs of concentric two-spherical-mirror anastigmats.**

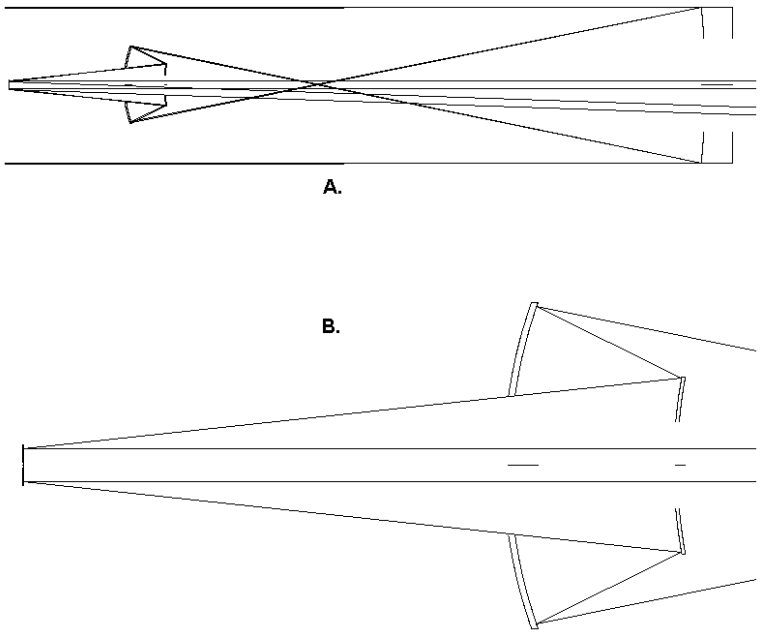


**Figure 10. An afocal four-spherical mirror anastigmat of the second kind. Unlike the solutions of figures 8 and 9, it has no special case that is comprised of coupled pairs of concentric mirrors.**

| | 8 A | 8 B | 9 A | 9 B | 10 | 11 A | 11 B |
|---|---|---|---|---|---|---|---|
| **R1** | −1.61838 | −2 | −2 | −2 | −2 | −2 | −2 |
| **T1** | −1.0 | −1.17050 | −1.17050 | −1.09550 | −1.49005 | −1.52005 | −1.51005 |
| **R2** | −0.61838 | −0.40401 | −0.40818 | −0.12618 | 0.29939 | 0.35087 | 0.35087 |
| **T2** | 0.10615 | 0.05809 | 0.09052 | 0.16859 | 0.10022 | 0.12631 | 0.12058 |
| **R3** | −0.17129 | −0.11475 | −0.15052 | −0.18226 | 0.30119 | 0.47371 | 0.57943 |
| **T3** | −0.10595 | −0.07272 | −0.11237 | −0.15859 | −0.39783 | −0.29493 | −0.27074 |
| **R4** | −0.06545 | −0.04015 | −0.03536 | −0.01375 | −0.18985 | −0.09802 | −0.07472 |
| **T4** | ∞ | ∞ | 0.11148 | 0.01289 | ∞ | 0.17378 | 0.09704 |

**Table 1. System parameters for the systems depicted in figures 8-11. Units are metres. R1-R4 are the radii of the primary – quaternary mirrors. T1–T4 are inter-mirror or in the case of T4, the mirror-focal plane separation. In each case the aperture stop has been set at the primary mirror, though as these systems are anastigmats the stop position can be set anywhere without affecting the correction of the third-order aberrations. The stop diameter (and hence that of the primary mirror) has been set at 0.4 m in all cases.**

## 5. CONCLUSION

A closed-form analytical solution for four-spherical-mirror anastigmats has been derived and used to map out all possible solutions for four-spherical-mirror anastigmatic telescopes with concave primary mirrors. This completes the set of simplest possible anastigmatic reflecting telescopes, a set that also includes two-conicoid-mirror systems and three-mirror systems with one conicoid. The four-spherical-mirror set as derived above can be considered to consist of five geometrically distinct families of solutions mapped over 3-space, the basis vectors of which are three constructional parameters of the system.

After exclusion of solutions that are deemed impractical due to large inter-element spacing or extremely large element diameters, there remain two sets of viable four-spherical mirror anastigmats. These are both novel and unique systems, the analytical approach employed here has shown that no other possibilities exist for rotationally-symmetrical, four- spherical-mirror anastigmats with concave primary mirrors.

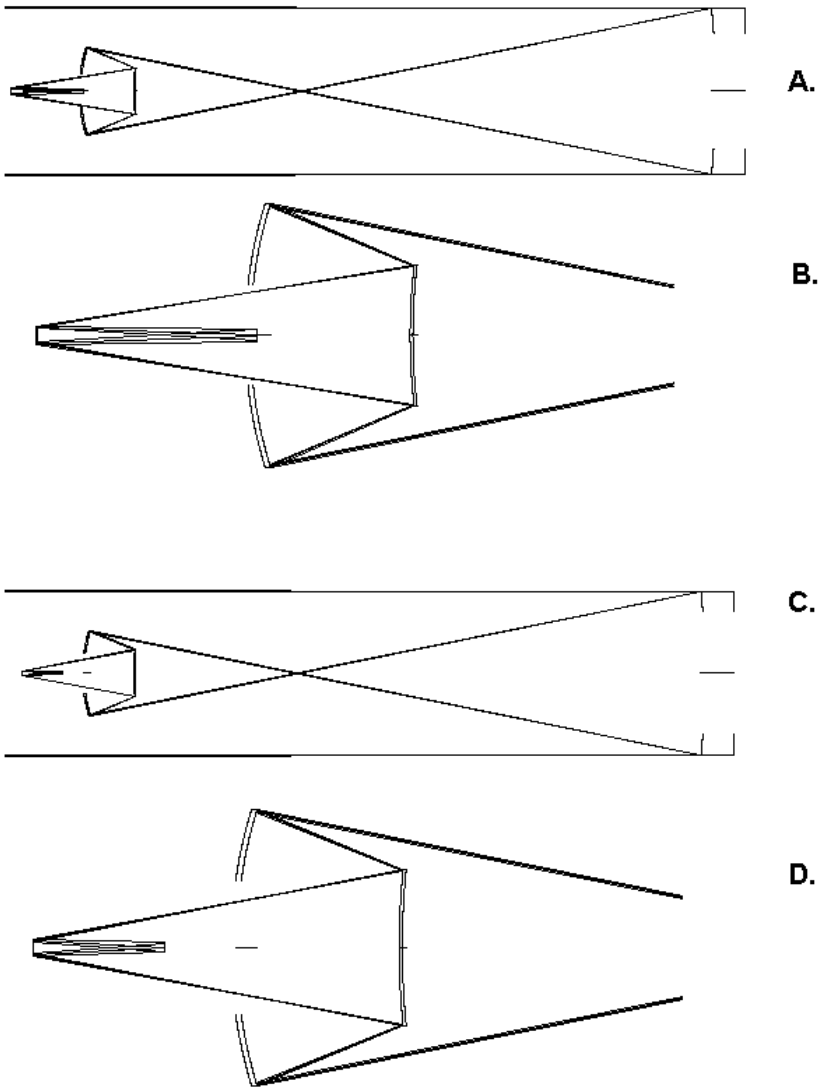


**Figure 11. Focal versions of the second type of solution as shown in figure 10. Drawings B and D give an expanded view of the last three elements of systems A and C respectively. There is a continuum of solutions with focal ratios ranging from the afocal case down to about f/8 (for the scale given for these systems). In practice the image could be picked off to a more convenient location with a fold mirror. This type of system in general suffers from less high-order aberration than the systems shown in figures 8 and 9. The minimum linear central obstructions achievable with this type of system are of the order of 67%.**

Ongoing investigation of the solution set will be aimed at extracting useful Schiefspiegler and multi-axis systems from the large number of possibilities. It is

expected that a survey off the full solution set for useful Schiefspiegler forms will result in the discovery of additional practical solutions.

Further work will also be done to identify potentially useful systems with convex primary mirrors.

The method documented here illustrates the good results that can be achieved by combining an analytical approach to optical design problems with modern computing power. For certain classes of

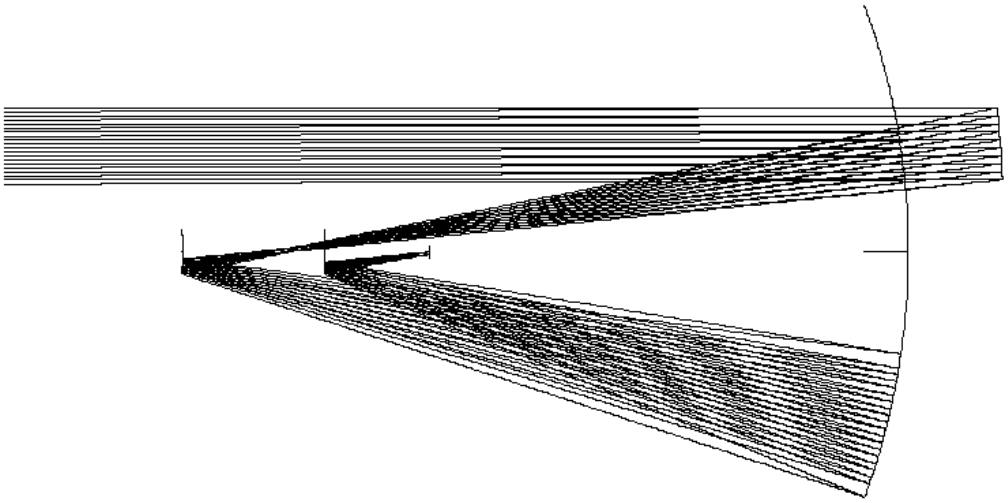

**Figure 12. An example of a four-spherical-mirror anastigmatic Schiefspiegler. Numerous examples of anastigmatic Schiefspiegler are likely to be uncovered Schiefspiegler-oriented sifting of the solution sets.**

system this approach is clearly capable of providing superior global results to those that would be obtainable with modern optical-design software. The fact that this method has produced the apparently novel on-axis, all-spherical, concave-primary-mirror anastigmatic optical designs, and simultaneously has shown that no others can exist, is a testament to the power of the technique.

It would be highly impractical if not impossible to achieve the results and comprehensive knowledge of solution space achieved here using ray tracing and global optimization algorithms alone.

**ACKNOWLEDGEMENT**

I take this opportunity to pay tribute to Mr. Norman Rumsey, a great friend and mentor, who died in January 2007. Norman has been teaching me optics since 1990 and none of my work in this field would have been possible without his patient guidance, based on his profound knowledge of the history, development and use of optical aberration theory.

## REFERENCES


1. M. Paul, “Systèmes correcteurs pour réflecteurs astronomiques”, Rev. d’Optique, **14**, pp. 169-202, 1935
2. M. Liang., L. Seppala, D. Sweeney, LSST Project Team, "The LSST Optical System," AAS Meeting 207, #26.20; Bulletin of the American Astronomical Society, **37**, p.1205, 2005
3. John Nella *et. al.*, “James Webb Space Telescope (JWST) Observatory architecture and performance”, *Proc. SPIE*, **5487**, pp 576-587, 2004
4. Aden B. Meinel, Majorie P. Meinel, Ding-Qiang Su, Ya-Nan Wang, “Four-mirror, spherical-primary submillimeter telescope design”, *Appl. Op.*, **23**, No. 17, 1984
5. P. Robb, “Three-mirror telescopes: design and optimization”, *Appl. Opt.*, **17**, 2677, 1978
6. A. Goncharov, “Optical Design for Advanced Extremely Large Telescopes”, *Proc. SPIE*, **5489**, pp. 518-525, 2004
7. R. N. Wilson, B. Delabre, “A new 4-mirror optical concept for very large telescope with spherical primary and secondary mirrors, giving excellent field and obstruction characteristics”, *Proc. SPIE*, **2199**, pp. 1052-1062, 1994.
8. R. Gilmozzi et al., “The future of filled aperture telescopes: Is a 100 m feasible?”, *Proc. SPIE*, **3352**, p. 778, 1998.
9. R.N. Wilson, “Reflecting Telescope Optics, I”, 2nd ed., §3.6.5, Springer-Verlag, Berlin-
   Heidelberg, November, 2003
10. W.H. Steele, “Etude des effets combinés des aberrations et d’une obturation centrale de la pupille sur les images. Application aux objectifs de microscope miroirs.”, *Thèses Soc. Phys. Paris*, Ser. A **2511**, No. 3383, 1953
11. D.R. Shafer, “Four-mirror unobscured anastigmatic telescopes with all-spherical surfaces”, *Appl. Op.*, **17**, No. 7, 1978
12. Joseph M. Howard, Bryan D. Stone, “Imaging with four spherical mirrors”, *Appl. Opt.*, **39**, No. 19, pp. 3232-3242, 2000.
13. Scott A. Lerner, Jose M. Sasian, Michael R. Descour, “Design approach and comparison of projection cameras for EUV lithography.”, *Opt. Eng.*, **39**, 3, pp. 792-802, 2000
14. M. F. Bal, F. Bociort, J. J. M. Braat, "Analysis, Search, and Classification for Reflective Ring-Field Projection Systems ," *Appl. Opt.* **42**, pp 2301-2311, 2003
15. D. Korsch, “Reflective Optics”, Academic Press, San Diego, 1991
16. R. N. Wilson, “Karl Schwarzschild lecture of the German Astronomical Society.”, *Reviews in Modern Astronomy*, **7**, 1, 1993.

17. Daniil T. Puryayev, Alexander V. Gontcharov, “Aplanatic four-mirror system for optical telescopes with a spherical primary mirror.”, *Opt. Eng.*, **37**, No. 8, pp. 2334-2342, 1998.
18. H.L. Aldis, “On the construction of photographic objectives”, *Photographic Journal*, **24**, pp. 291-299, 1900
19. C.R. Burch, “On the optical see-saw diagram”, *MNRAS*, **102**, pp. 159-165, 1942
20. C.R. Burch, “On aspheric anastigmatic systems”, *Proc. Phys. Soc.*, **55**, pp. 433-444, 1943
21. C.R. Burch, “Application of the Plate Diagram to reflecting telescope design”, *Optica Acta*, **26**, pp. 493-504, 1979
22. K. Schwarzschild, “Untersuchungen zur geometrischen optik I, II”, Göttinger Abh, Neue Folge, Band IV, No.1, 1905
23. A. Rakich, N.J. Rumsey, “A method for deriving the complete solution set for three-mirror anastigmatic telescopes with two spherical mirrors”, *JOSA A*, **19**, No. 7, pp. 1398-1405, 2002
24. A. Rakich, “Four families of flat-field three-mirror anastigmatic telescopes with only one mirror aspherised”, *Proc. SPIE*, **4768**, pp. 32-40, 2002
25. E.H. Linfoot, “Recent advances in optics”, Clarendon Press, Oxford, pp. 229-259, 1955
26. W. Welford, “Aberrations of the Symmetrical Optical System”, pp 143-170, Academic Press, London, 1974.
27. V. Mahajan, “Optical Imaging and Aberrations: Part 1. Ray Geometrical Optics”, pp 73-84, SPIE, Bellingham, Washington, 1998
28. A. Rakich, “Complete solution set for four-spherical-mirror anastigmatic telescope systems”, *Proc. SPIE*, **5249**, pp. 103-111, 2004
29. S. Rosin, “Inverse Cassegrain systems” *Appl. Op.*, **7**, No. 8., pp. 1483-1497, 1968
30. A. Kutter, “Der Schiefspiegler”, Verlag, Biberach, 1953.

# Appendix B: Four-mirror anastigmats II: A complete solution set for all-spherical telescopic systems

This paper was originally submitted to Optical Engineering in December 2006 and has been provisionally accepted with some revisions required.

# Four-mirror anastigmats II: Useful first-order layouts and minimum complexity.

Andrew Rakich [a,b.]
[a]EOS Space Systems, 111 Canberra Ave, Griffith, ACT 2603, Australia
[b]Department of Physics and Astronomy, Canterbury University, Private Bag 4800, Christchurch 8140, New Zealand

**ABSTRACT**

In the first paper of this series the author described a closed-form analytical approach to obtaining the complete solution set for four-mirror anastigmats in which all the mirrors were spherical. Two novel types of four-spherical-mirror anastigmat with concave primary were reported. This approach has been modified by setting up baseline systems with good first-order characteristics and adding the minimum number of aspheres necessary to provide anastigmatic correction. In this way, searches for useful four-mirror anastigmats with one, two or three-mirrors kept strictly spherical have been carried out. The example given in this paper shows that by using this technique a system with only one conicoid mirror can be found which has very similar first-order properties and equivalent correction to a system with three conicoids.

**Keywords: anastigmat, reflecting telescope, four-mirror, Schiefspiegler**

## 1. INTRODUCTION

In the first paper of this series the author produced an analytical solution for four-spherical mirror anastigmats with concave primary mirrors[1,2]. Nine distinct solutions were derived for each point in a 3-dimensional parameter space. The solution was applied iteratively over the 3-dimensional parameter space to map every possible solution for four-spherical mirror anastigmatic systems with concave primary mirrors.

This was the second example of an analytical solution for four-mirror systems in the published literature[3,4] and the only one that deals with four-spherical mirror anastigmatic telescopes. It was found that there were two types of axially-symmetric systems of practical interest. At the time of writing Ref. 1 no valid systems had been found, but a refined search method uncovered the two solution sets and these are reported in Ref. 2.

This paper has taken a different approach to obtaining useful four-mirror anastigmatic systems using an analytical method. Here the global solution technique previously developed for four-spherical mirror systems has been generalized to accommodate four-mirror systems with one or more conicoid surfaces.

Using this method, a practical unobstructed first-order layout is first produced. Using this baseline system, analytical solutions are first derived and then applied to find anastigmatic systems utilizing a decreasing numbers of conicoid surfaces (but retaining four-mirrors in all cases). In this way, systems with useful on-axis geometries and minimum optical complexity are uncovered. In the following section a brief description of the plate diagram method will be provided, followed by an outline of the technique used to solve for several cases of four-mirror telescopes with decreasing numbers of conicoids. These cases are:

• Four mirrors: three conicoids (with a spherical primary). This relatively trivial solution involves setting up an exact first-order layout, then solving for the three conic constants required to eliminate primary spherical aberration, coma and astigmatism. This set is included here as an interesting example of the relative simplicity of the method.

• Four mirrors: two conicoids. In this system two conic constants on two mirrors of fixed radii and position, together with the position and curvature of the quaternary mirror are free to vary. In this case three 1-dimensional solution sets are obtained.

• Four mirrors: one conicoid, the conic constant on the secondary mirror is allowed to vary. Also the tertiary and quaternary mirrors are free to vary in position and curvature. Three 2-dimensional solution sets in 2-parameter space are obtained.

The results obtained in the following examples show that the analytical method is capable of giving useful results similar to the baseline system as well as unexpected and potentially useful variants. The final section will consist of a brief discussion of these results.

## 2. METHOD

**THE PLATE DIAGRAM.**

Burch's "Plate Diagram method", a generalization of earlier work by Aldis[5], has been used to formulate the analytical solutions in this paper. The method has been described in detail elsewhere[1,2,.5,6,7,8,9] , and in particular section 3 of Ref. 2 describes the use of a plate diagram based approach to deriving solutions for four-spherical-mirror anastigmats. Only the briefest of summaries of the Plate Diagram method will be given here.

The Plate Diagram method utilizes a transformation in which systems of powered spherical or conicoid mirrors are converted to afocal systems comprised of zero-powered Schmidt plates. In these plate systems each plate gives an equal contribution to the third order system aberration sum as the spherical mirror or conicoid surface it replaces. A spherical mirror can be replaced with one plate, which lies at its centre of curvature if it is the primary mirror, or at the image of the centre of curvature in object space for subsequent mirrors in the system. A conicoid mirror is represented by two plates, one representing the vertex sphere as above, and the other representing the conicoid figure. The conicoid replacement plate lies either at the pole of the primary mirror or at the image of the pole of the mirror in object space for subsequent mirrors in the system.

These afocal systems replicate exactly the primary aberrations of the original powered systems that they have replaced, but allow for a relatively simple analytical treatment of the system aberration sums, as will be shown below. In all cases the assumption is made that these systems are operating in air.

To start with we consider a spherical mirror, with a primary spherical aberration coefficient in wavefront measure given by:

$$W = \frac{c^3 y_c^4}{4} \text{ in collimated incident light,}$$

$$\text{or } W = \frac{c i^2 y_c{}^2}{4} \text{ in non-collimated incident light.} \qquad (2.1)$$

Here $c$ is the curvature of the spherical mirror and $y_c$ is the height of the marginal ray of the axial paraxial pencil on the mirror and $i$ is the angle of incidence of the marginal ray of the paraxial axial pencil on the mirror. The "strength" of the Schmidt plate representing the spherical mirror can be thought of as $W$.

The plate representing a conicoid figure has a "strength", or primary wavefront spherical aberration coefficient given by:

$$W_k = \frac{kc^3 y_c^4}{4}. \tag{2.2}$$

Here $k$ represents the conic constant of the conicoid.

For multiple mirror telescope systems the positions of the plates are determined by imaging the center of curvature of spherical mirrors (or vertex spheres and mirror poles in the case of conic surface contributions), into infinite conjugate space ("star space" in Burch's terminology) through all preceding elements in the system. In the case where no infinite conjugate space exists naturally in the optical system, it is a simple matter to create one artificially for the purposes of the analysis, and this can be done without in any way modifying the properties of the system under investigation.

It can be shown[5,6,9] that the system sums of primary wavefront aberration coefficients for a system of $n$ plates arising from $n-a$ spherical mirrors and $\frac{a}{2}$ conicoid mirrors (where $n$ and $a$ are positive integers and $\frac{a}{2} \le n$) can be given as:

$$Spherical_{SYS} = \sum_{i=1}^{n} W_i \tag{2.3}$$

$$C_1 \times Coma_{SYS} = \sum_{i=1}^{n} x_i W_i \tag{2.4}$$

$$C_2 \times Astigmatism_{SYS} = \sum_{i=1}^{n} x_i^2 W_i \tag{2.5}$$

Here $x$ is the distance of the plate $W$ from the entrance pupil position. Note that equations 2.4 and 2.5 give system sums that are proportional to the respective aberrations through the constants $C_1$ and $C_2$ respectively. While it would be a simple extension to obtain actual values for system coma and astigmatism, our goal is to drive these aberrations to zero so only their relative quantities are required. The extra step of calculation is not necessary and the proportionality constants drop out in the next step of calculation and so can be ignored. In the methods outlined below, the system sums in 2.3-2.5 are simultaneously driven to zero to produce anastigmatic systems.

Note that while the systems derived below are corrected for primary, or third-order, aberrations, there will commonly be some residual of higher-order aberrations. In practice, and particularly for catoptric systems, fine tuning a third-order solution by optimization with optical design software and allowing the re-introduction of small amounts of third-order aberration to balance optimally against high-order residuals will lead to a well-corrected system that differs very little from the pure third-order solution. The third-order approximation to a baseline system is much better than the first-order approximation in this sense.

## 3. EXAMPLES

### FOUR-MIRRORS; THREE CONICOIDS.

The first case considered is the almost trivial case of four-mirrors with three of these mirrors being conicoids. Here we set up a system of spherical mirrors with a useful first-order layout such as that shown in figure 1. System constructional parameters for this and subsequent systems are given in table 1. Then three-mirrors are allowed to become conicoids and conic constants are found that simultaneously zero spherical aberration, coma and astigmatism. This is a trivial exercise in a modern ray-tracing program but the plate diagram approach is included here as an example.

With the radii and positions of the four-mirrors set we can immediately calculate plate strengths and positions in object space using equations 2.1, 2.2 and simple paraxial optics. Setting the position of the entrance pupil to any convenient location allows us to calculate $x_i$ and hence system sums for spherical aberration, coma and astigmatism following equations 2.3 – 2.5. To obtain the necessary combination of conicoids required for anastigmatic correction it is simply a matter of formulating and solving the following linear system of plate equations for $W_{ki}$, using standard paraxial optics relationships to determine the fixed values of $x_i$:

$$W_{k2} + W_{k3} + W_{k4} = -Spherical_{SYS} \tag{2.6}$$

$$x_{k2}W_{k2} + x_{k3}W_{k3} + x_{k4}W_{k4} = -C_1 \times Coma_{SYS} \tag{2.7}$$

$$x_{k2}^2W_{k2} + x_{k3}^2W_{k3} + x_{k4}^2W_{k4} = -C_2 \times Astigmatism_{SYS} \tag{2.8}$$

Here we have set up the system to have a spherical primary mirror, but in practice any of the four mirrors could be chosen to remain spherical. It then simply remains to rearrange equation 2.2 to obtain the three values of $k_i$. For the spherical primary example given in figure 1 these $k_i$ are; $k_2 = 3.166, k_3 = -0.351$ and $k_4 = -0.267$. The simplicity of this approach

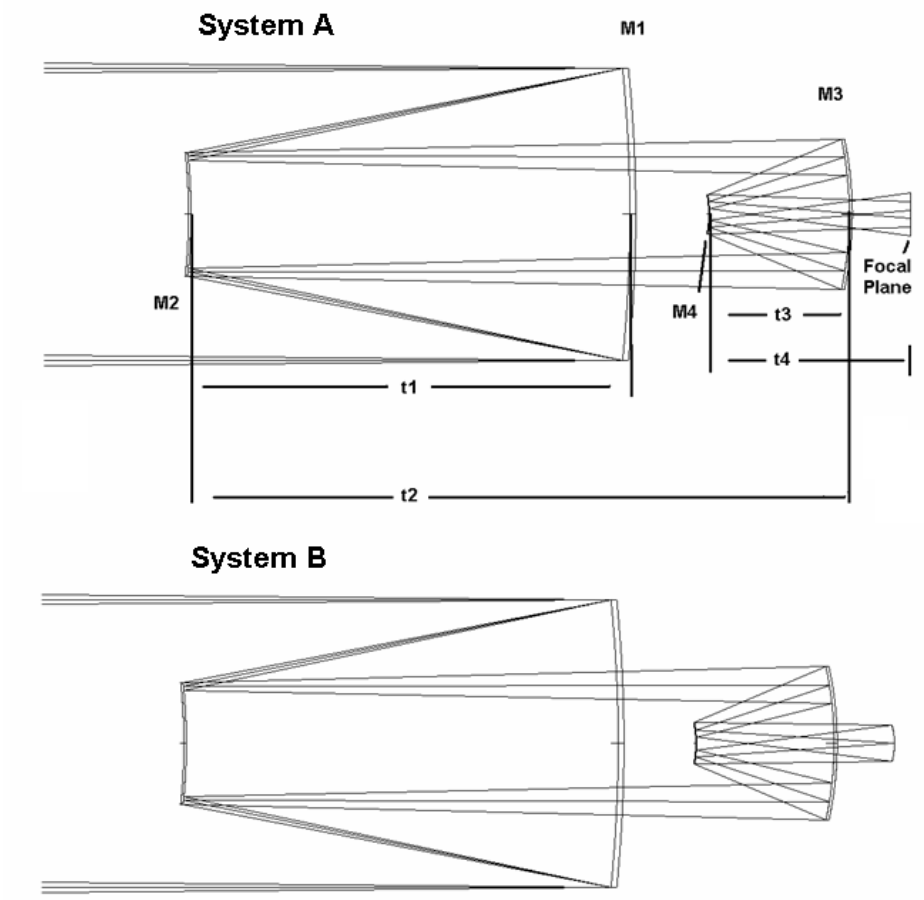


**Figure 1. First-order layout using spherical mirrors initially, giving a useful geometry but requiring three conicoids for anastigmatic correction. System A represents the first-order layout which can be seen to have large spherical aberration at the focal plane. In system B primary spherical aberration, coma and astigmatism have been corrected by an appropriate choice of conicoids. The three conicoid system parameters are given in table 1.**

compares favourably to that given by Korsch[3,4]. Furthermore, Korsch's approach required $n$ conicoid surfaces to correct $n$ Seidel aberrations, according to what Wilson describes as "the generalized Schwarzschild Theroem"[10]. The next two examples give examples of analytical solutions for systems in which $n$ Seidel aberrations are corrected with less than $n$ conicoid surfaces.

**FOUR-MIRRORS; TWO CONICOIDS.**

In this example two mirrors, the primary and quaternary mirrors, will remain strictly spherical. The secondary and tertiary mirrors are allowed to be conicoids.

To achieve anastigmatic correction the position and curvature of the quaternary mirror must be varied. This is only one of six possible arrangements of two conicoids amongst four mirrors, but serves as a representative example. In this case we will start with the primary, secondary and tertiary mirrors retaining some arbitrary but promising first-order layout, such as in the configuration given in figure 1. We then will solve for the position and radius of the quaternary mirror.

To proceed we imagine that the aperture stop is placed at the center of curvature of the quaternary mirror. Also, we assign some arbitrary position to the entrance pupil, which after imaging through primary, secondary and tertiary mirrors, will locate the center of curvature of the quaternary mirror. In this way, equations 2.7 and 2.8 are reduced to:

$$x_{k2}W_{k2} + x_{k3}W_{k3} = -C_1 \times Coma_{SYS} \tag{2.9}$$

$$x_{k2}^2W_{k2} + x_{k3}^2W_{k3} = -C_2 \times Astigmatism_{SYS} \tag{2.10}$$

That is, only contributions from the two conicoids provide variables to balance against system coma and astigmatism; by placing the stop on the center of curvature of the quaternary mirror the $x$ value for the plate associated with this mirror is now zero so its coma and astigmatism contributions are necessarily zero. Note that here $-Coma_{SYS}$ and $-Astigmatism_{SYS}$ are values calculated from the spherical primary and vertex spheres of the secondary and tertiary mirrors. Values of $x_{ki}$ can be obtained and equations 2.7 and 2.8 can be used to solve for $W_{ki}$ and hence, using equation 2.7, for $k_2$ and $k_3$. Using the values of $W_{ki}$ thus obtained we can now solve for the spherical aberration contribution of the quaternary mirror by rearranging equation 2.6 (and substituting $W_{quat}$ for $W_{k4}$ in this case):

$$W_{quat} = -Spherical_{SYS} - W_{k2} - W_{k3} \tag{2.11}$$

Now we have the position of the center of curvature of the quaternary mirror (from setting the initial position of the entrance pupil) and the spherical aberration contribution of the quaternary mirror from equation 2.11. Also, by simple paraxial optics we have $u_4$, the angle the marginal ray of the axial paraxial pencil makes with the axis after reflection from the tertiary. We can also calculate a quantity, $P$, which is the length of the perpendicular from the center of curvature of the quaternary mirror to the marginal ray of the axial paraxial pencil after reflection from the tertiary mirror. Using these, and the following relationship;

$$W_{quat} = -\tfrac{1}{4}c_4P^2(u_4 - c_4P)^2 \quad . \tag{2.12}$$

we can obtain the following cubic equation in $c_4$ (the curvature of the quaternary mirror):

$$-\tfrac{1}{4}c_4P^2(u_4-c_4P)^2-W_{quat}=0 \tag{2.13}$$

If we define:

$$a_0=\frac{-4W_{quat}}{P_4^4};\ a_1=\frac{u_4}{P_4^2};\ a_2=\frac{2u_4}{P_4}, \tag{2.14}$$

and further define:

$$Y=3a_1-a_2^2;\ Z=-27a_0+9a_1a_2-a_3^2;\ Q=\sqrt{4Y^3+Z^2}, \tag{2.15}$$

then the three solutions to 2.13 can be compactly expressed as:

$$SA=\frac{-a^2}{3}-\frac{\sqrt[3]{2}Y}{3\sqrt[3]{Z+Q}}+\frac{\sqrt[3]{Z+Q}}{3\sqrt[3]{2}} \tag{2.16}$$

$$SB=\frac{-a^2}{3}+\frac{(1-i\sqrt{3})Y}{3\sqrt[3]{4(Z+Q)}}-\frac{(1+i\sqrt{3})\sqrt[3]{Z+Q}}{6\sqrt[3]{2}} \tag{2.17}$$

$$SC=\frac{-a^2}{3}+\frac{(1+i\sqrt{3})Y}{3\sqrt[3]{4(Z+Q)}}-\frac{(1-i\sqrt{3})\sqrt[3]{Z+Q}}{6\sqrt[3]{2}}. \tag{2.18}$$

Using these three solutions, for each initial position of the entrance pupil (and therefore the position of center of curvature of the quaternary mirror) we obtain a maximum of three distinct anastigmatic telescopes. These telescopes differ only in the position and curvature of the quaternary mirror (and hence in other related parameters such as f/#, Petzval curvature and central obscuration). It remains to scan through the available solution space and build up a curve representing

available solutions. Figure 2 shows these solution curves in 2-parameter space;

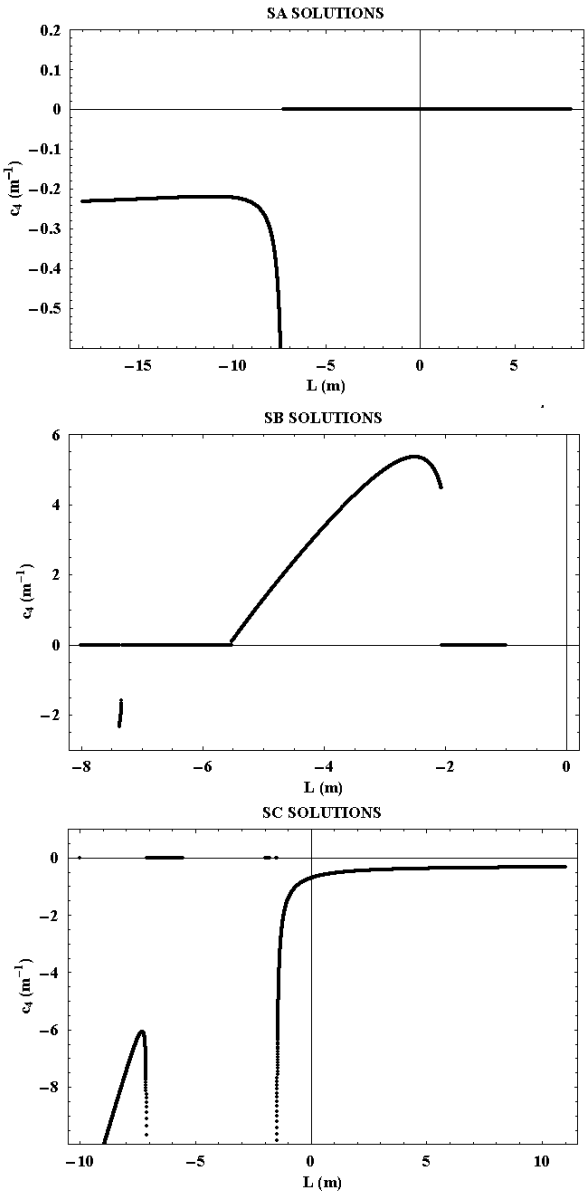


**Figure 2. SA, SB and SC solution curves for the case in which the baseline system is as given in table 1, and mirrors 2 and 3 are allowed to become conicoids. SA solutions are given by equation 2.16, SB by equation 2.17 and SC by equation 2.18. The horizontal axis here represents the initial position of the entrance pupil as measured from the primary mirror in object space, L, and the vertical axis represents the curvature of the quaternary mirror for each of the three solution sets, $C_4$. Representative examples of optical systems from these solution sets are given in figures 3-5 and table 1.**

the horizontal axis represents the initial position of the entrance pupil, and therefore is directly related to the original position of the centre of curvature of the quaternary mirror, whereas the vertical axis represents the curvature of the quaternary mirror (negative is concave). Note also that while the position of the aperture stop and hence entrance pupil was set initially to reduce the number of unknowns in equations 2.7 and 2.8, once an anastigmatic system is achieved the aperture stop can be moved to any convenient location without affecting the anastigmatic correction, as given by the stop-shift theorem.

Figure 3 shows some examples of optical systems represented by the solution curves in figure 2. Note that the "*SB*" solutions contain an example that is very close to the baseline system shown in figure 1. However in all of these solutions only two conicoids are required to produce anastigmatic correction.

A final point is that the anastigmats derived in this way are not necessarily practical systems, or even physically realizable. For example, if one or more of the solutions to equation 2.13 have imaginary components then this will not lead to an actual anastigmat. Also, there is no guarantee that the light path after each reflection will remain real.

Once physically meaningless systems have been disqualified, as they have been in the solution curves provided in figure 2, there is still the chance that the solution will be impractical, for example the quaternary mirror could become too large. Figure 3 gives an example of an impractical solution from the SA family of solutions. It can also be seen from figure 3 that practical off-axis solutions can still be extracted from impractical axially-symmetric parent systems.

Figure 4 shows a range of solutions from the SB curve in figure 2. The third system from the top in figure 2 is closely related to the baseline system of figure 1, but achieves anastigmatic performance with one less conicoid. Systems are arranged from top to bottom in figure 4 have decreasing values of $L$, and therefore are taken from points running from right to left on the SB family of solutions in figure 2. It can be seen the f/# of these solutions decreases from an afocal system in figure 4.A to a relatively fast f/2 system in figure 4.E.

Figure 5 shows SC solutions. While these solutions are valid anastigmatic solutions with usefully-low central obscurations, they are extremely fast and probably of limited practical value.
However, the solution sets SA, SB and SC have illustrated that starting from a first-order layout of interest, anastigmatic solutions can be found that lie close to the baseline solution in layout, and correct three Seidel aberrations with less than

three conicoids. Furthermore, the method has shown that it can generate potentially useful geometries that are quite different from the baseline geometry.

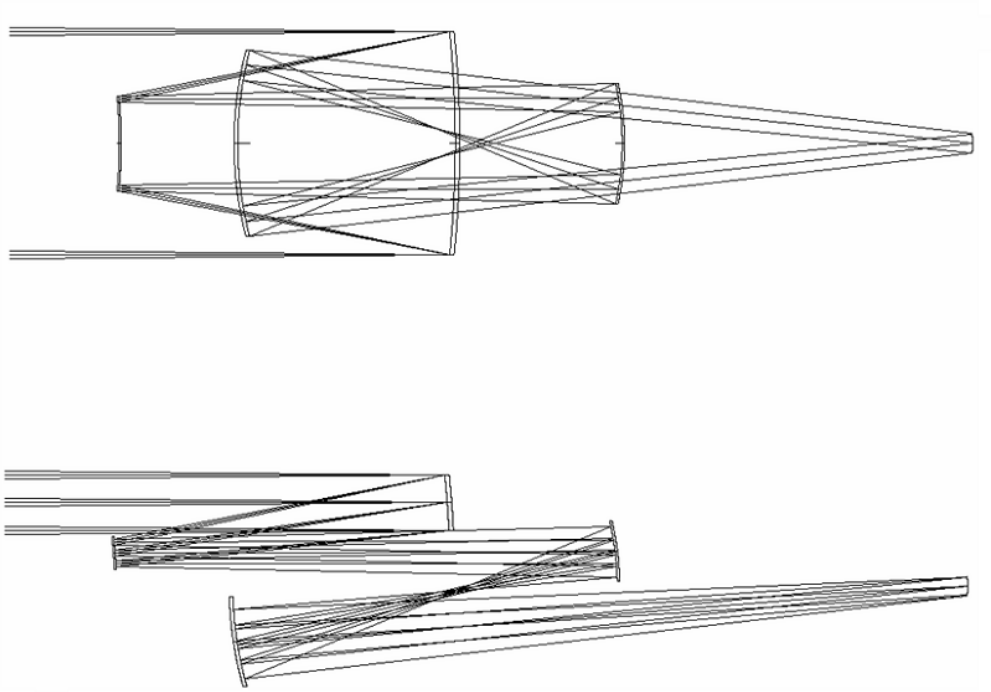

**Figure 3. An example of a solution for two-conicoid anastigmats using the SA solution. While the axially-symmetric system at top is clearly impractical due to 100% obscuration by the quaternary mirror of the light from the primary to the secondary mirror, a system obtained by using an off-axis portion of this parent system gives a useful unobstructed design.**

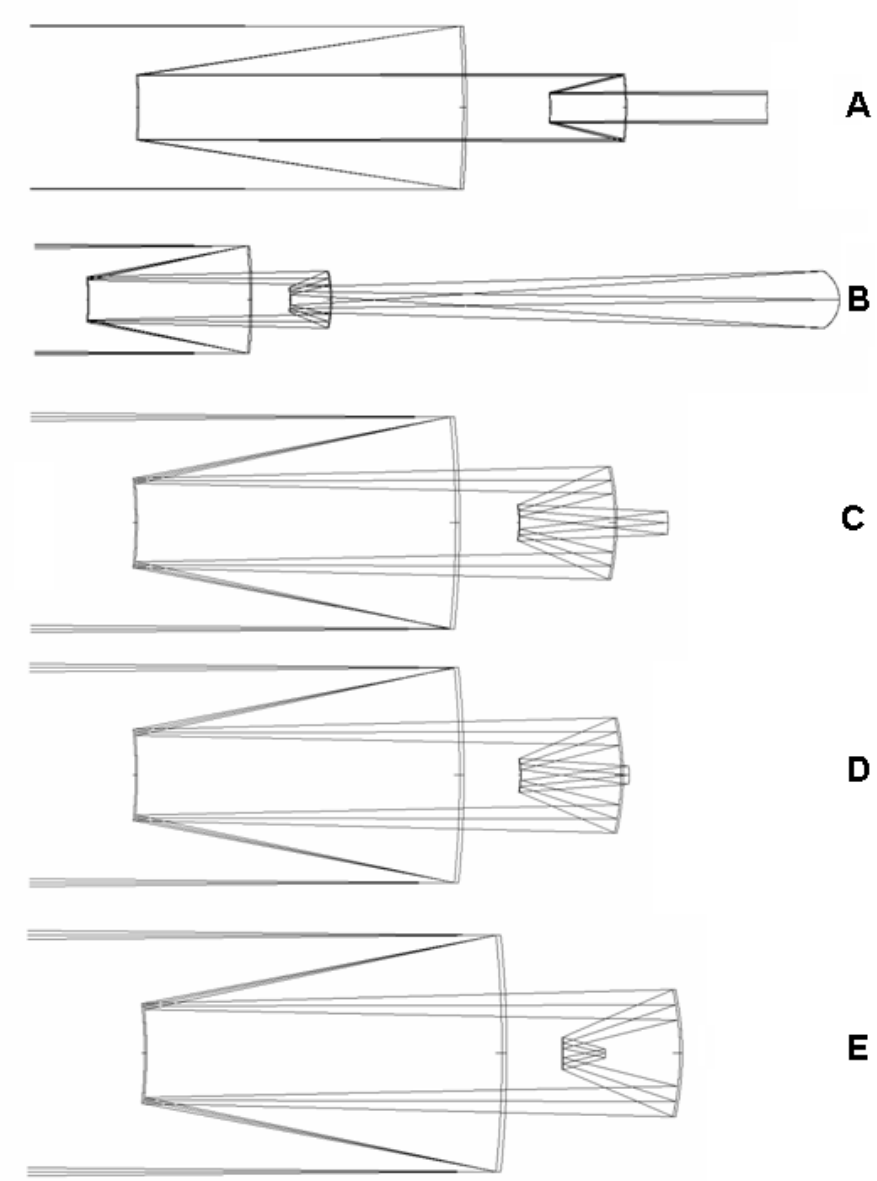


**Figure 4. Examples of the SB family of two-conicoid, two-sphere anastigmatic solutions. Systems ordered from A to E in this figure are solutions taken from points on the SB solution curve of figure 2 from right to left. Note that the system A is afocal, with systems of reducing (faster) focal ratio going down the page from A to E. System C is closely related to the baseline system in its first-order properties, and achieves anastigmatic correction with only two conicoids.**

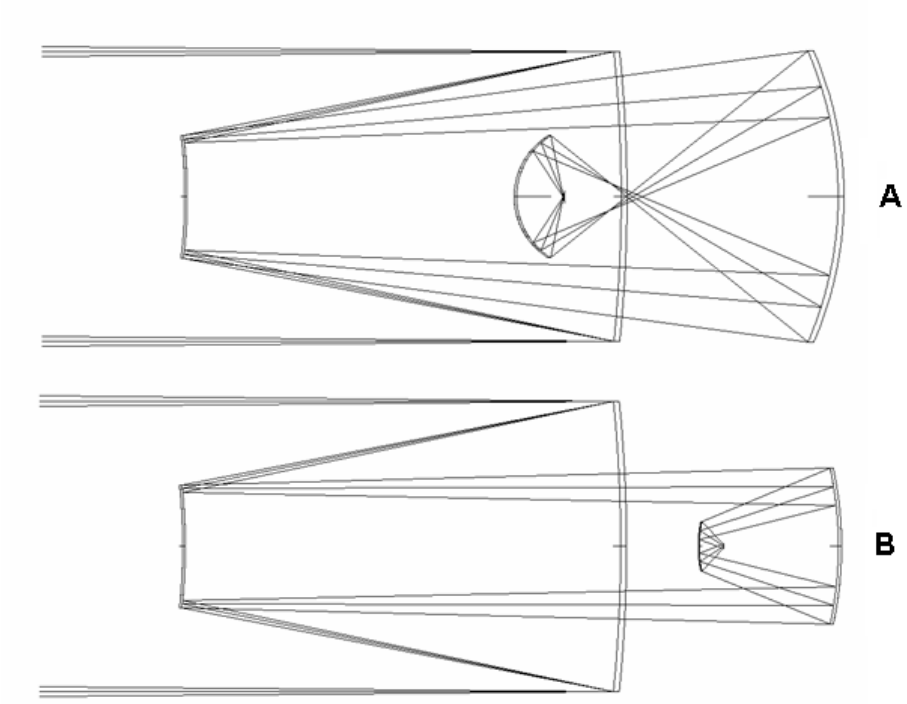


**Figure 5. Two examples of solutions from the SC curves shown in figure 2. While these systems do not exhibit a particularly favourable geometry, they serve as examples of the varied geometrical forms of valid anastigmatic system that can be produced by this method.**

**FOUR-MIRRORS; ONE CONICOID.**

In this final example we look at the case in which there is one conicoid mirror and three spheres. While in this case the secondary mirror has been chosen to be the conicoid, the method described below is readily adapted to accommodate any choice of mirror as the conicoid one. The primary and secondary mirrors have the same characteristics and positions as in figure 1. Now the curvatures and positions of the tertiary and quaternary mirrors are varied to solve for anastigmats. The first step is similar to that in the previous example. As in the previous example, the initial position of the aperture stop is chosen to eliminate one set of variables from the plate equations 2.7 and 2.8. In this case placing the aperture stop at the pole of the secondary mirror prevents the plate associated with the conic constant of the secondary mirror from having any effect on the coma or astigmatism of the system. Now we can form the equations:

$$x_{tert}W_{tert} + x_{quat}W_{quat} = -(x_{prim}W_{prim} + x_{sec}W_{sec}), \tag{2.19}$$

$$x_{tert}^2 W_{tert} + x_{quat}^2 W_{quat} = -(x_{prim}^2 W_{prim} + x_{\sec}^2 W_{sec}) . \tag{2.20}$$

Here "prim, "sec", "tert" and "quat" refer to quantities derived from the spherical primary through quaternary mirrors respectively (or vertex sphere in the case of the conicoid secondary mirror). Equation 2.19 is the condition for zero coma and equation 2.20 the condition for zero astigmatism. Quantities on the RHS are known. To proceed further we assign values to $t_2$, the separation of the secondary and tertiary mirrors and $r_3$, the radius of the tertiary mirror, from which we can calculate $x_{tert}$ and $W_{tert}$.

Moving all known quantities in the above equations to the $RHS$ and dividing equation 2.20 by 2.19 gives:

$$x_{quat} = \frac{x_{prim}^2 W_{prim} + x_{\sec}^2 W_{sec} + x_{tert}^2 W_{tert}}{x_{prim} W_{prim} + x_{sec} W_{sec} + x_{tert} W_{tert}} , \tag{2.21}$$

from which we obtain:

$$W_{quat} = -\frac{(x_{prim} W_{prim} + x_{sec} W_{sec} + x_{tert} W_{tert})}{x_{quat}} . \tag{2.22}$$

Now that all $W_i$ are known apart from the one associated with the conicoid, we can solve for the conicoid using the spherical aberration plate sum equation 2.6 and a rearranged 2.2:

$$k_2 = \frac{-4}{c_2^3 y_2^4} (W_{prim} + W_{\sec} + W_{tert} + W_{quat}) . \tag{2.23}$$

It is interesting to note that the necessary spherical aberration contribution from the quaternary mirror is thus defined before the radius or position of the quaternary mirror is determined. The final remaining step is to solve for the radius and position of the quaternary mirror, which is done exactly by deriving necessary paraxial quantities and solving equation 2.13. As in the previous case, this leads to three distinct systems for each choice of the starting values $t_2$ and $c_3$. Again, as in the previous case, each of the three exact algebraic solutions to equation 2.13 can be evaluated independently for a large number of initial values of the parameters $t_2$ and $c_3$. In this way a map of the solutions can be built up over this 2-parameter space, as is shown in figure 6 for solutions SA, SB and SC. In these maps anastigmats that are physically impossible can be filtered out, and there is also the opportunity to write custom filters targeting systems with

particular characteristics, for example sizes of mirrors, space envelope, central obscuration etc.

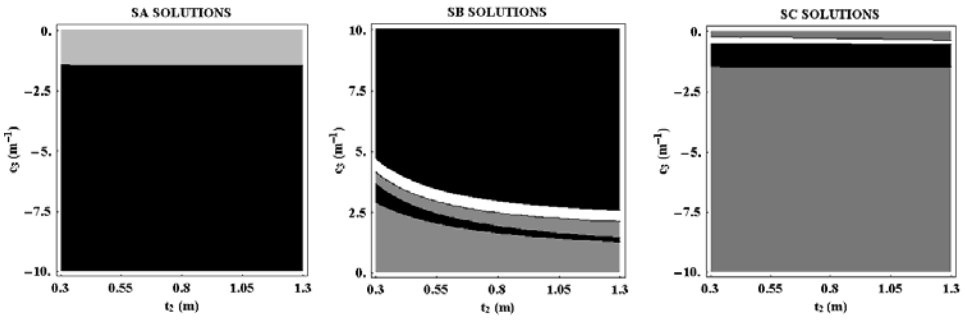


**Figure 6. Three independent sets of solutions for the case where only $M_2$ is allowed to be a conicoid. SA solutions are given by equation 2.16, SB by equation 2.17 and SC by equation 2.18. In these plots the vertical axis represents the curvature of the tertiary mirror while the horizontal axis represents the separation of the secondary and tertiary mirrors. Solutions are represented by either black or white regions, representing solutions with either negative or positive Petzval sums. Grey regions represent regions for which no valid anastigmatic solution exists. Note that there exist solution regions which have the corresponding coordinates in different sets. These represent systems that differ only in the radius and position of the quaternary mirror.**

Figure 7 gives an example of the type of system that would be removed by these custom filters. This SA type solution is a valid anastigmat in that it is a physically realizable solution, however it is obviously completely impractical. Figure 8 shows a selection of valid SB solutions. As with the two-conicoid case, in the one-conicoid case investigated here the SB solutions are the most closely related to the baseline solution. The system shown at the top of the figure places the focal plane at approximately the same place as it is in the baseline system, though here the focal ratio is increased to f/13.6. Details of this system are given in table 1. The third system from the top of figure 8 matches the focal ratio of the baseline system. Members of the SB family of solutions in this particular case can be seen to have useful first-order geometries and to achieve anastigmatic correction with only one conicoid surface.

An example from the family of SC solutions is presented in figure 9. The layout of this system bears some resemblance to one of the earliest four-mirror forms for imaging systems, proposed by Steele[11] in 1953. Steele gave several four-mirror concepts based on the idea of coupling pairs of corrected two-mirror systems. One of these pairs consisted of a Cassegrain front end and a Schwarzschild flat-

field rear end. A similar approach was later independently developed and extended by Shafer[12], to produce off-axis, all-spherical, four-mirror anastigmats.

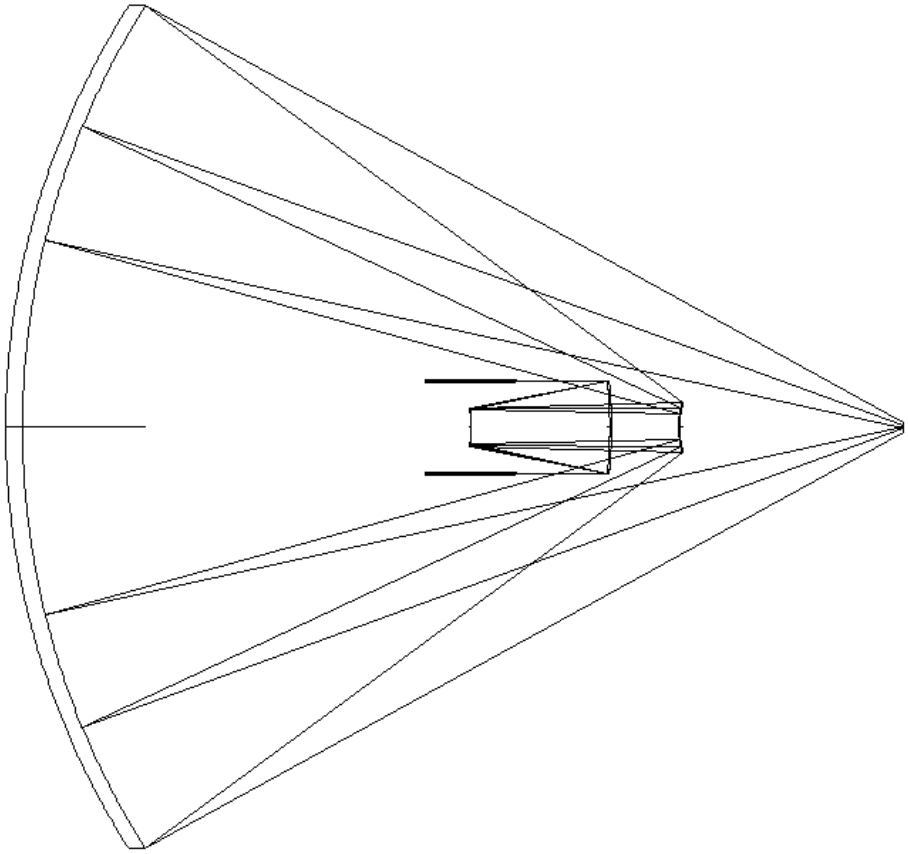

**Figure 7. An example of a completely impractical solution for the SA solution set of figure 6. When filters which exclude solutions with impractically large mirrors are applied, this solution set vanishes.**

The system shown in figure 9 is similar in appearance to one of Steele's four-mirror couplings of two-aspheric-mirror systems, but achieves anastigmatic correction with only one aspheric mirror. Details for this system are provided in table 1.

## 3. CONCLUSION

In previous work the author has presented the first example of a closed-form analytical solution for telescope systems consisting of four spherical mirrors. In this paper that solution has been generalized to include four-mirror systems in

which one, two or three mirrors are conicoids. The last case, deemed here the most trivial, is equivalent to Korsch's solution, where three conicoids are used to correct three Seidel aberrations.

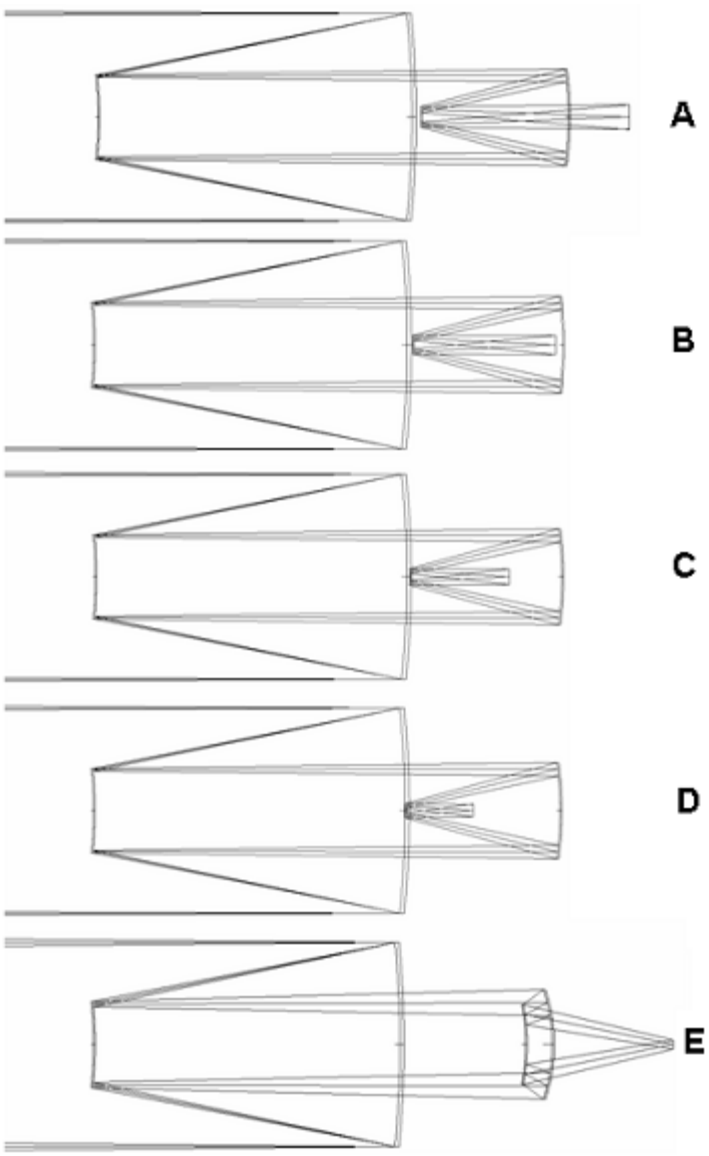


**Figure 8. Representative examples from the SB solution set shown in figure 6. In particular, systems A through D inclusive come from the thin black curving region in the SB solution plot, while system E is from the white region. System A most closely resembles the layout of the baseline system. This system has a focal ratio of f/13.6. System C most closely resembles the focal ratio of the baseline solution.**

| | baseline system (figure 1) | baseline with 3 conicoids (figure 1) | 2 conicoid SB solution (3rd from the top of figure 3) | 1 conicoid SB solution ( top of figure 8) | 1 conicoid SC solution (from figure 9) |
|---|---|---|---|---|---|
| **M1 radius** | −2.000 | −2.000 | −2.000 | −2.000 | −2.000 |
| **k1** | 0 | 0 | 0 | 0 | 0 |
| **t1** | −0.60000 | −0.60000 | −0.60000 | −0.60000 | −0.60000 |
| **M2 radius** | −0.800 | −0.800 | −0.800 | −0.8000 | −0.800 |
| **k2** | 0 | 3.166 | 3.189 | 2.752 | 2.301 |
| **t2** | 0.90000 | 0.90000 | 0.90000 | 0.90000 | 1.45000 |
| **M3 radius** | −0.500 | −0.500 | −0.5000 | −0.68729 | 1.551 |
| **k3** | 0 | −0.351 | −0.235 | 0 | 0 |
| **t3** | −0.19107 | −0.19107 | −.17384 | −0.28092 | −0.72812 |
| **M4 radius** | −0.150 | −0.150 | −0.194 | −0.14889 | 0.979 |
| **k4** | 0 | −0.26669 | 0 | 0 | 0 |
| **t4** | 0.27497 | 0.27497 | 0.35417 | 0.39834 | 0.72592 |

**Table 1. Optical parameters for several of the optical systems described in this paper are given here. The sign convention employed should be self-evident considering that the first column of data in the table corresponds to the baseline system of figure 1. In all cases presented in this paper the primary mirror was set with an aperture of 0.4 m. All mirror radii and mirror separations are given in units of meters. The stop is set on the primary mirror, but can of course be relocated anywhere in the system without adversely effecting the anastigmatic correction.**

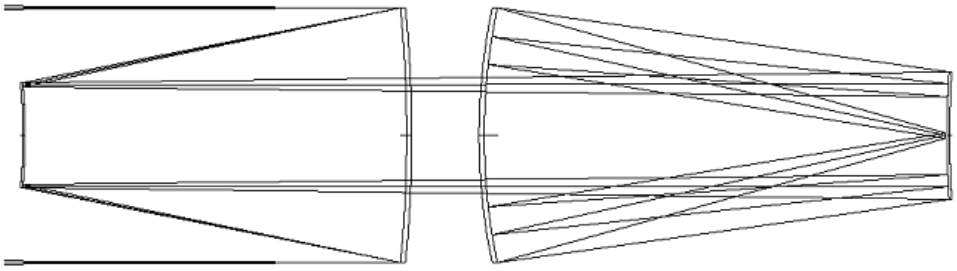

**Figure 9. This solution from the SC solution set of figure 6 bears some resemblance to a system proposed by Steele[11]. In this case however anastigmatic performance is achieved, and that with only one conicoid mirror.**

An example of the technique has been given where an initial system with a useful first-order layout is corrected using one, two or three conicoids. Starting from a baseline solution with useful first-order properties, it has been shown that corresponding anastigmatic systems with useful first-order geometries can be found even in the case where the number of conicoid surfaces used to correct the three targeted Seidel aberrations has been reduced to one. Moreover, the technique utilized here has demonstrated the potential to produce useful and unexpected geometries that are not so closely related to the baseline geometry.

This technique is readily generalizable to systems of more than four mirrors, and to systems in which both the object and image conjugates are finite, and therefore is potentially useful to the design of reflecting systems for a wide range of applications.

## REFERENCES


1. A. Rakich, "Complete solution set for four-spherical-mirror anastigmatic telescope systems",
   *Proc. SPIE*, **5249**, pp 103-111, 2004
2. A. Rakich, "Complete solution set for four-spherical-mirror anastigmatic telescope systems", *Opt. Eng.*, publication pending
3. D. Korsch, "Closed form solutions for imaging systems, corrected for third-order aberrations", *JOSA*, **65**, No. 6, pp. 667-672
4. D. Korsch, "Reflective Optics", Academic Press, San Diego, 1991
5. H.L. Aldis, "On the construction of photographic objectives", *Photographic Journal*, **24**, pp. 291-299, 1900
6. A. Rakich, N.J. Rumsey, "A method for deriving the complete solution set for three-mirror anastigmatic
   telescopes with two spherical mirrors", *JOSA A*, **19**, No. 7, pp. 1398-1405, 2002
7. C.R. Burch, "On aspheric anastigmatic systems", *Proc. Phys. Soc.*, **55**, pp.433-444, 1943
8. C.R. Burch, "Application of the plate diagram to reflecting telescope design", *Optica Acta*, **26**, pp. 493-504, 1979
9. Linfoot, E.H., "Recent advances in optics", Clarendon Press, Oxford, pp. 229-259, 1955
10. Wilson, R.N., "Reflecting Telescope Optics I", 2nd Edition, p.119, Springer Verlag, 2004
11. W.H. Steele, "Etude des effets combinés des aberrations et d'une obturation centrale de la pupille sur les images. Application aux objectifs de microscope miroirs.", *Thèses Soc. Phys. Paris*, Ser. A 2511, No. 3383, 1953
12. D.R. Shafer, "Four-mirror unobscured anastigmatic telescopes with all-spherical surfaces", *App. Op.*, **17**, No. 7, 1978

# Appendix C: Four-mirror anastigmats III: all-spherical systems with elements larger than the entrance pupil

This paper was submitted to Optical Engineering in February 2007 and is currently under review.

# Four-mirror anastigmats III: all-spherical systems with elements larger than the entrance pupil.

Andrew Rakich[a,b]
[a]Electro Optic Systems Pty., Locked Bag 2 Post Office, Queanbeyan NSW 2620, Australia
[b]Department of Physics and Astronomy, University of Canterbury, Private Bag 4800, Christchurch 8020, New Zealand
e-mail: arakich@eos-aus.com, Phone +61 2 62227935, Fax +61 2 62997687

**ABSTRACT**

In the first paper in this series closed-form analytical solutions for four-spherical-mirror anastigmats were developed and used to map the solution space for such systems. In all cases systems investigated had objects at infinity, concave primary mirrors, and the primary mirror was always the element with the largest diameter. This work extends the survey to include systems with elements larger than the primary mirror, and now includes both new types of concave-primary-mirror systems and also all of the convex-primary-mirror systems, which were previously excluded. Numerous systems are presented, including new forms of concentric-mirror systems and systems that have zero Petzval curvature. Also investigated are off-axis or Schiefspiegler forms, which include systems excluded from the previous survey due to large central obstructions when considered as on-axis systems. The fact that closed-form solutions are used to map out all solutions over the relevant parameter space means that the systems presented here (together with the first paper in this series) represent the full and final range of possibilities for four-spherical-mirror anastigmats for which at least one of the system imaging conjugates is infinite.

**Keywords: anastigmat, reflecting telescope, four-mirror, Schiefspiegler**

## 1. INTRODUCTION

All-reflecting or catoptric optical systems are useful in a range of applications in science and industry. A range of applications including but not limited to EUV lithography, high energy laser systems, microscopy,

projection and hyper-spectral imaging all benefit from the advantages catoptric systems offer, such as zero chromatic dispersion, high transmission efficiency, high damage thresholds and good correction of optical aberrations achievable with relatively simple systems.

This paper is concerned with catoptric systems comprised of four spherical mirrors in which the third-order aberrations that affect image sharpness, namely spherical aberration, coma and astigmatism, are simultaneously corrected; i.e. anastigmatic optical systems. In the first paper in this series[1] a closed-form analytical solution for four-spherical-mirror anastigmats was developed and applied to a survey of systems of potential usefulness as telescopes. This meant that the investigation was limited to systems in which the largest optical element was a concave primary mirror.

While this limitation is sensible in the case of astronomical telescopes systems, there are numerous types of optical system in which the largest optical element can be many times greater in diameter than the entrance pupil. For example catoptric microscope objectives, projection systems and camera objectives commonly have pupils and primary optics that are smaller than succeeding elements in the system. This paper presents the results of a broader survey of four-spherical-mirror anastigmats than that previously presented. As well as systems with larger optics, other systems that were excluded from the previous survey on the basis that the on-axis parent systems were 100% self-obstructed, are shown to become viable as "Schiefspiegler" or off-axis unobstructed systems.

This survey has resulted in the discovery of a large number of four-spherical-mirror anastigmatic systems, only one of which had previously been reported[2]. The nature of the survey technique means that it is certain that all possible types of four-spherical-mirror anastigmat have been now been discovered. This would be a difficult claim to make if one had attempted to employ a global optimization routine to determine these solutions. Another advantage of the analytical technique used here to find these solutions is that there is a clear mathematical basis for classifying the various solution families that arises from their underlying geometry. This will be discussed in the following section, together with a summary of the survey method.

## 2. METHOD

The closed form solution for four-spherical-mirror anastigmats employed here was developed and presented in full in earlier work[1,3]. In short, equations 3.1-3.21 of reference 1 develop an analytical solution for four-spherical-mirror anastigmats for given values of three input parameters. These parameters are the curvature of the secondary mirror, the separation of the primary and secondary mirrors and the position of the centre of curvature of the quaternary mirror. It is shown that for any point in this three-parameter space, anastigmatic systems can be found by solving two cubic equations, one each for the radii of curvature of the tertiary and quarternary mirrors. These cubics are given as equations 3.19 and 3.21 in reference 1.

Analytical expressions for the solutions for the general cubic equation:

$$a_0 + a_1 x + a_2 x^2 + x^3 = 0, \tag{2.1}$$

can be given as:

$$SA = \frac{-a_2}{3} - \frac{\sqrt[3]{2}Y}{3\sqrt[3]{Z+Q}} + \frac{\sqrt[3]{Z+Q}}{3\sqrt[3]{2}}, \tag{2.2}$$

$$SB = \frac{-a_2}{3} + \frac{(1-i\sqrt{3})Y}{3\sqrt[3]{4(Z+Q)}} - \frac{(1+i\sqrt{3})\sqrt[3]{Z+Q}}{6\sqrt[3]{2}}, \tag{2.3}$$

$$SC = \frac{-a_2}{3} + \frac{(1+i\sqrt{3})Y}{3\sqrt[3]{4(Z+Q)}} - \frac{(1-i\sqrt{3})\sqrt[3]{Z+Q}}{6\sqrt[3]{2}}, \tag{2.4}$$

where:

$$Y = 3a_1 - a_2^2; Z = -27a_0 + 9a_1a_2 - a_3^2; Q = \sqrt{4Y^3 + Z^2}. \tag{2.5}$$

By sampling the three-parameter space with sufficient density and solving each of the nine possible combinations of solutions for the two cubics for each sampled point one can build up nine sets of geometrically distinct anastigmatic systems. In the following presentation of results these geometrically distinct families will be grouped according to which of the three analytical solutions to the each of two cubics are employed to obtain the anastigmatic system. For example, the solution

set derived when the $SB$ solution is used to determine the radius of curvature of the tertiary mirror and the $SA$ solution is used to determine the radius of curvature of the quaternary mirror will be referred to as the "BA" family of solutions. If the $SC$ solution is used for the tertiary mirror radius of curvature and the $SB$ solution is used to obtain the quaternary mirror radius of curvature the solution set of anastigmatic systems thus obtained is referred to as the "CB" set, and so on.

Clearly it is possible for any of $SA$, $SB$ or $SC$ to have imaginary components. In the case where one of these solutions has an imaginary component the resultant system is not anastigmatic. Therefore the 3-D solution space for anastigmatic systems is comprised of volumes of valid solution and complementary volumes of invalid solutions.

The solutions thus found encompass every possible anastigmatic system comprised of four co-axial spherical mirrors and with an infinite object conjugate. In the survey undertaken in reference 1 the survey was limited to systems in which no element had a diameter exceeding that of the primary mirror, and all solutions had concave primary mirrors. In the survey undertaken here, elements have been allowed to exceed the diameter of the primary mirror by as much as 15 times, and both concave primary and convex primary mirror systems have been surveyed.

Filters are written into the algorithm for successively determining anastigmatic systems over a large numbers of points in the three-parameter space described above. These filters are used to exclude systems with excessive element sizes, excessive lengths and large or total central obscuration. Of the systems that are totally self-obstructing when considered as axially symmetrical systems a further test is used to determine whether or not useful Schiefspiegler can be obtained by using an off-axis portion of the pupil.

The algorithm for calculating system self-obstruction required the sorting of each system into one of sixteen possible arrangements of relative placement of mirrors and image surface. If we label the primary through quarternary mirrors as 1 through 4 and the image space as 5, then a five digit number comprised of these five numerals can be used to categorize the system according to the order that the optical components are arranged. For example, with incident collimated light traveling from left to right, a system designated "21435" would be a system in which the order of placement of elements from left to right would be secondary mirror, primary mirror, quaternary mirror, tertiary mirror and focal plane. An example of a 45231 system is given in figure 1.

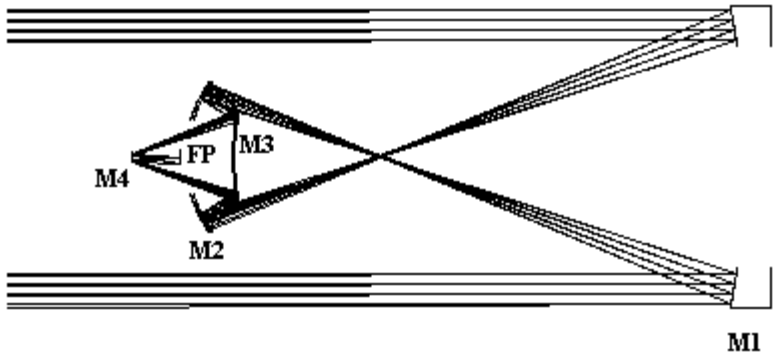


**Figure 1. Illustration of the five digit classification system. For the system shown, with the object to the left of the page, the order from left to right of the various surfaces is quaternary mirror, focal plane, secondary mirror, tertiary mirror, primary mirror. In the classification system used throughout this paper this system would be described as a 45231 arrangement.**

It turns out that there are 16 possible permutations of the "order of occurrence" of four mirrors and focal plane in valid four-mirror imaging systems. Using the system described above, these can be represented by the following sets of digits:

21435, 21453, 24513, 24153, 24135, 24531, 24351, 24315, 45213, 42513, 42153, 42135, 45231, 42531, 42351 and 42315.

This classification system can be useful. For example, when designing microscope objectives it would make sense to limit the investigation to systems with "5" as the last digit, representing systems for which the "image" was beyond all of the optics (though for a microscope objective the "image" here would typically be the object and the image space would have the infinite long conjugate).

Because of the large number of solutions found, only representative examples from each family of solutions will be presented in this paper. Several points should be noted about the solutions presented here. Firstly, these solutions are third-order solutions only. Better results will almost always be available if these solutions are used as starting points for optimization, and then thicknesses and curvatures are allowed to vary. In practice slight variations in system parameters from the third-order solution will allow the re-introduction of small amounts of third-order aberrations to balance optimally against high-order residuals. In most cases this high-order balancing can be achieved without noticeably changing the general configuration of the third-order solution.

Secondly, no attempt has been made to discuss the practicality or usefulness of the systems presented here. The fact that these systems exist at all and the disclosure of available forms of four-spherical-mirror anastigmat is the main point of this paper, and the suitability or otherwise of a particular system for a particular application will, in general, not be discussed.

Another important point is that while all of these solutions are geometrically distinct from each other, each unique solution can be scaled either in pupil or geometrically scaled in three dimensions without affecting the third-order correction. The former case allows for a certain range of selection of f/ratios for a given solution, and the latter case allows for sizing to match a given application. Of course, scaling the pupil will affect the ratio of high-order to third-order aberrations in the system. All systems presented here have a primary mirror diameter of 0.4 m, and the radius of curvature of the primary mirror is 2 m, unless otherwise stated.

Finally, while representative examples of the various families of solution are presented in this paper, the fact is that there are variations within each family which can not be fully described in one paper. It is suggested that designers interested in the full range of solutions available in a particular family follow the procedure outlined in reference 1, by which they can obtain every possible solution.

## 3. Results

### 3.1 AA SOLUTIONS

There are no AA-type solutions for concave primary mirror systems. Only one type of solution exists for convex primary AA-type solutions, as shown in figure 2. Optical design data for this figure are given in table 1. The relatively limited range of solutions in this family are all of the 42135 type.

### 3.2 AB SOLUTIONS

AB-type solutions exist for both concave and convex primary mirror types. Concave primary mirror solutions are shown in figures 3 and 4, with design data for these systems given in table 2. There exist two distinct sub-regions of solution in the AB concave primary mirror case. Examples from the first sub-region are given in figure 3. The three systems shown here can be classified as 24135, 24153 and 24513 systems, and they are indicative of the continuum of solutions within their solution family. Afocal versions also exist.

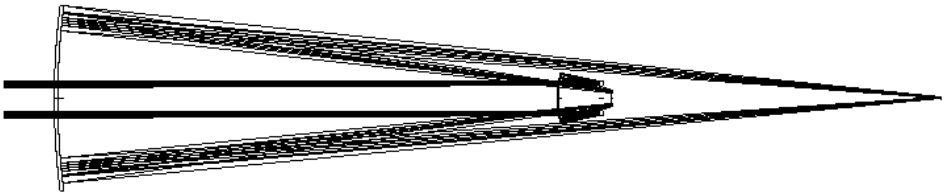

**Figure 2. An AA-type 42135 system with convex primary mirror. In this figure, and in all subsequent figures in this paper, collimated light from the object at infinity incident on the primary mirror is traveling from left to right.**

| System | R1 | t1 | R2 | t2 | R3 | t3 | R4 | t4 |
|---|---|---|---|---|---|---|---|---|
| Fig 2 | 2.0 | -0.47672 | 1.11099 | 0.62439 | 0.37561 | -6.51739 | 8.47899 | 10.403 |

**Table 1. Optical design data for the AA-type system shown in figure 2. The primary mirror in this and all other non-Schiefspiegler systems presented in this paper is 0.4 m diameter, though this is an arbitrary value as all these systems can be scaled. Units are meters. The sign convention employed should be obvious from the figure.**

24531, 24351 and 24315 versions of this family also exist and some of these were reported in reference 1. In these cases the tertiary mirror lies between the primary and secondary mirrors (the digit "3" is always between the digits "2" and "1" in the five digit naming system in these cases) and is in general smaller in diameter than the primary mirror. There are no members of this family for which Petzval curvature is zero.

Two solutions from the second solution sub-region are shown in figure 4. Within this particular family there also exist afocal solutions. Solution 4.a is an example of one of the members of this solution family that has zero Petzval curvature. This solution family, which can be seen to be geometrically distinct from the solution family shown in figure 3, contains 21435 and 21453 type solutions.

Convex primary mirror solutions are shown in figure 5. All of these solutions occupy a single connected "volume" in solution space. Within this solution family there exist examples of 21435 and 21453 systems. The system depicted in figure 5.c is a system previously described by Shafer[2]. Of the systems presented in this paper, this is the only one that has previously appeared in published literature. Shafer's system is an example of this solution type that has zero Petzval curvature. Optical design data for the convex primary systems can be found in table 2.

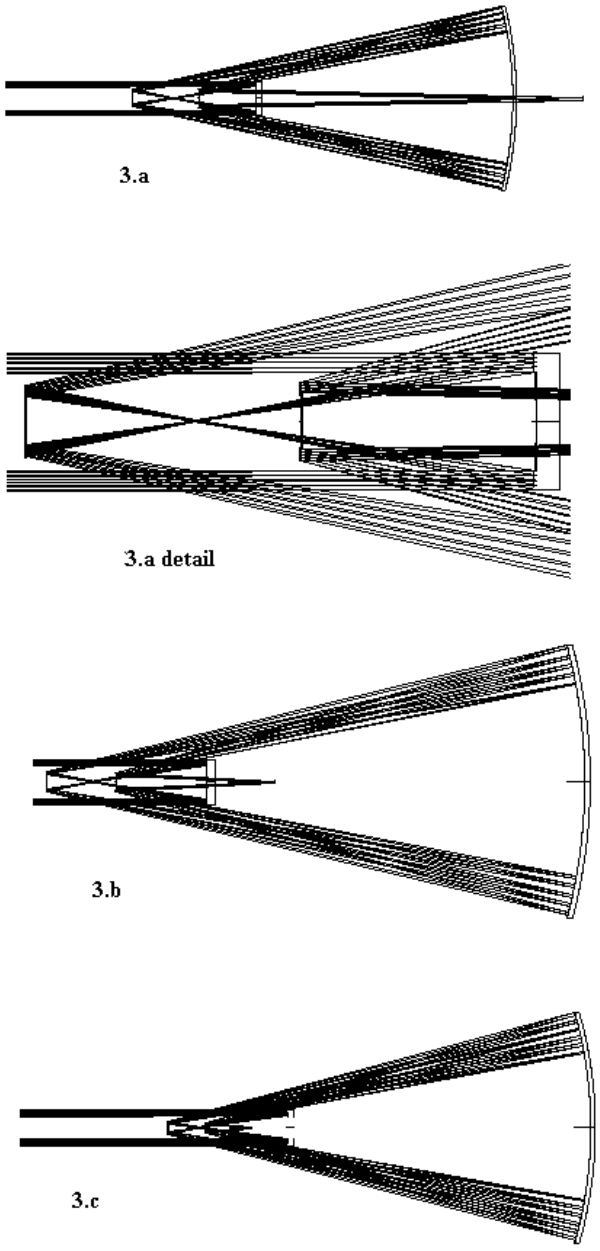


**Figure 3. Two examples, each from the first sub-region of AB-type concave primary mirror solutions.**

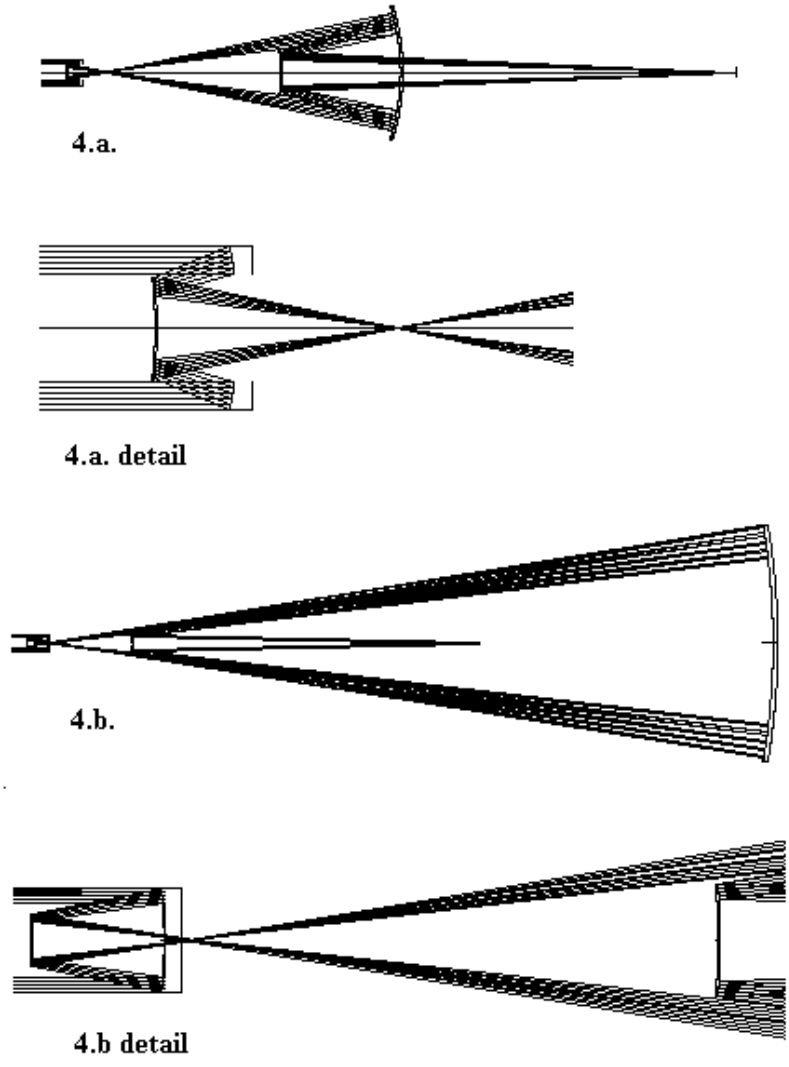


**Figure 4. Two examples, each from the second sub-region of AB-type concave primary mirror solutions.**

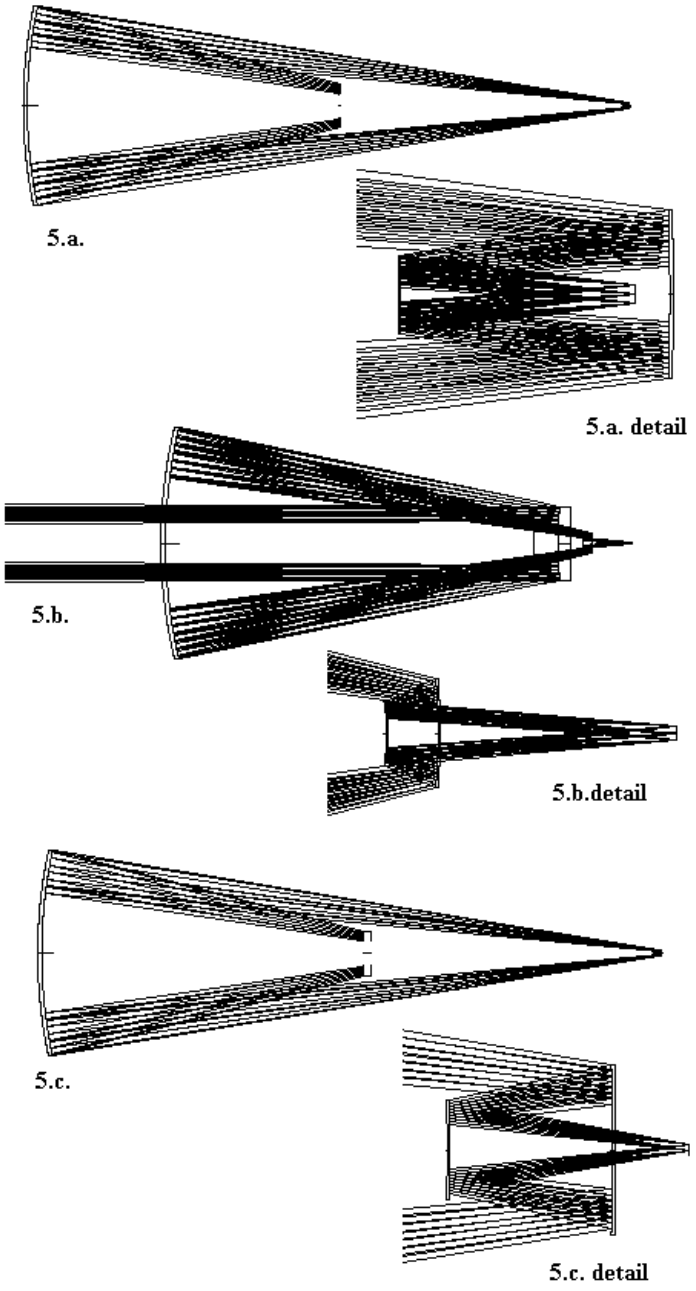


**Figure 5. Three examples from the single solution set for AB-type convex primary mirror systems. 5.a is a flat-field system originally given by Shafer[2] and is the only example of a flat-field, axially symmetrical four-spherical-mirror anastigmat with infinite object conjugate to have appeared in previously published literature.**

| System | R1 | t1 | R2 | t2 | R3 | t3 | R4 | t4 |
|---|---|---|---|---|---|---|---|---|
| **Fig 3.a** | -2.0 | -1.49005 | -10.0100 | 4.57732 | -4.57732 | -3.76881 | -0.96077 | 4.605 |
| **Fig 3.c** | -2.0 | -1.41005 | -5.00250 | 4.73340 | -4.73340 | -4.12223 | -0.77917 | 1.395 |
| **Fig 4.a** | -1.0 | -0.19774 | -1.22416 | 5.08832 | -3.38817 | -1.81143 | -2.09091 | 6.947 |
| **Fig 4.c** | -2.0 | -0.51005 | -5.0025 | 18.86250 | -17.8625 | -16.1996 | -3.02074 | 8.775 |
| **Fig 5.a** | 2.0 | -3.30005 | 6.28465 | 5.26039 | -3.78465 | -0.22825 | -1.62752 | 0.199 |
| **Fig 5.b** | 2.0 | -2.13005 | 2.77701 | 2.31242 | -0.61242 | -0.04667 | -0.18168 | 0.269 |
| **Fig 5.c** | 2.0 | -3.60794 | 5.60795 | 6.95518 | -1.34723 | -0.07000 | -1.27723 | 0.103 |

**Table 2. Optical design data for the AB-type systems shown in figures 3, 4 and 5.**

### 3.3 AC SOLUTIONS

No concave primary mirror AC-type solutions exist. A limited range of convex primary mirror AC-type solutions exist, and a typical example is given in figure 6. All of these systems are of the 45213 type. Optical design data for these systems are given in table 3. As can be seen in figure 6.a, these systems suffer from a high central obscuration ratio. One way around this problem is demonstrated in figure 6.b, which shows a wholly unobstructed system taken from an axially-symmetrical parent system. This family of solutions contains no afocal systems, and no systems for which the Petzval curvature is zero.

### 3.4 BA SOLUTIONS

There are no BA-type concave primary mirror solutions. There is a relatively limited range of BA convex primary solutions. Examples of 42315, 42135, 24135 and 21435 variants are given in figure 7, with system design parameters given in table 4. There are no variants free of Petzval curvature.

### 3.5 BB SOLUTIONS

One connected volume of BB-type concave primary mirror solutions exists. 24351, 24315, 42315, 42351, 42531, and 45231 variants are shown in figure 8, with optical design data given in table 5.

There is a relatively limited range of BB convex primary solutions. Examples of 45213, 42135 and 21435 variants are given in figure 9, with system design parameters given in table 5. There are no variants free of Petzval curvature. The system in figure 9.a only works as a Schiefspiegler due to self-obstruction in the axially symmetrical system. It is interesting to note the clear first-order differences between the 45213 system in figure 9.d. and the 45213 systems in figure 6.

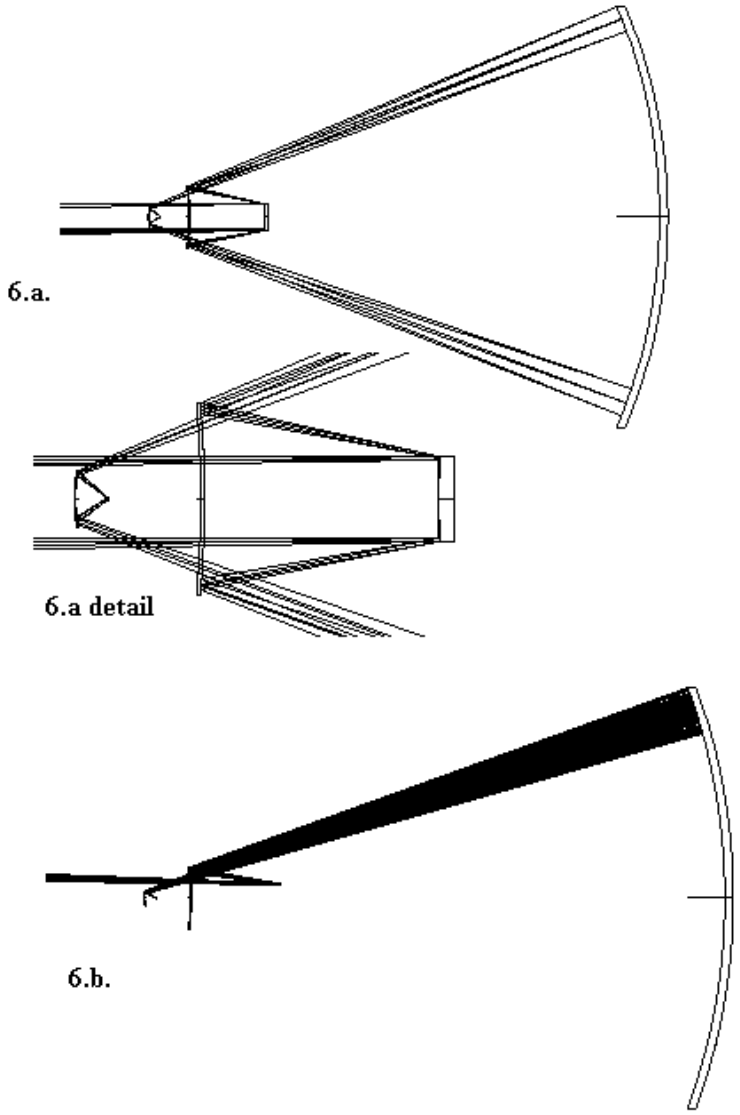


**Figure 6. AC-type convex primary mirror solutions all resemble this solution. 6.b shows a Schiefspiegler formed by using an off-axis portion of the 6.a system.**

| System | R1 | t1 | R2 | t2 | R3 | t3 | R4 | t4 |
|---|---|---|---|---|---|---|---|---|
| Fig 6 | 2.0 | -1.10000 | -5.00250 | 6.96588 | -7.96588 | -7.57213 | 0.80757 | 0.157 |

**Table 3. Optical design data for the AC-type system shown in figure 6.a. The Schiefspiegler shown in figure 6.b is simply a system produced by using an off-axis portion of the pupil of this system.**

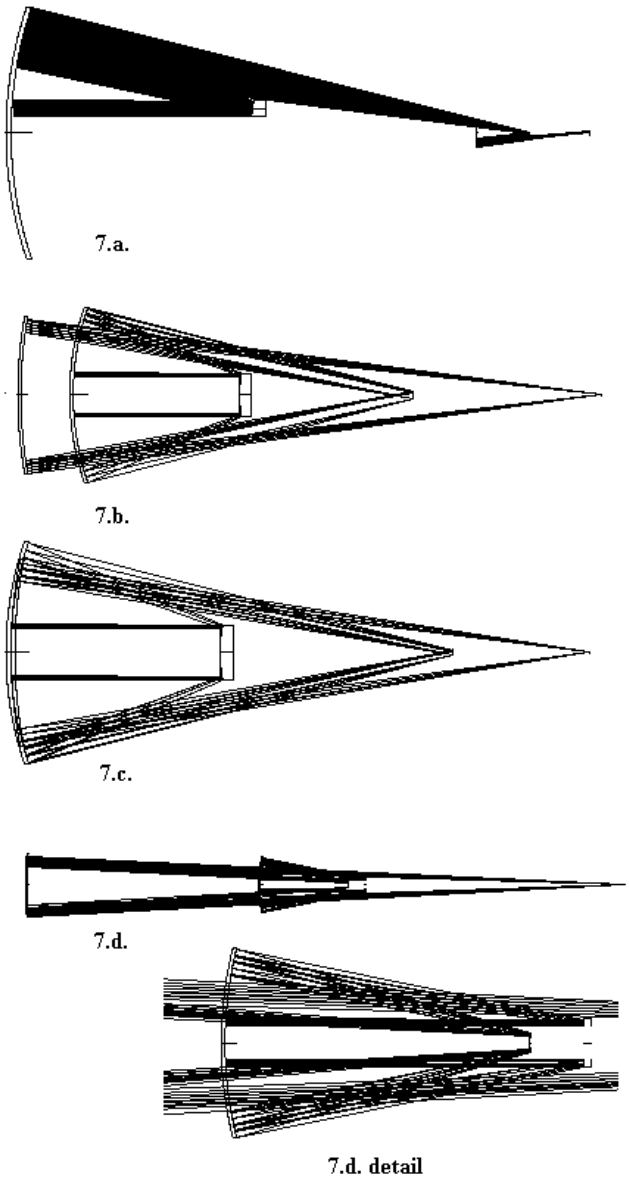


**Figure 7. BA-type convex primary mirror solutions. 7.a is an example of a 21435 system that only works as a Schiefspiegler, the axially symmetrical parent system is 100% self-obstructing. 7.b, 7.c and 7.d are all solution types from one connected volume of solutions within the solution space.**

| System | R1 | t1 | R2 | t2 | R3 | t3 | R4 | t4 |
|---|---|---|---|---|---|---|---|---|
| **Fig 7.a** | 1.0 | -1.51502 | 2.49875 | 3.27763 | 0.22237 | -0.33542 | 0.44547 | 0.713 |
| **Fig 7.b** | 2.0 | -3.06005 | 4.99750 | 6.24161 | 2.75839 | -7.20474 | 8.37344 | 10.671 |
| **Fig 7.c** | 2.0 | -3.04005 | 4.99750 | 6.42442 | 1.57558 | -6.36053 | 7.11601 | 8.379 |
| **Fig 7.d** | 2.0 | -3.02005 | 3.33222 | 2.56571 | 0.43429 | -9.31763 | 12.9222 | 17.367 |

**Table 4. Optical design data for BA-type systems as shown in figure 7. The figure 7.a. system is an example of a system that only works as a Schiefspiegler, the axially symmetrical system is totally self-obstructing.**

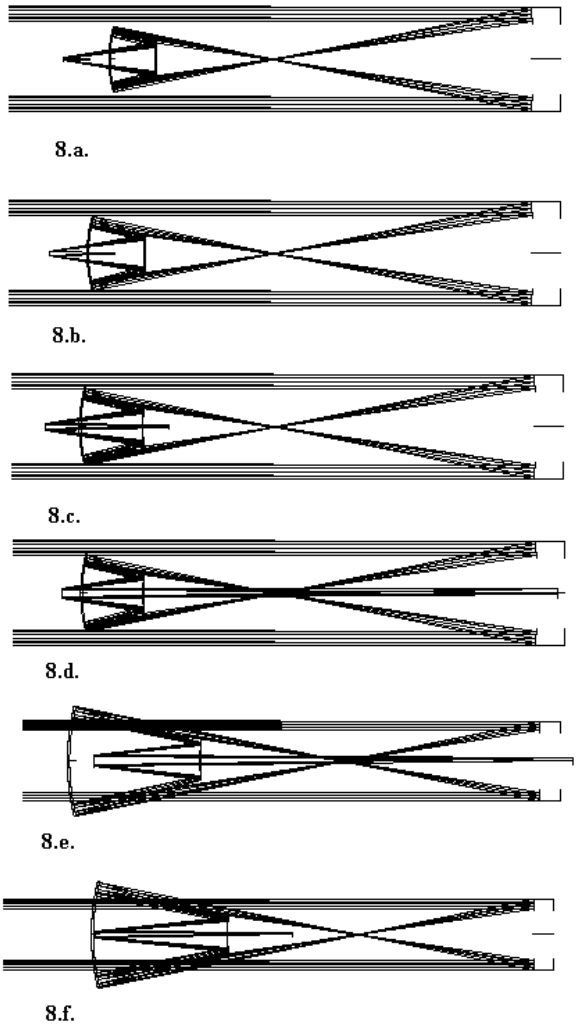


**Figure 8. BB-type concave primary solutions. The first four systems here, 8.a-8.d, were previously reported in reference 1, and are included here for comparison to other members of this solution family. The systems shown in 8.e and 8.f are clearly members of this family.**

| System | R1 | t1 | R2 | t2 | R3 | t3 | R4 | t4 |
|---|---|---|---|---|---|---|---|---|
| **Fig 8.a** | -2.0 | -1.61747 | 0.44803 | 0.17183 | 0.68119 | -0.34970 | -0.08908 | 0.100 |
| **Fig 8.b** | -2.0 | -1.70005 | 0.52081 | 0.21256 | 0.78744 | -0.36063 | -0.13957 | 0.250 |
| **Fig 8.c** | -2.0 | -1.74005 | 0.55246 | 0.23475 | 0.76525 | -0.36985 | -0.18222 | 0.470 |
| **Fig 8.d** | -2.0 | -1.72000 | 0.52869 | 0.22013 | 0.78703 | -0.28804 | -0.23104 | 1.860 |
| **Fig 8.e** | -2.0 | -2.37005 | 1.16266 | 0.65589 | 1.34411 | -0.53018 | -0.47801 | 2.40928 |
| **Fig 8.f** | -2.0 | -2.49005 | 1.28189 | 0.75225 | 1.24775 | -0.73961 | -0.44377 | 1.112 |
| **Fig 9.a** | 2.0 | -3.08005 | 4.9975 | 6.04405 | 3.95595 | -3.18582 | 4.67821 | 18.418 |
| **Fig 9.b** | 2.0 | -3.07005 | 4.99750 | 6.20993 | 2.79007 | -2.35117 | 3.48385 | 12.352 |
| **Fig 9.c** | 2.0 | -1.78765 | 3.33322 | 7.21546 | -5.21546 | -15.8551 | -3.12821 | 16.196 |
| **Fig 9.d** | 2.0 | -1.78385 | 3.33322 | 7.21216 | -5.21216 | -16.6497 | -2.33138 | 4.784 |

**Table 5. Optical design data for BB-type systems as shown in figures 8 and 9. The systems shown in figures 9.c and 9.d have been scaled in aperture to 1 m (the primary mirror has a 1 m diameter with the stop on the primary) for the sake of clarity.**

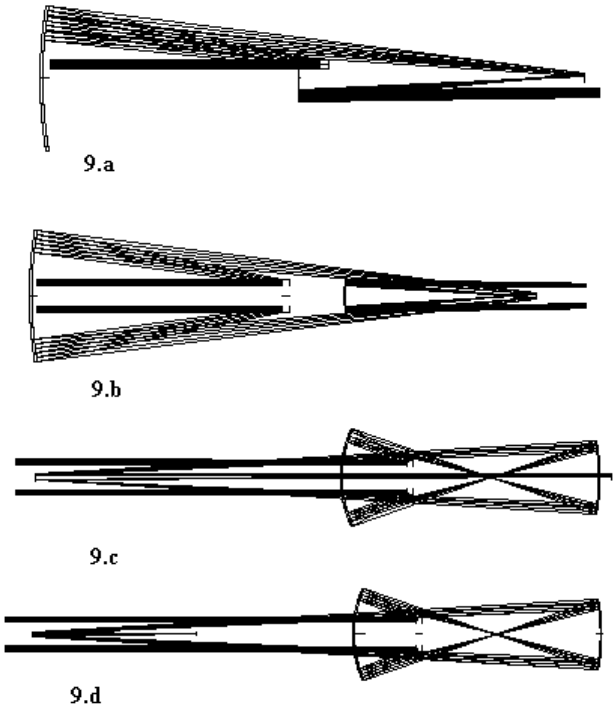


**Figure 9. BB-type convex primary mirror solutions. The 24135 system shown in 9.a is another example of a system that only works as a Schiefspiegler due to self-obstruction. 9.b, 9.c and 9.d are 21435, 42135 and 45213 type arrangements respectively.**

## 3.6 BC SOLUTIONS

No concave primary mirror BC-type solutions exist. There is one connected volume of BC solutions with convex primary mirrors. Within this family there exist 24153, 24513, 24531 and 21453 variants as shown in figures 10.a., 10.b., 10.c., and 10.d. respectively. The example given in figure 10.c. has zero Petzval curvature.

The first–order layout of the first two mirrors of the system in figure 10.d. is very similar to the two-mirror Schwarzschild flat-field anastigmat, though in that case, both the mirrors are conicoids. Here, instead of requiring two conicoid mirrors, correction of coma and astigmatism is achieved with the small set of tertiary and quaternary spherical mirrors. However the system has a curved focal plane. Optical design data for the BC solutions are given in table 6.

| System | R1 | t1 | R2 | t2 | R3 | t3 | R4 | t4 |
|---|---|---|---|---|---|---|---|---|
| **Fig 10.a** | 2.0 | -1.37005 | 1.99960 | 1.53636 | 0.46364 | -0.22866 | 0.30563 | 0.131 |
| **Fig 10.b** | 2.0 | -1.40005 | 1.999960 | 1.49873 | 0.50127 | -0.29596 | 0.35824 | 0.156 |
| **Fig 10.c** | 2.0 | -1.51005 | 1.99960 | 1.36335 | 0.63665 | -0.66006 | 0.62166 | 0.28887 |
| **Fig 10.d** | 2.0 | -2.85005 | 3.33222 | 2.90352 | 0.09648 | -0.02224 | 0.04863 | 0.019 |

**Table 6. Optical design data for BC-type solutions as shown in figure 10.**

## 3.7 CA SOLUTIONS

There are two separate solution volumes for CA-type systems with concave primary mirrors, and these are shown in figure 11, with optical design data in table 7. 42315 and 42351 arrangements exist. Both systems have relatively high numerical apertures. Also, both these systems are characterized by the high angles of incidence rays make on the tertiary mirror. These two facts mean that these systems are less well approximated by third-order theory than is the norm, as the proportion of high-order to low-order aberration in these types of system is much higher than in other systems so far presented.

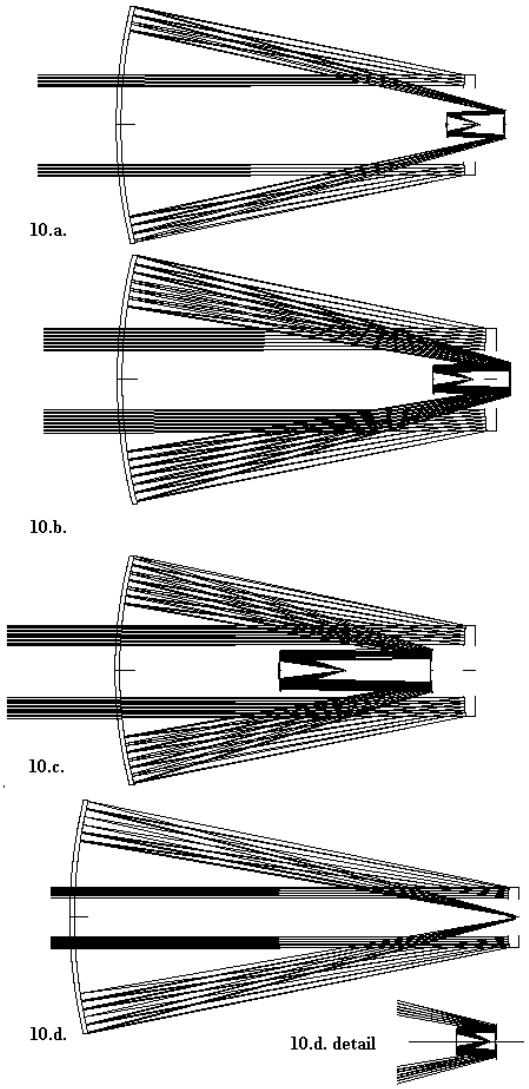


**Figure 10. BC-type convex primary mirror systems from one connected volume of solutions. The 24531 system in 10.c is an example of a flat-field anastigmat.**

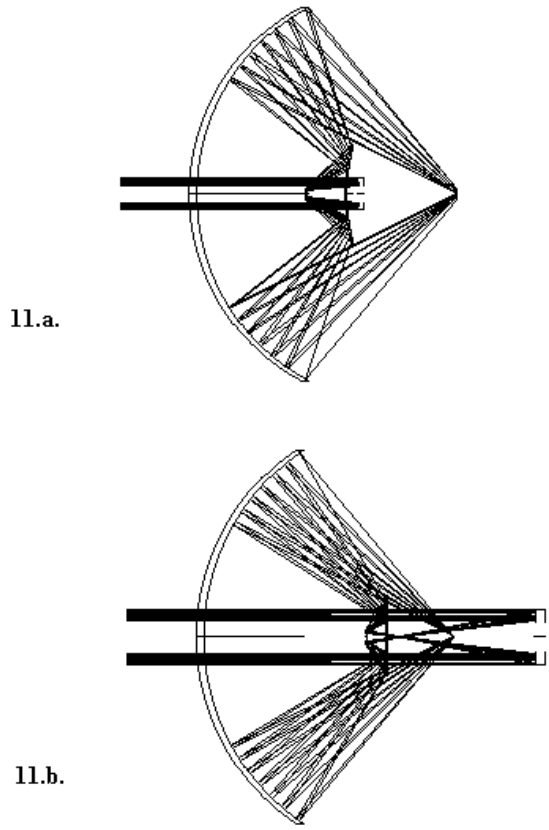


**Figure 11. CA-type concave primary mirror solutions, from two unconnected volumes of solution space. Both systems are characterized by high numerical aperture and large angles of incidence on the tertiary mirror.**

The convex primary CA-type systems are shown in figure 12. The solution set contains systems with 21435, 24135 and 42135 arrangements. All solutions come from one connected volume of solutions, and there are some interesting variants, including versions with zero Petzval curvature (shown in figures 12.a., 12.b., 12.c. and 12.d.). The flat-field system shown in figure 12.d is similar to the system shown in figure 10.d, though the arrangement of the "small corrector pair" of the tertiary and quaternary mirrors is somewhat different. Optical design data for these systems is given in table 7.

| System | R1 | t1 | R2 | t2 | R3 | t3 | R4 | t4 |
|---|---|---|---|---|---|---|---|---|
| **Fig 11.a** | -2.0 | -0.66005 | -0.14085 | 0.48884 | 2.51116 | -1.87143 | 2.69156 | 3.282 |
| **Fig 11.b** | -2.0 | -1.24005 | -0.13889 | 0.13430 | 6.8657 | -1.32947 | 1.65190 | 1.826 |
| **Fig 12.a** | 2.0 | -0.61005 | 1.24984 | 1.24944 | 0.75056 | -0.67398 | 0.96508 | 1.181 |
| **Fig 12.c** | 2.0 | -1.21005 | 1.99960 | 3.23066 | 4.76934 | -3.24174 | 5.06698 | 6.564 |
| **Fig 12.d** | 2.0 | -2.87005 | 3.33186 | 2.94074 | 0.05962 | -0.03519 | 0.05794 | 0.080 |
| **Fig 12.e** | 1.618 | -2.61798 | 4.23598 | 7.00000 | 1.28818 | -7.47487 | 8.76305 | 9.805 |

**Table 7. Optical design data for CA-type solutions as shown in figures 11 and 12. Figure 12.b is an example of a flat-field Schiefspiegler obtainable by using an off-axis portion of the pupil of the system in figure 12.a.**

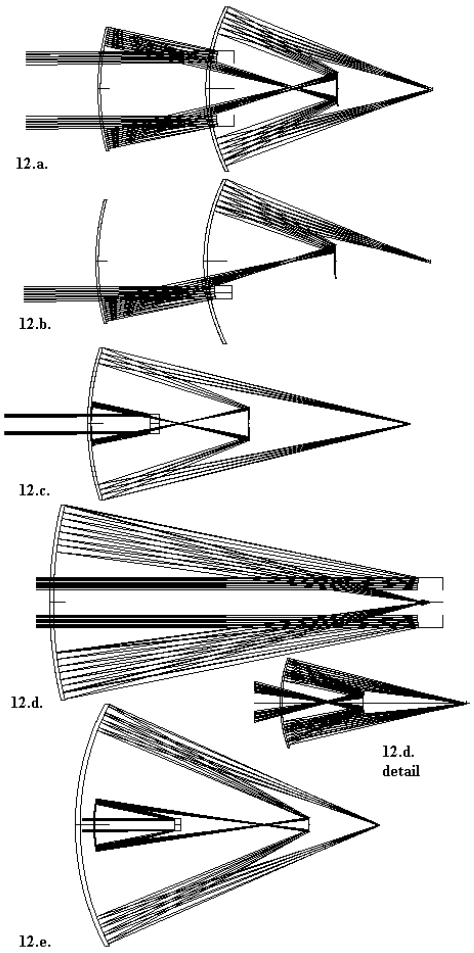


**Figure 12. Each of the first four CA-type convex primary mirror solutions shown here has zero Petzval curvature. 12.b is a Schiefspiegler with a relatively fast numerical aperture taken from the axially symmetrical parent in 12.a. The system in 12.e is comprised of two individually anastigmatic concentric spherical mirror pairs. Solutions such as this are a special case, lying in a 2-dimensional sub-space of the 3-dimesional solution space.**

The system shown in figure 12.e. is an example of a four-spherical mirror anastigmat that consists of two individually anastigmatic pairs of concentric spherical mirrors. In this case the primary and secondary mirrors form a two-concentric spherical-mirror anastigmat with the object at infinity, and the tertiary and quaternary mirrors are a two-concentric-spherical-mirror anastigmatic relay.

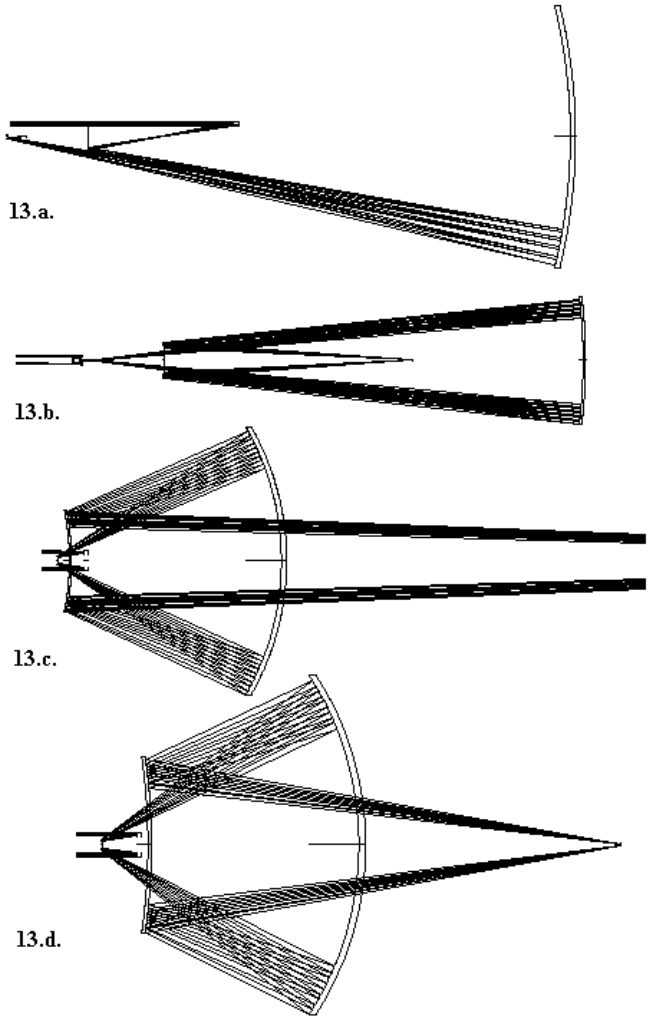


**Figure 13. Three distinct families of CB-type concave primary mirror solutions are shown here. The 45213 system in13.a comes from one family, the 21453 solution in 13.b from a second and the 24135 and 21435 systems in 13.c and 13.d from the third.**

## 3.8 CB SOLUTIONS

Concave primary CB-type solutions exist in three unconnected volumes within the solution space. 45213 solutions as shown in figure 13.a come from one of the solution volumes. These systems only work as Schiefspiegler, and have relatively uninteresting geometries. The 21453 solutions as in figure 13.b come from another distinct family of solutions and 21453- and 24135-type solutions as shown in figure 13.c come from the third. There are no afocal systems or systems with zero Petzval curvature among these solutions. Optical design data for these systems are given in table 8.

There is a relatively wide variety of convex primary mirror CB-type solutions, including flat-field systems and afocal systems. 21435, 24135, 42153, 42135 and 45213 geometries exist and examples are given in figure 14 and table 8. These solutions come from three unconnected volumes of solution. The 45213 example in figure 14.e. shows in effect a three-mirror anastigmat with the secondary mirror as a flat fold mirror. While technically the example given has four powered mirrors, there does exist a very similar system to the one shown in which the secondary mirror has no power.

| System | R1 | t1 | R2 | t2 | R3 | t3 | R4 | t4 |
|---|---|---|---|---|---|---|---|---|
| **Fig 13.a** | -2.0 | -1.95005 | -10.0100 | 6.46323 | -7.46323 | -7.55919 | -0.42120 | 0.264 |
| **Fig 13.b** | -2.0 | -0.38005 | -3.33440 | 23.8200 | -24.8200 | -19.5608 | -44.4246 | 11.610 |
| **Fig 13.c** | -2.0 | -0.54005 | -0.23256 | 4.65637 | -5.65637 | -4.38337 | -5.48759 | 25.449 |
| **Fig 13.d** | -2.0 | -0.58005 | -0.19608 | 4.26324 | -5.26324 | -3.45058 | -10.3864 | 7.797 |
| **Fig 14.a** | 2.0 | -2.01054 | 3.31934 | 4.54919 | 3.45264 | -0.71567 | 2.04974 | 5.056 |
| **Fig 14.b** | 2.0 | -2.25005 | 1.99960 | 7.24702 | -6.24702 | -5.37939 | -3.11477 | 12.531 |
| **Fig 14.c** | 2.0 | -1.82005 | 3.33220 | 20.8835 | -19.8835 | -23.1106 | -3.44192 | 4.166 |
| **Fig 14.d** | 2.0 | -1.29005 | -10.0100 | 3.18882 | -5.18882 | -9.15276 | 5.98398 | 22.530 |
| **Fig 14.e** | 2.0 | -1.00005 | 10000 | 2.23341 | -5.23341 | -6.80769 | -3.52854 | 0.043 |

**Table 8. Optical design data for CB-type systems as shown in figures 13 and 14.**

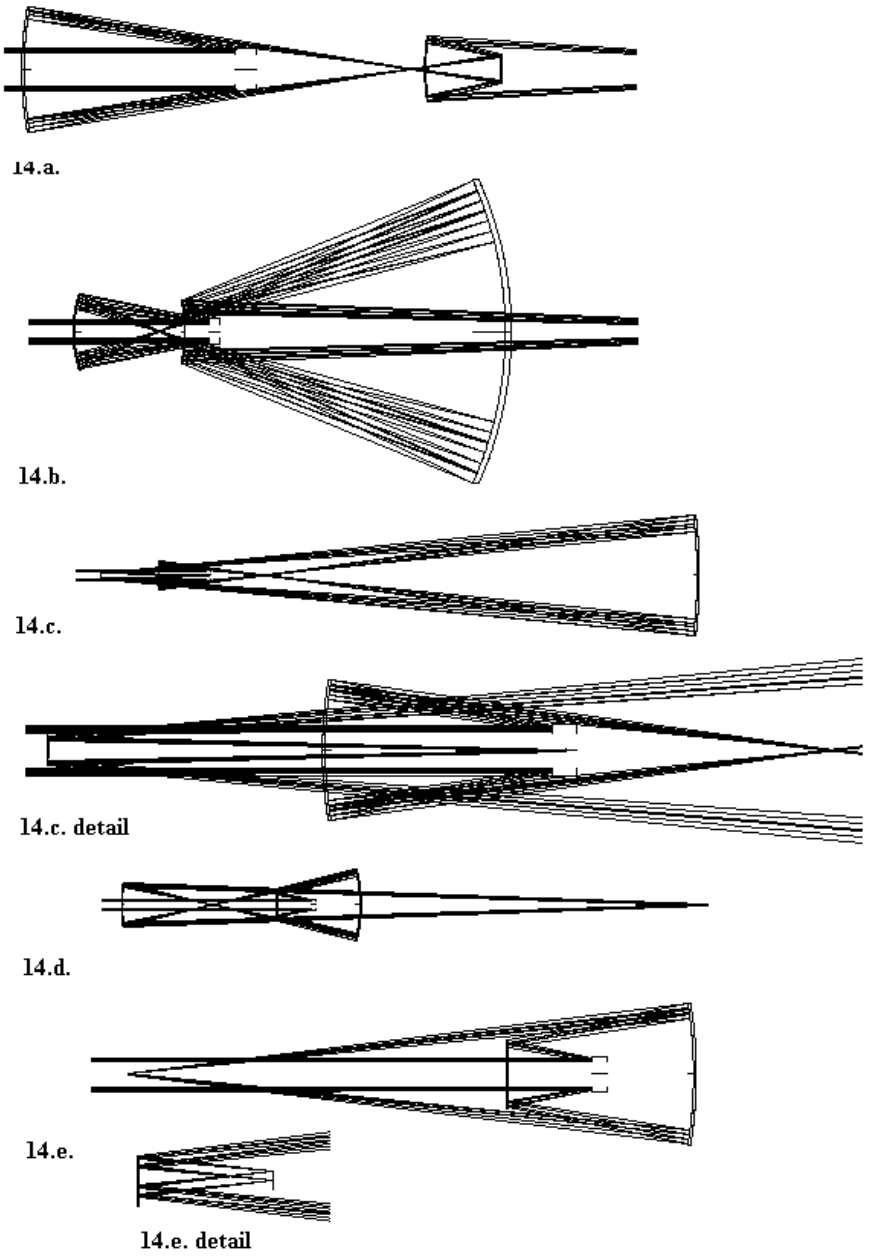


**Figure 14. Three distinct families if CB-type convex primary systems exist. 14.a is an example of a flat-field system from one of these families. 14.e is very close to a special case system in which the secondary mirror has zero power; essentially a three-spherical mirror anastigmat.**

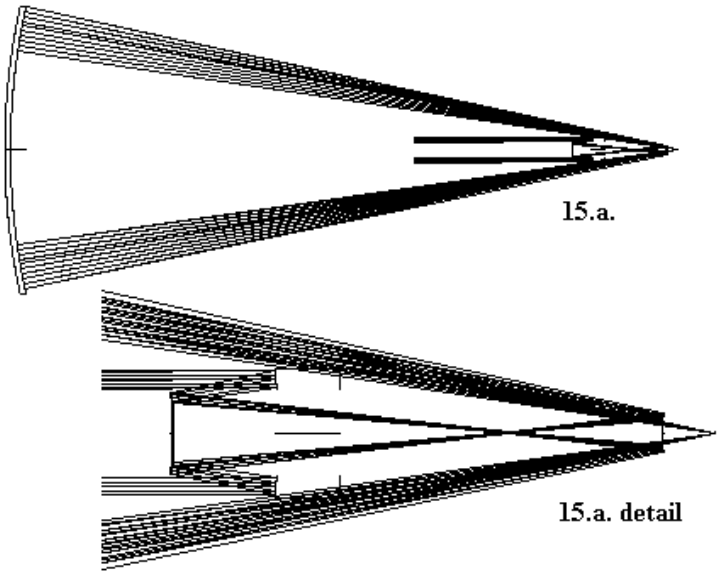


**Figure 15. The system depicted here is typical of the very limited range of available CC-type concave primary mirror systems.**

| System | R1 | t1 | R2 | t2 | R3 | t3 | R4 | t4 |
|---|---|---|---|---|---|---|---|---|
| **Fig 15** | -2.0 | -0.34005 | -3.33444 | 1.58416 | 1.41584 | -11.0188 | 11.2492 | 11.190 |
| **Fig 16.a** | 2.0 | -1.81005 | -1.42878 | 1.18685 | -2.18685 | -2.16756 | 3.71605 | 0.524 |
| **Fig 16.b** | 2.0 | -1.13005 | 1.11099 | 0.82160 | 0.17840 | -2.88205 | 2.89642 | 2.872 |
| **Fig 16.c** | 2.0 | -1.08005 | 1.11099 | 0.82612 | 0.17388 | -2.62531 | 2.64161 | 2.620 |
| **Fig 16.d** | 2.0 | -0.85005 | 1.11099 | 0.85118 | 0.14882 | -1.49641 | 1.52108 | 1.513 |

**Table 9. Optical design data for CC-type systems as shown in figures 15 and 16.**

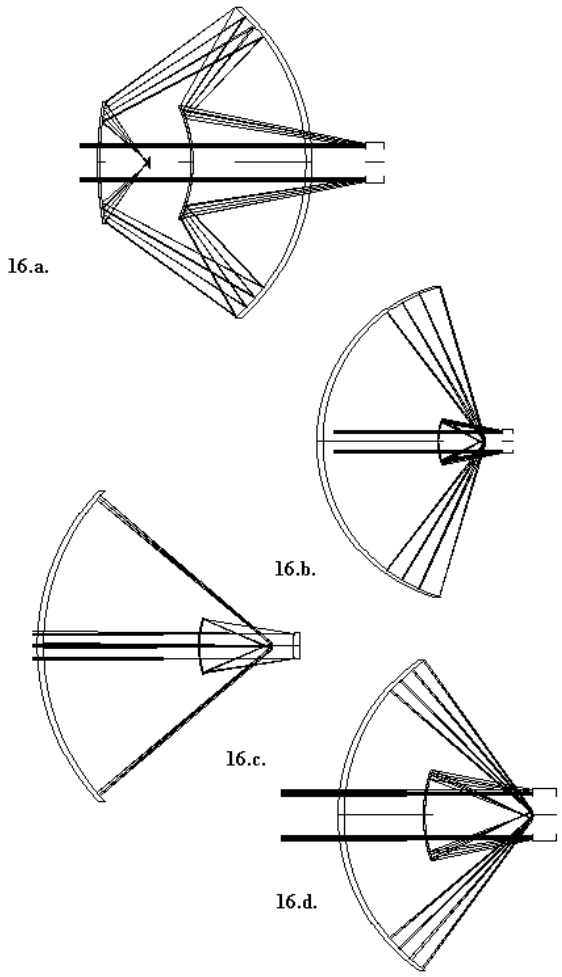


**Figure 16. CC-type convex primary mirror systems from the single available solution family are depicted here. All members of this family have relatively high numerical apertures.**

## 3.9 CC SOLUTIONS

A very limited range of concave primary CC-type solutions exists as shown in figure 15. All solutions of this type are in the 42135 configuration.

While there is somewhat more variety with the convex primary CC-type solutions, with 45231, 42531, 42351 and 42135 geometries available, all members of this family of solution are characterized by an extremely fast focal ratio. This means that the third-order aberration approximation is not so close to an optimum solution for this family of systems, as was the case with the CA concave

primary mirror systems. Convex primary CC-type solutions are shown in figure 16, with optical design data given in table 9.

## 4. Conclusion

A large number of solutions for four-spherical-mirror anastigmatic systems have been presented in this paper. Eleven geometrically distinct families of solution have been found to exist for convex primary systems. Nine geometrically distinct families of concave-primary mirror type solutions have been found. The solution families include focal and afocal systems. Numerous solutions have been found that have zero Petzval curvature. Of the sixteen possible arrangements of four mirrors and focal plane mentioned in section 2, only the 42513 arrangements have not been found in this survey.

Together with the systems discussed in reference 1, the systems described here represent the full range of available possibilities for four-spherical mirror anastigmats with the object at infinity. Of the systems discussed in this paper and in reference 1, only one has appeared in previously published work. This was an interesting system described by David Shafer[2], which can now be seen to be a member of the AB-type convex primary systems.

While many of these systems may seem somewhat impractical, the practicality or otherwise of a given system is strongly dependent on the application. The main purpose of this work has been to define the range of possible solutions, a task that would be very difficult if not impossible to achieve if conventional optical design software was employed.

## 5. Acknowledgement

This series of papers is dedicated to the memory of my great friend and mentor of almost 20 years, and as of late my Ph.D. supervisor, Norman Jack Rumsey. Norman died in January 2007, aged 84, after a career in optics spanning more than 60 years.

## References


1. A. Rakich, “Four-mirror anastigmats I: a complete solution set for all-spherical telescopic systems”, Submitted *OE*, 16/12/2006.
2. Shafer, D., “Galaxy Wars Optics”, *Optics News*, **14**, No. 6, 1988
3. A. Rakich, “Complete solution set for four-spherical-mirror anastigmatic telescope systems”, *Proc. SPIE*, **5249**, pp. 103-111, 2004

# Appendix D: Sample Mathematica File

This appendix presents as an example the Mathematica program used to generate one of the families of solutions as described in chapter 3 of this thesis. No attempt is made to explain the program, but it may prove useful to people interested in replicating the results presented in this thesis.

The core mathematical development occurs on the first two pages (pp 209-210). Subsequent pages are mainly concerned with filters used to determine practicality, and iteration.

```
g = 0; SCHp = 0.725; r1 = 2; h = 0; t1 = 1.0005; c2 = -3.5001; VALUES = {}; delt = 0.01; delc2 = 0.01;
delEp = 10; t1 = t1 - delt; Ep = 0; Label[RST]; Csum = 0; t1 = t1 + delt; r2 = 1/c2;
N1 = -1; N2 = 1; N3 = -1; N4 = 1; y1 = .2; c1 = 1/r1; Ø1 = (N2 - N1)/r1; Ø2 = (N3 - N2)/r2;
!Matrix Mirror 1;
m1 = {{1, 0}, {Ø1, 1}};
!T1 Matrix;
m2 = {{1, -t1}, {0, 1}};
!Matrix Mirror 2;
m3 = {{1, 0}, {Ø2, 1}};
M3 = m1.m2.m3;
UY2 = {0, .2}.M3;
u3 = -Part[UY2, 1];
y2 = Part[UY2, 2];
l2 = y2/u3;
!Distance from pole of secondary to marginal ray's intersection with the axis;
!Ep is the distance of the entrance pupil to the pole of the primary mirror in object space;
x1 = r1 - Ep;
x2 = r1 (t1 + r2)/(2 (t1 + r2) - r1) - Ep;
W1 = -.25 * N1 * c1^3 * y1^4;
u2 = (N2 - N1) * c1 * y1;
i2 = c2 * y2 - u2;
W2 = -.25 * N2 * c2 * i2^2 * y2^2;
x3 = (x1^2 * W1 + x2^2 * W2)/(x1 * W1 + x2 * W2);
W3 = -(x1 * W1 + x2 * W2)/x3;
W4 = -(W3 + W1 + W2);
x4 = 0;

LLL3 = -(Ep + x3);
UYLLL3 = {0.2/LLL3, 0.2}.M3;
L = Part[UYLLL3, 2]/Part[UYLLL3, 1];
P3 = y2 + L * u3;
a0 = -4 * W3/P3^4; a1 = u3^2/P3^2; a2 = 2 * u3/P3; Y = 3 * a1 - a2^2; Z = -27 * a0 + 9 * a1 * a2 - 2 * a2^3;
Q = (4 * Y^3 + Z^2)^.5;
```

$$\text{Sol1} = -\frac{a2}{3} + \frac{\left(1 - I\, 3^{0.5`}\right) Y}{3\, 2^{2/3}\, (Z + Q)^{1/3}} - \frac{\left(1 + I\, 3^{0.5`}\right) (Z + Q)^{1/3}}{6\, 2^{1/3}};$$

```
If[Abs[Im[Sol1]] > 10^-8, Goto[Imaginarysols]]; sola = Re[Sol1]; r3 = 1/sola; c3 = sola;
t2 = -r3 - L;
Ø3 = (N4 - N3) * c3;
!transfer2;
m4 = {{1, t2}, {0, 1}};
!mirror3;
m5 = {{1, 0}, {Ø3, 1}};
Mtert = M3.m4.m5;
UY3 = {0, 0.2}.Mtert;
```

```
y3 = Part[UY3, 2];
u4 = Part[UY3, 1];
i3 = c3 * y3 - u3;
LLL = -(x4 + Ep);
CoC4 = (Part[Mtert, 2, 2] * LLL + Part[Mtert, 1, 2]) / (Part[Mtert, 2, 1] * LLL + Part[Mtert, 1, 1]);
P4 = y3 - CoC4 * u4;
b0 = 4 * W4 / P4^4; b1 = u4^2 / P4^2; b2 = 2 * u4 / P4; Y = 3 * b1 - b2^2; Z = -27 * b0 + 9 * b1 * b2 - 2 * b2^3;
Q = (4 * Y^3 + Z^2)^.5; Sol2 = -b2/3 + (1 - I 3^0.5`) Y / (3 2^(2/3) (Z + Q)^(1/3)) - (1 + I 3^0.5`) (Z + Q)^(1/3) / (6 2^(1/3));
If[Abs[Im[Sol2]] > 10^-8, Goto[Imaginarysols]];
solb = Re[Sol2]; r4 = 1 / solb; c4 = solb;
t3 = CoC4 - r4; M4 = (N3 - N4) * c4;
m6 = {{1, -t3}, {0, 1}}; m7 = {{1, 0}, {M4, 1}}; Mquart = Mtert.m6.m7;
UY4 = {0, 0.2}.Mquart;
y4 = Part[UY4, 2]; u5 = -Part[UY4, 1]; t4 = y4 / u5;

If[t2 > 0, Goto[stepping]]; If[t3 < 0, Goto[stepping]]; If[t4 > 0, Goto[stepping]]; If[t3 < 0, Goto[stepping]];
If[t4 > 0, Goto[stepping]]; If[t2 < -2, Goto[stepping]]; If[t3 > 2, Goto[stepping]];
If[t2 > -0.01`, Goto[stepping]]; If[t3 < 0.01`, Goto[stepping]]; If[Abs[y4] > 0.8, Goto[stepping]];
If[Abs[y3] > 0.8, Goto[stepping]]; If[Abs[r3] < 0.005, Goto[stepping]]; If[Abs[r4] < 0.005, Goto[stepping]];
Goto[bobb]; Label[bob]; !Print["virtual airspaces"]; Goto[stepping]; Label[boob];
If[TrueQ[t3 === t4], Goto[stepping]]; Goto[goodsolution]; Label[Imaginarysols];
!imaginary solution to cubic; Goto[stepping]; Label[goodsolution];
If[t4 > -0.05, Goto[stepping]]; y5 = -.25 / Sin[u5] * 2 * y1 * .5 * Pi / 180;
!!!! 01 heights;


y1a = SCHp * y1; y2a = SCHp * y2; y3a = SCHp * y3; y4a = SCHp * y4; y5a = SCHp * y5; y1av = (y1 + y1a) / 2;
y2av = (y2 + y2a) / 2; y3av = (y3 + y3a) / 2; y4av = (y4 + y4a) / 2; y5av = (y5 + y5a) / 2;

!!!!! 12 heights;

m13 = {{1, -(t1 + t2)}, {0, 1}}; m14 = {{1, -(t1 + t2 + t3)}, {0, 1}}; m15 = {{1, -(t1 + t2 + t3 + t4)}, {0, 1}};

UY13 = {0, .2}.m1.m13; UY14 = {0, .2}.m1.m14; UY15 = {0, .2}.m1.m15;
UY13a = {0, .2 * SCHp}.m1.m13; UY14a = {0, .2 * SCHp}.m1.m14; UY15a = {0, .2 * SCHp}.m1.m15;
m12y3 = Part[UY13, 2]; m12y4 = Part[UY14, 2]; m12y5 = Part[UY15, 2];
m12y3a = Part[UY13a, 2]; m12y4a = Part[UY14a, 2]; m12y5a = Part[UY15a, 2];

m12y3av = (m12y3 + m12y3a) / 2; m12y4av = (m12y4 + m12y4a) / 2; m12y5av = (m12y5 + m12y5a) / 2;



!!!!!! 23 heights;
m21 = {{1, -t1}, {0, 1}}; m24 = {{1, (t2 + t3)}, {0, 1}}; m25 = {{1, (t2 + t3 + t4)}, {0, 1}};
UY21 = {0, 0.2}.M3.m21; UY24 = {0, 0.2}.M3.m24; UY25 = {0, 0.2}.M3.m25;
UY21a = {0, 0.2 * SCHp}.M3.m21; UY24a = {0, 0.2 * SCHp}.M3.m24; UY25a = {0, 0.2 * SCHp}.M3.m25;
m23y1 = Part[UY21, 2]; m23y4 = Part[UY24, 2]; m23y5 = Part[UY25, 2];
m23y1a = Part[UY21a, 2]; m23y4a = Part[UY24a, 2]; m23y5a = Part[UY25a, 2];
m23y1av = (m23y1 + m23y1a) / 2; m23y4av = (m23y4 + m23y4a) / 2; m23y5av = (m23y5 + m23y5a) / 2;
```

```
!!!!!!! 34 heights;

m31 = {{1, (t1 + t2)}, {0, 1}}; m32 = {{1, t2}, {0, 1}}; m35 = {{1, -(t3 + t4)}, {0, 1}};
UY31 = {0, 0.2}.Mtert.m31; UY32 = {0, 0.2}.Mtert.m32; UY35 = {0, 0.2}.Mtert.m35;
UY31a = {0, 0.2 * SCHp}.Mtert.m31; UY32a = {0, 0.2 * SCHp}.Mtert.m32; UY35a = {0, 0.2 * SCHp}.Mtert.m35;
m34y1 = Part[UY31, 2]; m34y2 = Part[UY32, 2]; m34y5 = Part[UY35, 2];
m34y1a = Part[UY31a, 2]; m34y2a = Part[UY32a, 2]; m34y5a = Part[UY35a, 2];
m34y1av = (m34y1 + m34y1a) / 2; m34y2av = (m34y2 + m34y2a) / 2; m34y5av = (m34y5 + m34y5a) / 2;


!!!!!!!! 45 heights;

m41 = {{1, -(t1 + t2 + t3)}, {0, 1}}; m42 = {{1, -(t2 + t3)}, {0, 1}}; m43 = {{1, -(t3)}, {0, 1}};
UY41 = {0, 0.2}.Mquart.m41; UY42 = {0, 0.2}.Mquart.m42; UY43 = {0, 0.2}.Mquart.m43;
UY41a = {0, 0.2 * SCHp}.Mquart.m41; UY42a = {0, 0.2 * SCHp}.Mquart.m42; UY43a = {0, 0.2 * SCHp}.Mquart.m43;
m45y1 = Part[UY41, 2]; m45y2 = Part[UY42, 2]; m45y3 = Part[UY43, 2];
m45y1a = Part[UY41a, 2]; m45y2a = Part[UY42a, 2]; m45y3a = Part[UY43a, 2];
m45y1av = (m45y1 + m45y1a) / 2; m45y2av = (m45y2 + m45y2a) / 2; m45y3av = (m45y3 + m45y3a) / 2;

!!! Sorting Schiefspiegler;
!!! type 213 or 231;
If[Abs[t2] > Abs[t1], Goto[213]];
!!! Type 231 here;
If[(t1 + t2 + t3) > t1, Goto[4231]];
!!!! Type 2431;
If[(t1 + t2 + t3 + t4) < 0, Goto[24315]];
!!!! Type 24531 or 24351;
If[(t1 + t2 + t3 + t4) < (t1 + t2), Goto[24351]];
!!!!! Type 24531;
Goto[24531];


!!!!!Type 24351;
!!!!!Type 24315;
Label[4231];
!!!!Type[4231];
If[(t1 + t2 + t3 + t4) > t1, Goto[45231]];
!!!!Type 42531 or 42351 or 42315;
If[(t1 + t2 + t3 + t4) < 0, Goto[42315]];
!!!!Type 42531 or 42351;
If[(t1 + t2) < (t1 + t2 + t3 + t4), Goto[42531]];
!!!!!Type 42351;
Goto[42351];
!!!!!Type[42531];
!!!!!Type 42315;
!!!!!Type 45231;
Label[213];
!!!Type 2143 2413 or 4213;
```

```
!!!!Type 2143;
!!!Type 21435 or 21453;
If[Abs[t4] > Abs[t3], Goto[21435]];
!!!!!Type 21453;
Goto[21453];
!!!!!Type21435 ;
Label[2413 or 4213];
If[(t1 + t2 + t3) < t1, Goto[2413]];
!!!!Type 4213;
!!! 45213 42513 42153 or 42135;
If[(t1 + t2 + t3 + t4) > t1, Goto[45213]];
If[(t1 + t2 + t3 + t4) < 0, Goto[42153 or 42135]];
!!!!!Type 42513;
Goto[42513];
Label[42153 or 42135];
If[(t1 + t2) > (t1 + t2 + t3 + t4), Goto[42135]];
Goto[42153];
Label[2413];
!!! 24513 24153 or 24135;
If[t1 + t2 + t3 + t4 < 0, Goto[24153 or 24135]];
Goto[24513];
Label[24153 or 24135];
If[t1 + t2 + t3 + t4 < t1 + t2, Goto[24135]];
Goto[24153];
Label[24531];
!!! 01 conditions;
If[Abs[y1av - y2av] < (Abs[(y1 - y1a)] + Abs[(y2 - y2a)]) / 2, Goto[stepping]];
If[Abs[y1av - y3av] < (Abs[(y1 - y1a)] + Abs[(y3 - y3a)]) / 2, Goto[stepping]];
If[Abs[y1av - y4av] < (Abs[(y1 - y1a)] + Abs[(y4 - y4a)]) / 2, Goto[stepping]];
If[Abs[y1av - y5av] < (Abs[(y1 - y1a)] + Abs[(y5 - y5a)]) / 2, Goto[stepping]];

!!! 12 conditions;
If[Abs[m12y3av - y3av] < (Abs[(m12y3 - m12y3a)] + Abs[(y3 - y3a)]) / 2, Goto[stepping]];
If[Abs[m12y4av - y4av] < (Abs[(m12y4 - m12y4a)] + Abs[(y4 - y4a)]) / 2, Goto[stepping]];
If[Abs[m12y5av - y5av] < (Abs[(m12y5 - m12y5a)] + Abs[(y5 - y5a)]) / 2, Goto[stepping]];

!!! 23 conditions;

If[Abs[m23y4av - y4av] < (Abs[(m23y4 - m23y4a)] + Abs[(y4 - y4a)]) / 2, Goto[stepping]];
If[Abs[m23y5av - y5av] < (Abs[(m23y5 - m23y5a)] + Abs[(y5 - y5a)]) / 2, Goto[stepping]];
```

```
!!! 34 conditions;
If[Abs[m34y5av - y5av] < (Abs[(m34y5 - m34y5a)] + Abs[(y5 - y5a)]) / 2, Goto[stepping]];

!!! no 45 conditions;

Print["24531"];
Goto[gdsol];

Label[24351];
!!! 01 conditions;
If[Abs[y1av - y2av] < (Abs[(y1 - y1a)] + Abs[(y2 - y2a)]) / 2, Goto[stepping]];
If[Abs[y1av - y3av] < (Abs[(y1 - y1a)] + Abs[(y3 - y3a)]) / 2, Goto[stepping]];
If[Abs[y1av - y4av] < (Abs[(y1 - y1a)] + Abs[(y4 - y4a)]) / 2, Goto[stepping]];
If[Abs[y1av - y5av] < (Abs[(y1 - y1a)] + Abs[(y5 - y5a)]) / 2, Goto[stepping]];

!!! 12 conditions;

If[Abs[m12y3av - y3av] < (Abs[(m12y3 - m12y3a)] + Abs[(y3 - y3a)]) / 2, Goto[stepping]];
If[Abs[m12y4av - y4av] < (Abs[(m12y4 - m12y4a)] + Abs[(y4 - y4a)]) / 2, Goto[stepping]];
If[Abs[(m12y5av - y5av)] < (Abs[(m12y5 - m12y5a)] + Abs[(y5 - y5a)]) / 2, Goto[stepping]];


!!! 23 conditions;

If[Abs[m23y4av - y4av] < (Abs[(m23y4 - m23y4a)] + Abs[(y4 - y4a)]) / 2, Goto[stepping]];

!!! No 34 conditions in this case;

!!! 45 conditions;
If[Abs[m45y3av - y3av] < (Abs[(m45y3 - m45y3a)] + Abs[(y3 - y3a)]) / 2, Goto[stepping]];

Print["24351"];
Goto[gdsol];

Label[24315];
!!! 01 conditions;
If[Abs[y1av - y2av] < (Abs[(y1 - y1a)] + Abs[(y2 - y2a)]) / 2, Goto[stepping]];
If[Abs[y1av - y3av] < (Abs[(y1 - y1a)] + Abs[(y3 - y3a)]) / 2, Goto[stepping]];
If[Abs[y1av - y4av] < (Abs[(y1 - y1a)] + Abs[(y4 - y4a)]) / 2, Goto[stepping]];

!!! 12 conditions;
If[Abs[m12y3av - y3av] < (Abs[(m12y3 - m12y3a)] + Abs[(y3 - y3a)]) / 2, Goto[stepping]];
If[Abs[m12y4av - y4av] < (Abs[(m12y4 - m12y4a)] + Abs[(y4 - y4a)]) / 2, Goto[stepping]];

!!! 23 conditions;

If[Abs[m23y4av - y4av] < (Abs[(m23y4 - m23y4a)] + Abs[(y4 - y4a)]) / 2, Goto[stepping]];

!!! no 34 conditions;

!!! 45 conditions;
If[Abs[m45y1av - y1av] < (Abs[(m45y1 - m45y1a)] + Abs[(y1 - y1a)]) / 2, Goto[stepping]];
If[Abs[m45y3av - y3av] < (Abs[(m45y3 - m45y3a)] + Abs[(y3 - y3a)]) / 2, Goto[stepping]];

Print["24315"];
Goto[gdsol];
```

```
Label[42351];
!!!01conditions;
If[Abs[y1av-y2av]<(Abs[(y1-y1a)]+Abs[(y2-y2a)])/2,Goto[stepping]];
If[Abs[y1av-y3av]<(Abs[(y1-y1a)]+Abs[(y3-y3a)])/2,Goto[stepping]];
If[Abs[y1av-y4av]<(Abs[(y1-y1a)]+Abs[(y4-y4a)])/2,Goto[stepping]];
If[Abs[y1av-y5av]<(Abs[(y1-y1a)]+Abs[(y5-y5a)])/2,Goto[stepping]];

!!!12conditions;
If[Abs[m12y3av-y3av]<(Abs[(m12y3-m12y3a)]+Abs[(y3-y3a)])/2,Goto[stepping]];
If[Abs[m12y5av-y5av]<(Abs[(m12y5-m12y5a)]+Abs[(y5-y5a)])/2,Goto[stepping]];

!!!NO 23 conditions IN THIS CASE;

!!! 34conditions;
If[Abs[m34y2av-y2av]<(Abs[(m34y2-m34y2a)]+Abs[(y2-y2a)])/2,Goto[stepping]];

!!! 45conditions;
If[Abs[m45y1av-y1av]< (Abs[(m45y1-m45y1a)]+Abs[(y1-y1a)])/2,Goto[stepping]];
If[Abs[m45y3av-y3av]< (Abs[(m45y3-m45y3a)]+Abs[(y3-y3a)])/2,Goto[stepping]];

Print["42351"];
Goto[gdsol];


Label[42315];
!!!01conditions;
If[Abs[y1av-y2av]<(Abs[(y1-y1a)]+Abs[(y2-y2a)])/2,Goto[stepping]];
If[Abs[y1av-y3av]<(Abs[(y1-y1a)]+Abs[(y3-y3a)])/2,Goto[stepping]];
If[Abs[y1av-y4av]<(Abs[(y1-y1a)]+Abs[(y4-y4a)])/2,Goto[stepping]];


!!!12conditions;
If[Abs[m12y3av-y3av]<(Abs[(m12y3-m12y3a)]+Abs[(y3-y3a)])/2,Goto[stepping]];

!!!NO 23 conditions IN THIS CASE;

!!! 34conditions;
If[Abs[m34y2av-y2av]<(Abs[(m34y2-m34y2a)]+Abs[(y2-y2a)])/2,Goto[stepping]];
```

```
!!! 45 conditions;
If[Abs[m45y1av - y1av] < (Abs[(m45y1 - m45y1a)] + Abs[(y1 - y1a)]) / 2, Goto[stepping]];
If[Abs[m45y2av - y2av] < (Abs[(m45y2 - m45y2a)] + Abs[(y2 - y2a)]) / 2, Goto[stepping]];
If[Abs[m45y3av - y3av] < (Abs[(m45y3 - m45y3a)] + Abs[(y3 - y3a)]) / 2, Goto[stepping]];

Print["42315"];
Goto[gdsol];

Label[42531];
!!! 01 conditions;
If[Abs[y1av - y2av] < (Abs[(y1 - y1a)] + Abs[(y2 - y2a)]) / 2, Goto[stepping]];
If[Abs[y1av - y3av] < (Abs[(y1 - y1a)] + Abs[(y3 - y3a)]) / 2, Goto[stepping]];
If[Abs[y1av - y4av] < (Abs[(y1 - y1a)] + Abs[(y4 - y4a)]) / 2, Goto[stepping]];
If[Abs[y1av - y5av] < (Abs[(y1 - y1a)] + Abs[(y5 - y5a)]) / 2, Goto[stepping]];

!!! 12 conditions;
If[Abs[m12y3av - y3av] < (Abs[(m12y3 - m12y3a)] + Abs[(y3 - y3a)]) / 2, Goto[stepping]];
If[Abs[m12y5av - y5av] < (Abs[(m12y5 - m12y5a)] + Abs[(y5 - y5a)]) / 2, Goto[stepping]];

!!! 23 conditions;
If[Abs[m23y5av - y5av] < (Abs[(m23y5 - m23y5a)] + Abs[(y5 - y5a)]) / 2, Goto[stepping]];


!!! 34 conditions;
If[Abs[m34y2av - y2av] < (Abs[(m34y2 - m34y2a)] + Abs[(y2 - y2a)]) / 2, Goto[stepping]];
If[Abs[m34y5av - y5av] < (Abs[(m34y5 - m34y5a)] + Abs[(y5 - y5a)]) / 2, Goto[stepping]];

!!! 45 conditions;
If[Abs[m45y2av - y2av] < (Abs[(m45y2 - m45y2a)] + Abs[(y2 - y2a)]) / 2, Goto[stepping]];


Print["42531"];
Goto[gdsol];
```

```
Label[45231];
!!!01conditions;
If[Abs[y1av-y2av]<(Abs[(y1-y1a)]+Abs[(y2-y2a)])/2,Goto[stepping]];
If[Abs[y1av-y3av]<(Abs[(y1-y1a)]+Abs[(y3-y3a)])/2,Goto[stepping]];
If[Abs[y1av-y4av]<(Abs[(y1-y1a)]+Abs[(y4-y4a)])/2,Goto[stepping]];
If[Abs[y1av-y5av]<(Abs[(y1-y1a)]+Abs[(y5-y5a)])/2,Goto[stepping]];

!!!12conditions;
If[Abs[m12y3av-y3av]<(Abs[(m12y3-m12y3a)]+Abs[(y3-y3a)])/2,Goto[stepping]];

!!!NO23conditionsINTHISCASE;


!!!34conditions;

If[Abs[m34y2av-y2av]<(Abs[(m34y2-m34y2a)]+Abs[(y2-y2a)])/2,Goto[stepping]];
If[Abs[m34y5av-y5av]<(Abs[(m34y5-m34y5a)]+Abs[(y5-y5a)])/2,Goto[stepping]];

!!!no45conditions;

Print["45231"];
Goto[gdsol];

Label[21453];
!!!01conditions;
If[Abs[y1av-y2av]<(Abs[(y1-y1a)]+Abs[(y2-y2a)])/2,Goto[stepping]];

!!!NO12conditionsINTHISCASE;

!!!23conditions;
If[Abs[m23y1av-y1av]<(Abs[(m23y1-m23y1a)]+Abs[(y1-y1a)])/2,Goto[stepping]];
If[Abs[m23y4av-y4av]<(Abs[(m23y4-m23y4a)]+Abs[(y4-y4a)])/2,Goto[stepping]];
If[Abs[m23y5av-y5av]<(Abs[(m23y5-m23y5a)]+Abs[(y5-y5a)])/2,Goto[stepping]];

!!!34conditions;

If[Abs[m34y5av-y5av]<(Abs[(m34y5-m34y5a)]+Abs[(y5-y5a)])/2,Goto[stepping]];

!!!no45conditions;


Print["21453"];
Goto[gdsol];

Label[21435];
!!!01conditions;
If[Abs[y1av-y2av]<(Abs[(y1-y1a)]+Abs[(y2-y2a)])/2,Goto[stepping]];

!!!NO12conditionsINTHISCASE;
```

```
!!! 23 conditions;
If[Abs[m23y1av - y1av] < (Abs[(m23y1 - m23y1a)] + Abs[(y1 - y1a)]) / 2, Goto[stepping]];
If[Abs[m23y4av - y4av] < (Abs[(m23y4 - m23y4a)] + Abs[(y4 - y4a)]) / 2, Goto[stepping]];

!!! No 34 conditions in this case;

!!! 45 conditions;
If[Abs[m45y3av - y3av] < (Abs[(m45y3 - m45y3a)] + Abs[(y3 - y3a)]) / 2, Goto[stepping]];

Print["21435"];
Goto[gdsol];

Label[42513];
!!! 01 conditions;
If[Abs[y1av - y2av] < (Abs[(y1 - y1a)] + Abs[(y2 - y2a)]) / 2, Goto[stepping]];
If[Abs[y1av - y4av] < (Abs[(y1 - y1a)] + Abs[(y4 - y4a)]) / 2, Goto[stepping]];
If[Abs[y1av - y5av] < (Abs[(y1 - y1a)] + Abs[(y5 - y5a)]) / 2, Goto[stepping]];

!!! 12 conditions;
If[Abs[m12y5av - y5av] < (Abs[(m12y5 - m12y5a)] + Abs[(y5 - y5a)]) / 2, Goto[stepping]];

!!! 23 conditions;
If[Abs[m23y1av - y1av] < (Abs[(m23y1 - m23y1a)] + Abs[(y1 - y1a)]) / 2, Goto[stepping]];
If[Abs[m23y5av - y5av] < (Abs[(m23y5 - m23y5a)] + Abs[(y5 - y5a)]) / 2, Goto[stepping]];

!!! 34 conditions;
If[Abs[m34y1av - y1av] < (Abs[(m34y1 - m34y1a)] + Abs[(y1 - y1a)]) / 2, Goto[stepping]];
If[Abs[m34y2av - y2av] < (Abs[(m34y2 - m34y2a)] + Abs[(y2 - y2a)]) / 2, Goto[stepping]];
If[Abs[m34y5av - y5av] < (Abs[(m34y5 - m34y5a)] + Abs[(y5 - y5a)]) / 2, Goto[stepping]];

!!! 45 conditions;
If[Abs[m45y2av - y2av] < (Abs[(m45y2 - m45y2a)] + Abs[(y2 - y2a)]) / 2, Goto[stepping]];

Print["42513"];
Goto[gdsol];

Label[42153];
!!! 01 conditions;
If[Abs[y1av - y2av] < (Abs[(y1 - y1a)] + Abs[(y2 - y2a)]) / 2, Goto[stepping]];
If[Abs[y1av - y4av] < (Abs[(y1 - y1a)] + Abs[(y4 - y4a)]) / 2, Goto[stepping]];


!!! NO 12 conditions IN THIS CASE;
!!! 23 conditions;

If[Abs[m23y1av - y1av] < (Abs[(m23y1 - m23y1a)] + Abs[(y1 - y1a)]) / 2, Goto[stepping]];
If[Abs[m23y5av - y5av] < (Abs[(m23y5 - m23y5a)] + Abs[(y5 - y5a)]) / 2, Goto[stepping]];

!!! 34 conditions;
If[Abs[m34y1av - y1av] < (Abs[(m34y1 - m34y1a)] + Abs[(y1 - y1a)]) / 2, Goto[stepping]];
If[Abs[m34y2av - y2av] < (Abs[(m34y2 - m34y2a)] + Abs[(y2 - y2a)]) / 2, Goto[stepping]];
If[Abs[m34y5av - y5av] < (Abs[(m34y5 - m34y5a)] + Abs[(y5 - y5a)]) / 2, Goto[stepping]];
```

```
!! 45 conditions;
If[Abs[m45y1av - y1av] < (Abs[(m45y1 - m45y1a)] + Abs[(y1 - y1a)]) / 2, Goto[stepping]];
If[Abs[m45y2av - y2av] < (Abs[(m45y2 - m45y2a)] + Abs[(y2 - y2a)]) / 2, Goto[stepping]];


Print["42153"];
Goto[gdsol];

Label[42135];
!!! 01 conditions;
If[Abs[y1av - y2av] < (Abs[(y1 - y1a)] + Abs[(y2 - y2a)]) / 2, Goto[stepping]];
If[Abs[y1av - y4av] < (Abs[(y1 - y1a)] + Abs[(y4 - y4a)]) / 2, Goto[stepping]];


!!! NO 12 conditions IN THIS CASE;
!!! 23 conditions;
If[Abs[m23y1av - y1av] < (Abs[(m23y1 - m23y1a)] + Abs[(y1 - y1a)]) / 2, Goto[stepping]];


!!! 34 conditions;
If[Abs[m34y1av - y1av] < (Abs[(m34y1 - m34y1a)] + Abs[(y1 - y1a)]) / 2, Goto[stepping]];
If[Abs[m34y2av - y2av] < (Abs[(m34y2 - m34y2a)] + Abs[(y2 - y2a)]) / 2, Goto[stepping]];

!!! 45 conditions;
If[Abs[m45y1av - y1av] < (Abs[(m45y1 - m45y1a)] + Abs[(y1 - y1a)]) / 2, Goto[stepping]];
If[Abs[m45y2av - y2av] < (Abs[(m45y2 - m45y2a)] + Abs[(y2 - y2a)]) / 2, Goto[stepping]];
If[Abs[m45y3av - y3av] < (Abs[(m45y3 - m45y3a)] + Abs[(y3 - y3a)]) / 2, Goto[stepping]];

Print["42135"];
Goto[gdsol];

Label[45213];
!!! 01 conditions;
If[Abs[y1av - y2av] < (Abs[(y1 - y1a)] + Abs[(y2 - y2a)]) / 2, Goto[stepping]];
If[Abs[y1av - y4av] < (Abs[(y1 - y1a)] + Abs[(y4 - y4a)]) / 2, Goto[stepping]];
If[Abs[y1av - y5av] < (Abs[(y1 - y1a)] + Abs[(y5 - y5a)]) / 2, Goto[stepping]];

!!! NO 12 conditions IN THIS CASE;

!!! 23 conditions;
If[Abs[m23y1av - y1av] < (Abs[(m23y1 - m23y1a)] + Abs[(y1 - y1a)]) / 2, Goto[stepping]];


!!! 34 conditions;
If[Abs[m34y1av - y1av] < (Abs[(m34y1 - m34y1a)] + Abs[(y1 - y1a)]) / 2, Goto[stepping]];
If[Abs[m34y2av - y2av] < (Abs[(m34y2 - m34y2a)] + Abs[(y2 - y2a)]) / 2, Goto[stepping]];
If[Abs[m34y5av - y5av] < (Abs[(m34y5 - m34y5a)] + Abs[(y5 - y5a)]) / 2, Goto[stepping]];
```

```
!!! no 45 conditions;

Print["45213"];
Goto[gdsol];

Label[24513];
!!!01conditions;
If[Abs[y1av-y2av]<(Abs[(y1-y1a)]+Abs[(y2-y2a)])/2,Goto[stepping]];
If[Abs[y1av-y4av]<(Abs[(y1-y1a)]+Abs[(y4-y4a)])/2,Goto[stepping]];
If[Abs[y1av-y5av]<(Abs[(y1-y1a)]+Abs[(y5-y5a)])/2,Goto[stepping]];

!!!12conditions;
If[Abs[m12y4av-y4av]<(Abs[(m12y4-m12y4a)]+Abs[(y4-y4a)])/2,Goto[stepping]];
If[Abs[m12y5av-y5av]<(Abs[(m12y5-m12y5a)]+Abs[(y5-y5a)])/2,Goto[stepping]];

!!! 23conditions;
If[Abs[m23y1av-y1av]<(Abs[(m23y1-m23y1a)]+Abs[(y1-y1a)])/2,Goto[stepping]];
If[Abs[m23y4av-y4av]<(Abs[(m23y4-m23y4a)]+Abs[(y4-y4a)])/2,Goto[stepping]];
If[Abs[m23y5av-y5av]<(Abs[(m23y5-m23y5a)]+Abs[(y5-y5a)])/2,Goto[stepping]];


!!! 34conditions;
If[Abs[m34y1av-y1av]<(Abs[(m34y1-m34y1a)]+Abs[(y1-y1a)])/2,Goto[stepping]];
If[Abs[m34y5av-y5av]<(Abs[(m34y5-m34y5a)]+Abs[(y5-y5a)])/2,Goto[stepping]];

!!! no 45conditions;

Print["24513"];
Goto[gdsol];

Label[24153];
!!!01conditions;
If[Abs[y1av-y2av]<(Abs[(y1-y1a)]+Abs[(y2-y2a)])/2,Goto[stepping]];
If[Abs[y1av-y4av]<(Abs[(y1-y1a)]+Abs[(y4-y4a)])/2,Goto[stepping]];

!!!12conditions;
If[Abs[m12y4av-y4av]<(Abs[(m12y4-m12y4a)]+Abs[(y4-y4a)])/2,Goto[stepping]];

!!! 23conditions;
If[Abs[m23y1av-y1av]<(Abs[(m23y1-m23y1a)]+Abs[(y1-y1a)])/2,Goto[stepping]];
If[Abs[m23y4av-y4av]<(Abs[(m23y4-m23y4a)]+Abs[(y4-y4a)])/2,Goto[stepping]];
If[Abs[m23y5av-y5av]<(Abs[(m23y5-m23y5a)]+Abs[(y5-y5a)])/2,Goto[stepping]];

!!! 34conditions;
If[Abs[m34y1av-y1av]<(Abs[(m34y1-m34y1a)]+Abs[(y1-y1a)])/2,Goto[stepping]];
If[Abs[m34y5av-y5av]<(Abs[(m34y5-m34y5a)]+Abs[(y5-y5a)])/2,Goto[stepping]];
```

```
!!! 45 conditions;
If[Abs[m45y1av - y1av] < (Abs[(m45y1 - m45y1a)] + Abs[(y1 - y1a)]) / 2, Goto[stepping]];


Print["24153"];
Goto[gdsol];

Label[24135];
!!!01conditions;
If[Abs[y1av - y2av] < (Abs[(y1 - y1a)] + Abs[(y2 - y2a)]) / 2, Goto[stepping]];
If[Abs[y1av - y4av] < (Abs[(y1 - y1a)] + Abs[(y4 - y4a)]) / 2, Goto[stepping]];


!!!12conditions;
If[Abs[m12y4av - y4av] < (Abs[(m12y4 - m12y4a)] + Abs[(y4 - y4a)]) / 2, Goto[stepping]];

!!! 23conditions;
If[Abs[m23y1av - y1av] < (Abs[(m23y1 - m23y1a)] + Abs[(y1 - y1a)]) / 2, Goto[stepping]];
If[Abs[m23y4av - y4av] < (Abs[(m23y4 - m23y4a)] + Abs[(y4 - y4a)]) / 2, Goto[stepping]];


!!! 34conditions;
If[Abs[m34y1av - y1av] < (Abs[(m34y1 - m34y1a)] + Abs[(y1 - y1a)]) / 2, Goto[stepping]];

!!! 45conditions;
If[Abs[m45y1av - y1av] < (Abs[(m45y1 - m45y1a)] + Abs[(y1 - y1a)]) / 2, Goto[stepping]];
If[Abs[m45y3av - y3av] < (Abs[(m45y3 - m45y3a)] + Abs[(y3 - y3a)]) / 2, Goto[stepping]];

Print["24135"];
Goto[gdsol];

Label[gdsol];
If[Abs[.5 / Sin[u5]] > 10, Goto[stepping]];
Csum = -c1 + c2 - c3 + c4;
Petz = 2 * (c1 - c2 + 1 / r3 - c4); Print["Petz = ", Petz];
If[Abs[Im[Sol1]] > 1 * 10^-10, Print "Imaginary Solution"];
Print["r1=  ", -r1, "  r2=  ", -r2, "  r3=  ", -r3, "  r4=  ", -r4];
Print["t1=  ", t1, "  t2=  ", t2, "  t3=  ", t3, "  t4=  ", t4];
Print["t1=  ", t1, " c2=  ", c2, "  L=  ", L];
Print["k2=  ", k2];
Print["y1=  ", y1, "  y2=  ", y2, "  y3=  ", y3, "  y4=  ", y4]; Print["Sol1=  ", Sol1];
Print["Sol2=  ", Sol2]; Print["f/number=  ", .5 / Sin[u5]];

!Stepping iterations;
```

```
Label[stepping];
VALUES = Append[VALUES, Csum];
h = h + 1;
g = FractionalPart[h / 1000];
!!!"If[g<0.000001,Print[h],h=h+0]";
If[t1 > 2.4, Goto[c2iteration]];
Goto[RST];
Label[c2iteration];
If[c2 > -0.5, Goto[LStep]]; c2 = c2 + delc2; t1 = 1.00005;
Goto[RST];
 Label[LStep]; VALUES = Delete[VALUES, 1]; "Print[Dimensions[VALUES]]"; Va = VALUES;
 t = Partition[VALUES, 140];
 ListContourPlot[t, Contours -> {-.000001, 0, .000001}, ColorFunction -> GrayLevel, Axes →True, PlotLabel → Ep];
 Ep = Ep + delEp;
 VALUES = {};
 t = {};
 c2 = -3.5001;
 If[Ep > 100, Goto[omega]];
 Goto[RST];
Label[omega]; End)
```

# Appendix E: Schwarzschild Paper

The following paper was published in the Proceedings of SPIE, Volume 5875, in 2005, from the 2005 conference "Novel Optical Systems Design and Optimization VIII". This paper describes Schwarzschild's first two 1905 optics papers, which are referred to extensively throughout this thesis.

# The 100th Birthday of the conic constant and Schwarzschild's revolutionary papers in optics.

Andrew Rakich
EOS Space Systems, 111 Canberra Ave, Griffith, ACT 2603, Australia

**ABSTRACT**

In 1905 Karl Schwarzschild published three papers on optics, two of which revolutionized the field of reflecting telescope optics. In his first paper he developed a full theory of the aberrations of reflecting telescopes, generalizing the Eikonal of Bruns to take into account systems with an infinite long conjugate. In the second paper Schwarzschild applied his formulation to a masterful analysis of 2 mirror anastigmatic systems, along the way discovering the so called Ritchey-Chrétien aplanat, 18 years Ritchey and Chrétien's announcement. Numerous other innovations are given in what must be seen as being among the most important papers on the aberrations of optical systems ever written.

**Keywords: anastigmat, reflecting telescope, Schwarzschild**

## 1. INTRODUCTION

There is a famous quotation attributed to George Satayana "Those who forget the lessons of history are doomed to repeat them". This is certainly true in the field of optical design, where there are numerous examples of published work presented as novel despite clear prior examples existing in the literature. There are many misconceptions and ambiguities surrounding Schwarzschild's 1905 work in optics, works of immense significance and historical importance to the development of the aberration theory of reflecting optical systems.

For example there is the widespread misconception that Schwarzschild discovered the concentric 2-spherical-mirror anastigmat (he didn't). Numerous textbooks and papers refer to this as the "Schwarzschild anastigmat". The fact is that the true originator of this system is unclear. It has also been attributed to C.R. Burch, but inspection of Burch's publications reveals that he makes no claim of invention and treats the concentric two-spherical-mirror anastigmat as an already well known system[1]. While Schwarzschild's formulation of an aberration theory for two mirror systems lead to the two-concentric-spherical-mirror system as a trivial result, Schwarzschild himself never sought this solution, almost

certainly because of his focus on systems with flat-focal planes and of practical use to astronomy.

Likewise, it does not seem to be well known that Schwarzschild presented the formulation for the two-mirror aplanatic telescope 17 years before Ritchey and Chrétien[2], or that Schwarzschild was a pioneer in the field of high-order aberration theory.

This year, as the world celebrates the International Year of Physics, with its strong emphasis on the 100th anniversary of Einstein's 1905 papers, and as SPIE celebrates its 50th anniversary, it seems fitting to make some mention of the 100th anniversary of Karl Schwarzschild's monumental achievements in optics

## 2. BACKGROUND

Karl Schwarzschild was born in Frankfurt in 1873, the eldest of six children in the family of a well to do Jewish businessman. He was the only member of his family to pursue a career in science. At the age of 16 he had published his first two papers, on the orbital dynamics of binary stars.

After obtaining his Doctorate from the University of Munich, Schwarzschild went on to work as an assistant at a Vienna Observatory. It was here that he developed an interest in the relatively new field of photographic astronomy. He was the first to realize the significance in the difference in stellar magnitudes obtained visually and photographically (that these differences were related to the temperatures of the stellar atmospheres).

In 1901 Schwarzschild took up a position at Göttingen Observatory, first as an extraordinary professor; within a year he had been promoted to full professor. Here he developed his interests in the application of photography to the science of astronomy and in 1910 published the first part of the one of the first large scale photographic surveys of stellar magnitudes. It was most likely his interest in photographic astronomy that led him into geometrical optics.

To better understand the significance of Schwarzschild's contribution to geometrical optics it is helpful to consider his work in its historical context. To this end the following brief synopsis of relevant developments in the field in chronological order is presented:

• **Early visual reflecting telescopes:** Spherical aberration solutions by Descartes, Mersenne, Gregory, Newton and Cassegrain. Slow relative apertures

and limited field of view eyepieces mean that there is little pressure to correct field aberrations.

• **1795, G.S. Klügel:** The invention of iterative trigonometric ray tracing through successive surfaces on a single axis.

• **1829, J. Fraunhofer:** The heliometer for Königsberg was roughly corrected for field coma as well as for spherical aberration. How this was achieved is unclear.

• **1833, W.R. Hamilton:** Hamilton defined the "Characteristic Function", a general definition of the nature of the aberrations of a centered optical system in terms of fundamental system parameters.

• **1835-1840, The early development of practical photography:** For the first time there is real pressure for the development of a practical field aberration theory, since significant angular fields were required.

• **1835-1840, C.F.Gauss:** The "first-order" theory of a centered optical system.

• **1843, J. Petzval:** Probably the first to possess a practical theory of primary (and secondary) aberrations in the sense that he could calculate them from constructional parameters. Schwarzschild himself refers to Petzval's 5th order aberration theory in his first optics paper. Sadly, none of this work was published (a manuscript for a book was stolen from his house and his wife burned all his papers on his death).

• **1856, L. Seidel:** First to publish a complete and practical theory of third-order aberrations, named the Seidel aberrations in his honor.

• **1873, E. Abbé:** Abbé discovered the "sine condition", a general condition for freedom from spherical aberration and coma, and defined the term "aplanatic" for a system free of these aberrations.

• **1873-1890:** This period saw much development of optical design techniques using ray tracing and third-order theory. No significant work done on reflecting systems.

• **1895, H. Bruns:** Bruns developed the "Eikonal", a set of differential equations giving the optical path length and relating object and image space, an extension of Hamilton's approach. Bruns took the Eikonal which he was familiar with from his use of it in mechanics and applied it to optics, apparently ignorant of the fact that Hamilton had first developed his characteristic function as an optical theory.

• **ca. 1900:** Astronomical photography with slow emulsions was pushing thinking towards faster relative apertures and larger fields than had previously been sought in astronomical telescopes.

In the early 1900's, when Schwarzschild was working towards large scale photographic sky surveys, astrograph objectives were exclusively refracting systems. In particular the Cooke Triplet anastigmats were providing the right combination of good aberration correction over a wide field of view and fast relative aperture.

Reflecting systems were considered useless for this sort of work as they were generally limited by field aberrations to slow relative apertures and narrow fields of view. In this environment Schwarzschild began his investigations into the aberration theory of optical systems, leading to some remarkable breakthroughs.

## 2. INVESTIGATIONS INTO GEOMETRICAL OPTICS I.

There is no better introduction to Schwarzschild's optics papers than his own introduction to his first paper, which is translated below:

***1. The current report presents a general introduction*** *to the aberration theory of optical systems with the intention on the one hand to give the non-specialist reader a compact overview on the area and on the other hand to produce for my own benefit a source of reference material to be used in future investigations. The representation is based on Hamilton's "Characteristic Function" which I will name together with Mr. Bruns as the "Eikonal". I would like to show herewith that the practical calculating optician does not have to fear the Eikonal as something highly theoretical, that one can get very comfortably from the Eikonal to the practical laws and especially to Seidel's formulae. Hamilton himself must have been very conscious on the applicability of his theorems, but completed (or at least published) investigations of only a few very simple cases of several lenses with axial object points. The derivation of the general calculation formulae directly from the Eikonal does not appear anywhere. This might have been caused by difficulties in the elimination of the so-called "intermediate variables", which can be overcome simply by the introduction of the "Seidel Variables" and the "Seidel Eikonal" (below 5 & 6).*

*The advantage of the application of the Eikonal is no less significant in investigations of 5$^{th}$ order aberrations than in the theory of 3$^{rd}$ order aberrations (which Seidel's formulae refer to). The*

*compilation of complete terms for the 5th order aberrations of a given optical system would not be too complicated following the formulae in § 5. The number of independent aberrations of the 5th order amounts, without more detail, to 9. Petzval, the calculator of the first "portrait lens" gave this number as 12, from which seems to follow that despite his calculations extending to aberration coefficients of the 9th order, he did not see through the relationship all too deeply. Apart from the general outline on the 5th order aberrations of an optical system in 11 this report presents therefore only well-known facts in a changed form. New material will be developed in my subsequent investigations.*

There are several interesting points to take from this introduction. First and foremost, Schwarzschild explicitly refers to a derivation of high-order aberration coefficients by Joseph Petzval. This is of great historical importance as no record of this work survives today; Schwarzschild's comments add to a large body of evidence suggesting that Petzval had a well developed aberration theory, including high-order aberration coefficients, at least a decade before Seidel published.

Schwarzschild's somewhat disparaging reference to Petzval having got the number of 5th order aberration coefficients wrong is in fact further evidence for the case that Petzval had indeed correctly derived high-order aberration coefficients. Recently de Meijere and Velzel[3] showed that one could obtain either 9 or 12 independent 5th order aberration coefficients depending on the choice of pupil-coordinate definitions.

While Schwarzschild modestly states that "this report presents therefore only well-known facts in a changed form", this is far from the case, as is shown below.

After outlining the Bruns Eikonal Schwarzschild immediately went on to develop the first significant innovation in this paper, the "Angle Eikonal". The Bruns Eikonal was only able to deal with systems with finite conjugates, and with his astronomical interests this clearly was not satisfactory to Schwarzschild. His Angle Eikonal generalized Bruns's work to allow the treatment of systems with infinite conjugates, as is the case with astronomical telescopes. A further development leads to what Schwarzschild calls the "Seidel variables", which he uses to obtain primary wavefront aberration coefficients. Schwarzschild points out the advantage of these wavefront aberration coefficients in that the individual surface contributions for each aberration are simply additive to give the system sum, unlike the transverse coefficients given by Seidel and others. In this connection Schwarzschild makes the following comments:

*This equation shows that* **the aberrations of the $3^{rd}$ order of an entire system are made up from the accumulated aberrations of the individual systems.** *If this result seems simple the credit for this is solely due to the use of the Seidel variables and the definition of the individual image aberrations by the coefficients of the Eikonal expansion especially with these variables. As soon as you turn to other linear combinations of the Seidel variables, which change from system to system, one obtains for each expansion coefficient of the combined Eikonal a complicated linear equation of all the aberrations of the individual Eikonals. So this is the point, where the advantage of the Seidel variables is clearly evident. The formula (39) shows that the 5th order aberrations are not directly subjected to the accumulative rule, but their composition is readily aparrent.*

*The transition from the composition of two surfaces to an abitrary number is so obvious, that writing of equations is unnecessary, I suppose.*

The discovery that individual primary wavefront aberration coefficients are simply additive to give system sums must be regarded as a very significant one. Also Schwarzschild noted that the simple additvity of primary aberration coefficients did not continue with secondary aberrations. The simple additivity of primary wavefront aberration coefficients had far reaching implications and is deserving of recognition as a fundamental discovery in the aberration theory of optical systems. Schwarzschild puts this result to work with immediate effect.

Schwarzschild proceeded to make what was, to the author's knowledge, the first clear published statement of what is known today as the stop-shift theorem. This is another fundamental theorem in the aberration theory of optical systems, and another first in this remarkable work.

As mentioned previously Schwarzschild then goes on to derive aberration coefficients for the nine 5th order aberrations. To date the author is unaware of any prior publication of the complete set of 5th order aberration coefficients and so, in the absence of surviving work by Petzval, it seems that Schwarzschild deserves recognition for his priority here. There does not seem to be any widespread recognition of Schwarzschild's priority in the development of the complete set of 5th order aberrations.

The final development in this paper is to apply this newly developed algebra to the analysis of a general axially symmetrical lens system of n elements. In doing so Schwarzschild introduces yet another innovation, the now famous "Schwarzschild constant" or as it is more commonly known "conic constant". The fact that this constant is almost universally used in modern optics to define conicoid surfaces is a testament to the fact that, while in hindsight it was a seemingly trivial innovation to replace $-e^2$ with $b$, where $e$ is the eccentricity of

a conicoid, it was a very handy one and another "first" for Schwarzschild in his first optics paper.

## 3. INVESTIGATIONS INTO GEOMETRICAL OPTICS 2.

Having developed a very powerful set of tools in his first paper, Schwarzschild in his second paper embarks on a voyage of discovery. The field of reflecting telescope optics had been left unmodified for more than two centuries, with no significant innovations since the work of Newton, Cassegrain and Gregory. In one paper Schwarzschild lays the framework for the entire edifice of 20th century reflecting telescope aberration theory.

Schwarzschild makes it clear in his opening comments of the second paper that his main purpose is in this work is to find the reflecting equivalents of Cooke triplets:

***1. In the competition between refractors and reflectors**, the reflectors are at present gaining ground. Many and various of the former doubts concerning the precision and stability of large mirrors have been dismissed by the technical progress of recent years. At present glass mirrors with a silver-plated front side are commonly used. As the thickness of the silver layer turns out very even from experience, the exact form giving process used in the fabrication of lenses is also suitable for the fabrication of mirrors. Warping and temperature related strain can be reduced to a harmless measure by suitable mounting (Ritchey, Chicago). The low weather resistance (the silver layer quickly loses its high gloss) is compensated for by arranging the elements in such a way that the mirror can easily be taken out and can be freshly silvered during the course of a single day.*

*With this obstacle removed, the advantages of reflecting telescopes are plainly shown, two of which stand in first place. The first to emphasize is the economic advantage offered by reflectors. An ordinary achromatic lens has four polished surfaces, the reflecting telescope (apart from the small plane mirror) has only one and the quality demand of the glass mass of the mirror (although it must be good) is not the very highest. Consequently, the price ratio between lenses and mirrors of the same diameter can rise up to 10:1 with large dimensions.*
*In addition the mirror is free from all colour aberrations. While the secondary spectrum of the so-called achromatic lens is still it's worst defect, no colour separation at all occurs at the mirror. As well has having zero dispersion, the reflection capability of silver reaches far into the ultra violet, which is very valuable for photographic and spectral recordings.*

*These advantages are opposed by one substantial disadvantage at least with the present reflecting telescopes: the restriction of the visual field. A parabolic mirror delivers a perfect image on the axis, but only half a degree from the axis with an aperture ratio of 1/4, a coma the size of 29" appears. In the following investigation the question is asked whether*

*progress cannot be achieved in this point by using two mirrors of a suitably calculated shape instead of the commonly used parabolic mirrors with diagonal plane mirrors. The answer is a positive one. It is possible to design telescopes with 2 mirrors, that deliver the same expansion of the usable visual field (2°-3° diameter) at an aperture ratio of 1/3, corresponding, for example, to the refractors of the same diameter commonly used in the enterprise of producing photographic sky maps. With this, it seems another application area is opening up for reflecting telescopes.*

Schwarzschild proceeds to lay the ground work for his investigations into two mirror systems by conducting an analysis of the field aberrations of a single mirror. While the results of Seidel for lens systems had been available for 50 years, Schwarzschild was apparently the first to produce a complete third-order analysis of the aberrations of a single mirror.

Using the results from his first paper this analysis is completed easily, Schwarzschild provides an example of an f/10 paraboloid mirror, which he shows compares favorably to an f/10 refracting objective of similar aperture. He also points out that at f/3 a paraboloid mirror suffers badly from coma and is unsuitable as an "astrograph objective" as the coma causes apparent stellar positions to be a function of their brightness.

Immediately he moved on to an investigation of two mirror systems, and in the first paragraph he gives the formulation for what is to become the most significant astronomical telescope form of the 20th century, the so-called Ritchey-Chrétien telescope:

***8. Explicit aberration terms.*** *The conditions required to make the spherical aberration and the coma disappear for 2 mirrors are given below:*

23)
$$B = h_1^4\left(\frac{b_1}{r_1^3}+\frac{K_1^2}{r_1}\right)+h_2^4\left(\frac{b_2}{r_2^3}+\frac{K_2^2}{r_2}\right)=0,$$
$$F = h_1^3H_1\left(\frac{b_1}{r_1^3}+\frac{K_1L_1}{r_1}\right)+h_2^3H_2\left(\frac{b_2}{r_2^3}+\frac{K_2L_2}{r_2}\right)=0.$$

*Astigmatism and image curvature are defined by:*

24)
$$D = h_1^2 H_1^2 \left\{ \frac{b_1}{r_1^3} + \frac{K_1(2L_1 - K_1)}{r_1} \right\} + h_2^2 H_2^2 \left\{ \frac{b_2}{r_2^3} + \frac{K_2(2L_2 - K_2)}{r_2} \right\},$$

$$C - D = \frac{1}{r_1} + \frac{1}{r_2}.$$

*From the first two equations one can see that with any arbitrary arrangement of the mirror system one can choose the deformations $b_1$ and $b_2$ so that spherical aberration and coma disappear. We ask, what image blurring aberrations then still remain?*

This statement, "that with any arbitrary arrangement of the mirror system one can choose the deformations $b_1$ and $b_2$ so that spherical aberration and coma disappear" is the clear invention of the two-mirror aplanatic telescope. It should be noted that this invention was published 18 years prior to the publication of Ritchey and Chrétien[2]. However, a mere aplanat was not suitable for Schwarzschild's purposes. After answering his own question posed above (the answer was "unacceptably large"), Schwarzschild concluded that what was required was a flat-field anastigmat.

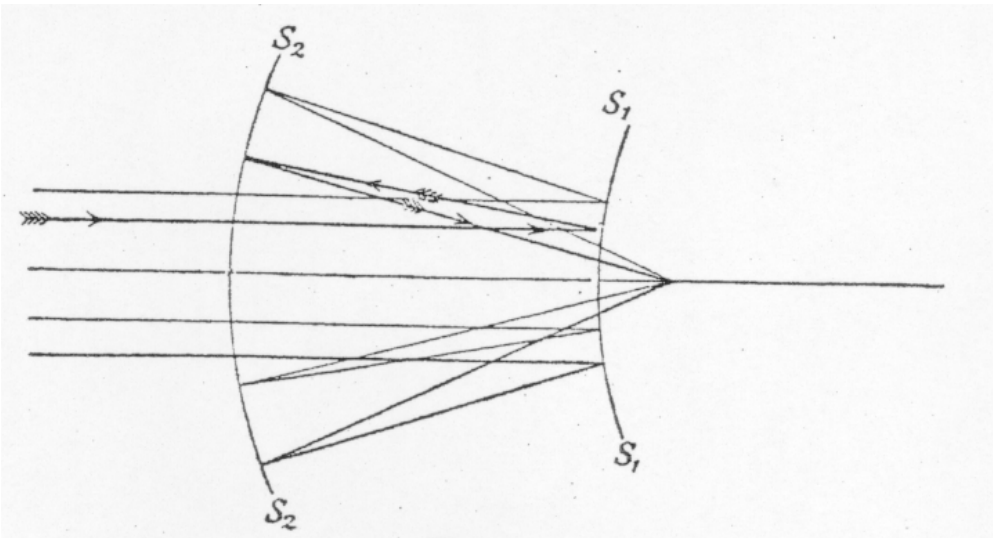


**Figure 1. The Schwarzschild flat-field two mirror anastigmat (both mirrors are oblate spheroids).**

The ease with which he proceeded to the only possible solution (figure 1) is a tribute to the power and clarity of his analysis.

This system was a disappointment to Schwarzschild, who had been hoping for a concave-primary-mirror flat-field anastigmat. He saw the convex-primary solution as impractical for astronomical purposes and immediately discounted it. The system was subsequently picked up by microscopists, in particular the great C.R. Burch produced modified versions of it[4,5], and it has also been used as a spectrograph camera. It is interesting to note that many textbooks on optical design wrongly attribute the concentric-spherical-mirror-pair anastigmat to Schwarzschild. While this system was implicit in his formulation, and would have been a trivial result had Schwarzschild turned his attention to spherical mirror pairs, Schwarzschild was clearly not interested in systems with convex primary mirrors and certainly did not produce it.

The concentric mirror pair has also been attributed by some to C.R. Burch, but again, Burch does not claim novelty and discusses the concentric mirror pair as an already well known system in the 1940's. Schwarzschild has in fact a far greater claim to naming rights to the Ritchey-Chrétien telescope as was shown previously.

After failing to find an acceptable flat-field anastigmat, Schwarzschild turned his attention to concave primary systems in which some astigmatism was allowed to flatten the field. He produced a design with two concave mirrors which met his performance goals, giving superior performance to that obtainable with a Cooke triplet of comparable field and relative aperture.

Due to manufacturing difficulties and inconvenient focal plane position few of these were ever made. Apparently two were made in the USA, a 12" and a 24" version, in the period between WWI and WWII[6]. A better performing system was later obtained by Couder[7] by correcting astigmatism fully and obtaining a flat-field using a field flattening lens.

However, Wilson[8] makes the point well: "the precise form of the original Schwarzschild proposal is completely unimportant. His aims were later satisfied by Schmidt telescopes, and either by the primary foci of large telescopes with field correctors, or by Cassegrain foci with focal reducers. The fundamental importance of his work was the theoretical formulation in third-order theory which opened the design path to all modern telescope solutions."

## 4. CONCLUDING COMMENTS

Schwarzschild's first two optics papers stand as monumental works in the field of the geometrical aberration theory of optical systems. The author is unaware of any other work in optical aberration theory in which so much new material is developed, so much new ground opened up, at once. A third paper was presented in this set of papers that the author has not had translated. This dealt with the application of Schwarzschild's techniques to the design of refracting systems.

Karl Schwarzschild's career continued on its upward trajectory in the years following his work in geometrical optics. He took up a prestigious role as the director of the Astrophysical Observatory at Potsdam in 1909 and was elected to the Berlin academy in 1913.

On the outbreak of war in 1914 Schwarzschild enlisted in the army, to the amazement of his colleagues. When questioned as to why he would abandon his luminous career in science to join the army he replied that "as a German Jew I feel duty bound to stand up and fight for the state of Prussia, which has been the most hospitable state to the Jewish people in all of Europe"[9].

Schwarzschild died of a disease he contracted while serving on the Eastern front in 1916, unaware of the bitter historical irony of his sacrifice.

## Acknowledgement

The author wishes to thank Dr. Raymond Wilson, 1992 Schwarzschild Medalist, for his encouragement, many useful discussions and helpful suggestions. Dr. Werner Friedrich, an engineer at Industrial Research Limited, New Zealand, provided the bulk of the translation, struggling with a much changed and archaic form of German (the language has apparently changed much more significantly than English in the last 100 years), and technical terms from outside of his field and experience.

## References


1. C.R. Burch, "On aspheric anastigmatic systems", *Proc. Phys. Soc.*, **55**, pp.436, 1943

2. Chrétien, H., Rev. d'Opt., **1**, 13, 19. 1922

3. de Meijere, J.L.F., Velzel, C.H.F., "Dependence of third- and fifth-order aberration coefficients on the definition of pupil coordinates", *JOSA A*, **6**, No. 10, pp. 1609-1617, 1989

4. C.R. Burch, "Reflecting Microscopes", *Proc. Phys. Soc.*, **59**, pp 41-46, 1947

5. C.R. Burch, "Reflecting Microscopes", *Letter to Nature,* **152**, pp 748-749, 1943

6. Wilson, R.N., "Reflecting Telescope Optics I", 2nd Edition, p.119, Springer Verlag, 2004

7. Couder, A., C.R. Acad. Sci. Paris, **183** (II), 1276

8. Wilson, R.N., "Reflecting Telescope Optics I", 2nd Edition, p. 119, Springer Verlag, 2004

9. Schwarzschild, K., Gessammelte Werke (Collected Works}, Voight H. H. (ED), Springer Verlag, 1992

# Appendix F: SPIE Four-spherical-mirror paper

The following paper was the presented at the SPIE "Optical Design and Engineering" conference in 2003, and published in SPIE proceedings volume 5249 in 2004. This paper was the basis for the paper presented in Appendix A and for material presented in chapter 3 of this thesis.

# Complete solution set for four-spherical-mirror anastigmatic telescope systems

Andrew Rakich [*,a,b], Norman J. Rumsey [b]
[a]Electro Optic Systems Pty., Locked Bag 2 Post Office, Queanbeyan NSW 2620, Australia
[b]Department of Physics and Astronomy, University of Canterbury, Private Bag 4800, Christchurch 8020, New Zealand

## ABSTRACT

The concept of the simplest possible reflecting anastigmat is discussed and anastigmats consisting of four spherical mirrors are introduced in this context as being the last remaining family for which the solution set has not been thoroughly mapped. A method for mapping the solution space for four-spherical-mirror anastigmats is described and results are presented. Analysis of the large number of solutions obtained in this way is in its initial stages, and some of the early results are presented here.

**Keywords: anastigmat, reflecting telescope, 4-mirror, Schiefspiegler**

## 1. INTRODUCTION

Optical systems in which spherical aberration, coma and astigmatism are all well corrected in the image are known as anastigmats. In the Seidel (or third-order) approximation the lowest orders of spherical aberration, coma and astigmatism are brought to zero. While the aberration function of a real optical system will in general contain higher order terms as well, systems for which the Seidel aberrations are made zero are usually very close to optimum solutions in which small amounts of non-zero Seidel aberrations balance against higher order aberrations. The Seidel aberration approximation to a system's aberration function is particularly useful in all-reflecting, or catoptric, systems. This is because, for a given power, a reflecting surface will in general have ~ ¼ of the curvature of a refracting surface, and the contribution of a surface to the increasingly high-order terms in the aberration function grows as increasingly high powers of this curvature. Therefore for a given power the Seidel approximation will be better for a reflecting surface than for a refracting

* arakich@eos-aus.com; phone +612 62988033; fax +612 62997687; www.eos-aus.com

surface. The anastigmats referred to in the following are all anastigmats in the Seidel aberration sense.

In 1900 Aldis[1] showed that an optical system consisting of four spherical surfaces could produce an anastigmatic image. This work was later generalized by C.R. Burch[2,3,4] who showed that systems of two conicoid surfaces, three surfaces, one of which was a conicoid, or four spherical surfaces could all produce anastigmatic images. Burch's generalization of Aldis' work utilized a means of describing and manipulating the Seidel aberrations of an optical system in wavefront measure, which he termed the "plate diagram" analysis. Plate diagram analysis lends itself naturally to the formulation of algebraic systems for multi-mirror telescopes, and a plate diagram based approach to determining four-mirror anastigmats will be described in detail in the following section.

Anastigmats consisting of two conicoid mirrors were completely described by Schwarzschild[5] in his classic optics papers of 1905. Two distinct families of solution exist, one with concave primary mirrors and the other with convex primary mirrors (figure 1). The Schwarzschild anstigmat set has only two interesting points on the solution curves, one representing a solution with a flat field (an anastigmat with zero Petzval curvature) and the other representing a very special case where both mirrors are strictly spherical. Clearly, the range of advantageous geometries for two-mirror anastigmats is very limited.

Rakich and Rumsey[6,7,8] described the complete solution set for three-mirror anastigmats that consist of one conicoid and two spherical mirrors. A representative sample of the solution set is given below (figure 2). The solution set for simplest

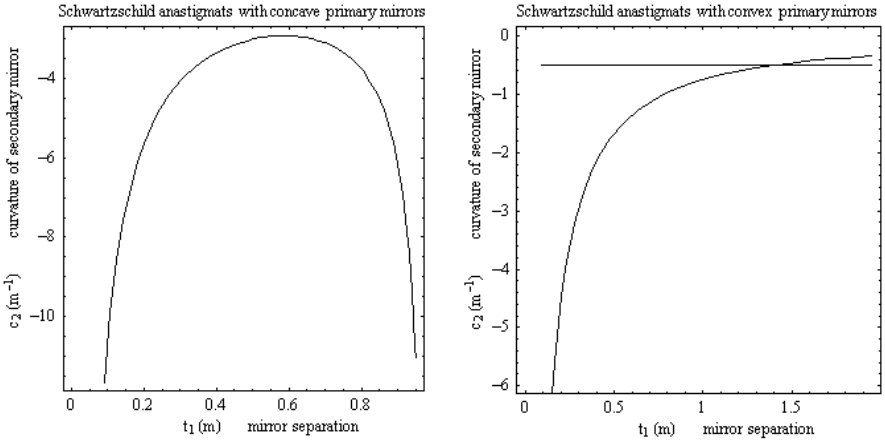


**Figure 1. These two plots represent the complete solution set for two-mirror or Schwarzschild anastigmats. In both cases the primary mirror has been set with a focal length of +/- 1 m (so $c_1$ = +/- 0.5 $m^{-1}$). In both cases the secondary mirrors are concave. The horizontal line in the right hand plot intersects the solution curve at the point representing a flat-field anastigmat. In both cases the mirrors are in general conicoids.**

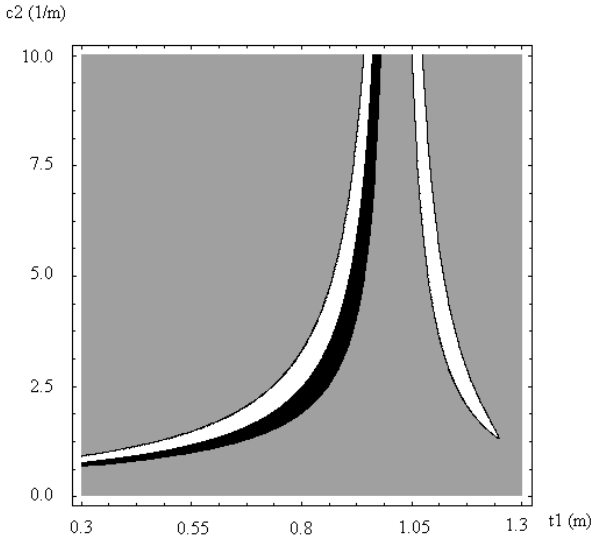


**Figure 2. One of seven plots representing all possible three-mirror anastigmats in which two mirrors are spherical and one mirror is a conicoid. This example represents one of three families in which the primary mirror is aspherised. White regions represent solutions with positive Petzval curvature and black regions represent regions with negative Petzval curvature, while grey regions represent configurations for which no solutions exist. Flat-field solutions exist at points where black regions abut directly onto white regions.**

possible three-mirror anastigmats contains many more possible system geometries than the two-mirror solution set. In the three-mirror case the solutions occupy 2-dimensional regions of the $t_1$, $c_2$ parameter space, and there are seven distinct families of solutions, with most of the families containing two or more geometrically distinct "sub-families" of solutions.

These solution sets were obtained by first producing 7 distinct sets of equations, each of which gave, for given input values of $t_1$ and $c_2$, the remaining constructional parameters required to define an anastigmat. Then each of the 7 sets of equations was solved repeatedly for a large number of points in the $t_1$, $c_2$ plane, thus mapping solution sets. A modest amount of computing was able to produce every possible variant within this class of system, leading to the discovery of previously unknown forms of three-mirror anastigmat, including three previously unknown types of flat-field three-mirror anastigmat in which only one mirror is aspherised.

A similar method has now been applied to the problem of four-mirror anastigmats consisting entirely of spherical mirrors. The solution for four-spherical mirror systems completes Burch's "triplet" of simplest possible reflecting anastigmats. The derivation and some of the initial analysis are presented here.

## 2. Method

Burch's plate diagram method has been described in detail elsewhere[2,7,9], so only a brief summary will be given here. The plate diagram analysis of an optical system gives a system of Schmidt plates in collimated light which reproduce exactly the wavefront primary aberration condition of a system consisting of any number of concave or convex, conicoid or spherical, refracting or reflecting surfaces. In this work we are limited to considering systems of mirrors. A spherical mirror will be replaced by a Schmidt plate which contributes exactly the same spherical aberration in wavefront measure as the mirror it replaces. In the case of the primary mirror of a telescope this plate will lie at the center of curvature of the original mirror, in the case of any subsequent mirror in the system the Schmidt plate is placed at the Gaussian image in object space of the center of curvature of the mirror as imaged sequentially through any preceding elements starting with the immediately preceding element.

Conicoid mirrors are represented by two Schmidt plates, one representing the primary wavefront spherical aberration contribution of the underlying vertex sphere of the conicoid, positioned as described above, and the other giving the same primary wavefront spherical aberration contribution as the mirror's asphericity. This second plate lies at the pole of the mirror if it is the primary mirror or otherwise at the Gaussian image of the pole of the mirror in object space.

Once a plate system is produced in this way the only other quantities required to completely determine the primary spherical aberration, coma and astigmatism of the system are the displacements of each of the plates from the system's entrance pupil. Then if we denote the spherical aberration contribution of the ith plate as $W_i$ and the displacement of this plate from the entrance pupil as $x_i$ then the following sums give the system spherical aberration, coma and astigmatism:

$$\sum_1^n W_i \qquad \text{(spherical aberration sum),} \tag{1}$$

$$\sum_1^n W_i x_i \qquad \text{(coma sum),} \tag{2}$$

$$\sum_1^n W_i x_i^2 . \qquad \text{(astigmatism sum).} \tag{3}$$

Equating these sums to zero and solving simultaneously will give an anastigmatic plate system. The minimum number of plates required for the general solution will be four (with some notable exceptions; for example the Schmidt camera for which only two plates are required for anastigmatic performance).

In the case of four spherical mirrors there are four plates, one for each of the mirrors. If the height of the marginal paraxial ray on the primary mirror is $y_1$ and the reciprocal of the radius of the primary is $c_1$, then the plate strength, $W_1$, of the plate replacing the primary mirror is given by:

$$W_1 = -\frac{N_1 c_1^3 y_1^4}{4}. \tag{4}$$

Subsequent mirrors in the system will not in general be in collimated light so the plate strengths of these mirrors can be found by:

$$W_i = -\frac{N_i c_i i_i^2 y_i^4}{4}, \tag{5}$$

where $i_i$ is the angle of incidence of the marginal paraxial ray and $N_i$ is the refractive index in the space immediately preceding the ith mirror, following the convention for mirrors in air that the refractive index is of unit magnitude and changes sign on reflection.

Without loss of generality we can fix the radius of the primary mirror as $2\,m$ (unit focal length) and the diameter as
0.4 $m$. Then , by (4), we have:

$$W_1 = 0.00005m \tag{6}$$

Setting up the system of simultaneous equations described above gives:

$$0.00005m + W_2 + W_3 + W_4 = 0 \text{ (spherical aberration zeroed)} \tag{7}$$

$$0.00005m \times x_1 + W_2 x_2 + W_3 x_3 + W_4 x_4 = 0 \text{ (coma zeroed)} \tag{8}$$

$$0.00005m \times x_1^2 + W_2 x_2^2 + W_3 x_3^2 + W_4 x_4^2 = 0 \text{ (astigmatism zeroed)} \tag{9}$$

An interesting step at this point is the key to solving these equations. The position of the entrance pupil is of fundamental importance to the plate equations, as all $x_i$ are measured from this. If we now state that the aperture stop for the system lies at the center of curvature of the quaternary mirror we can immediately simplify (8) and (9), as $x_4$ will be zero. It is important to note that while setting the position of the aperture stop is an important step in this formulation, the resultant anastigmat is not limited by this, as, by the Stop Shift Theorem, the aperture stop can later be placed anywhere in the system without disturbing the anastigmatic correction (8) and (9) can be rearranged to give:

$$W_3 x_3 = -W_2 x_2 - 0.00005m \times x_1 \tag{10}$$

$$W_3 x_3^2 = -W_2 x_2^2 - 0.00005m \times x_1^2 \tag{11}$$

At this point two further simplifications are made. Firstly the entrance pupil position is set, and it can be to any point in object space. The entrance pupil position is also the location of the image of the center of curvature of the quaternary mirror from above. We are free to place the entrance pupil anywhere in object space because at this point the secondary and tertiary mirrors are undefined. With the entrance pupil position defined we can immediately evaluate $x_1$. At this point we also assign arbitrary values to $t_1$, the separation of primary and secondary mirrors, and $c_2$, the curvature of the secondary mirror. With these $W_2$ and $x_2$ can be calculated using (5) and standard relationships in paraxial optics. Now the right hand side of equations (10) and (11) can be completely evaluated.

This allows us to calculate $W_3$ and $x_3$ by first dividing (11) by (10) to give $x_3$ and then dividing (10) with the newly acquired value of $x_3$ to give $W_3$. At this point $W_4$ can also be obtained by substituting the values for $W_1, W_2$ and $W_3$ into (7).

We now need to translate the plate quantities $x_3$ and $W_3$ back into optical system constructional parameters. These are needed to determine the actual position of the center of curvature of the quaternary mirror, and finally the curvature of the quaternary mirror.

To proceed we make use of the following relationship:

$$W_3 = -\tfrac{1}{4} N_3 c_3 P_3^2 (u_3 - c_3 P_3)^2 \rightarrow -\tfrac{1}{4} N_3 c_3 P_3^2 (u_3 - c_3 P_3)^2 - W_3 = 0 \qquad (12)$$

Here $u_3$ is the angle the marginal paraxial ray from the secondary to the tertiary mirror makes with the optical axis and $P_3$ is the length of the perpendicular from the center of curvature of the tertiary mirror to the marginal paraxial ray from the secondary mirror to the tertiary mirror. (12) is cubic in $c_3$ and as all other quantities in (12) can be obtained from standard paraxial relationships, $c_3$ can immediately be evaluated. At this point the three solutions for the cubic are obtained.

With each of the three values of $c_3$ thus obtained, a different position of the center of curvature of the quaternary mirror can now be calculated by imaging the previously fixed position of the entrance pupil back through mirrors $M_1, M_2$

and $M_3$. This determines the position of the center of curvature of the quaternary mirror. With the system up to the tertiary mirror defined (three times, once for each solution of $c_3$) the quantities $u_4$ and $P_4$ can be determined, and $W_4$ can be obtained from rearranging (7):

$$W_4 = -(W_2 + W_3 + 0.00005m) \tag{13}$$

Now it only remains to formulate a similar cubic to (12) and solve for $c_4$:

$$W_4 = -\tfrac{1}{4} N_4 c_4 P_4^2 (u_4 - c_4 P_4)^2 \rightarrow -\tfrac{1}{4} N_4 c_4 P_4^2 (u_4 - c_4 P_4)^2 - W_4 = 0 \tag{14}$$

This completes the derivation of the constructional parameters of nine distinct four-spherical-mirror anastigmats for given input values of $t_1, c_2$, and $\varepsilon$, where $\varepsilon$ is the position of the entrance pupil with respect to the origin of whatever coordinate system was chosen.

## 3. Results

Using the method described above nine distinct anastigmatic solutions are obtained, because as we have seen for each of the three values of $c_3$ there are three different values of $c_4$. These nine anastigmats can justifiably be thought of as belonging to geometrically distinct families; the other members of each family can be found by repeating the method described above for a large number of different points $t_1, c_2$, and $\varepsilon$. By choosing and solving for enough points in this parameter space the entire set of solutions for four-spherical-mirror anastigmats can be mapped with a large but not unmanageable amount of computing.

The solutions obtained in this way are not necessarily physically realizable anastigmats. Physically unrealizable solutions fall into two categories. In one, the solution involves at least one mirror located in a virtual space. Obviously in this case the systems are not physically practical. The other case is a result of the derivation given above requiring the solution of two cubic equations. Two of the three algebraic expressions for the solution of a cubic equation allow for a solution with an imaginary component. Any solutions with imaginary components will not be physically realizable anastigmats.

It is a relatively simple matter to sift the solutions to remove these physically meaningless solutions during the mapping process. The plot in figure 2 shows one map made in this way, in that case for three-mirror anastigmats with two spherical mirrors. In this map gray points represent physically unrealizable

solutions, while white and black points are possible anastigmats. Once a set of physically realizable solutions is achieved various conditions for practicality can be used to further refine the set, but the physically realizable set represents the complete range of possible solutions, a truly global solution set.

Possible impracticalities include mirrors with huge diameters, large inter-mirror distances, and large or complete self-obscuration by system elements. Removing such systems from consideration is simply a matter of writing "filters" into the program used to map the solution space. This filtering approach can be used in many ways, for example one can specify a certain maximum acceptable central obscuration, mirror size, total system length, minimum back focal length etc.

The mapping of four-spherical-mirror anastigmat sets has now been carried out. Of the nine distinct families of solution, four were empty sets when physically unrealizable solutions were filtered out. The remaining solution sets contain a large amount of data. Figure 3 is an example of several cross sections of one of the five three-dimensional solution sets. The "out of the page" axis represents $\varepsilon$, the entrance pupil position parameter, and $t_1$ and $c_2$ are system parameters as defined for figures 1 and 2. As in figure 2, gray areas represent physically unrealizable solutions, and white and black regions represent solutions with positive and negative Petzval curvature respectively.

An initial investigation of these results indicates that there are no physically realizable four-spherical-mirror anastigmats with an acceptably low central obstruction when on axis systems are considered. Wilson[10] anticipated this disappointing result. A more detailed analysis of the solution sets will soon be undertaken to confirm that no reasonably unobstructed axially symmetrical four-spherical-mirror anastigmats exist.

Ongoing investigation will also focus on identifying viable four-spherical-mirror anastigmatic Schiefspiegler and multi-axis systems. In this study Schiefspiegler will be taken as systems that use off-axis portions of the pupil, are off-axis in field (do not include the axial pencil say) or both. However, the center of curvature of the component mirrors will remain co-axial, the degrees of freedom available by breaking this symmetry are not covered in this analysis. Examples of multi-axis four-mirror anastigmats with conicoid surfaces can be found in Wilson[11]. A significant positive feature of solutions available from the four-spherical-mirror anastigmat set is that there is a greatly reduced manufacturing and alignment difficulty for systems with off axis spherical mirrors, which of course remain spherical. This is very advantageous when compared to Schiefspiegler obtained from systems with conicoid or other aspheric components.

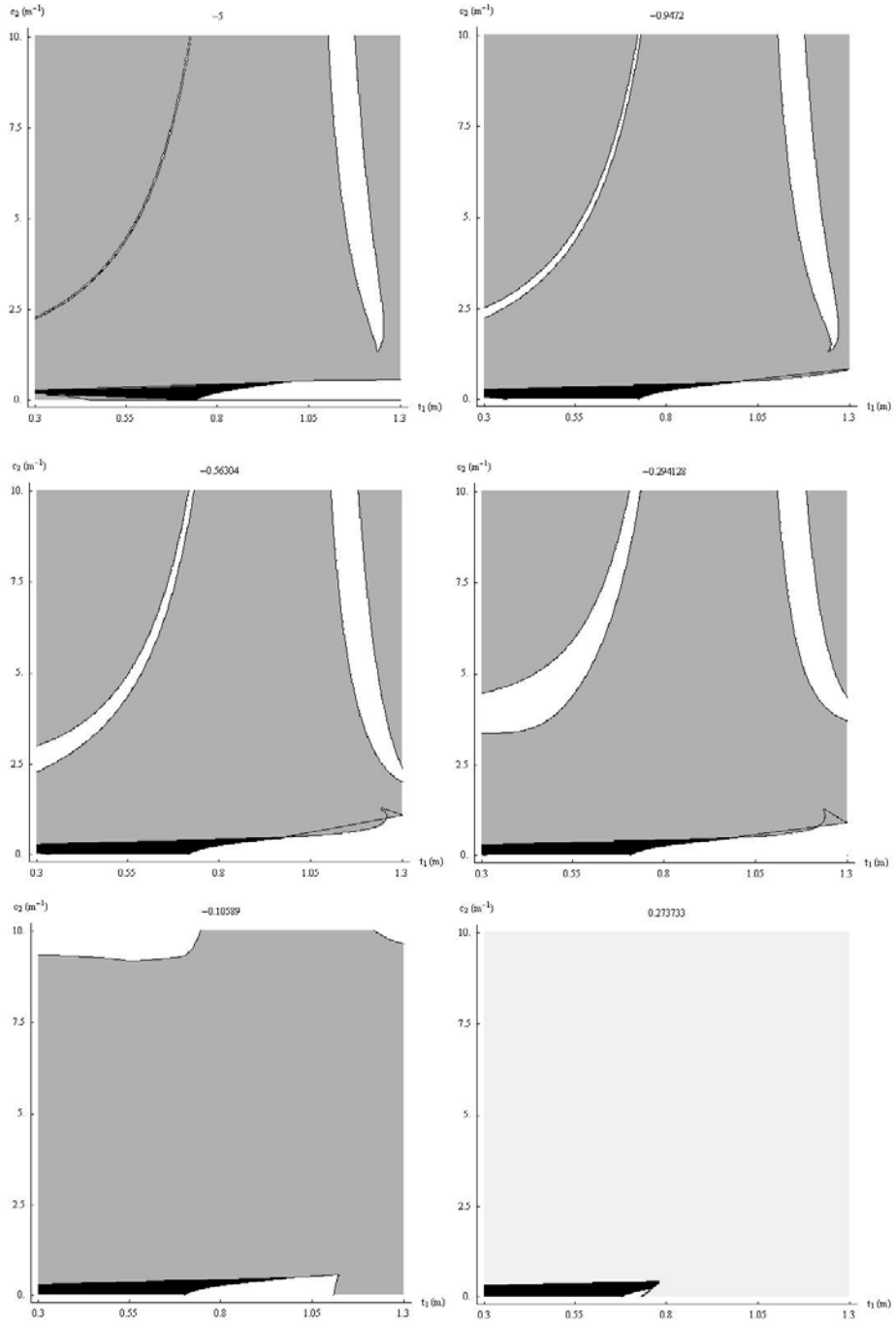


**Figure 3. These plots are a number of cross-sections taken from one of the five solution families. The horizontal and vertical axes represent $t_1$ and $c_2$ respectively, the number in the center top of each plot is related to $\mathcal{E}$, the initial position of the entrance pupil, for each cross section.**

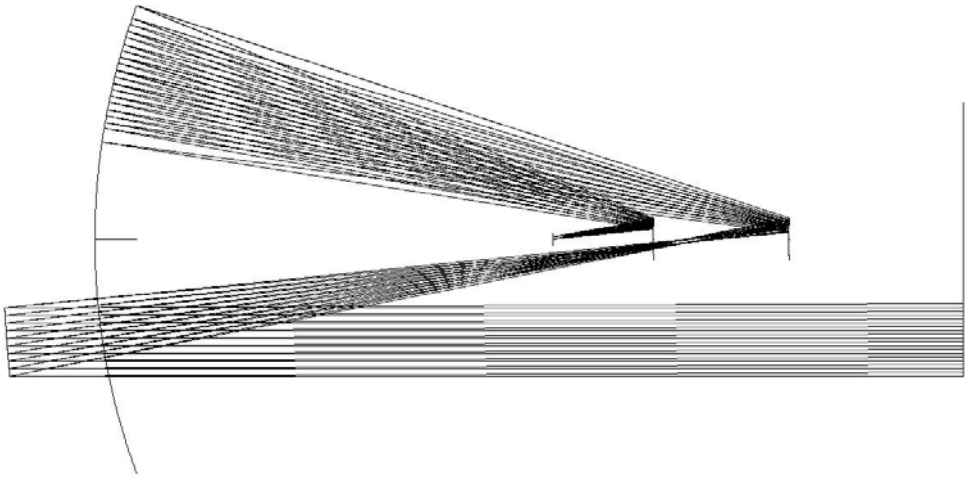

**Figure 4. An example of a four-spherical-mirror anastigmatic Schiefspiegler. Numerous examples of anastigmatic Schiefspiegler, including flat-field examples, are likely to be uncovered in a more detailed analysis of the solution sets.**

## 4. Conclusion

The method outlined in section two has been used to map out all possible solutions for four-spherical-mirror anastigmatic telescopes. This completes the set of simplest possible reflecting anastigmatic telescopes, a set that also includes two-conicoid mirror systems and three-mirror systems with one conicoid. The four-spherical-mirror set as derived above can be considered to consist of five geometrically distinct families of solutions mapped over 3-space, the basis vectors of which are three constructional parameters of the system.

Initial investigation of the solution set indicates that rotationally symmetrical solutions will all suffer from unacceptably high central obstruction. Ongoing investigation of the solution set will be aimed at extracting useful Schiefspiegler and multi-axis systems from the large number of possibilities.

The method documented here illustrates the good results that can be achieved by combining an analytical approach to optical design problems with modern computing power. For certain classes of system this approach is clearly capable of

providing superior global results to those that would be obtainable with modern optical design software.

## Acknowledgement

Andrew Rakich wishes to thank his employer, EOS, for their support in this endeavor, and Dr. Raymond Wilson, for his encouragement and helpful suggestions.

## References

1. H.L. Aldis, "On the construction of photographic objectives", *Photographic Journal*, **24**, pp. 291-299, 1900

2. C.R. Burch, "On the optical see-saw diagram", *MNRAS*, **102**, pp.159-165, 1942

3. C.R. Burch, "On aspheric anastigmatic systems", *Proc. Phys. Soc.*, **55**, pp.433-444, 1943

4. C.R. Burch, "Application of the plate diagram to reflecting telescope design", *Optica Acta*, **26**, 493-504, 1979

5. K. Schwarzschild, "Untersuchungen zur geometrischen optik I, II", Göttinger Abh, Neue Folge, Band IV, No.1, 1905

6. A. Rakich, "A complete survey of three-mirror anastigmatic reflecting telescope systems with one aspheric surface", M.Sc. Thesis, University of Canterbury, Canterbury, New Zealand, 2001

7. A. Rakich, N.J. Rumsey, "A method for deriving the complete solution set for three-mirror anastigmatic telescopes with two spherical mirrors", *JOSA A*, **19**, No. 7, pp. 1398-1405, 2002

8. A. Rakich, "Four families of flat-field three-mirror anastigmatic telescopes with only one mirror aspherised", *Proc. SPIE*, **4768**, pp 32-40, 2002

9. R.N. Wilson, "Reflecting Telescope Optics, I", 2nd ed., §3.6.5.1 and §3.7.2.4, Springer-Verlag, Berlin-Heidelberg, November, 2003

10. R.N. Wilson, Private communication, 2001-2003.

11. R.N. Wilson, "Reflecting Telescope Optics, I", 1st ed., pp 242-245, Springer-Verlag, Berlin-Heidelberg, 1996

# Appendix G: SPIE 1, 2 or 3 conicoid mirror paper

The following paper was the presented at the SPIE "Novel Optical Systems Design and Optimization" conference in 2004, and published in SPIE proceedings volume 5524 in 2004. This paper was the basis for the paper presented in Appendix B and material in chapter 4 of this thesis.

# Four-mirror anastigmats with useful first-order layouts and minimum complexity.

Andrew Rakich [a,b.]
[a]Electro Optic Systems Pty., Locked Bag 2 Post Office, Queanbeyan NSW 2620, Australia
[b]Department of Physics and Astronomy, University of Canterbury, Private Bag 4800, Christchurch 8020, New Zealand

## ABSTRACT

Recently the author described a method that gave the complete solution set for four-mirror anastigmats in which all the mirrors were spherical[1]. Even though a large variety of such systems were shown to exist, most of these were not practical due to large central obstructions. The author has now modified his previous approach by setting up "partial" systems with good first-order characteristics and adding the minimum number of aspheres necessary to give anastigmatic correction. In this way, surveys of useful four-mirror anastigmats with one, two or three-mirrors kept strictly spherical can be carried out.

**Keywords: anastigmat, reflecting telescope, 4-mirror**

## 1. INTRODUCTION

Primary, or Seidel, aberrations are particularly well suited to surveys of reflecting, as opposed to refracting, optical systems. This is because a mirror will achieve the same power as a refracting surface with approximately ¼ of the curvature. High-order aberration terms grow with increasing powers of the curvature of an optical surface, so a reflecting surface will give rise to less high-order aberration than an refracting surface of equal power, making the primary aberration approximation more accurate for reflecting systems than for refracting systems of equal power.

Burch[2] showed that there are three families of "simplest possible" reflecting anastigmats. They are systems consisting of two conicoid mirrors, three-mirrors of which only one is a conicoid, and four spherical mirrors.

In 1905 Schwarzschild published a paper[3] in which he laid down the mathematical basis for solving for the first of these families, two-mirror anastigmats with two conicoid mirrors. Designs he presented included a two-

mirror anastigmat with two hyperboloid mirrors and zero Petzval curvature, and a system with two concave mirrors, as shown in Figure 1. Figure 2 shows a plot of all available solutions for the two cases in which the primary mirror is either convex or concave. The solution set for the two-mirror anastigmat family is shown as a one dimensional set in a 2-parameter space where the axes are defined by two of the constructional parameters of the optical systems.

The second family of simplest possible reflecting anastigmats consists of three-mirror anastigmats in which only one mirror is a conicoid. The first three-mirror anastigmat was of this family, the Paul[4] anastigmat, which was later independently re-discovered by Baker[5].

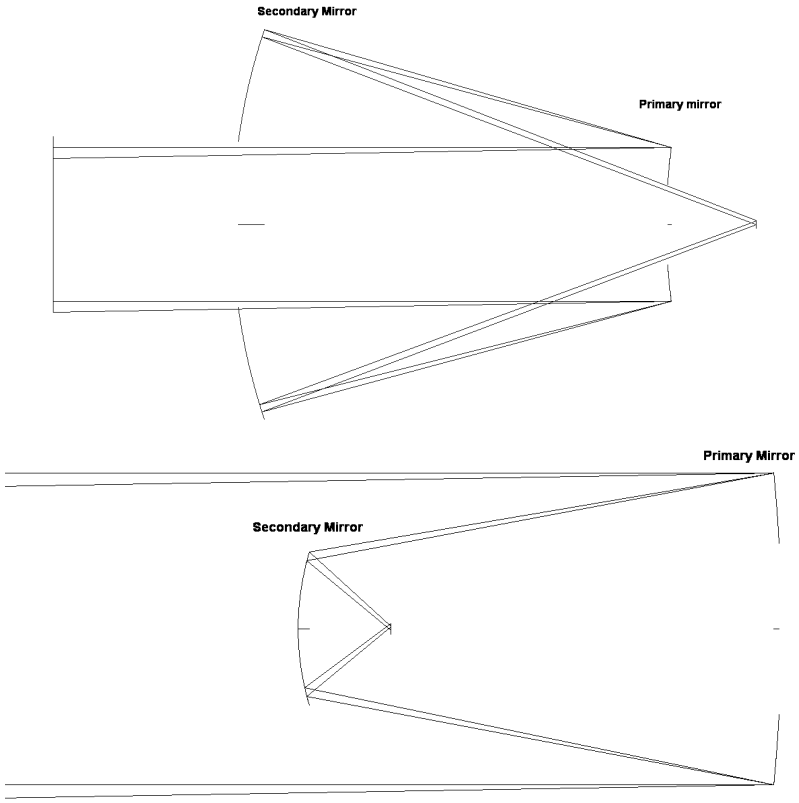


**Figure 1. Two examples of two-mirror anastigmats, similar to examples given by Schwarzschild. The upper system has a convex primary mirror, both mirrors are oblate spheroids and the Petzval curvature is zero. The lower system is a concave primary system. In his 1905 paper Schwarzschild reintroduced astigmatism to this system to flatten the field. As with all two-mirror anastigmats, the separation of the two-mirrors is equal to twice the system focal length.**

Since Paul's first paper in 1935 numerous other examples of three-mirror anastigmats with one conicoid mirror have been published, notably by Cook[6], Rumsey[7] and Korsch[8]. In 2002 the author together with Rumsey[9] presented a paper in which the complete solution set for three-mirror telescopes with one conicoid mirror (and concave primary mirrors) was presented. The solutions were mapped over the same 2-parameter space as used in Figure 2 for the Schwarzschild solutions. The conicoid can occur on either the primary, secondary or tertiary mirrors, giving three main divisions of solution.

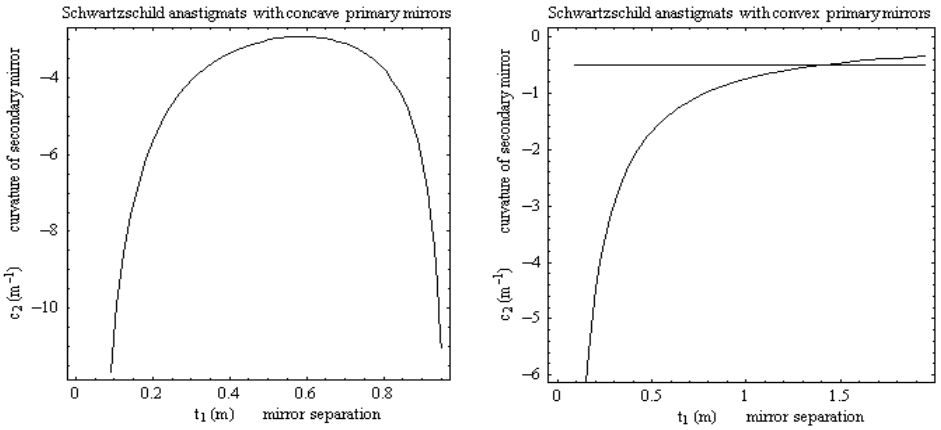


**Figure 2. These two plots represent the complete solution set for two-mirror or Schwarzschild anastigmats, mapped over a parameter space defined by the curvature of the secondary mirror and the separation of the two-mirrors. In both cases the primary mirror has been set with a focal length of +/- 1 m (so $c_1$ = +/- 0.5 $m^{-1}$). In both cases the secondary mirrors are concave. The horizontal line in the right hand plot intersects the solution curve at the point representing a flat-field anastigmat shown in Figure 1. In both cases the mirrors are in general conicoids.**

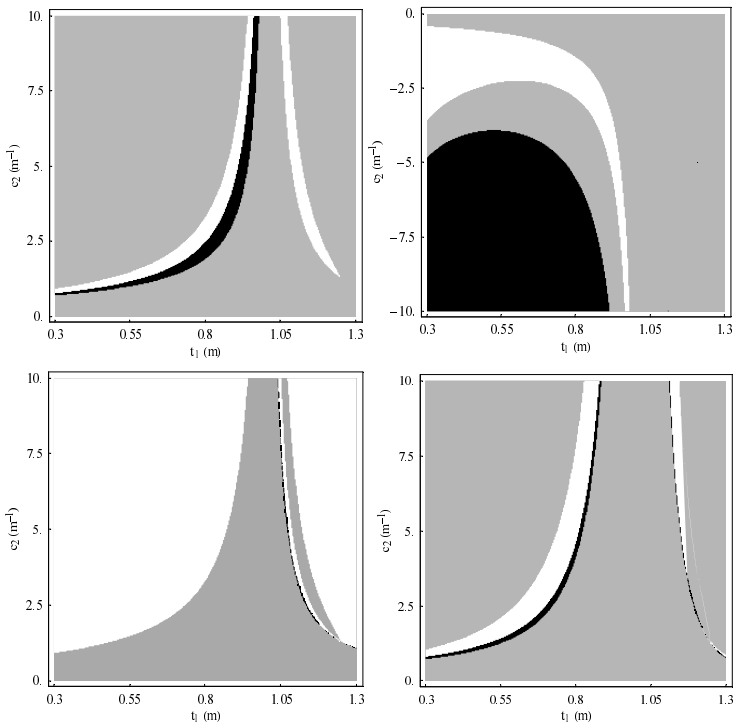


**Figure 3. These plots are four out of the seven plots representing the complete solution set for three-mirror anastigmats with two strictly spherical mirrors. In these plots solutions with positive Petzval curvature are plotted white and solutions with negative Petzval curvature are plotted black (gray points correspond to non-physical solutions). Hence flat-field solutions lie along loci where black and white regions abut directly onto each other. Clearly there are 4 families of flat-field three-mirror anastigmat with two spherical mirrors, only one of these appeared in the literature prior to this work.**

In the cases where the conicoid was on the primary or secondary mirrors, three distinct anastigmatic systems can be found for each point in the 2 parameter space used. In the case of a conicoid tertiary a numerical method yielded single solutions for each point in the two parameter space. Excluding physically unrealizable solutions (solutions with virtual images or imaginary components) leaves maps of parameter space with regions containing all possible anastigmats.

This complete mapping of the solution space included all previously described anastigmats of this type, and uncovered a number of geometries not previously described in the literature. In particular, four families of flat-field anastigmats were uncovered, only one of which had previously appeared in the literature[10]. Figure 3 shows the seven independent solution regions found using this method.

In 2003 the author described the application of the same solution mapping technique to telescope systems consisting of four spherical mirrors[1]. The complete mapping of solution space for four spherical mirror anastigmats completed Burch's triplet of simplest possible reflecting anastigmats. It was found that five distinct families of solutions could be obtained over a 3-dimensional parameter space. An example of cross-sections from one of these 3-dimensional solution sets is shown in Figure 4. In this case the parameters forming the basis of the solution 3-parameter space were the curvature of the secondary mirror, the separation of the primary and secondary mirrors and the position of the image of the center of curvature of the quaternary mirror as imaged by all preceding mirrors in the system, that is, the image in object space.

It was found that no solution from the large variety of solutions for four spherical mirror anastigmats was useful when they were considered as rotationally symmetrical systems due to self-obstruction by one or more of the systems mirrors. There are, however, a number of interesting off-axis or "Schiefspiegler" solutions that can be obtained from suitable rotationally symmetrical bases. These systems can use either an off-axis portion of the pupil, a field centered on a non-axial field point, or a combination of both of these. The off-axis solutions are particularly attractive in this case as they consist of purely spherical mirrors so there is none of the difficulty usually associated with systems of off-axis aspheres. The identification of useful Schiefspiegler from among the large variety of possible solutions is the subject of an ongoing investigation.

Following the "null-result" for on-axis four spherical mirror anastigmats the author has investigated applying the global solution technique to four-mirror systems in which desirable first-order layouts are first produced. Searches around these solutions are then carried out with decreasing numbers of conicoid surfaces (but retaining four-mirrors in all cases). In this way it is hoped that systems with useful on-axis geometries and minimum optical complexity will be uncovered. In the following section a brief description of the plate diagram method will be given and an outline of the technique used to solve for several cases of four-mirror telescope with decreasing numbers of conicoids. These cases are:

• Four-mirrors: three conicoids (with a spherical primary). This trivial solution involves setting up an exact first-order layout, then solving for three conicoids required to eliminate primary spherical aberration, coma and astigmatism. This set is included here for completeness.

• Four-mirrors: two conicoids, quaternary mirror free to vary in position and curvature. In this case three1-dimensional solution sets in 2-parameter space are obtained, similar to those in Figure 2.

• Four-mirrors: one conicoid, tertiary and quaternary mirrors free to vary in position and curvature. In this case three 2-dimensional solution sets in 2-parameter space are obtained, similar to those in Figure 3.

The final section will consist of a brief discussion of initial results.

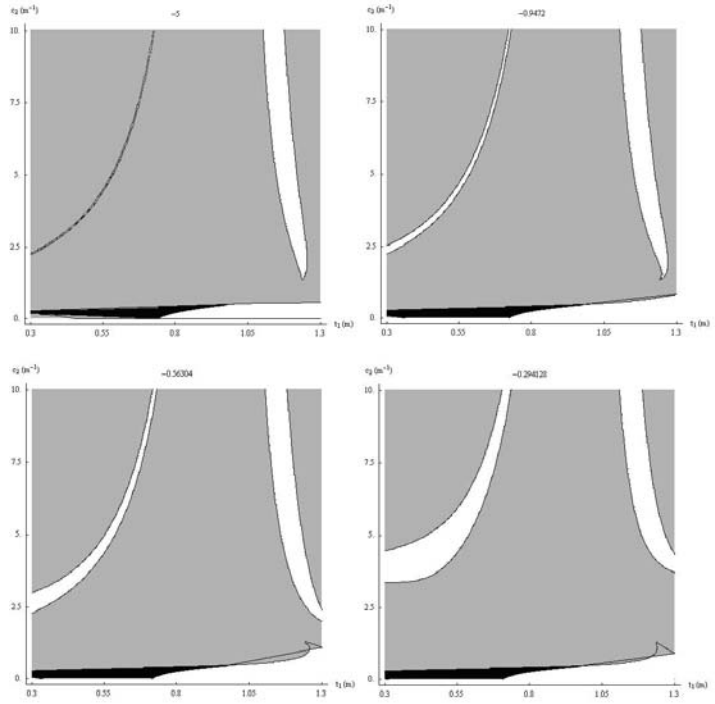

**Figure 4. These plots are a number of cross-sections taken from one of the five solution families for four spherical mirror anastigmats. The horizontal and vertical axes represent the separation of the primary and secondary mirrors and the curvature of the secondary mirrors respectively, the number in the center top of each plot is related to $\mathcal{E}$ , the position of the image of the center of curvature of the quaternary mirror as imaged by all preceding mirrors, in object space, for each cross section.**

## 2. METHOD

### THE PLATE DIAGRAM.

Burch's plate diagram method has been used in deriving all the solutions discussed in this paper. The method has been described in detail elsewhere[2,11,12,13], but it seems to be a largely forgotten analysis technique, particularly among the younger generation of optical designers, so a brief summary will be given here.

The plate diagram analysis of an optical system gives a system of Schmidt plates in collimated light which reproduce exactly the wavefront primary aberration condition of a system consisting of any number of concave or convex, conicoid or spherical, refracting or reflecting surfaces. In this work we are limited to considering systems of mirrors. Figure 5 shows how a spherical mirror can be replaced by an "anti- Schmidt plate" which contributes exactly the same aberrations as the mirror it replaces, without contributing any power. Primary wavefront spherical aberration for a mirror in air with collimated incident light can be given as:

$$W = \frac{c^3 y_c^4}{4}, \tag{2.1}$$

where $c$ is the curvature of the spherical mirror and $y_c$ is the height of the marginal ray of the axial paraxial pencil on the mirror. The "strength" of the anti-Schmidt plate representing the spherical mirror can be thought of as $W$. In the case where the mirror is in convergent or divergent light an alternative expression must be used:

$$W = \frac{ci^2 y^2}{4}. \tag{2.2}$$

Here $i$ is the angle of incidence of the marginal ray of the paraxial axial pencil on the mirror. Primary wavefront coma can be given as:

$$Coma = 4\frac{y_{pc}}{y_c}W, \tag{2.3}$$

and astigmatism as:

$$Astigmatism = 2\frac{y_{pc}^2}{y_c^2}W. \tag{2.4}$$

Here $y_{pc}$ is the height of the principal (chief) ray of the most oblique (paraxial) pencil, which will be zero if the plate is at the center of curvature of the spherical mirror, and non-zero as the plate moves away from the center of curvature of the mirror. As can be seen from Figure 6, $y_{pc}$ is directly proportional to $x$, the axial distance from the stop to the plate, so we have the following proportionalities:

$$Coma \propto xW, \tag{2.5}$$

$$Astigmatism \propto x^2 W. \tag{2.6}$$

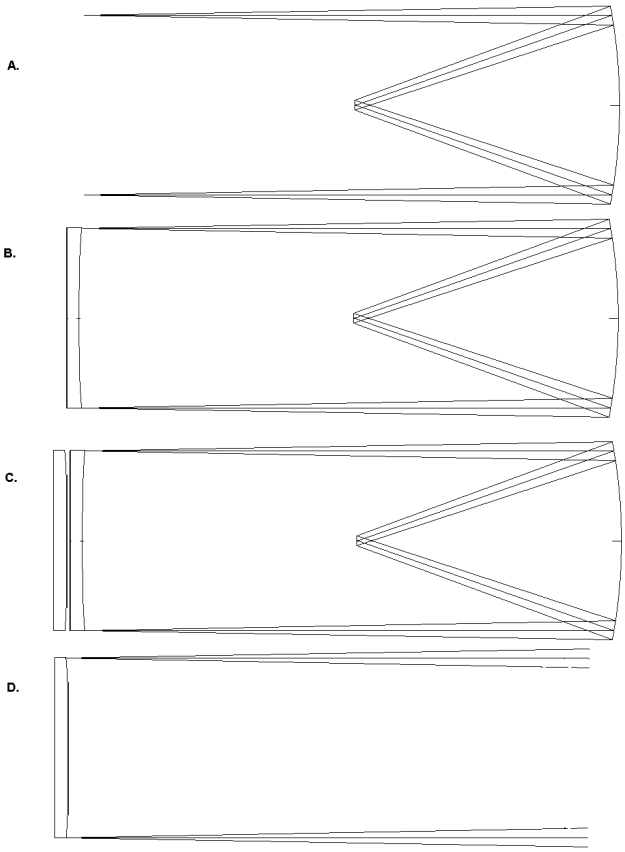


**Figure 5.**

- **A. Spherical mirror with the aperture stop at the center of curvature. Coma and astigmatism free but image suffers from spherical aberration over a curved field.**
- **B. Introducing a Schmidt plate with a spherical contribution equal in magnitude and opposite in sign to that of the mirror, at the center of curvature, corrects spherical aberration. By the stop-shift theorem, the stop can now be moved anywhere without re-introducing coma or astigmatism.**
- **C. Introducing an "anti-Schmidt plate" cancels the correction described in B, returning the aberration condition to that of the original spherical mirror.**
- **D. Removing the original spherical mirror and Schmidt correcting plate leaves the anti-Schmidt plate, giving the same aberrations as the original spherical mirror, including astigmatism and coma as the stop moves away from the plate.**

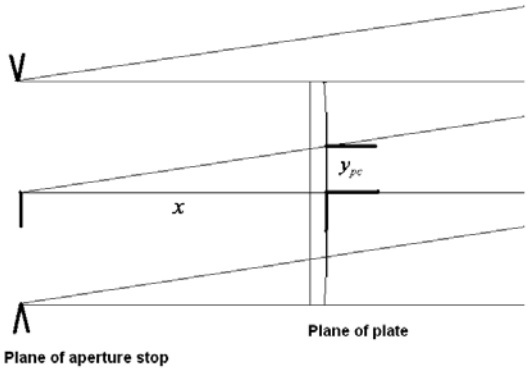


**Figure 6. As the plate is moved axially away from the stop $y_{pc}$, the height of the intercept of the principal ray of the most oblique pencil with the plate grows in direct proportion to the axial separation of the plate and the stop, $x$.**

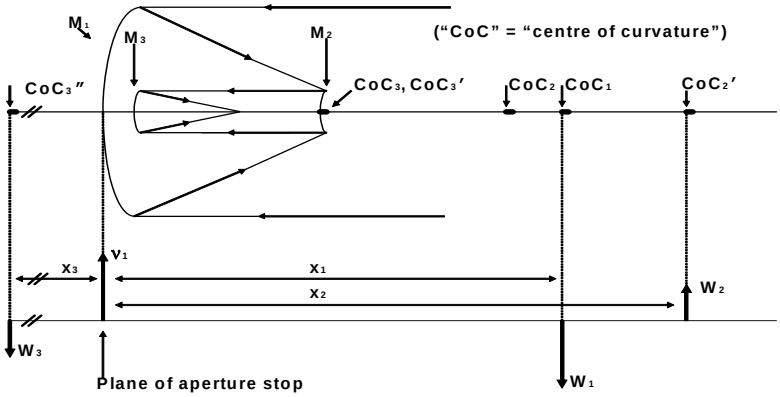


**Figure 7. Plate diagram for a Paul three-mirror anastigmat. The primary mirror is a paraboloid giving rise to two plates, $W_1$ from the vertex sphere and $\nu_1$ from the conic departure. Note that the plates are of equal magnitude and opposite sign, the paraboloid has no spherical aberration. The plate representing the spherical secondary mirror, $W_2$, is in object space at CoC$_2$', the image of the center of curvature of the secondary mirror through the primary. Similarly the plate representing the spherical tertiary mirror, $W_3$ is at CoC$_3$", the image of the center of curvature of the tertiary mirror through the secondary, then the primary. Note that $W_2$ and $W_3$ are also equal in magnitude and opposite in sign, so the system spherical aberration is zero, and that the plate $\nu_1$ representing the paraboloid lies on the entrance pupil, so it has no contribution to coma or astigmatism.**

In a similar way a conicoid mirror can be thought of as consisting of two plates. One plate represents the vertex sphere as described above, and the other plate represents the primary wavefront spherical aberration induced by the aspheric departure, given by:

$$W_{Conicoid} = \frac{kc^3 y_c^4}{4}. \tag{2.7}$$

Here $k$ represents the conic constant of the conicoid. This plate lies on the pole of the conicoid mirror. Coma and astigmatism introduced by this plate arise exactly as for the spherical mirror as described in 2.3 - 2.6.

For multiple mirror telescope systems the positions of the plates are determined by imaging the center of curvature of spherical mirrors (or vertex spheres) and mirror poles in the case of conic contributions, into infinite conjugate space ("star space" after Burch) through all preceding elements in the system. Figure 7 gives an example of the plate diagram for a Paul three-mirror anastigmat.

With plate strengths and distances from the entrance pupil evaluated for multiple mirrors it is a simple matter to determine the aberration condition of a multi-mirror system. The primary wavefront aberration contributions from each mirror are simply additive, so the system sum for each aberration can be given as:

$$Spherical_{SYS} = \sum_{i=1}^{n} W_i \tag{2.8}$$

$$Coma_{SYS} \propto \sum_{i=1}^{n} x_i W_i \tag{2.9}$$

$$Astigmatism_{SYS} \propto \sum_{i=1}^{n} x_i^2 W_i \tag{2.10}$$

Note that in using $x$ instead of $y_{pc}$ we are not solving for coma and astigmatism exactly. As our goal is to drive these aberrations to zero only their relative quantities are required. The extra step of calculation is not necessary. For actual values of coma and astigmatism equations 2.3 and 2.4 could be substituted into 2.9 and 2.10 respectively. In the methods outlined below, the system sums such as in 2.8-2.10 are simultaneously driven to zero to produce anastigmatic systems.

**FOUR-MIRRORS; 3 CONICOIDS.**

The first case considered is the almost trivial case of four-mirrors with three of these mirrors being conicoids. Here we set up a system of spherical mirrors with

a useful first-order layout such as that shown in Figure 8. Then three-mirrors are allowed to become conicoids and conic constants are found that simultaneously zero spherical aberration, coma and astigmatism. This is a trivial exercise in a modern ray-tracing program but the plate diagram approach is included here as an example.

With the radii and positions of the four-mirrors set we can immediately calculate plate strengths and positions in object space using equations 2.1, 2.2 and simple Gaussian optics. Setting the position of the entrance pupil to any convenient location allows us to calculate $x_i$ and hence system values for spherical aberration, coma and astigmatism following equations 2.8 – 2.10. To obtain the necessary combination of conicoids required for anastigmatic correction it is simply a matter of formulating and solving the following linear system of plate equations for $W_{ki}$, using Gaussian optics to determine the values of $x_i$:

$$W_{k1} + W_{k2} + W_{k3} = -Spherical_{SYS}, \tag{2.11}$$

$$x_{k1}W_{k1} + x_{k2}W_{k2} + x_{k3}W_{k3} = -Coma_{SYS}, \tag{2.12}$$

$$x_{k1}^2W_{k1} + x_{k2}^2W_{k2} + x_{k3}^2W_{k3} = -Astigmatism_{SYS}. \tag{2.13}$$

It then simply remains to rearrange equation 2.7 to obtain the three values of $k_i$. For the spherical primary example given in Figure 8 these $k_i$ are; $k_1 = 74.885, k_2 = -3.952$ and $k_3 = -1.061$. This example should serve to illustrate the relative ease of use of the plate equations in solving for multi-mirror anastigmats. The next examples should serve to illustrate the power of the technique.

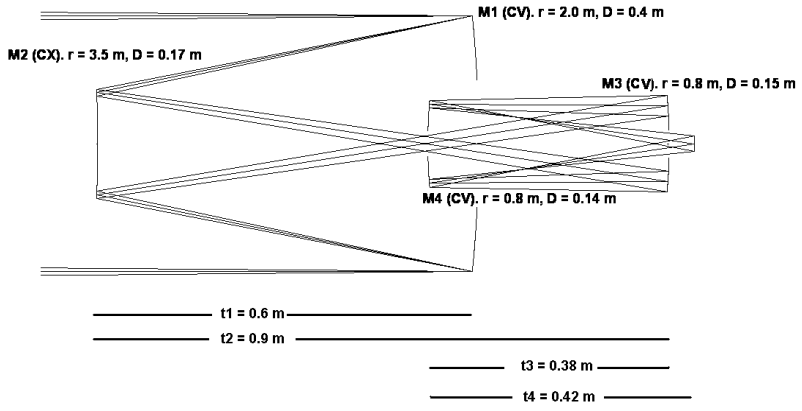


**Figure 8. First-order layout using spherical mirrors initially, giving a useful geometry but requiring three conicoids for anastigmatic correction.**

**FOUR-MIRRORS; 2 CONICOIDS.**

In this example two-mirrors, the primary and quaternary mirror, will remain strictly spherical. The secondary and tertiary mirrors are allowed to be conicoids. To achieve anastigmatic correction the position and curvature of the quaternary mirror must be varied. This is only one of 6 possible arrangements of two conicoids on four-mirrors, but serves as a representative example. In this case we will start with the primary, secondary and tertiary mirrors retaining some arbitrary but useful first-order layout, such as in the configuration given in Figure 8. To proceed we imagine that the aperture stop is placed at the center of curvature of the quaternary mirror. Also, we assign some arbitrary position to the entrance pupil, which after imaging through primary, secondary and tertiary mirrors, will locate the center of curvature of the quaternary mirror. In this way, equations 2.12 and 2.13 are reduced to:

$$x_{k1}W_{k1} + x_{k2}W_{k2} = -Coma_{SYS} \tag{2.14}$$

$$x_{k1}^2W_{k1} + x_{k2}^2W_{k2} = -Astigmatism_{SYS}\,. \tag{2.15}$$

That is, only contributions from the two conicoids contribute to the system coma and astigmatism; by placing the stop on the center of curvature of the quaternary mirror the $x$ value for the plate associated with this mirror is now zero so its coma and astigmatism contributions are necessarily zero. Note that here $-Coma_{SYS}$ and $-Astigmatism_{SYS}$ are values calculated from the spherical primary and vertex spheres of the secondary and tertiary mirrors. Values of $x_{ki}$ can be obtained and equations 2.14 and 2.15 can be used to solve for $W_{ki}$ and hence, using equation 2.7, for $k_1$ and $k_2$. Using the values of $W_{ki}$ thus obtained we can now solve for the spherical aberration contribution of the quaternary mirror by rearranging equation 2.11 (and substituting $W_{quat}$ for $W_{k3}$ in this case):

$$W_{quat} = -Spherical_{SYS} - W_{k1} - W_{k2}\,. \tag{2.16}$$

Now we have the position of the center of curvature of the quaternary mirror (from setting the initial position of the entrance pupil) and the spherical aberration contribution of the quaternary mirror from equation 2.16. Also, we have $u_4$, the angle the marginal ray of the axial paraxial pencil makes to the axis after reflection from the tertiary. We can also calculate a quantity, $P$, which is the length of the perpendicular from the center of curvature of the quaternary mirror to the marginal ray of the axial paraxial pencil after reflection from the tertiary mirror. Using these, and the following relationship;

$$W_{quat} = -\tfrac{1}{4} c_4 P^2 (u_4 - c_4 P)^2 \quad , \tag{2.17}$$

we can obtain a cubic equation in $c_4$ (the curvature of the quaternary mirror) which can be solved to give a maximum of three distinct quaternary mirrors.

$$-\tfrac{1}{4} c_4 P^2 (u_4 - c_4 P)^2 - W_{quat} = 0 \, . \tag{2.18}$$

In this way, for each initial position of the entrance pupil (and therefore the position of center of curvature of the quaternary mirror) we obtain a maximum of three distinct anastigmatic telescopes. These telescopes differ only in the position and curvature of the quaternary mirror. It remains to scan through the available solution space and build up a curve representing available solutions. Figure 9 in the next section shows curves in 2-parameter space, the horizontal axis is the separation of the tertiary and quaternary mirrors and the vertical axis represents the curvature of the quaternary mirror (negative is concave). Note the similarity in the dimensionality of the solution sets to those for the Schwarzschild solution set shown in Figure 2. Note also that while the position of the aperture stop and hence entrance pupil was set initially to reduce the number of unknowns in equations 2.14 and 2.15, once an anastigmatic system is achieved the aperture stop can be moved to any convenient location without affecting the anastigmatic correction, as given by the stop-shift theorem.

A final point is that the anastigmats derived in this way are not necessarily practical systems, or even physically realizable. For example, if one or more of the solutions to equation 2.18 have imaginary components then this will not lead to an actual anastigmat (unless one can make mirrors with imaginary components as well). Also, there is no guarantee that the light path after each reflection will remain real. Simple filters can be built into the evaluation algorithm to disqualify such solutions as they arise.

**FOUR-MIRRORS; 1 CONICOID.**

In this final example we look at the case in which there is one conicoid mirror and three spheres. Here the secondary mirror has been chosen to be the conicoid. The primary and secondary mirrors have the same characteristics and positions as in Figure 8. Now the curvatures and positions of the tertiary and quaternary mirrors are varied to solve for anastigmats. The first step is similar to that in the previous example. As in the previous example the initial position of the aperture stop is chosen to eliminate one set of variables from the plate equations. In this case placing the aperture stop at the pole of the secondary mirror stops the plate associated with the conic constant of the secondary mirror from having any affect

on the coma or astigmatism of the system (analogous to the way the paraboloid in Figure 7 makes no contribution to the system coma or astigmatism when the entrance pupil is on the primary mirror). Now we can form the equations:

$$x_{tert}W_{tert} + x_{quat}W_{quat} = -(x_{prim}W_{prim} + x_{sec}W_{sec}), \tag{2.19}$$

$$x_{tert}^2W_{tert} + x_{quat}^2W_{quat} = -(x_{prim}^2W_{prim} + x_{\sec}^2W_{sec}). \tag{2.20}$$

Here "prim, "sec", "tert" and "qaut" refer to quantities derived from the spherical primary through quaternary mirrors respectively (or vertex sphere in the case of the conicoid secondary mirror). Quantities on the $RHS$ are known. To proceed further we assign values to $t_2$, the separation of the secondary and tertiary mirrors and $r_3$, the radius of the tertiary mirror, from which we can calculate $x_{tert}$ and $W_{tert}$.

Moving all known quantities in the above equations to the $RHS$ and dividing 2.20 by 2.19 gives:

$$x_{quat} = \frac{x_{prim}^2W_{prim} + x_{\sec}^2W_{sec} + x_{tert}^2W_{tert}}{x_{prim}W_{prim} + x_{sec}W_{sec} + x_{tert}W_{tert}}, \tag{2.21}$$

from which we obtain:

$$W_{quat} = -\frac{(x_{prim}W_{prim} + x_{sec}W_{sec} + x_{tert}W_{tert})}{x_{quat}}. \tag{2.22}$$

Now that all $W_i$ are know apart from that associated with the conicoid we can solve for the conicoid using the spherical aberration plate sum and a rearranged equation 2.7:

$$k_2 = \frac{-4}{c_2^3y_2^4}(W_{prim} + W_{\sec} + W_{tert} + W_{quat}). \tag{2.23}$$

The final remaining step is to solve for the radius and position of the quaternary mirror, which is done exactly by deriving necessary Gaussian quantities and applying equations 2.17 and 2.18. As in the previous case, this leads to three distinct systems for each choice of starting values for $t_2$ and $c_3$. Again as in the previous case each of the three exact algebraic solutions to 2.18 can be applied independently to a large number of initial values of the parameters $t_2$ and $c_3$. In

this way a map of the solutions can be built up over this 2-parameter space, similar to the maps in Figure 3. In these maps anastigmats that were physically impossible can be filtered out, and there is also the opportunity to write custom filters targeting systems with particular characteristics, for example sizes of mirrors, space envelope, central obscuration etc.

## 3. RESULTS AND CONCLUSION

At the time of writing this paper the methods outlined in the previous section have been successfully implemented and some solution sets of anastigmats have been obtained for the 2-conicoid and 1-conicoid cases starting from several different base systems (the 3-conicoid case is trivial, the solution set consists of 1 member for each configuration). Figure 9 shows an example of results from the 2-conicoid case and Figure 10 shows an example of a solution set from the 1-conicoid case. A full investigation of solutions is a relatively laborious task and is still in its very early stages.

Similar techniques to those described in this paper have proven to be successful means of surveying the simplest possible three and four-mirror anastigmat cases, revealing previously unknown optical configurations with good correction and minimum complexity. Examples of a further generalization of these techniques to more complicated optical systems of four-mirrors have been presented here. While the technique is now established, a full evaluation as to whether this approach will provide a useful tool for the optical design of the type of system presented in this paper still needs to be carried out. Initial results show that this method will be capable of yielding useful systems of minimum complexity, but the efficiency of this method as opposed to methods employing modern optical design software remains to be determined.

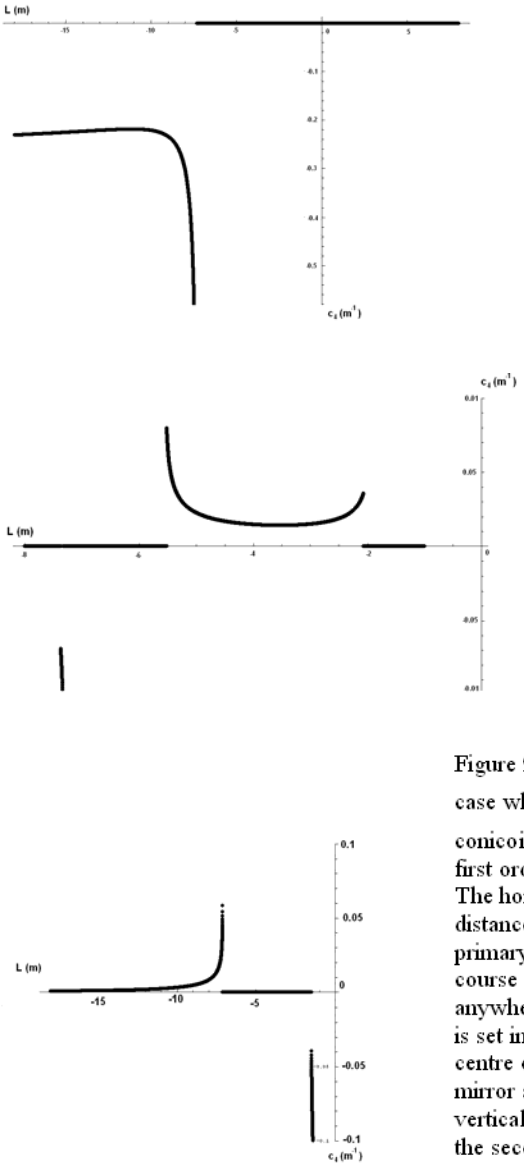


Figure 9. Three solution sets for the case where $M_2$ and $M_3$ are conicoids (in this case for a different first order layout than that in Figure 8). The horizontal axis is the initial distance of the entrance pupil from the primary mirror in object space. Of course the entrance pupil can be shifted anywhere in an anastigmat, the position is set initially to fix the position of the centre of curvature of quaternary mirror and remove variables. The vertical axis represents the curvature of the secondary mirror.

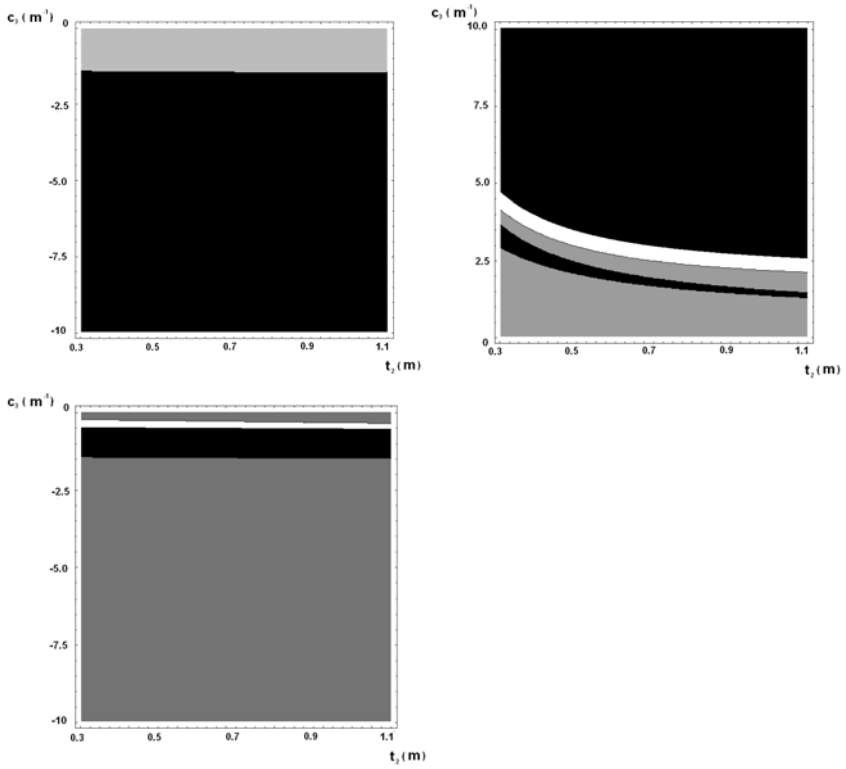


**Figure 10. Three independent sets of solutions for the case where only $M_2$ is allowed to be a conicoid. Note that there exist solution regions which have the same coordinates in each set, these represent systems that differ only in the radius and position of the quaternary mirror.**

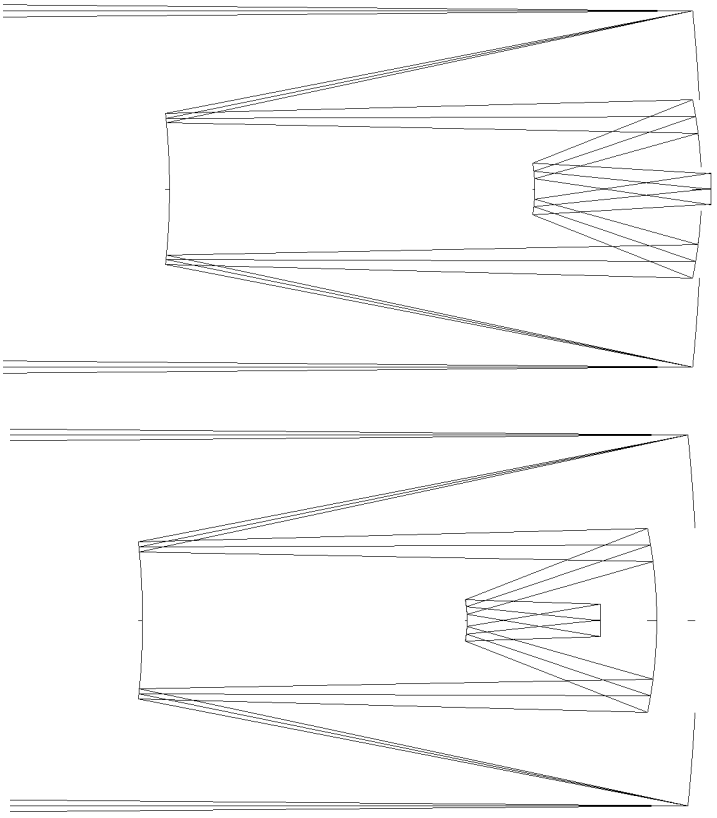

**Figure 11. The upper layout diagram is a four-mirror anastigmat which was given an initial first-order layout, then was rendered anastigmatic by solving for three conicoids. The lower diagram is a solution taken from a set similar to those in Figure 10, with only the secondary mirror a conicoid.**

## Acknowledgement

Andrew Rakich wishes to thank his employer, EOS (and EOST), for their support in this endeavor, and Mr. Norman Rumsey and Dr. Raymond Wilson, for their encouragement and helpful suggestions.

## References


1. A. Rakich, "Complete solution set for four-spherical-mirror anastigmatic telescope systems",
   *Proc. SPIE*, **5249**, pp 103-111, 2004

2. C.R. Burch, "On the optical see-saw diagram", *MNRAS*, **102**, pp.159-165, 1942

3. K. Schwarzschild, "Untersuchungen zur geometrischen optik II", Göttinger Abh, Neue Folge, Band IV, No.1,
   1905, translation available from author on request.

4. M. Paul, "Systèmes correcteurs pour réflecteurs astronomiques", *Rev. d'Optique* **14**, pp. 169-202, 1935

5. J.G. Baker, "On improving the effectiveness of large telescopes", *IEEE; Trans. AES,* **AES-5**, No. 2, pp. 261-
   272, 1965

6. L.G. Cook, "Wide field of view three-mirror anastigmat (TMA) employing spherical secondary and tertiary
   mirrors", *Proc. SPIE* **766**, pp. 158-162, 1987

7. N.J. Rumsey, "Pairs of spherical mirrors as field correctors for paraboloid mirrors", *Proc. ASA* **2**, pp. 22-23,
   1971

8. D. Korsch, "Reflective Optics", Academic Press, San Diego, 1991

9. A. Rakich, N.J. Rumsey, "A method for deriving the complete solution set for three-mirror anastigmatic
   telescopes with two spherical mirrors", *JOSA A*, **19**, No. 7, pp. 1398-1405, 2002

10. A. Rakich, "Four families of flat-field three-mirror anastigmatic telescopes with only one mirror aspherised",
    *Proc. SPIE*, **4768**, pp 32-40, 2002

11. C.R. Burch, "On aspheric anastigmatic systems", *Proc. Phys. Soc.*, **55**, pp.433-444, 1943

12. C.R. Burch, "Application of the plate diagram to reflecting telescope design", *Optica Acta*, **26**, 493-504, 1979

13. Linfoot, E.H., "Recent advances in optics", Clarendon Press, Oxford, 229-259 (1955).

# References


Aldis, H.L., 1900, "On the construction of photographic objectives", *Photographic Journal*, **24**, pp. 291-299

Baker, J.G., 1969, "On improving the effectiveness of large telescopes", *IEEE; Transactions of Aerospace and Electronic Systems*, **AES-5**, No. **2**, pp 261-271

Brumberg, E.M., 1943, "Colour Microscopy in Ultra-Violet Rays", *Nature*, **152**, p 357.

Buchdahl, H.A., 1954, "Optical aberration coefficients", Oxford Univ. Press

Burch, C.R., 1943-1, "Reflecting Microscopes", *Nature*, **152**, pp 748-749

Burch, C.R., 1943-2, "On aspheric anastigmatic systems", *Proc. Phys. Soc.*, **55**, pp. 433-444

Burch, C.R., 1947, "Reflecting Microscopes", *Proc. Phys. Soc.*, **59**, pp 41-46

Chrétien, H., 1922, *Rev. d'Opt.*, **1**, 1-28

Clay, R.S., 1939, "Some new non-electrical instruments", *J. Sci. Instrum.*, **16**, 49

Cook, L.G., 1987, "Wide field of view three-mirror anastigmat (TMA) employing spherical secondary and tertiary mirrors", Recent trends in optical system design, computer lens design workshop, *Proc. SPIE*, **776**, pp 158-162

Danjon, A and Couder, A, 1935, "Lunettes et Télescopes", Reprinted 1979 by Blanchard, Paris

De Meijère, J.L.F. and Velzel, C.H.F., 1989, "Dependence of third- and fifth-order aberration coefficients on the definition of pupil coordinates", *JOSA A*, **6**, Issue 10, p 1609

Dimitrov, G.Z., and Baker, J.G., 1945, "Telescopes and accessories", The Blakistone, New York

Epps, H.W. and Tadeka, M., 1983, "Optimization and practical designs for three-mirror telescopes", *Ann. Tokyo Astron. Obs. 2nd series*, **19**, No. 3, pp 401-412

Erdös, P., 1959, "Mirror anastigmat with two concentric spheres", *JOSA,* **49**, No. 9, p 877

Gelles, R., 1975, "Unobscured-aperture two-mirror systems", *JOSA*, **65**, No. 10, pp 1141-1143

Gilmozzi, R. et al., 1998, "The future of filled aperture telescopes: Is a 100 m feasible?", *Proc. SPIE*, **3352**, p. 778

Goncharov, A., 2004, "Optical Design for Advanced Extremely Large Telescopes", *Proc. SPIE*, **5489**, pp. 518-525

Grey, D.S., 1951, "Computed aberrations of spherical Schwarzschild reflecting microscope objectives", *JOSA*, **41**, 3, pp 183-192

Hamilton, W.R., 1833, *Report Brit. Assoc.*, **3**, 360

Hannan, P.G., 1992, "General analysis of two-mirror relay systems", *Appl. Opt.*, **31**, No. 4, pp 513-518

Hopkins, H.H., 1950, "Wave theory of aberrations", Clarendon Press, Oxford

Howard, J.M. and Stone, B. D., 2000, "Imaging with four spherical mirrors", *Appl. Opt.*, **39**, No. 19, pp. 3232-3242

King, H.C., 1955, "The history of the telescope", Charles Griffin and Co., London, p 182

Kingslake, R., 1980, "A history of the photographic lens", pp 82-98 Academic Press, San Diego

Korsch, D., 1973, "Closed-form solutions for imaging systems, corrected for third-order aberrations", *JOSA*, **63**, p 667

Korsch, D., 1991, "Reflective optics", Academic Press, San Diego

Kutter, A., 1953, "Der Schiefspiegler", Verlag, Biberach

Lerner, S.A., Sasian, J.M., Descour, M.R., 2000, "Design approach and comparison of projection cameras for EUV lithography.", *Opt. Eng.*, **39**, 3, pp. 792-802

Linfoot, E.H., 1938, *J. Sci. Instr.*, **15**, 405

Linfoot, E.H., 1943, *Mon. Not. Roy. Astron. Soc.*, **103**, No. 4, 210

Maksutov, D., 1932, U.S.S.R. Patent No. 40859, Dec 13th

McCarthy, E.L., 1940, Contributions from the McDonald Observatory, **1**, pp

97-102

Meinel, A.B. and M.P., Su, D.Q., Wang, Y.N., 1984, "Four-mirror, spherical-primary submillimeter telescope design", *Appl. Opt.,* **23**, No. 17, p 3020

Paul, M. 1935, "Systèmes correcteurs pour réflecteurs astronomiques", *Rev. d'Opt.*, **14**, pp. 169-202

Piazzi-Smyth, C., 1874, *Brit. J. of Phot. Alman*., **43**

Rakich, A., 2001, "A complete survey of three-mirror anastigmatic reflecting telescope systems with one aspheric surface", M.Sc. Thesis, University of Canterbury, Christchurch, New Zealand

Rakich, A., 2004, "Complete solution set for four-spherical-mirror anastigmatic telescope systems", *Proc. SPIE*, **5249**, pp. 103-111

Rakich, A., 2005, "The 100th birthday of the conic constant and Schwarzschild's revolutionary papers in optics", *Proc. SPIE*, **5875**, pp 1-8

Rakich, A., 2007-1, "Evidence supporting Petzval's primacy in the development of aberration theory", *Proc. SPIE*, abstract accepted February 2007.

Rakich, A., 2007-2, "Four-mirror anastigmats I: a complete solution set for all-spherical telescopic systems", Accepted for publication by *Opt. Eng.*, March 2007.

Robb, P.N., 1978, "Three-mirror telescopes: design and optimization", *Appl. Opt.*, **17**, No. 17, p 2677

Rosin, S., 1968, "Inverse Cassegrain systems" *Appl. Opt.*, **7**, No. 8., pp. 1483-1497

Rumsey, N.J., 1970, "A compact three-reflection astronomical camera", Optical Instruments and Techniques, Oriel Press, Newcastle-on-Tyne, pp 514-520

Rumsey, N.J., 1971, "Pairs of spherical mirrors as field correctors for paraboloid mirrors", *Proc. ASA*, **2**, pp. 22-23,

Rumsey, N.J., 1972, "Pairs of spherical mirrors as prime focus correctors for the Anglo Australian telescope", *Proc. ASA,* **2**, pp 126-127

Rumsey, N.J. and Rakich, A., 2002, "A method for deriving the complete solution set for three-mirror anastigmatic telescopes with two spherical mirrors", *JOSA A*, **19**, No. 7, pp. 1398-1405

Sasian, J.M., 1987, "Flat-field, anastigmatic, four-mirror optical system for large telescopes", *Opt. Eng.*, **26**, No. 12, pp 1197-1199

Sasian, J.M., 1990, "Design of a Schwarzschild flat-field, anastigmatic, unobstructed, wide-field telescope", *Opt. Eng.*, **29**, No. 1, pp 1-5

Schmidt, B., 1931, *Centr. Ztg. f. Opt. u. Mech.*, **52**, 25

Schwarzschild, K., 1905-1, "*Untersuchungen zur geometrischen Optik I*", Göttinger Abh., Neue Folge, Band IV, No.1, 1905

Schwarzschild, K., 1905-2, "*Untersuchungen zur geometrischen Optik II*", Göttinger Abh., Neue Folge, Band IV, No.1, 1905

Seidel, L., 1856, *Astron. Nachr*., **43**, p 289

Shafer, D.R., 1978, "Four-mirror unobscured anastigmatic telescopes with all-spherical surfaces", *Appl. Opt.*, **17**, No. 7, pp 1072-1074

Shafer, D.R., 1988, "Galaxy Wars Optics", *Optics News*, **14**, No. 6, 1988

Stavroudis, O.N., 1967, "Two-mirror systems with spherical reflecting surfaces", *JOSA*, **17**, No. 6, pp 741-748

Steele, W.H., 1953, "Etude des effets combinés des aberrations et d'une obturation centrale de la pupille sur les images. Application aux objectifs de microscope miroirs.", *Thèses Soc. Phys. Paris*, Ser. A **2511**, No. 3383

Stevick, D., 1993, "The Stevick-Paul off-axis reflecting telescope", *Amateur Telescope Making*, **3**, p 10

Stone, B. D., Forbes, G.W., 1991, "First-order layout of asymmetrical systems composed of three-spherical mirrors", *JOSA*, 9, No. 1, pp 110-120

von Rohr, M., 1899, "Theorie und geschichte des photographischen Objektivs", Springer, Berlin, pp 246-271

Wilson, R.N., 2004, "Reflecting Telescope Optics I" 2nd ed., Springer-Verlag, Berlin-Heidelberg, a) pp 88-89, b) p 119, c) pp 148-254, 419-449, d) pp 232-233, e) p 89

Wilson, R.N. and Delabre, B., 1994, "A new 4-mirror optical concept for very large telescope with spherical primary and secondary mirrors, giving excellent field and obstruction characteristics", *Proc. SPIE*, **2199**, pp. 1052-1062

Willstrop, R.V., 1984, "The Mersenne-Schmidt: a three-mirror survey telescope", *Mon. Not. Roy. Astron. Soc.*, **210**, pp 597-609

Willstrop, R.V., 1985, "The flat-field Mersenne-Schmidt", *Mon. Not. Roy. Astron. Soc.*, **216**, pp 411-427

Wynne, C.G., 1969, "Two-mirror anastigmats", *JOSA*, **59**, No. 5, pp 572-578

Yamashita, Y. and Nariai, K., 1983, Three-mirror telescopes", *Ann. Tokyo Astron. Obs.*, 2nd Series, **19**, No. 8, pp 375-400